EVALUATION OF 2-(1H-IMIDAZOL-1-YL)-N-(PYRIDIN-2-YL) AN ACETAMIDE DERIVATIVE SYNTHESIZED BY LIGAND AND STRUCTURE BASED PHARMACOPHORE MODELLING OF AMINOPYRIDINE & IMIDAZOLE AS A NOVEL EPIGENETIC MODULATOR IN HUMAN NON-SMALL CELL LUNG CANCER CELL LINE

Thesis submitted to Bharathidasan University for the award of

Doctor of Philosophy in Biochemistry

By K. SARAVANAN

Research Supervisor

Dr. V. RAVIKUMAR

Associate Professor and Head



Department of Biochemistry (DST- FIST Sponsored) School of Life Sciences Bharathidasan University Tiruchirappalli – 620 024 Tamil Nadu, India.

April – 2022

Dr. V. Ravikumar, PhD. Associate Professor and Head,

Cancer Biology Lab

Phone: 91-431-2407071 Ext 485

Mobile: 91-9444162763

Email: ravikumarbdu@gmail.com

drvr@bdu.ac.in



BHARATHIDASAN UNIVERSITY

Accredited with A⁺ Grade by NAAC Third cycle & 53rd Rank by NIRF 2019 DEPARTMENT OF BIOCHEMISTRY

(DST-FIST Sponsored)

Tiruchirappalli, Tamilnadu - 620 024

Phone: 91-431-2407071 Fax: 91-431-2407045

CERTIFICATE

This is to certify that this thesis entitled, "Evaluation of 2-(1H-imidazol-1-yl)-N-(pyridin-2-yl) an acetamide derivative synthesized by ligand and structure based pharmacophore modelling of aminopyridine & imidazole as a novel epigenetic modulator in human non-small cell lung cancer cell line" submitted by Mr. K. SARAVANAN for the degree of Doctor of Philosophy in Biochemistry to the Bharathidasan University, Tiruchirappalli – 620 024, Tamil Nadu, India, and this work is based on the results of studies carried out by him under my guidance and supervision. This thesis or any part thereof has not been submitted elsewhere for any other degree.

Place: Tiruchirappalli

Date: (V. Ravikumar)

DECLARATION

I do hereby declare that this work entitled "Evaluation of 2-(1H-imidazol-1-yl)-N-

(pyridin-2-yl) an acetamide derivative synthesized by ligand and structure based

pharmacophore modelling of aminopyridine & imidazole as a novel epigenetic modulator

in human non-small cell lung cancer cell line" was originally carried out by me under the

guidance and supervision of Dr. V. Ravikumar, Associate Professor and Head,

Department of Biochemistry, School of Life Sciences, Bharathidasan University and this

work has not been submitted elsewhere for any other degree, diploma or similar titles of any

institute.

Place: Tiruchirappalli

Date:

(K. SARAVANAN)



Document Information

Analyzed document Saravanan thesis final 31.03.22.docx (D132133603)

Submitted 2022-03-31T11:50:00.0000000

Submitted by Dr. V. Ravikumar

Submitter email drvr@bdu.ac.in

Similarity 2%

Analysis address drvr.bdu@analysis.urkund.com

Sources included in the report

W	URL: https://ar.iiarjournals.org/content/40/11/6039 Fetched: 2022-03-31T11:49:51.6670000	1
W	URL: https://www.ncbi.nlm.nih.gov/pmc/articles/PMC6331900/ Fetched: 2019-10-14T19:12:20.9070000	6
W	URL: https://www.ncbi.nlm.nih.gov/pmc/articles/PMC8198376/ Fetched: 2022-03-31T11:49:52.1070000	1
W	URL: https://journals.plos.org/plosone/article?id=10.1371/journal.pone.0129874 Fetched: 2019-10-30T08:47:41.6470000	1
W	URL: https://bmccancer.biomedcentral.com/articles/10.1186/s12885-016-2585-6 Fetched: 2022-01-04T06:59:06.0370000	1

Dedicated to

my Beloved Family

Acknowledgement

The journey of Ph.D. project is both an enjoyable and painful experience. It is just like climbing a high peak, step by step, accompanied with happiness, excitement, fun, hardship, frustration, encouragement and belief. Now, as I stand at the threshold of completing my doctoral work, I take this special moment to express my sincere appreciation and praise for those who have contributed substantially in making this thesis to take its present shape.

First and foremost, I would like to express my deepest sense of gratitude to my research supervisor, **Dr. V. Ravikumar**, Associate professor and Head, Department of Biochemistry, Bharathidasan University, Tiruchirappalli, for his excellent guidance, steadfast inspiration, valuable suggestions, constant motivation, support, constructive comments and discussions. I am grateful to him for his valuable guidance, care and patience that helped me to perform many arduous tasks. His wide knowledge and his logical way of thinking have been of great help for me. He showed me different ways to approach a research problem. I am thankful to him for his constant guidance and having faith in my abilities. His inspiring and encouraging way to guide me to a deeper understanding of knowledge work and his invaluable comments during the whole work with this research. It is purely because of his constant encouragement and much effort I could complete my Ph.D. research successfully.

I would like to thank **Dr.** (**Mrs.**) **K.S.** Shivashangari Ravikumar, Senior Scientific Officer, Regional Forensic Science Laboratory, Tiruchirappalli, for her constant support throughout my research career.

I also extend my heartfelt gratitude and thanks to my doctoral committee members **Dr. C. Prahalathan**, Associate Professor, Department of Biochemistry, Bharathidasan University, Tiruchirappalli, and **Dr. Velu Rajesh Kannan**, Associate Professor, Department of Microbiology, Bharathidasan University, Tiruchirappalli, who spent their time to critically review my work from time to time. Their guidance served me well and I owe them my heartfelt appreciation.

My profound thanks to **Dr. C. Ramesh Kumar**, Associate Professor, Department of Chemistry, Madras Christian College, Chennai. His kind help, encouragement, appreciation, guidance whenever needed and marvellous support have been of great value in this study. His optimistic suggestions, admirable advice, boosting words and constructive comments during the tenure of my research.

I express my special thanks to **Prof. Vasanthi Nachiappan**, UGC BSR Faculty Fellow, Department of Biochemistry, Bharathidasan University, Tiruchirappalli. I express this opportunity to acknowledge **Dr. C. Prahalathan**, Associate Professor, Department of Biochemistry, Bharathidasan University, Tiruchirappalli, for his help with gel documentation studies. I express this opportunity to acknowledge. **Dr. A. Antony Joseph Velanganni**, Assistant Professor, Department of Biochemistry, Bharathidasan University, Tiruchirappalli, for his help with fluorescence microscope studies. **Dr. Anusuyadevi Jayachandran**, Department of Biochemistry, Bharathidasan University, Tiruchirappalli, for supporting my research work. I also thank Dr. Prabhash, Dr. Senthil Kumar, and Dr. J. Kalaiarasi Guest lecture, Department of Biochemistry. Bharathidasan University, Tiruchirappalli, for him support.

I also thank **Dr. M. Karthikeyan**, Department of Bioinformatics, Alagappa University, Karaikudi, for their molecular docking studies.

I also express my heartfelt thanks to Ms. S.H. Kavya, Research Scholar Department of Chemistry, Vel Tech University, Chennai for their instant and timely helps in synthesizing and characterizing of the compounds. I am also thankful to Mr. J. John Marshal, Mr. Manikandan Selvaraj, Research Scholar, Department of Bioinformatics, Alagappa University, Karaikudi, for their molecular docking studies

I am extremely fortunate to have worked with a wonderful team of colleagues. My heartfelt thanks goes to my beloved seniors Dr. S. Karthik, Dr. R. Sankar, Dr. (Mrs). A. Kalaiarasi, Dr. C. Anusha, Dr. K. Varunkumar, whose constant support, encouragement and friendly attitude is a source of inspiration to auccodully finish my work and dear colleagues., Mr. D. Uma Maheswara Rao, Mr. S. Prabhu, Ms. Suhadha Parveen, Mr. Sanjay whose presence perpetually refreshed, helped and gave me such a memorable time when working together. I am thankful to them for providing a pleasant working environment throughout the tenure of my research work. I extend my hearty grade to our

lab M.Sc., M. Phil., Project Students for their unconditional help offered to me during the tough times of my experimental analysis.

I am very much obliged to Dr. Theodore Lemuel Mathuram. Dr. Durairaj Karthick Rajan, Dr. Srinath Rajeswar, Mr. M. Azarudeen, Mr. M. Rajesh Kannan, Mr. Arul Mativannan, Mr. U. Devan, and Mr. Chandhru Srinivasan.

I also express my heartfelt thanks to my dearest friends, Dr. Baskar Subramani, Mr. Paramasivan @ Sudhakar, Mr. Pandiyaraj, and Mr. Mugaesh, for their voluntary help during my research work. For their unconditional support and caring attitude would be the stretch of great friendship. I am really blessed to have them in my life as they were all along with me in all my happiness and sorrows. My heartfelt thanks to all my classmates for being friendly, helpful and for extending their help whenever I needed it.

I have been associated with a fantastic set of seniors, batch-mates, juniors and all supported me in every stage. A special thanks to Dr. K. Selvaraju, Dr. C. Sivaprakasam, Dr. A. William James, Dr. C. Karthick, and Mr. K. Arun Kannan, My heartfelt thanks to all my fellow researchers at Bharathidasan University, Tiruchirappalli, from whose might's and suggestions, I have benefited greatly and borrowed freely.

I take this opportunity to thank Mrs. Raja Lakshmi and Mr. Rajangam Non-teaching Staffs, Department of Biochemistry, Bharathidasan University. Tiruchirappalli for their instant assistance in official matters.

Last but not least, I wish to honour my lovable parents Mr. L. Kandasamy, K. Amaravathi, for leading me all these years by teaching me the value of life Words fail, making me helpless in expressing my heartfelt thanks for all their love, care, sacrifice, patience, selflessness, unflinching support and stood as pillars shouldering me from teaching everything tills this doctorate, stagnating dreams and craving to see me in this form.

Words are inadequate to express my gratitude to my beloved sister Mrs. K. Jothi, my lovable brother Mr. K. Arul, my beloved brother-in-law Mr. M. Rajiv Gandhi, for their love, moral support and treasured advice, has taken the load off my shoulder. I owe them for being selfless in letting my passions and ambitions come true. I would also like to record

my grateful acknowledgement to my endearing buddies R. Madhusudan, and R. Madhunika Sri, all for their constant love.

Financial assistance provided to me by Bharathidasan University in the form of Indian Council of Medical Research (ICMR-SRF) Fellowship is gratefully acknowledged.

I thank the Bharathidasan University, Administrative staffs, University informatics centre personnel and Estate maintenance department staffs who helped with the basic necessities

Above all, I offer my calmest thanks to The Lord Almighty for giving me the intellect to understand the complexity of research and giving me the strength to complete this thesis

I would like to express my deep sense of gratitude and indebtedness to my parents for their loves, guidance care and sacrifice in shaping my life in the right direction.

Ever with fraternal

K. Saravanan

CONTENTS

			Page No
1.0	INTR	ODUCTION	1 - 52
1.1.	Cance	er e e e e e e e e e e e e e e e e e e	1
	1.1.1	General characteristic features of cancer cells as compared to normal cells	2
	1.1.2	Molecular mechanisms in normal and cancer cell	3
1.2	Differ	rent types of cancer	4
	1.2.1	Categories of cancers that begin in specific types of cells	5
	1.2.1.	1 Carcinoma	5
1.3	The Q	Quantitative Burden Based on Cancer Statistics	8
1.4	What	is lung cancer?	13
	1.4.1	Non-Small Cell Lung Cancer (NSCLC)	14
		1.4.1.1 Adenocarcinoma	14
		1.4.1.2 Squamous Cell Carcinoma	15
		1.4.1.3 Large Cell Carcinoma	15
	1.4.2	Small Cell Lung Cancer	16
		1.4.2.1 Limited Stage	16
		1.4.2.2 Extensive Stage	16
1.5	Stages	s of Lung Cancer	17
	1.5.1	The number system of staging lung cancer	17
	1.5.2	TNM staging of lung cancer	18
1.6	Lung	cancer incidence and mortality	23
1.7	What	are the Risk factors for Lung cancer?	24
1.8	Treatr	ments of Lung cancer	25
1.9	Epige	netics	27
	1.9.1	Epigenetics mechanisms in normal cells	27
	1.9.2	Epigenetics in Cancer	29
	1.9.3	Aberrant reprogramming of the epigenome in cancer	30
	1.9.4	DNA methylation aberrations in cancer	31

	1.9.5 Histone modification	32				
	1.9.6 Acetylation	33				
	1.9.7 Methylation	34				
	1.9.8 Phosphorylation	34				
	1.9.9 Ubiquitination	35				
	1.9.10 Sumoylation	35				
	1.9.11 Changes in histone modifications in cancer	35				
1.10	Histone acetyltransferases	37				
1.11	Histone deacetylases	37				
	1.11.1 Mechanism of Histone deacetylase	39				
	1.11.2 Expression of histone deacetylase in cancer cells	40				
	1.11.3 An emerging as a Histone Deacetylase enzyme (Inhibitors) in Cancer Treatment	40				
	1.11.4 Mechanism of histone deacetylase inhibitor in signalling pathways	41				
	1.11.5 Classification of histone deacetylase inhibitors	42				
	1.11.6 Computational approaches for enzyme inhibitor design	44				
1.12	Imidazole					
	1.12.1 Pharmacological Activities	47				
	1.12.1.1 Antibacterial Activity	47				
	1.12.1.2 Anticancer activity	48				
	1.12.1.3 Antitubercular activity	49				
	1.12.1.4 Antifungal activity	49				
	1.12.1.5 Anti-HIV activity	50				
2.0	AIM AND OBJECTIVES	53 - 54				
3.0	MATERIALS AND METHODS	55 - 69				
3.1	Chemicals	55				
3.2	Procedure for the synthesis of ethyl (2, 5-diphenyl-1H-imidazole-4-yl) acetate	55				
3.3	Synthesis of 2-(1H-imidazol-1-yl)-N-(pyridin-2-yl) acetamide (2)	56				

3.4	2-Chloro-N-(pyridine-2-yl) acetamide (1)	56			
3.5	2-(1H-imidazol-1-yl)-N-(pyridin-2-yl) acetamide (2)	57			
3.6	Characterization of synthesised compounds	57			
3.7	Fourier transform infrared spectroscopy (FT-IR)	57			
3.8	Nuclear Magnetic Resonance (NMR)	57			
3.9	High resolution mass spectra (ESI)	57			
3.10	Mass Spectroscopy	58			
3.11	High –performance liquid chromatography (HPLC)	58			
3.12	Melting Point	58			
3.13	Homology modeling and validation	58			
3.14	Protein and Ligand preparation	58			
3.15	Molecular docking analysis	59			
3.16	Molecular dynamics simulations (MDs)	60			
3.17	Cell culture	60			
3.18	Cell viability assay	61			
3.19	Morphological changes of the C3 compound in A549 cells	61			
3.20	Colony formation inhibition assay	61			
3.21	DNA fragmentation assay	62			
3.22	HDAC Activity	62			
3.23	Reverse transcription polymerase chain reaction (RT-PCR)	63			
	3.23.1 Total RNA Isolation	63			
	3.23.2 RNA quantification and cDNA construction	64			
	3.23.3 RT-PCR	64			
3.24	Western blotting				
	3.24.1 Protein estimation	66			
	3.24.2 Separation of protein by SDS-gel electrophoresis and detection	66			
3.25	Cell Cycle distribution analysis by flow cytometry	66			
3.26	Measurement of Reactive Oxygen Species (ROS) Level	67			
3.27	Mitochondrial membrane potential (ΔΨm)	67			
3.28	Nuclear damage by Hoechst staining	68			

3.29	Propio	dium iodide Staining	69					
3.30	Statist	ical analysis	69					
4.0	RESU	JLTS	70 - 103					
4.1	Fourier transform infrared spectroscopy analysis of compounds							
	4.1.1	Nuclear magnetic resonance spectroscopy analysis of synthesised compounds	71					
	4.1.2	High Resolution Mass Spectroscopy Analysis of Synthesised Compounds	73					
	4.1.3	High performance liquid chromatography (HPLC) analysis of 2-(1H-imidazol-1-yl)-N-(pyridin-2-yl) acetamide compound	73					
	4.1.4	Molecular docking validation of the synthesized compounds	74					
	4.1.5	Molecular dynamics simulation (MDs) of ethyl (2, 5-diphenyl-1H-imidazole-4-yl) acetate (C3) compound	75					
	4.1.6	Homology modelling and validation	77					
	4.1.7	Molecular docking analysis	79					
	4.1.8	DFT analysis and salvation energy calculation	81					
4.2.	Biological evaluation of the synthesized compounds							
	4.2.1	Cytotoxicity assay of compounds against in A549 cells using MTT	82					
	4.2.2	Morphological changes of A549 cells treated with 2-(1H-imidazol-1-yl)-N-(pyridin-2- yl) acetamide compound using phase contrast microscopy	84					
	4.2.3	Clonogenic (CFU) assay	85					
	4.2.4	DNA fragmentation assay	86					
	4.2.5	5 Histone deacetylase enzyme colorimetric activity in A549 cells						
	4.2.6	Effect of 2-(1H-imidazol-1-yl)-N-(pyridin-2-yl) acetamide regulating various classes of HDACs	88					
	4.2.7	2-(1H-imidazol-1-yl)-N-(pyridin-2-yl) acetamide increase the acetylation State of Histone H3 and H4	91					
	4.2.8	Effect of tested compound on the expression of p53 and p21 in A549 cells	92					
	4.2.9.	Induction of cell cycle arrest by 2-(1H-imidazol-1-yl)-N-(pyridin-2-yl) acetamide in A549 cells	94					

6.	.0 SUMN	MARY AND CONCLUSION	114 - 116
5.	0 DISC	USSION	104 - 113
	4.2.15	Role of Phosphoinositide 3-kinase (PI3K)/Akt signalling in A549 cells.	102
	4.2.14	2-(1H-imidazol-1-yl)-N-(pyridin-2-yl) acetamide induces excessive ROS accumulation induced apoptosis by increasing oxidative stress and altering mitochondrial functions	101
	4.2.13	2-(1H-imidazol-1-yl)-N-(pyridin-2-yl) acetamide induce downregulation of MMP2 and MMP 9 expression in A549 cells	99
	4.2.12	Effect of tested compound on pro-apoptotic proteins Bax and Anti-apoptotic proteins Bcl-2 in A549 cells.	98
	4.2.11	2-(1H-imidazol-1-yl)-N-(pyridin-2-yl) acetamide triggers the apoptotic regulating proteins.	96
	4.2.10	Effect of 2-(1H-imidazol-1-yl)-N-(pyridin-2-yl) acetamide inhibits Tumour necrosis factor (TNF- α) mediated Cyclooxygenase (COX-2) expression	95

ABBREVIATIONS

ALP - Alkaline phosphate

AO - Acridine orange

Bax - Bcl2 - associated X protein

 $BCIP/NBT \qquad \text{-} \qquad \text{5-broma -4 -chloro} \\ -3 - inodyl - phosphate \\ / \text{ Nitro blue tetrazolium}$

Bcl – XL - B- cell lymphoma- extra large

Bcl 2 - B cell lymphoma 2

Bp - Base pare

CDKN - Cyclin- dependent kinase inhibitor

Cdna - complementary DNA

CoA - Coenzyme A

CU - Connect unit

CTCL - Cutaneous T- cell lymphoma

DCFH-DA - 2',7' - dichlorofluorescein - diacetate

DMEM - Dulbecco's modified Eagle's medium

DMSO - Dimethyl sulfoxide

DNA - DNA

EB - Ethidium bromide

EDTA - Ethylene diamine tetra acetic acid

F - Forward

FBS - Fetal bovine serum

FDA - Food and Drug Administration

FT-IR - Fourier transform infrared spectroscopy

GAPDH - Glyceraldehyde – 3 – phosphate dehydrogenase

H - Hours

HAT - Histone acetyltransferases

HDAC - Histone deacetylase

HDACi - Histone deacetylase inhibitor

HMT - Histone methyltransferases

HPLC - High performance liquid chromatography

IARC - International Agency for Research on Cancer

IC50 - Inhibitory concentration

IGFBP - Insulin – like growth factor binding protein

KD - Kilo Dalton

IL 6 - Interleukin 6

IL 8 - Interleukin 8

MM - Multiple myeloma

MMPs - Matrix metallo proteinases

MTT - 3-(4, 5 Dimethylthiazol 2-yl) - 2,5 - diphenyltetrazolium bromide

mRNAs - Messenger RNA

mg - Milligram

mL - Milliliter

Mm - Milli molar

nm - nanometer

nM - nanomole

NAD - Nicotinamide adenine dinucleotide

NMR - Nuclear Magnetic Resonance

NSCLC - Non Small Cell Lung Cancer

PI - Propidium iodide

PBS - Phosphate buffered saline

PMSF - Phenylmethylsulfonyl fluride

PTCL - Peripheral T – cell lymphoma

PTM - Post translational modification

R - Reverse

Rb - Retinoblastoma

RBCs - Red blood cells

RH123 - Rhodamine 123

RNA - Ribonucleic acid

RT-PCR - Reverse transcription polymerase chain reaction

ROS - Reactive oxygen species

SCLC - Small cell lung cancer

SDS -PAGE - Sodium dodecyl sulfate polyacrylamide gel electrophoresis

SRM - Surface recognition moiety

TBS - Tris – buffered saline

TBST - Tris – buffered saline and Tween 20

TIMP - Tissue inhibitor of metalloproteinase

 $TNF\alpha \qquad \quad - \quad Tumor \ necrosis \ factor \ alpha$

TRAIL - Tumor necrosis factor – related apoptosis inducing ligand

TSA - Trichostatin A

VEGF - Vascular endothelial growth factor

ZBG - Zinc binding group

 $\Delta \Psi m$ - Mitochondrial membrane potential

 μg - Microgram

μl - Microliter

 μM - Micro molar

Abstract

Histone deacetylase enzymes are involved in the remodelling of chromatin and have a pivotal role in balancing acetylation and deacetylation status of chromatin eventually ensures the epigenetic regulation of gene expression. Its aberrant activity was reported in several forms of cancer considering it as a potential target for cancer treatment. Histone deacetylase inhibitors emerged as new class of antineoplastic drugs. Recent developments in understanding the mechanism of interaction between drug and targeted molecule encourages rational development of new class of HDAC inhibitors directing global or gene specific histone acetylation. In the present study, we designed 14 imidazole-based derivatives abiding the common pharmacophore structure like CAP, Spacer, and Zinc binding group (ZBG) shared among the established HDAC inhibitors and was explored for its epigenetic modulator candidature targeting histone modifying enzymes through docking experiments. Among them the 2-(1H-imidazol-1-yl)-N-(pyridin-2-yl) acetamide was tightly bound to the isoforms of the HDAC enzymes at their receptor regions with high binding score. Our Second generation acetamide compound was synthesized and characterized experimentally by IR and NMR techniques. The synthesized compound were subjected to cell proliferation inhibition in A549 lung cancer cell by inducing cytotoxicity and increasing ROS generation eventually disrupting mitochondrial permeability as evidenced from deflection in (ΔΨM). From this study we revealed that 2-(1H-imidazol-1-yl)-N-(pyridin-2-yl) acetamide a novel imidazole derivative, that inhibits highly expressed HDAC enzyme in non-small cell lung cancer cell lines by epigenetic modification. Our Second generation acetamide compound is a potent dual - target i.e. one directed towards inhibiting histone deacetylases (HDAC) and simultaneously stimulating PI3K/AKT signalling. The antiproliferative effects of this compound were demonstrated using Clonogenic assays and apoptotic stimulation was detected by caspase cascade pathway against A549 cancer cell line and L-132 cell line (Epithelial normal lung cells). Acetylated state of histones proteins H3 and H4 were analysed by HDAC colorimetric assay. In addition, Matrix metalloproteinase (MMPs 2 and 9) were identified by western blot analysis and scratch-wound assay was used to analyse the migration of collective cells in A549 cells. Our compound had a significant antiproliferative effect and induces apoptosis when compared with the established HDAC inhibitor. It leads to hyperacetylation of the histones H3 and H4 as well as the HDAC family. Moreover, A549 cells showed a significant reduction in antiproliferative properties when phosphatidylinositol3 kinase was inhibited. The 2-(1H-imidazol-1-yl)-N-(pyridin-2-yl) acetamide accelerates the acetylation of histone proteins and chromatin remodelling by inhibiting HDAC, which may be the important mechanism of its antitumor effect.

Introduction

1. Introduction

1.1 Cancer

Cancer is a group of diseases which is characterized by the abnormal growth of cells which tend to proliferate in an uncontrolled manner [1]. Cancer results from a sequence of molecular events that fundamentally alter the normal properties of the cells. These alterations in the cellular genome affecting the expression or function of genes controlling cell growth and differentiation are considered to be the main cause of cancer. These cells develop new characteristic changes including cell structure, decreased cell adhesion, and production of new enzymes. These heritable changes allow the cell and its progeny to divide and grow, even in the presence of normal cells that typically inhibit the growth of nearby cells such changes allow the cancer cells to spread and invade other tissues.

Cancer development and evolution have been exposed to be dependent on the cellular accumulation of different genetic and epigenetic events. The abnormalities in cancer cells usually results from mutations in protein-encoding genes that regulate the cell division process. These mutations give arises to sub clones within tumours each with conflicting properties so that most tumours are heterogeneous in nature [2]. This often because the genes make the proteins normally they play a pivotal role in the DNA repair process are themselves not functioning correctly because they are also mutated [3]. Thus, mutations begin to increase in the cell, causing further aberrations in that cell and the daughter cells. Some of these mutated cells die, but other alterations may stretch the atypical cell a selective advantage that allows it to multiply much more rapidly than the normal cells. This enhanced growth describes most cancer cells gained functions in their original location, they are considered as benign. If the cancer cells have become invasive, they are considered as

malignant. Cancer cells in malignant tumours can often metastasize, distribution the cancer cells to distant places in the body where new tumours may form.

Approximately 35,000 genes have been associated with cancer in the human genome. Variations in a similar gene often are related to the different forms of cancer [4]. These malfunctioning genes are can be generally categorized into three groups. The first group, called proto-oncogenes, produces protein products that typically enhance cell division or inhibit normal cell death. The mutated forms of these genes are called oncogenes. The second group, called tumour suppressors, makes proteins that normally prevent cell division or cause cell death. The third group, called DNA repair genes, which help to prevent mutations that lead to cancer [5, 6]. Each of these novel capabilities acquired during tumour development represents the successful breaching of an anticancer defense mechanism hardwired into cells and tissues.

1.1.1 General characteristic features of cancer cells as compared to normal cells

Living organisms are made of cells. To endure life is a healthy manner. These cells must perform in biologically crucial ways. At any moment, cells in the body are being born, growing, dividing, and being destroyed all to maintain a healthy balance called homeostasis. Intermittently, when the normal cell regulation process is disturbed a chain reaction of cellular malfunction can occur which leads to diseases. Such disease that results from a malfunction in cellular regulation called cancer. Cancer cells differ from healthy cells in serious ways that make them harmful to the body. As they develop, they begin to ignore the signals sent by the body telling them when and when not grow or even when to die and they divide uncontrollably without stopping. Cancer cells develop referred to as metabolic autonomy which means they can self-medicate growth and division instead of being stimulated by an external signal like a normal cell [7]. As compared to normal cells, cancer cells show a notable number of different features as shown in (Fig.1).

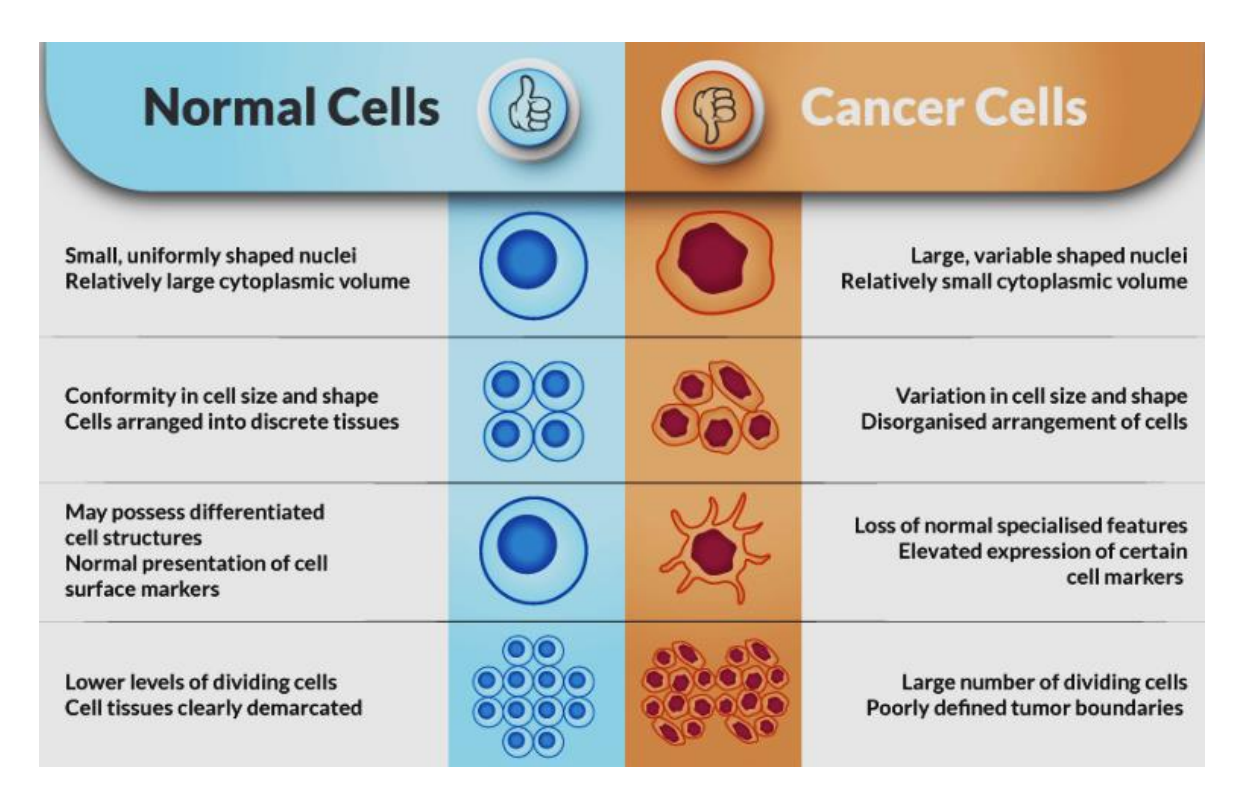


Fig. 1. General characteristic features of Normal cell Vs Cancer cell

1.1.2. Molecular mechanisms in normal and cancer cell

Normal cellular functions are managed and maintained by a network of collaborative interactions among several cellular pathways, which include cell cycle proteins, regulated apoptotic process, functional tumour suppressor proteins, responsible cellular receptors, regulated signal transduction network and active DNA-repair mechanisms. Together, these pathways make up what is known as the "six important rules" necessary for the maintenance of cells at normal cellular status. The heir maintains the normal cellular function, but if there is a significant break in any one of the mechanisms of this circuit, it can be led to a pathological state of the cell that might lead to cancer [8]. Cancer development involves mutated tumour suppressor proteins, activated angiogenesis, inactivated cell cycle checkpoints, anti-apoptotic property, active growth signalling, and deficient DNA repair systems (Fig.2) [9-11]. Also, each of these mechanisms is in turn regulated by a complex network of protein-protein interactions.

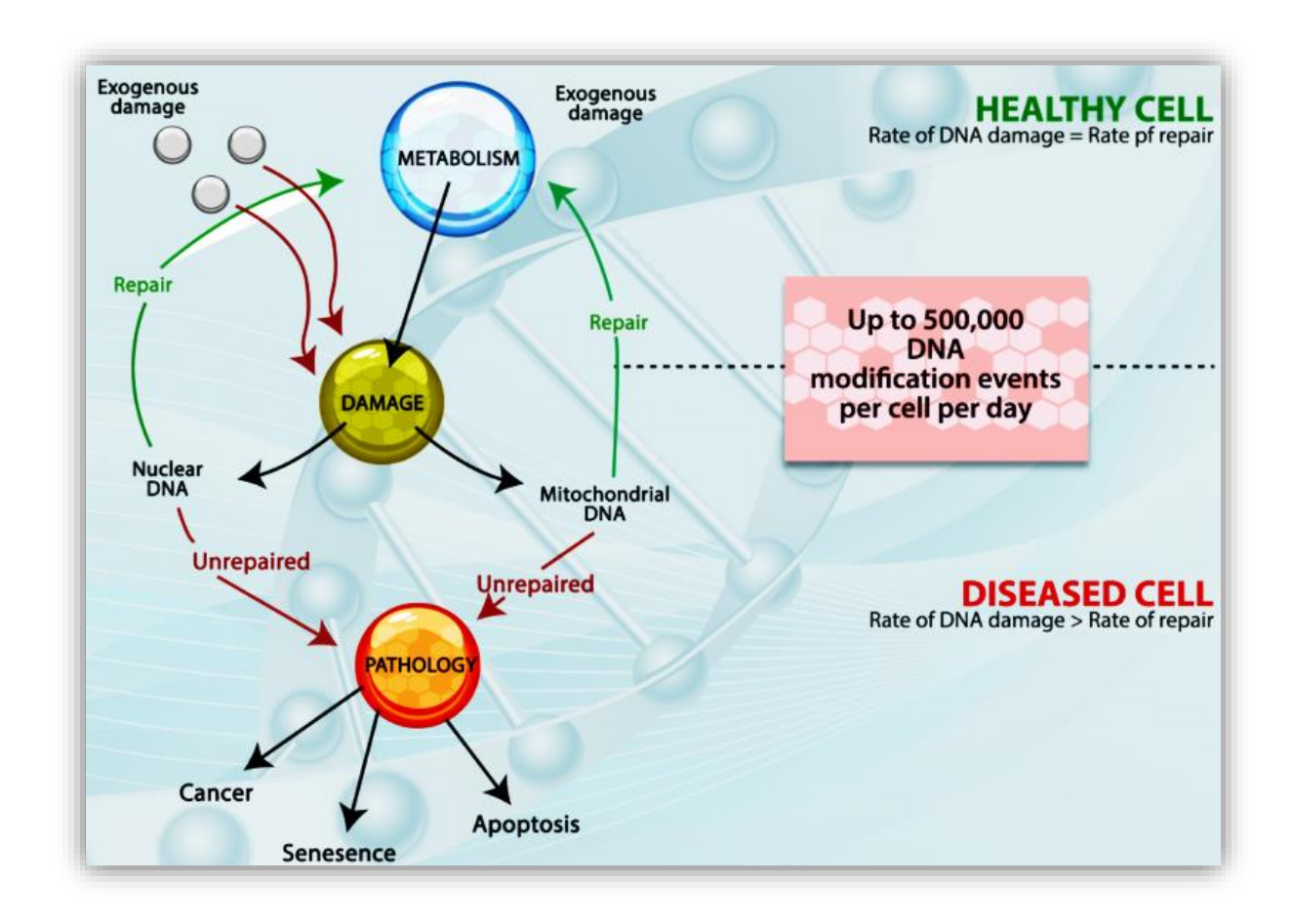


Fig. 2. Molecular mechanism behind the normal cell and cancer cell

1.2 Different types of cancer

More than 100 types of cancer worldwide. Usually, types of cancer are named for the organs or tissues where the cancers form (**Fig.3**). For example, lung cancer starts in cells of the lung, and brain cancer starts in cells of the brain. Cancers also may be described by the type of cell that formed them, such as an epithelial cell or a squamous cell. Specific types of cancer-based on the cancer's location in the body or our A to Z List of Cancers by using NCI's website (https://www.cancer.gov/types, https://www.cancer.gov/ types/by-body-location) [13]. We also have collections of information on childhood cancers and cancers in adolescents and young adults.

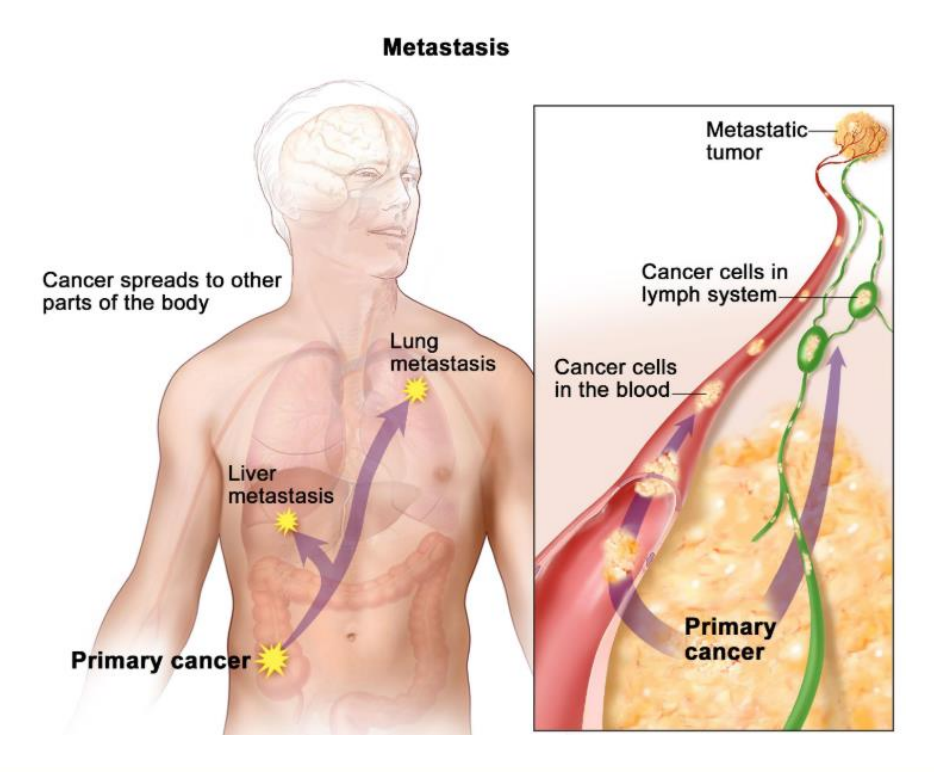


Fig. 3. In metastasis, cancer cells where they first formed (primary cancer), travel through the blood or lymph system and form new tumors (metastatic tumors) in other parts of the body

1.2.1 Categories of cancers that begin in specific types of cells

1.2.1.1 Carcinoma

The most common type of cancers are carcinoma. They are formed by epithelial cells, which are the cells that cover the inside and outside surfaces of the body. There are many types of epithelial cells, which frequently have a column-like shape when viewed under a microscope.

Carcinomas that begin in different epithelial cell types have specific names:

Adenocarcinoma is a cancer that forms in epithelial cells that produce fluids or mucus. Tissues with this type of epithelial cell are sometimes called glandular tissues. Most of the cancers breast, colon, and prostate are adenocarcinomas.

Basal cell carcinoma is a cancer that begins in the lower or basal (base) layer of the epidermis, which is a person's outer layer of skin.

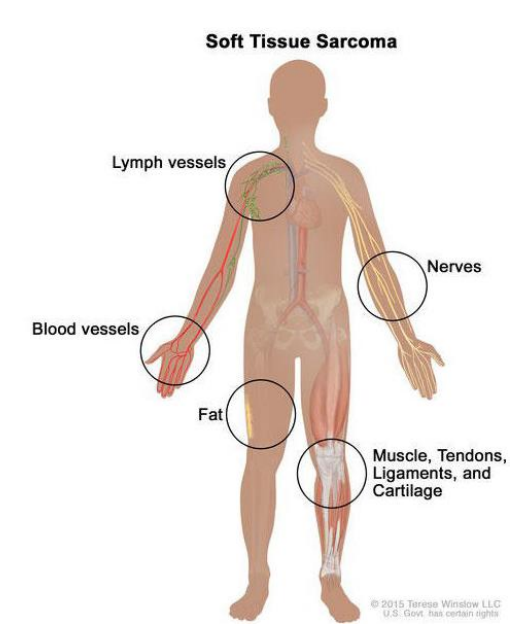
Squamous cell carcinoma is cancer that forms in squamous cells, which are epithelial cells that lie just beneath the outer surface of the skin. Squamous cells also link many other organs, including the stomach, intestines, lungs, bladder, and kidneys. Squamous cells look like a flat (like fish scales) when viewed under a microscope. Squamous cell carcinomas are sometimes called epidermoid carcinomas.

Transitional cell carcinoma is a cancer that forms in a type of epithelial tissue called transitional epithelium, or urothelium. This tissue, which is made up of many layers of epithelial cells that can get bigger and smaller, is found in the linings of the bladder, ureters, and part of the kidneys (renal pelvis), and a few other organs. Some cancers of the bladder, ureters, and kidneys are transitional cell carcinomas.

Sarcoma

Sarcomas are cancers that form in bone and soft tissues, including muscle, fat, blood vessels, lymph vessels, and fibrous tissue (such as tendons and ligaments).

Osteosarcoma is the most common cancer of the bone. The most common types of soft tissue sarcoma are leiomyosarcoma, Kaposi sarcoma, malignant fibrous histiocytoma, liposarcoma and dermatofibrosarcoma protuberans.



Leukemia

Cancers that begin in the blood-forming tissue of the bone marrow are called leukemias. These cancers do not form solid tumors. There are four common types of leukemia, which are grouped based on how quickly the disease gets worse (acute or chronic) and on the type of blood cell cancer starts in (lymphoblastic or myeloid).

Lymphoma

Lymphoma is cancer that begins in lymphocytes (T cells or B cells). These are disease-fighting white blood cells that are part of the immune system. In lymphoma, abnormal lymphocytes build up in lymph nodes and lymph vessels, as well as in other organs of the body.

There are two main types of lymphoma:

Hodgkin lymphoma – People with this disease have abnormal lymphocytes that are called Reed-Sternberg cells. These cells usually form from B cells.

Non-Hodgkin lymphoma – This is a large group of cancers that start in lymphocytes. The cancers can grow quickly or slowly and can form from B cells or T cells.

Multiple Myeloma

Multiple myeloma is cancer that begins in plasma cells, another type of immune cell.

Multiple myeloma is also called plasma cell myeloma and Kahler disease.

Melanoma

Melanoma is cancer that begins in cells that become melanocytes, which are specialized cells that make melanin (the pigment that gives skin its color). Most melanomas form on the skin, but melanomas can also form in other pigmented tissues, such as the eye.

Brain and Spinal Cord Tumors

There are different types of brain and spinal cord tumors. These tumors are named based on the type of cell in which they formed and where the tumor first formed in the central nervous system.

Other Types of Tumors

Germ Cell Tumors

Germ cell tumors are a type of tumor that begins in the cells that give rise to sperm or eggs. These tumors can occur almost anywhere in the body and can be either benign or malignant.

Neuroendocrine Tumors

Neuroendocrine tumors form from cells that release hormones into the blood in response to a signal from the nervous system.

Carcinoid Tumors

Carcinoid tumors are a type of neuroendocrine tumor. They are slow-growing tumors that are usually found in the gastrointestinal system (most often in the rectum and small intestine). Carcinoid tumors may spread to the liver or other sites in the body, and they may secrete substances such as serotonin or prostaglandins, causing carcinoid syndrome.

1.3 The Quantitative Burden Based on Cancer Statistics

International Agency for Research on Cancer (IARC) was founded by a Resolution of the World Health Assembly in September 1965 [7]. The continued growth and aging of the world's population will greatly affect the future cancer burden. By 2030, it could be expected that there will be 27 million incident cases of cancer, 17 million cancer deaths annually, and 75 million persons alive with cancer. Human societies have always traded and

migrated, yet the growth of powerful economic institutions and globalization is accelerating, mixing many cancer risk factors.

Understanding the burden of cancer survivorship also requires a quantitative appreciation of the incidence of cancer, the mortality of the disease, and the resulting number of accumulating survivors. The American Cancer Society publishes an annual summary of cancer statistics (Fig.4) [14]. Based on data from the National Cancer Institute and mortality data from the National Center for Health Statistics, estimated that in the United States for 2019, a total of 870,970 new cancer cases of males and 891,480 new cancer cases of females and estimated deaths are male 321,640 and 285,210 of females.

Cancer is a leading cause of death worldwide. In 2015, 8.8 million deaths were attributed due to cancer, particularly in developing countries such as India. [15]. According to GLOBOCAN 2018 data, in 2019 there were 1,157,294 new cancer cases in India in both men and women, 784821 and 2,258,208 people living with cancer (within 5 years of diagnosis). Top 5 cancers that affect the Indian population are Breast, Lip and Oral cavity, Cervix Uteri, Lung and Stomach [GLOBOCON 2018] (Table.1).



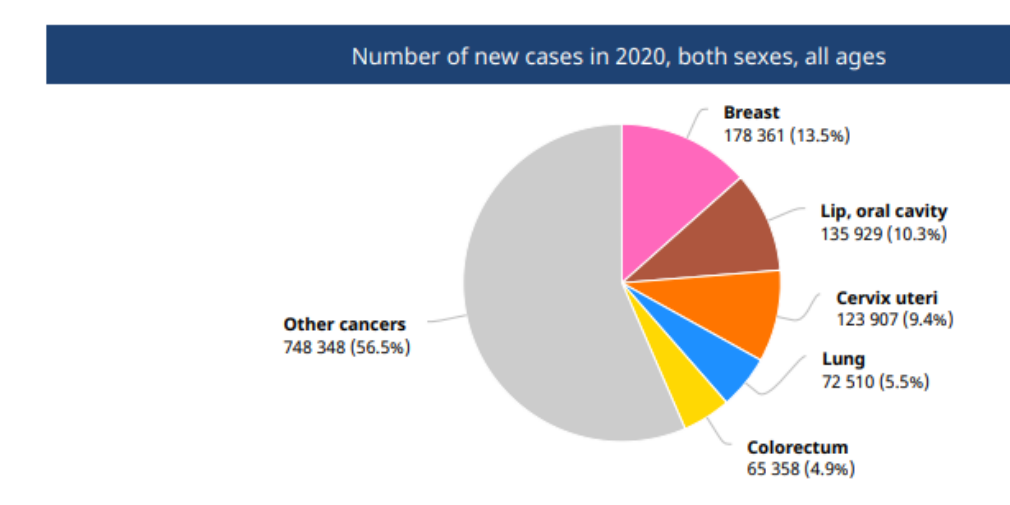
Fig.4. Estimate the leading sites of new cancer cases and deaths-2020

The latest estimates of global cancer incidence show that (Fig. 5) cancer has become the leading cause of cancer deaths among men and women. Critically, new cancer risk factors have also appeared, concurrent with globalization: modern diet, addictive products, pharmaceuticals, toxic and waste products will increase cancer rate.

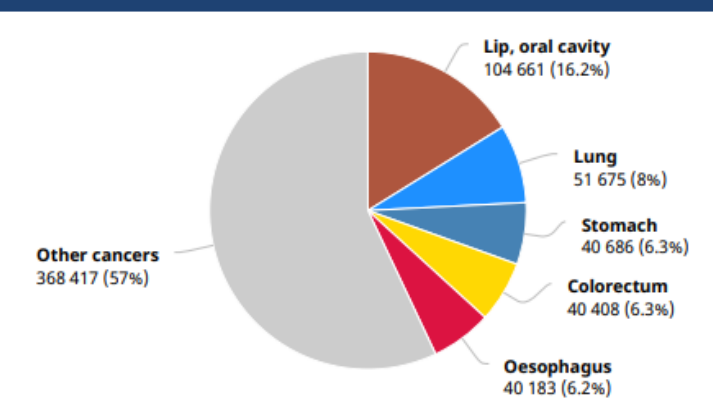
		Inc	idence, N	Mortality and P	revalence by	cancer si	te			
	New cases Deaths					5-year prevalence (all ages)				
Cancer	Number	Rank	(%)	Cum.risk	Number	Rank	(%)	Cum.risk	Number	Prop. (per 100 000)
Breast	178 361	1	13.5	2.81	90 408	1	10.6	1.49	459 271	69.28
Lip, oral cavity	135 929	2	10.3	1.09	75 290	3	8.8	0.62	300 413	21.77
Cervix uteri	123 907	3	9.4	2.01	77 348	2	9.1	1.30	283 842	42.82
Lung	72 510	4	5.5	0.67	66 279	4	7.8	0.61	80 817	5.86
Oesophagus	63 180	5	4.8	0.57	58 342	5	6.9	0.53	68 607	4.97
Stomach	60 222	6	4.5	0.53	53 253	6	6.3	0.48	81 270	5.89
Leukaemia	48 419	7	3.7	0.31	35 392	7	4.2	0.24	127 493	9.24
Ovary	45 701	8	3.5	0.74	32 077	9	3.8	0.57	103 716	15.65
Non-Hodgkin lymphoma	35 828	9	2.7	0.28	20 390	12	2.4	0.17	88 272	6.40
Liver	34 743	10	2.6	0.32	33 793	8	4.0	0.32	38 602	2.80
Larynx	34 687	11	2.6	0.32	21 660	11	2.5	0.21	82 087	5.95
Prostate	34 540	12	2.6	0.64	16 783	14	2.0	0.28	67 909	9.47
Colon	31 646	13	2.4	0.28	19 236	13	2.3	0.17	65 493	4.75
Brain, central nervous system	31 460	14	2.4	0.22	26 656	10	3.1	0.20	74 398	5.39
Hypopharynx	28 489	15	2.2	0.26	11 443	20	1.3	0.11	39 750	2.88
Rectum	28 260	16	2.1	0.24	16 149	15	1.9	0.13	62 827	4.55
Bladder	21 096	17	1.6	0.19	11 154	21	1.3	0.10	49 257	3.57
Oropharynx	20 617	18	1.6	0.19	12 703	17	1.5	0.12	44 398	3.22
Thyroid	20 432	19	1.5	0.15	4 895	25	0.57	0.04	55 248	4.00
Gallbladder	19 570	20	1.5	0.17	14 736	16	1.7	0.13	25 138	1.82
Kidney	16 861	21	1.3	0.14	9 897	22	1.2	0.09	39 150	2.84
Corpus uteri	16 413	22	1.2	0.29	6 385	23	0.75	0.11	43 484	6.56
Multiple myeloma	14 641	23	1.1	0.14	12 556	18	1.5	0.12	30 640	2.22
Pancreas	12 642	24	0.95	0.11	12 153	19	1.4	0.11	11 928	0.86
Penis	10 677	25	0.81	0.20	4 760	26	0.56	0.08	26 280	3.66
Hodgkin lymphoma	9 221	26	0.70	0.06	3 513	28	0.41	0.03	24 928	1.81
Salivary glands	7 850	27	0.59	0.07	5 127	24	0.60	0.05	20 448	1.48
Nasopharynx	5 697	28	0.43	0.05	4 148	27	0.49	0.03	14 196	1.03
Vagina	5 518	29	0.42	0.09	2 723	30	0.32	0.05	12 315	1.86
Anus	5 452	30	0.41	0.05	2 776	29	0.33	0.03	12 278	0.89
Testis	4 681	31	0.35	0.06	1 252	34	0.15	0.02	14 812	2.07
Melanoma of skin	3 916	32	0.30	0.03	2 296	31	0.27	0.02	9 637	0.70
Vulva	3 447	33	0.26	0.06	1 694	32	0.20	0.03	8 928	1.35
Mesothelioma	1 709	34	0.13	0.01	1 543	33	0.18	0.01	2 223	0.16
Kaposi sarcoma	66	35	0.00	0.00	43	35	0.01	0.00	156	0.01
All cancer sites	1 324 413			10.43	851 678			7.05	2 720 251	197.1

Table 1: Incidence, Mortality, and Prevalence by cancer site 2020 in India

Total: 1 324 413

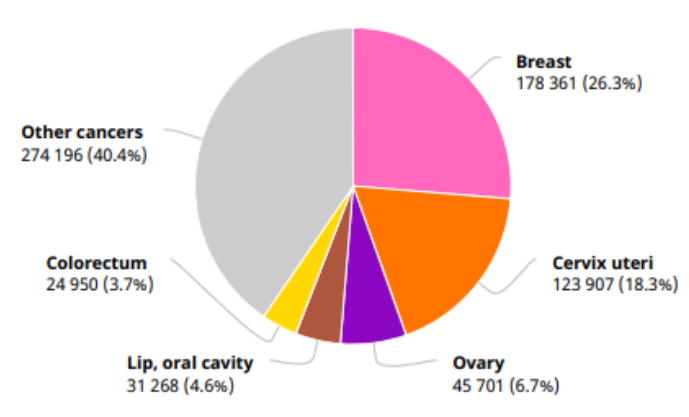


Number of new cases in 2020, males, all ages



Total: 646 030

Number of new cases in 2020, females, all ages



Total: 678 383

Summary	statistic 2020
---------	----------------

	Males	Females	Both sexes
Population	717 100 976	662 903 415	1 380 004 378
Number of new cancer cases	646 030	678 383	1 324 413
Age-standardized incidence rate (World)	95.7	99.3	97.1
Risk of developing cancer before the age of 75 years (%)	10.4	10.5	10.4
Number of cancer deaths	438 297	413 381	851 678
Age-standardized mortality rate (World)	65.4	61.0	63.1
Risk of dying from cancer before the age of 75 years (%)	7.4	6.7	7.1
5-year prevalent cases	1 208 835	1 511 416	2 720 251
Top 5 most frequent cancers excluding non-melanoma skin cancer	Lip, oral cavity	Breast	Breast
(ranked by cases)	Lung	Cervix uteri	Lip, oral cavity
	Stomach	Ovary	Cervix uteri
	Colorectum	Lip, oral cavity	Lung
	Oesophagus	Colorectum	Colorectum

Fig. 5 Latest estimate of Cancers GLOBOCON 2020 in India

1.4 What is lung cancer?

The lungs are a pair of sponge-like cone-shaped organs in the chest. These are part of our respiratory system. The main function of the lungs is to exchange gases between the air we breathe and the blood. When we breathe in (inhale), oxygen enters into the body through the lungs and when we breathe out (exhale) carbon dioxide is sent out of the body (Fig. 6). Lung cancer is one of the deadliest carcinomas in the world that affects the lungs. It originates from the tissues of the lungs, usually from cells lining in air passages. The abnormal cells do not develop into healthy lung tissues, they divide rapidly and forms tumors (Fig.7). Primary lung cancer initiates in the lungs, while secondary lung cancer starts somewhere else in the body. Lung cancer cells can travel via the bloodstream to other parts of the body where they continue to grow as metastasizes and reaches the lungs [16]. Almost 40% of those people newly diagnosed with lung cancer already have metastasis to other parts of the body e.g. lymph nodes, liver, bone, and adrenal gland, etc. Lung cancer grows when normal lung cells exposed to cigarette smoke, excess radiation, and other environmental carcinogens along with genetic damage that eventually leads to uncontrolled cell proliferation [14]. It is the second most common cancer in men and the fifth most common cancer in both men and women together. An estimated 228,150 new cases of lung cancer will be diagnosed in the US in 2019.

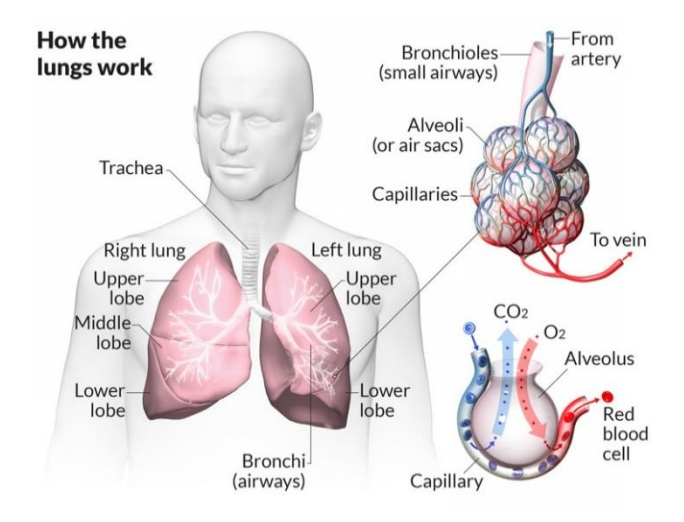


Fig. 6. How the Lungs work in our Respiratory System

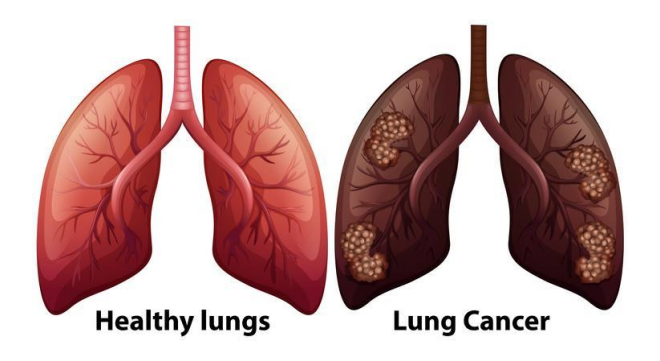


Fig.7. Structurally Difference Between Normal Lung and Cancer Lung

For a better understanding and treatment of lung cancer. Signs of lung cancer vary at different stages and the treatment is considered to be more effective when diagnosed at an early stage. The lung cancer is subdivided into two sub-categories namely: Non-Small Cell Lung Cancer (NSCLC) and Small Cell Lung Cancer (SCLC).

1.4.1 Non-Small Cell Lung Cancer (NSCLC)

Everywhere 80 to 85% of the lung cancer patients are suffering from Non-Small Cell Lung Cancer (NSCLC). The common cause of NSCLC was observed behind is smoking and exposure of asbestos. Symptoms of NSCLC like chest pain, coughing, fatigue, weight loss, body pain, coughing up blood, etc. The massive drawback of NSCLC is that is doesn't show any symptoms at the initial stage. According to severity, Non-Small Cell Lung Cancer (NSCLC) is further divided into three types:

1.4.1.1 Adenocarcinoma

Out of 80 to 85% of Non-Small Cell Lung Cancer patients, about 40% of them are suffering from Adenocarcinoma [17]. Usually, the accumulation of substances like Mucus on the walls of airways causes adenocarcinoma. This Non-small cell lung cancer targets the outer parts of the lungs. Consequently, the efficiency of the growth of infected cells is quite low as compared to other lung cancer types and it is easy to diagnose too (In

Adenocarcinoma, the effect on the internal parts of lungs is minimum). Therefore, Adenocarcinoma is classified as the initial stage of lung cancer.

1.4.1.2 Squamous Cell Carcinoma

This type of non-small cell lung cancer type is about 25%. Squamous Cell Lung Cancer is generally found in the middle of the lungs [18]. It affects the squamous cells present in the airways in the lungs. Moreover, this type of lung cancer is also called epidermoid carcinoma (cancer which is developed by the infected squamous cells) (**Fig. 8**). The primary symptoms which are experienced in this type of NSCLC are cough, chest pain, trouble breathing, etc. Although the primary causes overdue this type of lung cancer is smoking, age, genes, second-hand smoke, asbestos, radon, metal dust.

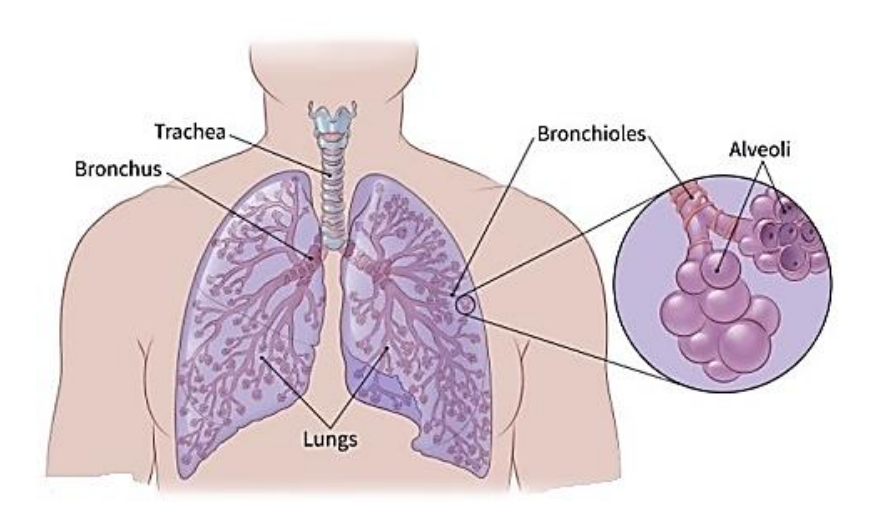


Fig. 8. Structure of squamous cell carcinoma

1.4.1.3 Large Cell Carcinoma

About 10% of people suffering from this type of lung cancer is called Large Cell Carcinoma. This type of tumor can view under the microscope because of its tumor cell size (**Fig. 9**). Infected cells in this type of cancer are found in the central part of the lungs. Also, the cells grow faster in Large Cells Carcinoma and affect the nearby lymph nodes in quick succession [19].

1.4.2 Small Cell Lung Cancer

Small Cell Lung Cancer is those who have a habit of smoking many cigarettes in a day or a long-time smoker or second-hand smokers. All of these people have the same probability of getting diagnosed with SCLC. Out of 100 Lung cancer patients, 10% of them fall under this type of Lung Cancer. Small cell lung cancer possesses a faster growth rate and affects the nearby parts easily [20] (**Fig.10**). The primary signs of Small cell lung cancer are Chest Pain, Breathing Problem, coughing, loss of appetite, fatigue, swelling of face, weight Loss. Small Cell Lung Cancer is largely diagnosed in Men. Small cell lung cancer (SCLC) is another form of lung cancer and has two main stages-

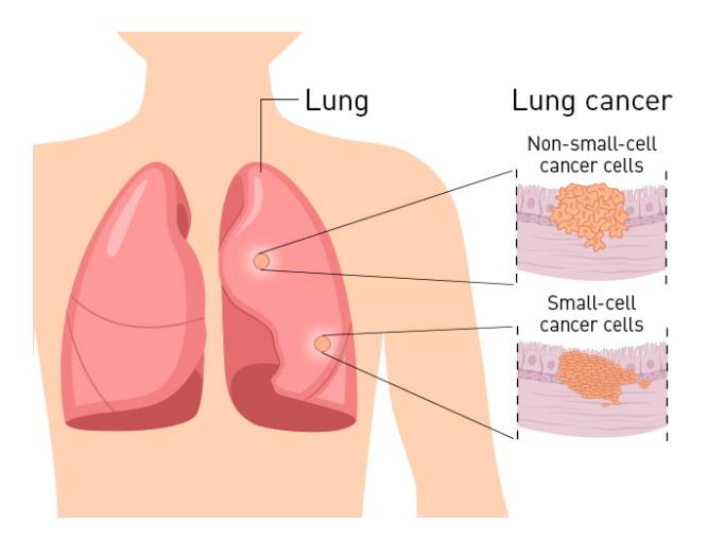


Fig.10. Structurally difference between SCLC and NSCLC

1.4.2.1 Limited Stage

Cancer is found in a small portion of only one lung and lymph nodes on the same side of the chest.

1.4.2.2 Extensive Stage

In this stage, cancer begins to spread to the entire lung and gradually moves to the other lung and lymph nodes around it. It also infects lung fluids, bone marrow, and other organs. Most often people suffering from SCLC are diagnosed at an extensive stage.

1.5 Stages of Lung Cancer

There are two types of staging systems used to stage lung cancer. They are a number system and TNM staging system [21, 22].

1.5.1 The number system of staging lung cancer

Stage I:

The tumor size is less than 5 cms and it is limited to lungs only. There is no involvement of lymph nodes (**Fig.11**).

Stage II:

- Tumor size is more than 5 cms
- Lymph nodes are involved
- Larger than 7cm with no involvement of lymph nodes
- Spread to the following areas the chest wall, the muscle under the lung (diaphragm), the phrenic nerve, or the layers that cover the heart (mediastinal pleura and parietal pericardium)
- In the main airway (bronchus) close to where it divides to go into each lung
- Making part of the lung collapse
- Any size but there is more than one tumor in the same lobe of the lung

Stage III:

There is a presence of any one of these following conditions

- Complete lung collapse
- Has spread into the chest wall, the muscle under the lung (diaphragm), or the layers
 that cover the heart (mediastinal pleura and parietal pericardium)
- Spread into lymph nodes on the opposite side of the chest

• The involvement of major structures in the chest include the heart, the windpipe (trachea), the food pipe (esophagus) or a main blood vessel.

Stage IV:

Cancer has spread to a distant part of the body such as the liver, bones or the brain.

1.5.2 TNM staging of lung cancer

TNM stands for Tumor, Node, and Metastases. This staging system describes

Tumor (T)

- T1 the tumor is contained within the lung and is smaller than 3 cm across
- T2 the tumor is between 3 and 7cm across
- T3 the tumor is larger than 7cm
- T4 the tumor has grown into one of the following structures: mediastinum, the heart, a major blood vessel, the windpipe, food pipe, a spinal bone, the nerve that controls the voice box

Nodes (N)

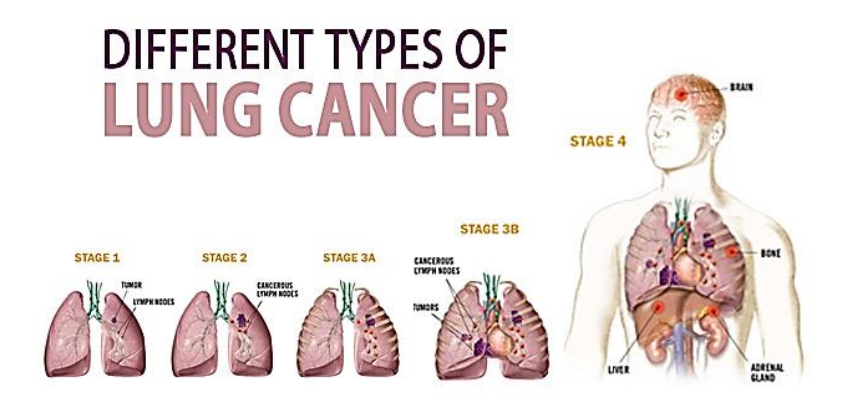
The N stages for lung cancer are

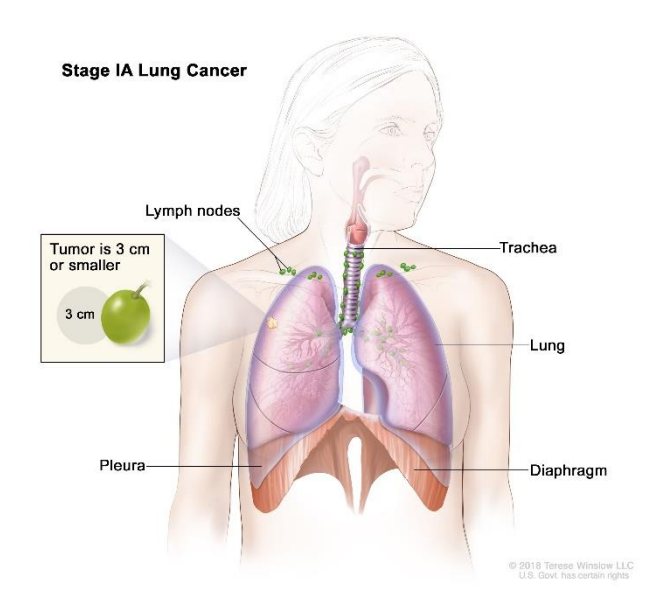
- NO there is no cancer in any lymph nodes
- N1 there is cancer in the lymph nodes nearest the affected lung
- N2 there is cancer in lymph nodes in the mediastinum but on the same side as the affected lung or there is cancer in lymph nodes just under where the windpipe branches off to each lung
- N3 there is cancer in lymph nodes on the opposite side of the chest from the affected lung or in the lymph nodes above either collar bone or the lymph nodes at the top of the lung

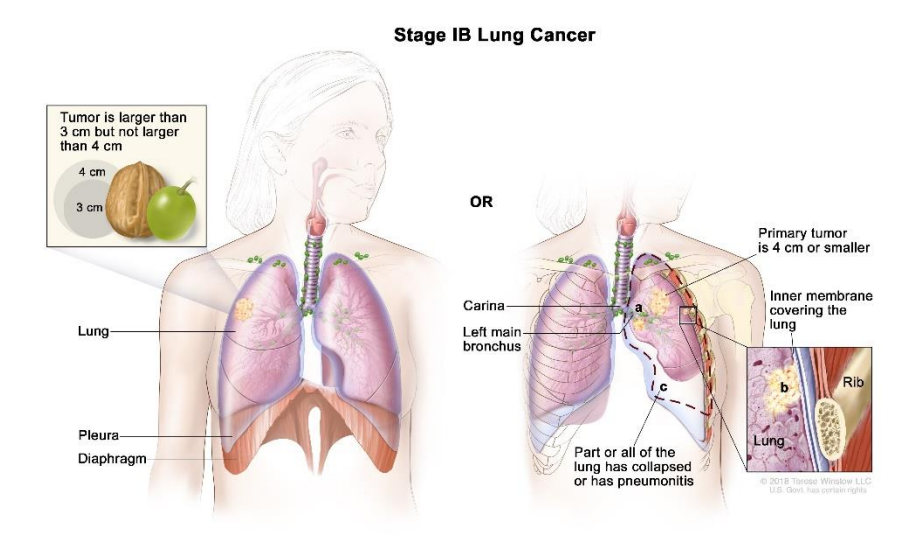
Metastases (M)

The M stages for lung cancer are

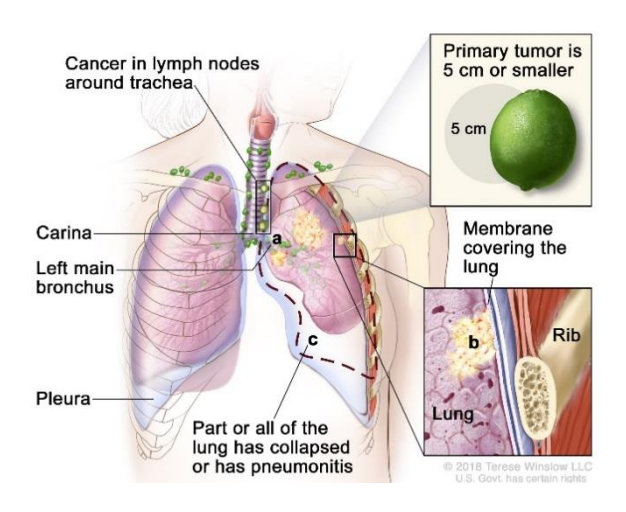
- M0 there are no signs that the cancer has spread to another lobe of the lung or any other part of the body
- M1 there are signs that the cancer has spread to another lobe of the lung or any other part of the body

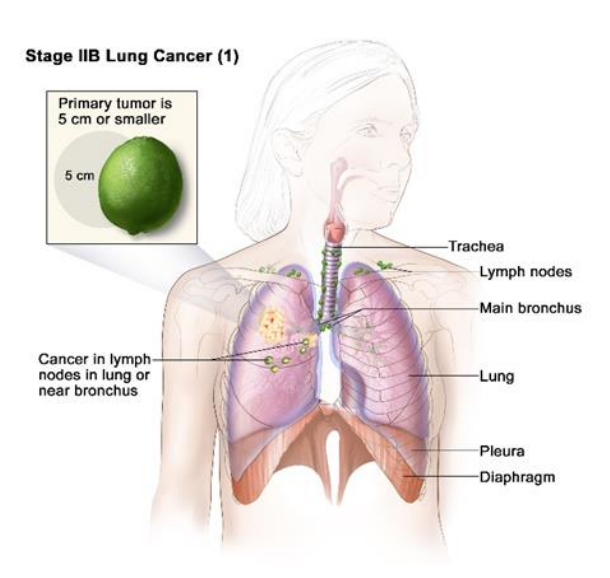


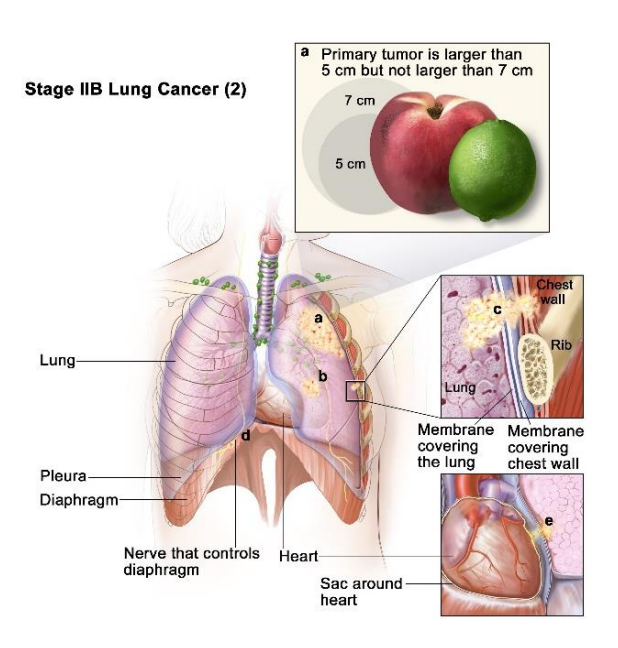


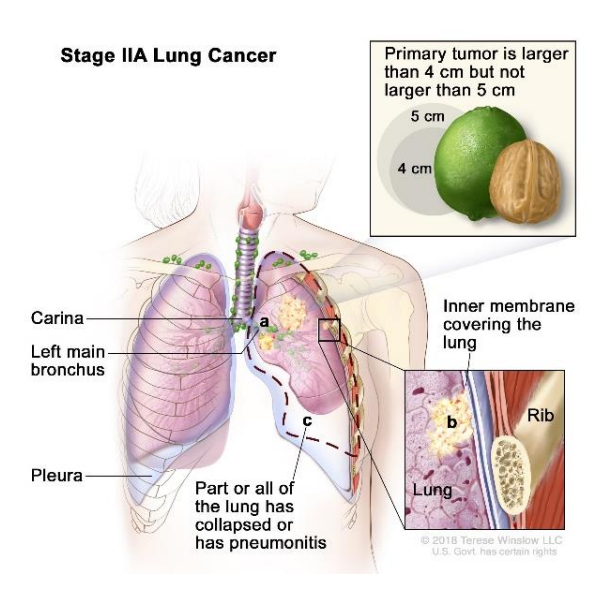


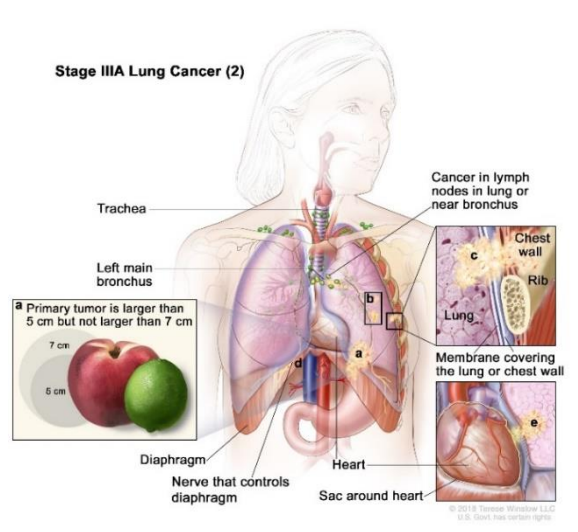
Stage IIIA Lung Cancer (1)



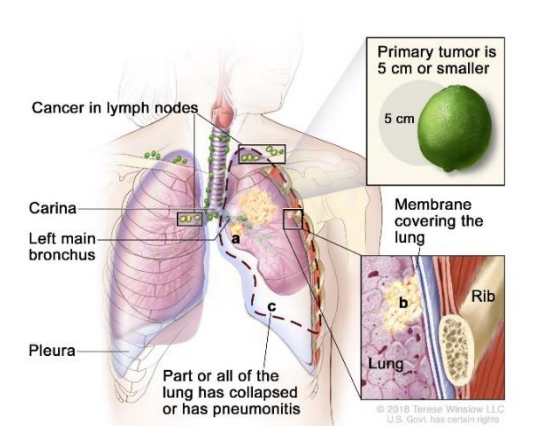


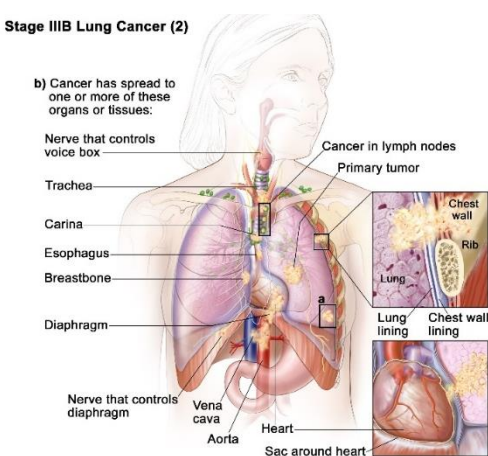






Stage IIIB Lung Cancer (1)





STAGE 1

The cancer is small (no larger than 3 cm for stage 1A; up to 5cm for stage 1B) and has not spread to the lymph nodes.

STAGE 3A

The cancer has started to extend into surrounding tissues and structures, such as the lining of the lung and chest wall and has spread to lymph nodes on the same side of the chest as the tumor.

STAGE 2

The tumor is up to 7 cm in diameter and may have spread to nearby lymph nodes

STAGE 3B

Two or more tumors are present, and the cancer has spread to the lung and lymph nodes on the opposite side of the chest.

STAGE 4

The cancer has spread to form new tumors in other parts of the body, such as the bone, brain, liver and adrenal gland.

Fig. 11. Stages of Lung Cancer

1.6 Lung cancer incidence and mortality

According to GLOBOCON 2012, an estimated 14.1 million new cancer cases and 8.2 million cancer-related deaths occur in 2012, compared with 12.7 million and 7.6 million, respectively, in 2008. The most commonly diagnosed cancer worldwide was those of the lung (1.8 million, 13.0% of the total), breast (1.7 million, 11.9%), and colorectal (1.4 million, 9.7%). The most common cancer deaths are lung cancer (1.6 million, 19.4% of the total), liver (0.8 million, 9.1%), and stomach (0.7 million, 8.8%). Projections based on the GLOBOCON 2012 estimates predict an applicable increase to 19.3 million new cancer cases per year by 2025, due to the growth and aging of the global population.

In India, lung cancer is the fifth most common cancer. According to GLOBOCON 2008, India showed 47,010 new lung cancer cases among males and 11,557 of females affected by lung cancer. The report further showed 41,865 deaths due to lung cancer among males and 10,040 death among females. The age-standardized incidence/100,000 is reported to be 10.9 for males and 2.5 for females in India [23, 24]. The recent report of GLOBOCON 2018 in India, showed 48, 698 new lung cancer cases of males and 19,097 of females affected by lung cancer. The further report showed that 45, 363 deaths among males and 18, 112 death among females. The most common cancer cases are lung cancer 67,795 death rate should be attained 63,475 nearby to the cancer cases [25].

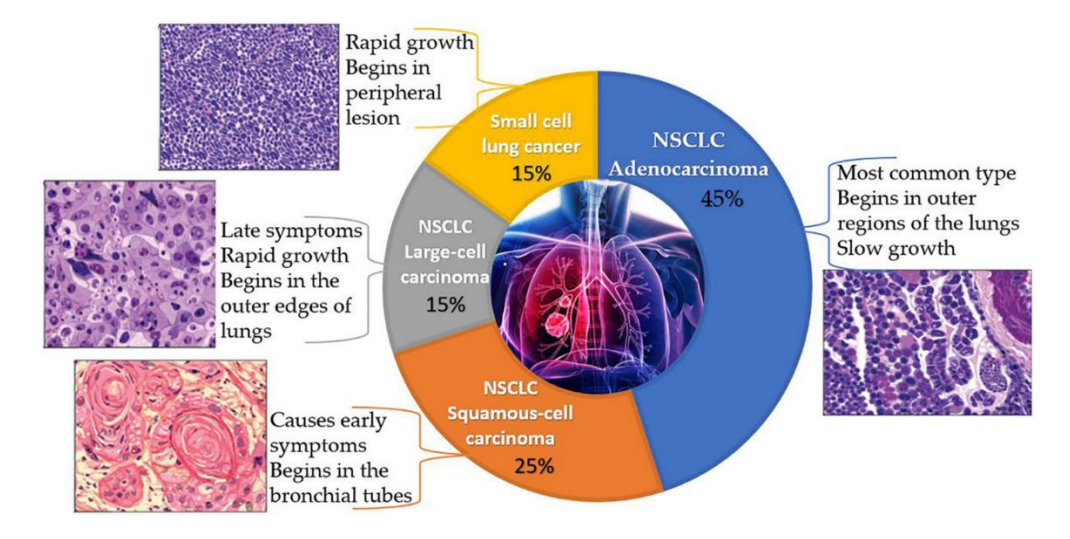
Lung cancer	New cases	Death
Men	48,698	45,363
Women	19, 97	18,112
Both Sexes	67,795	63,475

The mean age for getting lung cancer: 54.6 years. The majority of lung cancer patients are more than 65 years of age

Males predominate with a Male: Female ratio of 4.5:1 and this ratio varies with age and smoking status.

The ratio increases progressively up to 51-60 years and then remains the same.

The smoker to non-smoker ratio is high up to 20:1 in various studies.



Flow chart represents the types of carcinomas affected by Lung cancer

1.7 What are the Risk factors for Lung cancer?

The burning of a tobacco cigarette produces multiple chemical compounds that are released through mainstream smoke, which is inhaled by the smoker, and through side stream smoke, which is the smoke that is given off by the burning cigarette. Second-hand smoke, which is a combination of side stream smoke and the mainstream smoke that is exhaled by the smoker, has been demonstrated by several scientific studies to cause disease. Among 40 chemicals in side stream smoke have been identified that negatively impact human health, leading to the development of cancer or other conditions, such as immune system dysfunction, liver toxicity, cardiac arrhythmias, pulmonary edema, and neurological dysfunction (**Fig. 12**). Moreover, second-hand smoke has been found to anchorage at least 250 compounds that are known to be toxic, carcinogenic or both. Some major classes of

carcinogens in second-hand smoke are polyaromatic hydrocarbons (PAHs), N-nitrosamines, aromatic amines, formaldehyde, and acetaldehyde.

Tobacco and second-hand smoke are considered to be carcinogenic. Exposure to second-hand smoke can cause lung cancer in individuals who are not tobacco users themselves. It is estimated that the risk of developing lung cancer is increased by up to 30 percent in non-smokers who live with an individual who smokes in the house, as compared to non-smokers who are not regularly exposed to second-hand smoke. Children are especially affected by second-hand smoke. Children who live with an individual who smokes inside the home have a larger number of lower respiratory infections, which are associated with hospitalizations, and a higher risk of sudden infant death syndrome (SIDS). Second-hand smoke in the home has also been linked to a greater number of ear infections in children, as well as worsening symptoms of asthma [26].

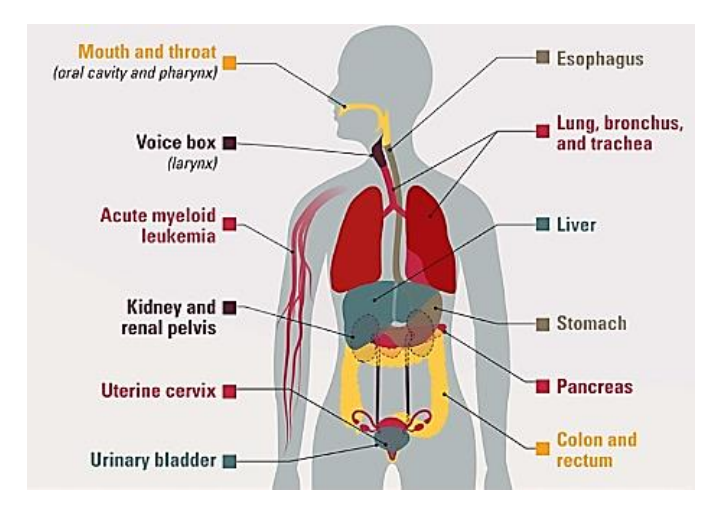


Fig. 12. Tobacco use causes cancer throughout the body

1.8 Treatments of Lung cancer

The most commonly available treatments depend on the lung cancer stages and other patient-related and disease-related characters. The treatments are different for small cell lung cancer and non-small cell lung cancer. Small cell lung cancer is typically treated with chemotherapy. Surgery is only suitable if there is no sign that the cancer has spread to the

lymph glands in the center of the chest. This is rare with small cell lung cancer. It has usually spread at the time of diagnosis. So, chemotherapy is usually the main treatment. Non-small cell lung cancer can be treated with surgery, chemotherapy, radiotherapy or a combination of these, depending on the stage when the cancer is diagnosed. Some people with advanced lung cancer may have biological therapy (**Fig. 13**) [27, 28]. There are endless probable chemotherapy agents has been identified to treat lung cancer, due to their poor bioavailability, drug-resistant and low therapeutic index lung cancer seems to be one of the most elusive diseases in the worldwide [29]. Hence, active researches are needed to overcome the problem with the currently available chemotherapy agents.

FDA APPROVES IMMUNOTHERAPY-BASED DRUG FOR LUNG CANCER TREATMENT

The drug pembrolizumab, marketed as Keytruda, underwent 4 years of testing before receiving first-line approval for the treatment of non-small cell lung cancer (NSCLC). Keytruda is an immunotherapy-based drug, in contrast to older classes of drugs called signal-transduction inhibitors.

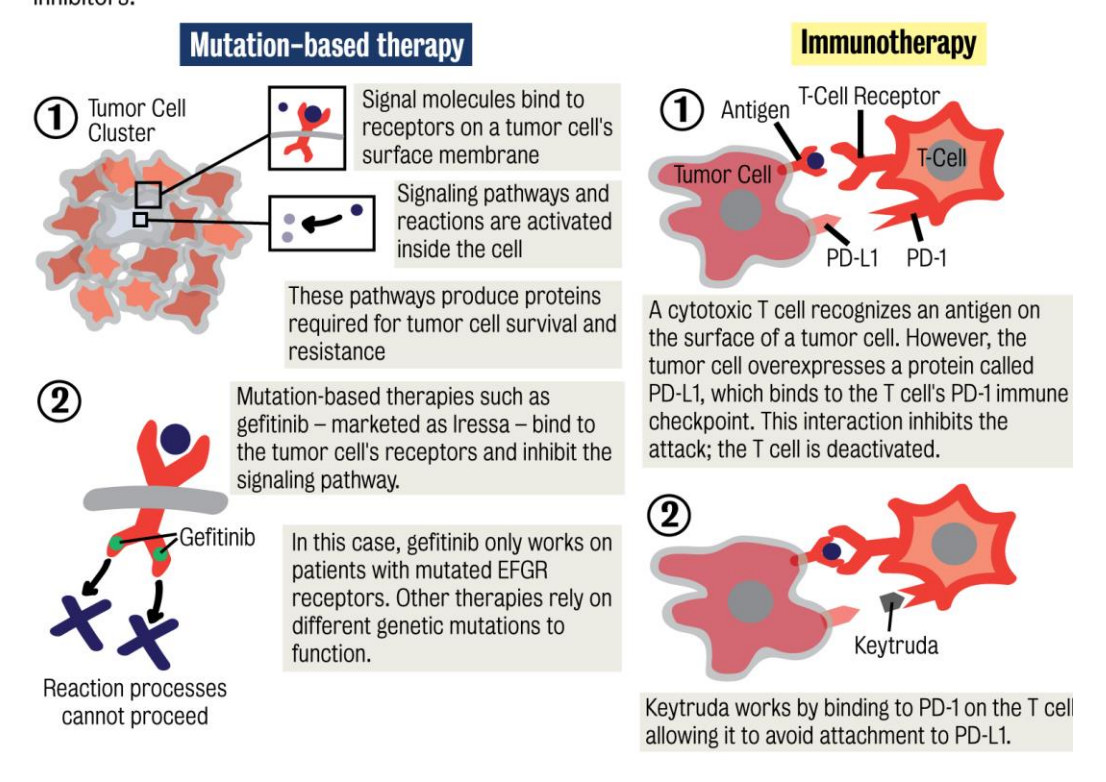


Fig.13. Treatment for Lung cancer

1.9 Epigenetics

Epigenetics is the learning of biological mechanisms that will switch genes on and off, to be put as a beginner's definition. Cells are essential working units of every human being. All the instructions required to direct their activities are contained within the chemical deoxyribonucleic acid, also known as DNA. DNA from humans is made up of approximately 3 billion nucleotide bases. Four fundamental types of bases comprise DNA – adenine, cytosine, guanine, and thymine, commonly abbreviated as A, C, G, and T, respectively.

1.9.1 Epigenetics mechanisms in normal cells

Chromatin is made of repeating units of nucleosomes, which consist of ~146 base pairs of DNA wrapped around an octamer of four core histone proteins (H3, H4, H2A, and H2B) [30]. Epigenetic mechanisms that modify the chromatin structure can be sub-divided into four main classes namely: DNA methylation, covalent histone modifications, non-covalent mechanisms such as the incorporation of histone variants and nucleosome remodelling and non-coding RNAs including microRNAs (miRNAs). These changes regulate the activity of the genome by altering the local structural dynamics of chromatin, primarily regulating its accessibility and firmness. The relationship of these modifications generates an 'epigenetic landscape' that regulates the way the mammalian genome displays itself in different cell types, developmental stages and disease states, including cancer [31-33]. Here, we will discuss about the important key features of the epigenetic mechanisms present in normal cells (Fig. 14) [34]. In contrast, the epigenome of differentiated tissue displays a relatively restricted structure that is stably maintained through multiple cell divisions.

DNA methylation

All cell types

Stable heritable modification

Gene silencing

Chromatin organization

Imprinting, X-chromosome inactivation, silencing of repetitive elements Mediated by DNMTs

ES cells

Bimodal distribution pattern

Global CpG methylation

CpG islands unmethylated

Pluripotency gene promoters unmethylated

Somatic cells

Tissue-specific methylation of some CpG islands and most non-CpG island promoters

Pluripotency gene promoters methylated

Covalent histone modifications

All cell types

Labile heritable modification

Both gene silencing (H3K9me, H3K27me etc.) and gene activation (H3K4me, acetylation etc.)

Specific distribution patterns of histone marks contribute to chromatin organization

Mediated by HMTs, HDMs, HATs and HDACs etc.

ES cells

Bivalent domains—coexistence of active and repressive marks (H3K4me and H3K27me) at promoters of developmentally important genes

Plastic epigenome

Somatic cells

Loss of bivalency and restricted epigenome

Establishment of tissue-specific monovalent H3K27me and H3K4me domains

Presence of large organized chromatin K9 modifications

Nucleosome positioning and histone variants

All cell types

Labile epigenetic regulatory mechanism

Both gene silencing and gene activation by modulating chromatin accessibility

Mediated by ATP-dependent chromatin-remodeling complexes

Both sliding of existing and incorporation of new nucleosomes

H2A.Z and H3.3 preferentially localized to gene promoters that are active or poised for activation

Acetylated H2A.Z associates with euchromatin and ubiquitylated H2A.Z with facultative heterochromatin

miRNAs

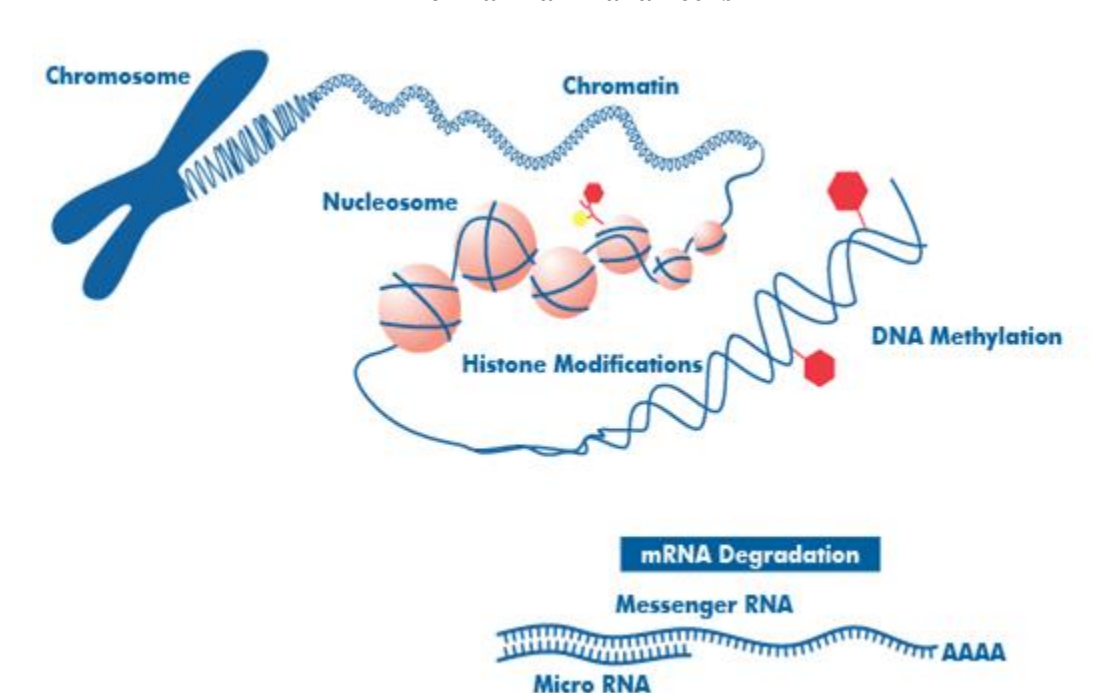
All cell types

Labile epigenetic regulatory mechanism

Gene silencing

Tissue-specific expression

Can be epigenetically regulated



Epigenetic mechanisms involved in regulating gene expression and chromatin structure in normal mammalian cells

Fig .14. Mechanism of Epigenetics

1.9.2 Epigenetics in Cancer

Epigenetic mechanisms are crucial for normal development and maintenance of tissue-specific gene expression patterns in mammals. The disorder of epigenetic processes can lead to altered gene function and malignant cellular transformation. Global changes in the epigenetic landscape are a "hallmark of cancer". The latest developments in the rapidly growing field of cancer epigenetics have shown extensive reprogramming of every component of the epigenetic machinery in cancer including DNA methylation, histone modifications, nucleosome positioning, and non-coding RNAs, specifically microRNA expression. The complement of these modifications collectively referred to as the epigenome provides a mechanism for cellular diversity by regulating what genetic information can be accessed by cellular machinery. Failure of the proper maintenance of heritable epigenetic marks can result in inappropriate activation or inhibition of various

signalling pathways and lead to disease states such as cancer. The reversible nature of epigenetic aberrations has led to the development of the auspicious field of epigenetic therapy, which is already making progress with the recent FDA approval of three epigenetic drugs for cancer treatment [35, 36].

Recent developments in the field of epigenetics have exposed that human cancer cells harbor global epigenetic abnormalities, in addition to numerous genetic alterations [35, 37]. These genetic and epigenetic alterations interact at all stages of cancer development, working together to promote cancer progression [38]. The genetic origin of cancer is generally accepted; but, recent studies suggest that epigenetic alterations may be the key initiating events in some forms of cancer [38]. These definitions have led to an overall resourcefulness to understand the role of epigenetics in the initiation and propagation of cancer [39].

1.9.3 Aberrant reprogramming of the epigenome in cancer

The exact epigenomic landscape present in normal cells endures general distortion in cancer [37]. These epimutations, along with extensive genetic alterations, play a significant role in cancer initiation and progression [37]. Epimutations can lead to the silencing of tumor suppressor genes autonomously and also in aggregation with deleterious genetic mutations or deletions; thus, serving as the second hit required for cancer initiation conferring to the 'two-hit' model suggested by Alfred Knudson [38]. Meanwhile, epigenetic alterations, like genetic mutations, are mitotically heritable, they are selected for in a rapidly growing cancer cell population and converse a growth advantage to tumor cells resulting in their uncontrolled growth (Fig. 15).

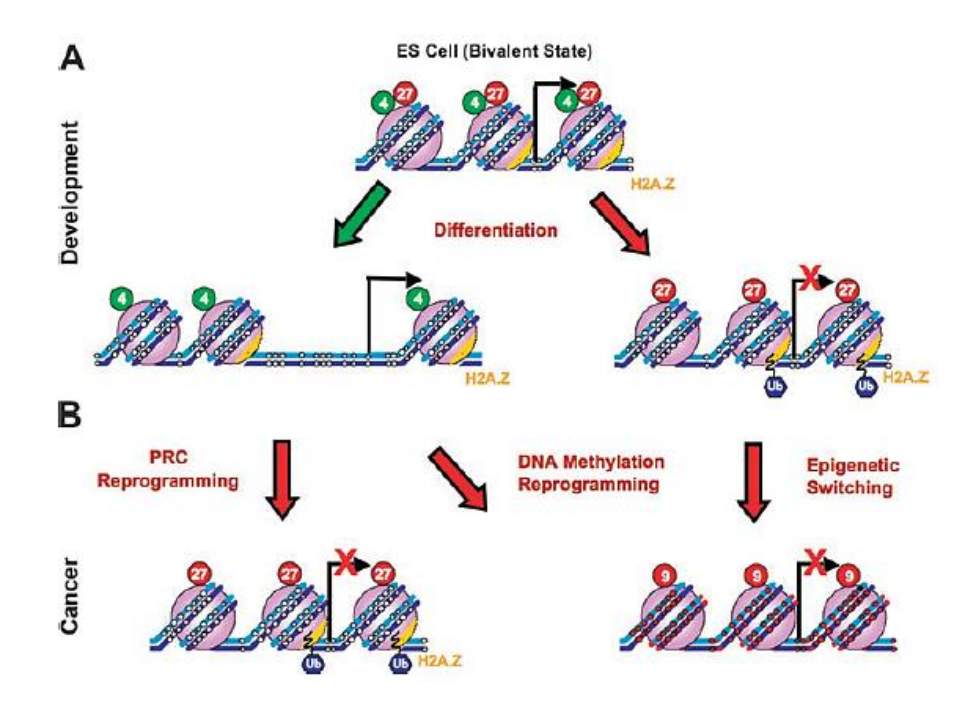


Fig.15. Reprogramming of the epigenome during development and tumorigenesis. (A) In ES cells, developmentally important genes are marked by a unique 'bivalent domain' structure, consisting of the active H3K4 methylation (green circles, 4) and repressive H3K27 methylation (red circles, 27) marks together with H2A.Z. Such bivalent domains are important for maintaining epigenomic plasticity that is required during development. During differentiation, the bivalent domains are lost, giving way to the establishment of a more rigid 'monovalent domain' structure that is either active (indicated by the green arrow) or repressive (indicated by the red arrow) depending upon which mark is maintained. (B) In cancer, cells undergo aberrant somatic reprogramming that results in gene silencing through the formation of a compact chromatin structure. Silencing can occur through PRC (Polycomb Repressive Complex) reprogramming-silencing of active genes by the polycomb group; DNA methylation reprogramming-silencing through de novo hypermethylation (small red circles on DNA strands) accompanied by H3K9 methylation (red circles, 9) or epigenetic switching replacement of gene repression by the polycomb mark with long-term silencing through DNA methylation; Ub, ubiquitination.

1.9.4 DNA methylation aberrations in cancer

Cancer initiation and progression are accompanied by intense changes in DNA methylation that were the first epigenetic alterations notorious in cancer [40, 41]. A cancer epigenome is manifest by genome-wide hypomethylation and site-specific CpG island promoter hypermethylation (**Fig. 16**) [36]. Whereas the underlying mechanisms that initiate these global changes are still under investigation, recent studies indicate that some changes

occur very early in cancer development and may contribute to cancer initiation [39]. Global DNA hypomethylation plays a significant role in tumorigenesis at various genomic sequences including repetitive elements, retrotransposons, CpG poor promoters, introns and gene deserts [42]. DNA hypomethylation at repeat sequences leads to increased genomic instability by promoting chromosomal rearrangements [36, 43]. Loss of DNA methylation and genomic instability is concerned with a variety of human cancers [44].

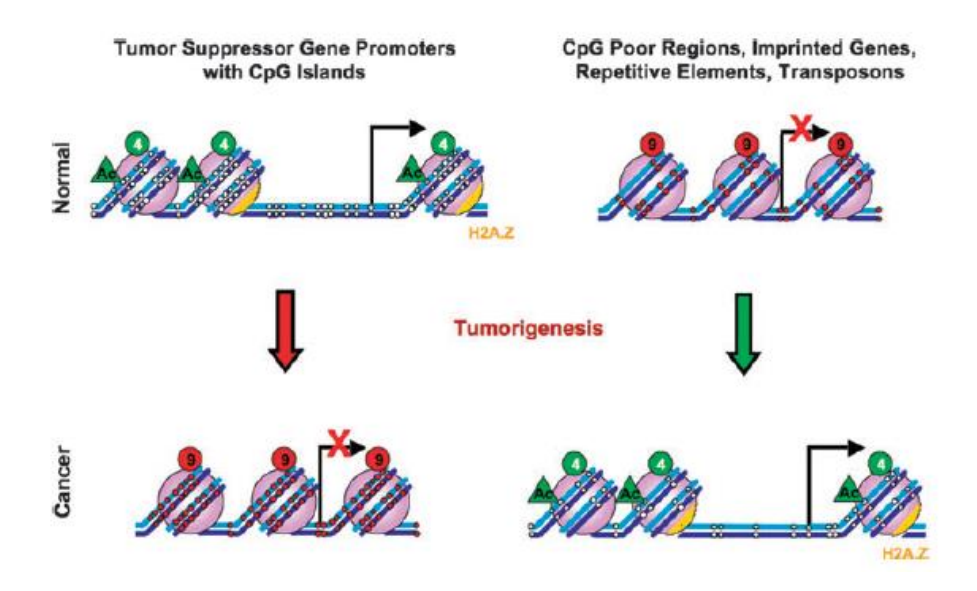


Fig. 16. DNA methylation changes in cancer

1.9.5 Histone modification

Histone modification is a covalent post-translational modification (PTM) to histone proteins which includes methylation, phosphorylation, acetylation, ubiquitination, and sumoylation [45]. The PTMs of histones can impact gene expression by altering chromatin structure or recruiting histone modifiers. Histone proteins act to package DNA, which wraps around the eight histones into chromosomes. Histone modification acts in the diverse biological process such as transcriptional activation/repression, chromosome packaging, and DNA damage/repair.

In most species, histone H3 is primarily acetylated at lysine 9, 14, 18, 23 and 56 methylated at arginine 2 and lysine 4, 9, 27, 36 and 79 phosphorylated Ser10, Ser28, Thr3, and Thr11. Histone 4 is primarily acetylated at lysine 5, 8, 12 and 16 methylated at arginine 3 and lysine 20 and phosphorylated at serine 1. Thus, quantitative detection of various histone modifications would provide useful information for a better understanding of epigenetic regulation of cellular process and the development of histone-modifying enzymetargeted drugs. The complement of modifications is proposed to store the epigenetic memory inside a cell in the form of a "histone code" that determines the structure and activity of different chromatin regions [46].

1.9.6 Acetylation

Eukaryotic DNA is packed into chromatin by histone proteins, which assemble the DNA into an organized, higher-order structure. The precise organization of chromatin is essential for the faithful execution of DNA-mediated reactions such as transcription, DNA repair, and DNA recombination. The organization of chromatin is considered to be regulated by a variety of post-transcriptional modifications of histones. Histone acetylation is important in the regulation of gene expression and is normally associated with transcriptionally active gene-dense regions, referred to as euchromatin [47]. Histone acetylation can be transient and must be maintained by enzymatic activity. Histone acetyltransferases (HAT) transfer the acetyl group (COCH₃) from acetyl coenzyme A to lysine residues. Equally, Histone deacetylase (HDAC) removes the acetyl groups. Both HAT and HDAC are also able to modify a large variety of non-histone proteins whose activity depends on their acetylation status, such as transcription factors, chaperone proteins, signal transduction mediators, structural proteins and inflammation mediators [48]. In general, HAT can modify more than one lysine residues but some limited specificity has been detected (Fig. 17).

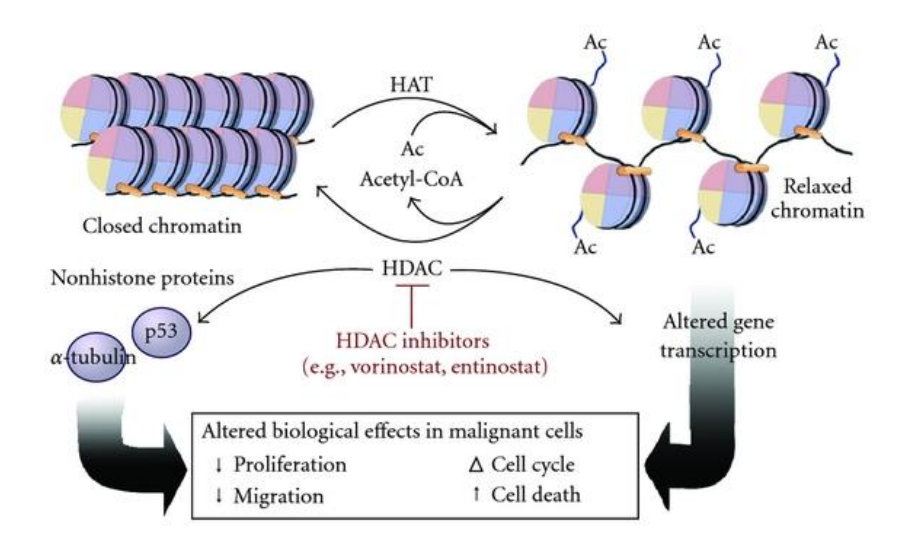


Fig.17. Histone acetylation and deacetylation

1.9.7 Methylation

Histone methylation is a process by which methyl groups are transferred to amino acids of histone proteins that make up nucleosomes, which the DNA double helix wraps around to form chromosomes. Histone methylation causes transcription repression or activation, depending on the target sites [49]. Histone methyltransferases (HMT) control or regulate DNA methylation through chromatin-dependent transcription repression or activation. The methylation of lysine in histones by specific histone methylation is also implicated in changes in chromatin structure and gene regulation. The methylation of lysine-4 in histone-3 is associated with an open chromatin configuration and gene expression. On the other hand, methylation of lysine-9 in histone-3 is associated with condensed and repressive chromatin [50]. This histone modification and the acetylation/deacetylation of histones to influence gene expression are called the histone code.

1.9.8 Phosphorylation

Phosphorylation is best known for its role in the cellular response to DNA damage. However, it also has crucial roles in chromatin remodelling linked to another nuclear process such as transcription regulation and chromatin condensation associated with mitosis, meiosis, and apoptosis [51]. Histone phosphorylation can occur on serine, threonine and tyrosine residues. All four nucleosomal histone tails contain acceptor sites that can be phosphorylated by several protein kinases and dephosphorylated by phosphatases.

1.9.9 Ubiquitination

Ubiquitination is a very large modification found on histones H2A and H2B and it's associated with either transcriptional repression or activation. Because histones are the most abundant ubiquitinated proteins, this modification has a critical role in many processes in the nucleus, including transcription, maintenance of chromatin structure and DNA repair. Conversely, its specification functions are still less well understood than other histone modifications such as methylation and acetylation [52].

1.9.10 Sumoylation

Sumoylation is also a very large modification that has been shown to take place on all four core histones, antagonizing both acetylation and ubiquitination, which occur on the same Lysine residues. In humans, there are four small ubiquitin-like modifiers (SUMO) isoforms (SUMO-1 to 4) encoded by different genes. Although SUMO proteins are associated with transcriptional regulation, recent work using Hela cells showed that a relatively high percentage of the most active genes (49%) had their promotors modified with bound SUMO-1 [53].

1.9.11 Changes in histone modifications in cancer

Recent developments in high-throughput sequencing have empowered the genome-wide mapping of chromatin changes occurring during tumorigenesis. From these studies revealed that a global loss of acetylated H4- lysine 16 (H4K16ac) and H4-lysine 20 trimethylation (H4K20me3) [52]. Such loss of histone acetylation, which is facilitated by

HDACs, results in gene repression. HDACs are habitually found overexpressed in various types of cancer [54, 55]. HATs, which work in concert with HDACs to maintain histone acetylation levels, can also be altered in cancer. Mistargeting of such deleterious fusion proteins contributes to global alterations in histone acetylation patterns in cancer. In addition to changes in histone acetylation, cancer cells also show widespread changes in histone methylation patterns. Alterations in H3K9 and H3K27 methylation patterns are associated with aberrant gene silencing in various forms of cancer [56, 57]. Dysregulation of HMTs responsible for repressive marks results in the altered distribution of these marks in cancer and leads to aberrant silencing of tumor suppressor genes. Besides histones, HAT and HDACs also target non-histone proteins including a variety of transcription factors, cell cycle proteins and in doing so have a major impact on the control cell fate. The inactivation of HATs and aberrant HDACs activity is closely associated with the development of the transformed state of human tumors, due to transcriptional repression of tumor suppressor genes and activation of oncogenes [58-62] (Fig. 18).

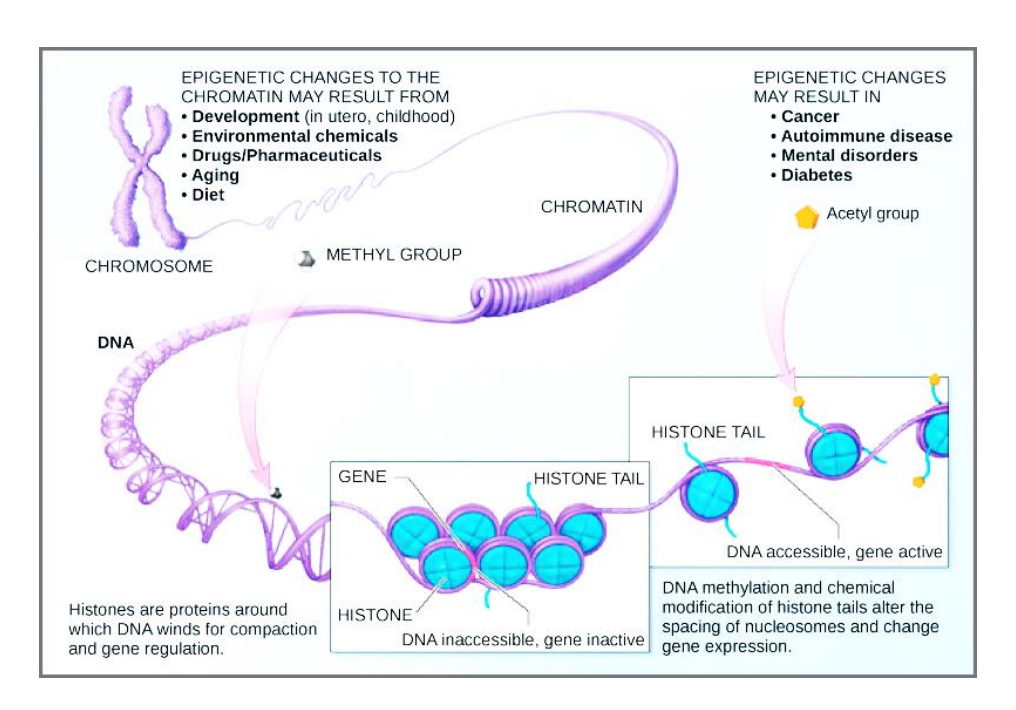


Fig. 18. Schematic representation of the modifications affect nucleosome spacing and gene expression.

1.10 Histone acetyltransferases

Histone acetyltransferase (HAT) is that acetylate conserved lysine residuals on histone proteins by transferring an acetyl group from acetyl CoA to form ϵ -N-acetyl-lysine. This modification neutralizes the positive charge of lysine and may thus disrupt the interaction between DNA and histone tails. HATs are traditionally divided into two different classes based on their subcellular localization [63]. Acetylated histones are generally associated with euchromatin and transcriptional activation. In contrast to histone acetylation, deacetylation restricts DNA accessibility through the positive charge of the lysine, permitting interaction between DNA and the histone tails and thus chromatin compaction.

1.11 Histone deacetylases

Histone deacetylases (HDAC) play a major role in the epigenetic regulation of gene expression through their effects on the compact chromatin structure [64]. Histone deacetylases are the class of enzymes involved in many biological pathways and one of their best-known properties is their ability to remove acetyl groups from the lysine residues on amino-terminal histone tails allowing the histones to wrap the DNA more tightly. The reversible deacetylation of core histone residues is normally associated with transcriptional termination. This is not surprising considering that histone acetylation is often associated with transcriptional activation and HAT and HDACs have contrary functions [65]. These enzymes exist in dynamic equilibrium within the cell and the acetylation status of histones and non-histone proteins is governed by the opposing actions of these enzymes. Similar to HATs, historically it was hypothesized that HDACs functioned by relieving the positively charged lysine residues of the negatively charged acetyl moiety. The restoration of positively charged lysine residues within the histone tails was thought to result in increased nucleosome-nucleosome and nucleosome-DNA interactions so "closing" the chromatin and

preventing access to co-activators [66]. Undeniably, it has been demonstrated that non-acetylated histone residues promote the association of repressors [67].

There are two protein families with HDAC activity: the recently discovered SIR2 family of NAD+-dependent HDACs, and the classical HDAC family. Members of the classical HDAC family fall into two different phylogenetic classes, namely class I and class II. The class I HDACs (HDAC1, 2, 3 and 8) are most closely related to the yeast transcriptional regulator RPD3. Class II HDACs (HDAC4, 5, 6, 7, 9 and 10) share domains with similarity to HDA1, another deacetylase found in yeast. Recently a new member of the HDAC family has been identified, HDAC11. This protein contains all the necessary features to be designated as an HDAC, and although it is tempting to conclude from that HDAC11 is most closely related to the class I HDACs, no classification of HDAC11 to class I, II or the SIR2 family could be made since the overall sequence similarity is too low. Currently, it is thought that HDACs of class I are expressed in most cell types, whereas the expression pattern of class II HDACs is more restricted suggesting that they might be involved in cellular differentiation and developmental processes [68].

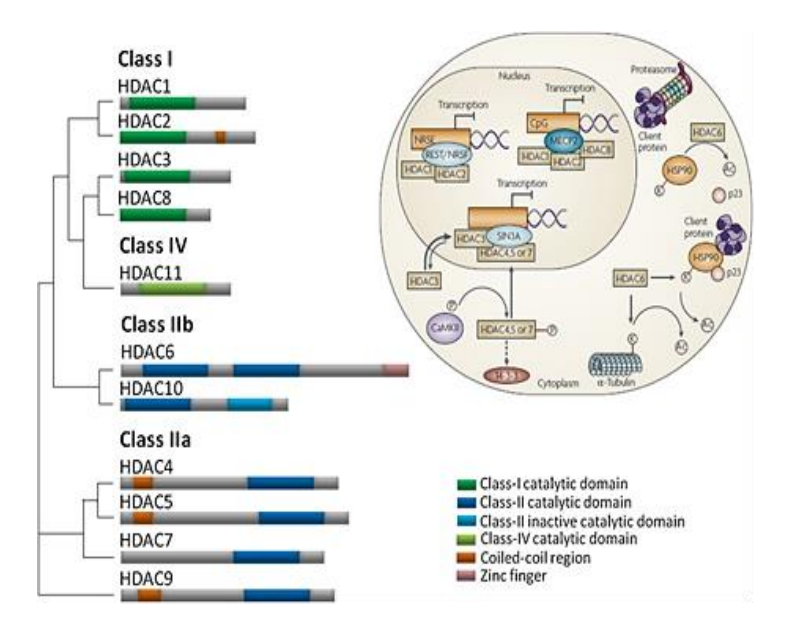
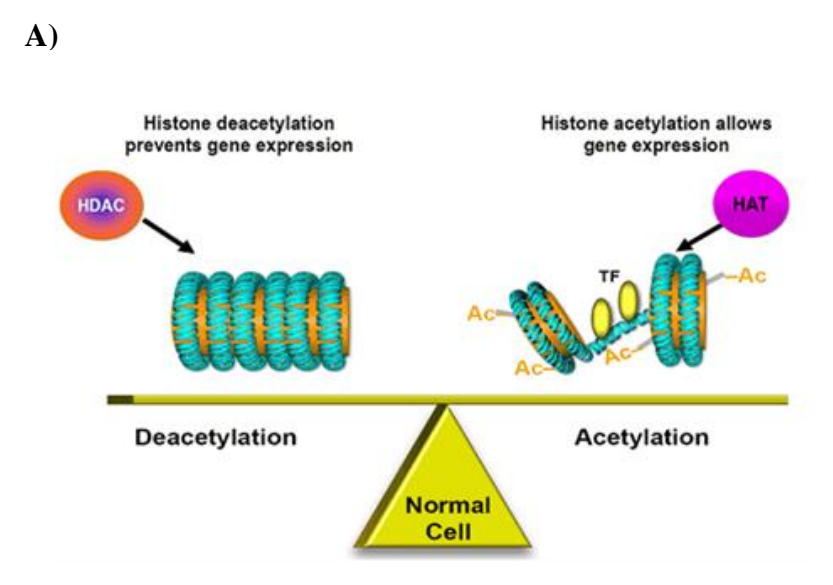


Fig.19. Classification, structures and cellular localization of Zn²⁺ dependent histone deacetylase isoforms

1.11.1 Mechanism of Histone deacetylase

Acetylation and deacetylation of histones provide a balance between an open conformation and a closed chromatin conformation for the regulation of transcription. This regulation is complex but is principally regulated by the HAT. HDAC is part of a vast family of enzymes that have a crucial role in numerous biological processes, largely through their repressive influence on transcription. Contrarily, the re-establishment of the positive charge in N-terminal tails of core histones catalyzed by HDACs is thought to tighten the interaction between histones and DNA, leading to chromatin condensation and transcriptional repression [69]. Besides histones, HAT and HDACs also target non-histone proteins including a variety of transcription factors, cell cycle proteins and in doing so have a major impact on the control of cell fate. The inactivation of HATs and aberrant HDACs activity is closely associated with the development of the transformed state of human tumors (Fig. 20).



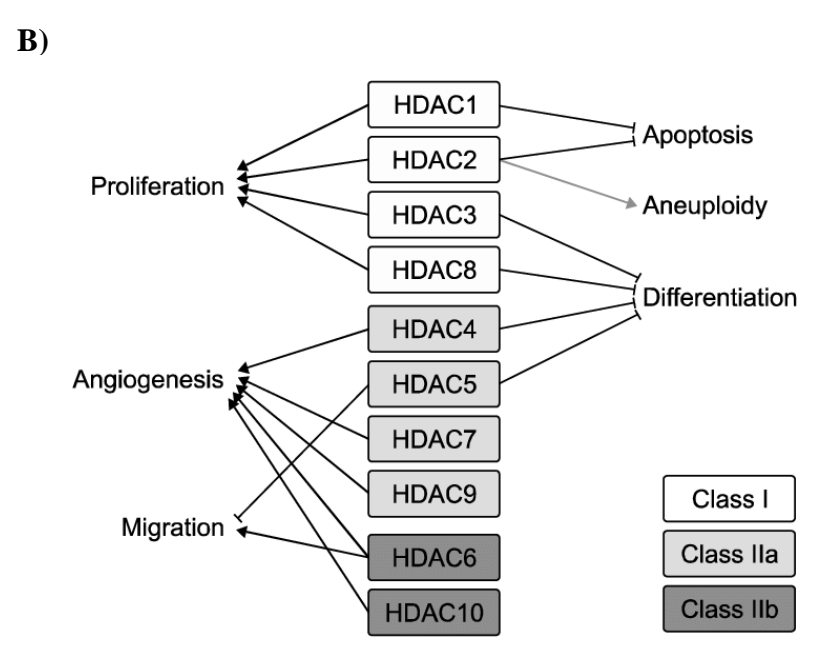


Fig. 20. A) A balance between normal cell level in HDAC and HAT. B) The Role of HDACs in cancer biology.

1.11.2 Expression of histone deacetylase in cancer cells

The significant roles of HATs and HDACs, their function is strictly regulated by modulation of protein amount, enzyme activity and availability for interaction with specific transcription factors [70]. Aberrant expression and/or mutations of HATs and HDACs have been described in a variety of human cancers [71]. For example, deletions, translocations and point mutations in the P³⁰⁰, PCAF and CBP genes have been detected in colorectal cancer [72]. HDAC-1 has been described to be overexpressed in hormone refractory prostrate, gastric, colon and breast cancer as well as oesophageal squamous cell carcinomas [73, 74]. Also, HDAC-2 overexpression is observed in colorectal, cervical and gastric cancer [71] and overexpression of HDAC-6 has been observed in breast cancer [75].

1.11.3 An emerging as a Histone Deacetylase enzyme (Inhibitors) in Cancer Treatment

Given these insights into the function of HDACs, it is not surprising that HDAC inhibitors (HDACi) are emerging as promising new agents for cancer therapy. HDACi are

a new class of antineoplastic agents that were originally recognized by their capacity to reverse the transformed phenotype [76]. For them, their anticancer activities were observed in pre-clinical studies of a broad range of different cancer cell lines both *in-vitro* and *in-vivo* (lung, thyroid, breast, pancreatic, colon and ovarian cancer) [77]. By blocking the activity of HDACs, restore the expression of some tumor suppression genes, induce cell differentiation, growth arrest and apoptosis of tumors cells [78, 79]. HDACi is preferentially cytotoxic for tumor cells, whereas normal cells are 10-fold or more resistant [80].

Moreover, many HDACi have been enhanced their anticancer activity while combining with a large number of traditional chemotherapeutic drugs such as vincristine and epotoside, DNA methyltransferases inhibitors and also other therapeutic regimens such as TRAIL [81, 83]. Because of a generally low toxicity and an impressive efficiency in preclinical cancer models. Several HDACi are currently in clinical trials as a single agent or combination with other therapeutic agents for the treatment of both solid and haematological malignancies [84, 85].

1.11.4 Mechanism of histone deacetylase inhibitor in signalling pathways

HDACi can induce tumor cell apoptosis, growth arrest, senescence, differentiation, and immunogenicity and inhibit angiogenesis as shown in (Fig. 21). Almost, the biological effects and the therapeutic outcomes will depend on the genetic lesions driving the tumor of interest and the HDACi under investigation. While HDACi were historically identified based on their ability to induce tumor cell differentiation, induction of tumor cell apoptosis is the biological outcome most often reported [79]. However, divergent views exist regarding the importance of the intrinsic apoptotic pathway mediated by the interplay between proapoptotic and anti-apoptotic Bcl-2 family proteins [86]. There is a link between altered gene expression and the induction of apoptosis, with histone hyperacetylation observed at promoters of apoptosis-inducing genes such as TRAIL, proapoptotic Bcl-2

family member Bcl-2 modifying factor (BMF) and changes in the activity of transcription factors due to acetylation, such as inhibition of SP1 and C/EBP α , leading to down-regulation of the antiapoptotic protein Bcl-2 [87], following HDACi treatment. It is therefore likely that both the threshold of apoptosis induction and the mechanism by which death can be triggered by HDACi is determined by the interaction between the oncogenic lesions and the intrinsic apoptosis signalling pathways active within each cell.

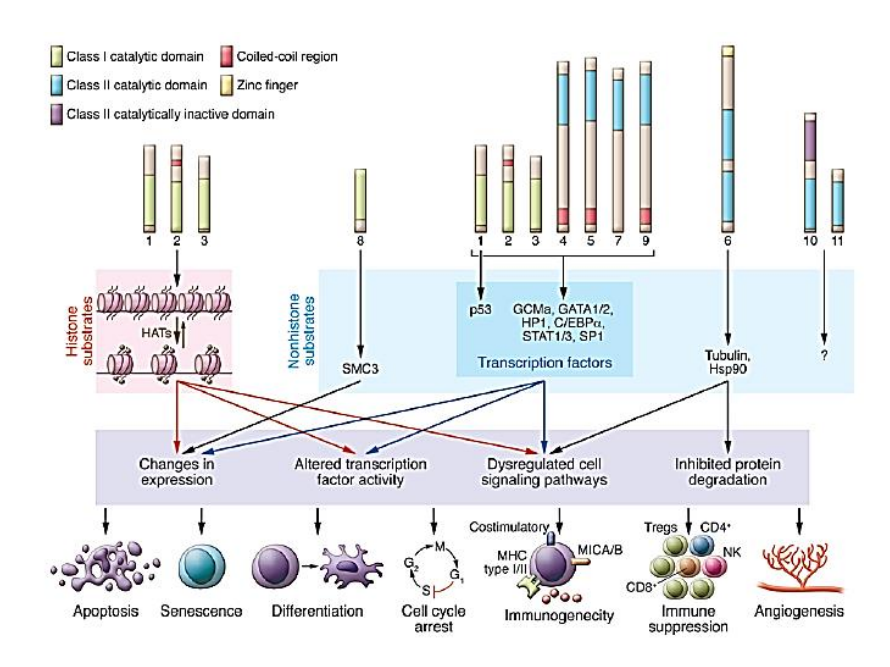


Fig.21. The molecular targets of HDACs, downstream cellular pathways, and anticancer outcomes of HDAC inhibition.

1.11.5 Classification of histone deacetylase inhibitors

More than 80 novel HDACi and their analogues have been purified as natural products or synthetic compounds which can be divided into six groups including hydroxamic acids, short-chain fatty acids, cyclic peptides, ketones, benzamides and miscellaneous compounds [88]. Although structurally different, all HDACi's contain a surface recognition site, the metal-binding domain that interacts with the Zn²⁺ and a linker domain. Different HDACi inhibit Class-I and Class II HDACs activity by directly chelating the Zn2+ ion the cofactor of the enzymes (Table 2) [89].

Tradename	Chemical names	FDA approved indication	Classification	Structure	Clincal trials
Zolinza®	Vorinostat SAHA	CTCL	Hydroxamate	The state of the s	Multiple myeloma Mesothelioma Neuroblastoma Glioblastoma Non-Hodgkin lymphoma
Istodax [®]	Romidepsin FK228	CTCL PTCL	Cyclicpeptide	CH ₃ HN S HN O CH ₃ H ₃ C H NH HN O CH ₃ H CH ₃	Multiple myeloma Breast cancer Lymphoma Sarcoma Small cell lung cancer
$\mathbf{Beleodaq}^{\circledR}$	belinostat, PXD101	Multiple melanoma	Hydroxamate	C C C C C C C C C C C C C C C C C C C	CUP Ovarian cancer Hepatocarcinoma Soft tissue sarcoma NSCLC AML and MDS
Farydak [®]	Panobinostat LBH-589	CTCL	Hydroxamate		Multiple myeloma CML Hodgkin's lymphoma Metastatic melanoma Prostat cancer
$\mathbf{Depacon}^{\mathbb{R}}$	Valproic acid	Epilepsy Seizures Bipolar disorder Migraine	Carboxylate	$\label{eq:ch3} \begin{array}{c} \operatorname{CH_3} & - \operatorname{CH_2} & - \operatorname{CH_2} \\ \\ \operatorname{CH_3} & - \operatorname{CH_2} & - \operatorname{CH_2} \\ \end{array}$	Cervical cancer Ovarian cancer Breast cancer AML and MDS Spinal muscular atrophy
On trial	Entinostat MS-275		Benzamide	NH ₂ H N N	Hormone receptor-positive advanced breast cancer Breast cancer Hodgkin's lymphoma NSCLC Colorectal cancer

Table 2. FDA approved HDAC inhibitors are listed by chemical names, indications, classifications, structures, and ongoing clinical trails

Among different HDACi, TSA is the first natural product that has been exposed to possess the HDACi activity, shows generally the highest activity [90]. Another HDACi, depsipeptide (romidepsin), belonging to the cyclic peptides group, is a natural product extracted from *Chromobacetrium violaceum* [91]. Until now more than 20 HDACi have entered clinical studies and to date, four HDACi, vorinostat, Romidepsin, Panobinostat and Belinostat crossed the journey by gaining FDA approved agents for treating different malignancies [92]. In addition to these four FDA-approved agents, the butyrates, valproic acid, and compounds such as givinostat, mocetinostat, belinostat, and entinostat have been

extensively studied in the clinic with varying results [93, 94]. However, currently known HDACi exhibit limited isoform specificity, off-target activity and undesirable pharmaceutical properties [95]. In the intensifying efforts to discover new, hopefully, more therapeutically efficacious HDAC inhibitors, molecular modeling-based rational drug design has played an important role in identifying potential inhibitors that vary in molecular structures and properties. However, due to their high toxicity nature, it was used only in the pre-clinical studies up to now. Compared with TSA, SAHA has milder activity, but more stable, making it the most broadly used HDACi in cancer treatment.

1.11.6 Computational approaches for enzyme inhibitor design

Computer-aided molecular design is an important aspect of drug design and discovery. In general, computational methods for drug discovery and design may be divide into two categories [96]. The first category is structure-based drug design. Using available 3D structural and other important biological information concerning the target protein, the binding strength of small molecule inhibitors is optimized [96]. In this case, the second category of computational techniques. Ligand-based methods such as QSAR are used. From the dataset obtained from a series of lead compounds, 2D or 3D descriptors are generated. QSAR equations are derived based on the 2D descriptors and usually, a pharmacophore model is created from the 3D descriptors. The QSAR equation and the pharmacophore model are used to suggest new compounds with improved activity [97]. Recently, many compounds have been identified that inhibit the activities of HDAC-1 and II. HDAC inhibitors block the activity of HDAC enzymes leading to the activation of acetylated histones [98]. They alter the expression of 7-10% of genes and induce cell growth arrest, differentiation, and apoptosis. Consequently, HDACs are popular targets for drug development and HDAC inhibitors are a potential drug for many diseases.

Molecular modelling – based rational drug design to play an important role in identifying potential inhibitors. Synthetic chemistry is also used to design new compounds or improving the efficacy or safety of readily used drugs in cancer therapy. Synthetic chemistry is also used to design new compounds or improving the efficacy or safety of drugs already in use for cancer therapy.

Heterocyclic molecules are well known to play a pivotal role in health care and pharmaceutical drug design [99]. A number of heterocyclic compounds are available and approved by FDA as anticancer drugs such as Lynparza® (Olaparib), Zydelig® (Idelalisib), Zycadia[®] (Ceritinib), Farydak[®] (Panobinostat), Lenvima[®] (Lenvatinib) and Ibrance[®] (Palbociclib). Full description of all currently investigated compounds is an unfeasible task, and here in the examples depicted and addressed are based upon the most frequent ring scaffolds in FDA approved drugs [100]. Innovativeness and categorization of heterocyclic drugs were addressed by taking previously approved therapies and their perspective molecular drugs by assessing internal FDA databases and listed drugs from the centre for drug evaluation and research (CDER) into account (Research, C. for D.E. and New Drugs at FDA 2015) [101]. Imidazoles are well known heterocyclic compounds and have an important feature of a variety of medicinal agents. The high therapeutic properties of the imidazole related drugs have encouraged the medicinal chemists to synthesize a large number of novel chemotherapeutic agents. The structural features of the imidazole ring with desirable electron rich characteristics are beneficial for imidazole derivatives to readily bind with a variety of enzymes and receptors in the biological system. The imidazole derivatives readily bind with a variety of enzymes and proteins molecules and receptors compared with other heterocyclic rings [102]. This potency and wide applicability of the imidazole pharmacophore can be attributed to its hydrogen bond donor-acceptor capability, p-p stacking interactions, co-ordination bonds with metals (e.g. Mg, Fe, and Zn) as ligands, van der Waals, polarization and hydrophobic forces. Synthesis of imidazole containing compounds by multicomponent reaction and their anti-cancer potential of against the panel of National Cancer Institute 60 cancer cell line panel. 2,20-(2- (3-(cyclopentyloxy)-4-methoxyphenyl)-1-isobutyl-1H-imidazole- 4,5- diyl) dipyridine imidazole derivative is shown to have antiproliferative activity in A549 epithelial cancer cells by affecting proliferation, migration, anchorage independent growth, and by inducing cell cycle arrest in the G2/M Phase plus the activation of apoptosis [102]. 2, 4, 5-Trisubstituted and 1, 2, 4, 5-tetrasubstitutedimidazoles are present in compounds possessing versatile pharmacological activities such as p38 MAP kinase inhibitors, B-Raf kinase inhibitors, cannabinoid receptor antagonists, CSBP kinase inhibitors and glucagon receptor antagonists. In recent years, applications of imidazole derivatives in medicinal chemistry have achieved remarkable progress in cancer. But there is no sufficient work to prove imidazole having HDAC inhibition property to inhibit HDACs in non-small cell lung cancer cells

1.12. Imidazole

The imidazole nucleus is present in several well-known components of human organisms, including the amino acid histidine, Vitamin B₁₂, a component of DNA base structure, as well as purines, histamine, and biotin. It can also be found in many natural or synthetic drugs, such as cimetidine, azomycin, or metronidazole. These molecule containing drugs have a wide scope of applications in clinical medicine [103]. The first imidazole was synthesized by Heinrich Debus in 1858, but numerous derivatives of imidazole had already been discovered as early as the 1840s. His synthesis used glyoxal and formaldehyde in ammonia to produce imidazole [104]. Medicinal chemistry concerns with the discovery,

development, interpretation, and identification of the mechanism of action of biologically active compounds at the molecular level [105].

1.12.1 Pharmacological Activities

The imidazole derivatives are heterocyclic compounds that are commonly found in a variety of medicinal agents. Based on various literature surveys, imidazole derivatives show the following pharmacological attributes:

- (i) Antibacterial activity;
- (ii) Anticancer activity;
- (iii) Antitubercular activity;
- (iv) Antifungal;
- (v) Analgesic activity;
- (vi) Anti-HIV activity.

1.12.1.1 Antibacterial Activity

A series of substituted 4-(2, 6-dichlorobenzyloxy) phenyl thiazole, oxazole, and imidazole derivatives were synthesized by Lu et al. Their derivatives were screened for in vitro antibacterial activity against *S. aureus*, *E. coli*, *S. pneumonia*, *S. pneumonia*, Penicillinresistant, *P. aeruginosa* and *C. Perfringens*. The antibacterial screening revealed that the tested compounds have good inhibition against various tested microbial strains when compared to standard drug streptomycin [106].

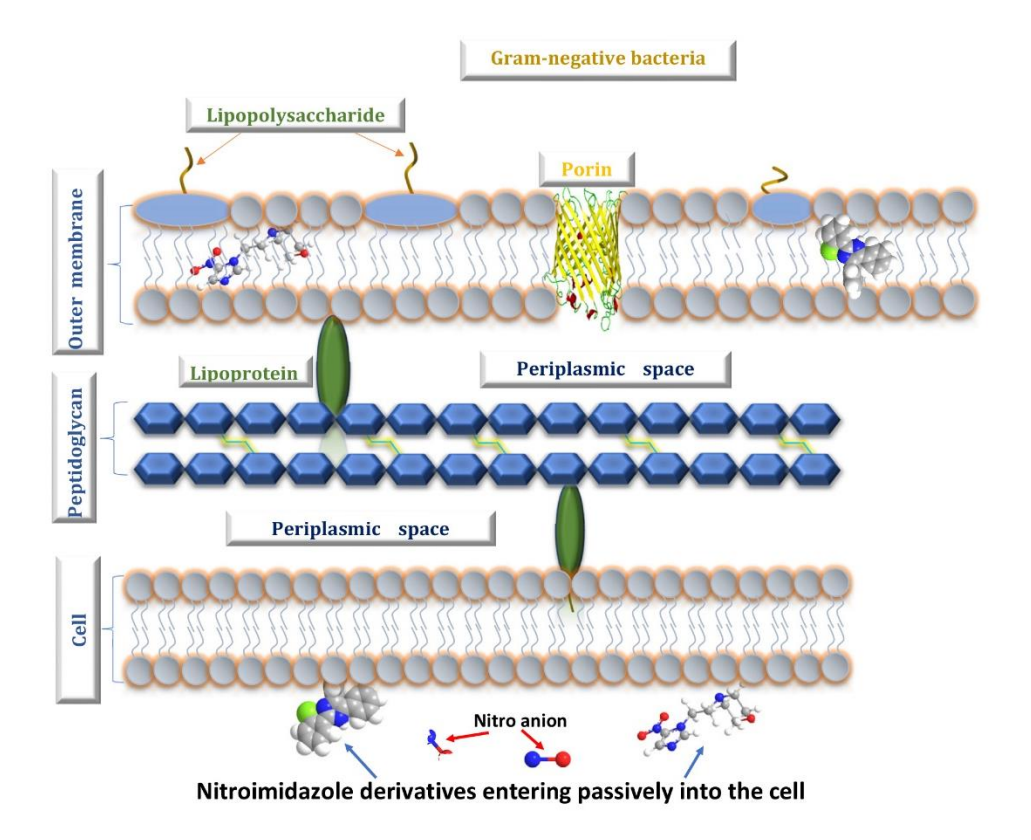


Figure 22. Imidazole derivatives and their antibacterial activity

1.12.1.2 Anticancer activity

In drug discovery, imidazole-based compounds present a desirable target for the design of novel chemical structures. Imidazole derivatives have achieved remarkable progress in medicinal chemistry over the past few years. The imidazole derivatives readily bind with a variety of enzymes and protein molecules and receptors compared with the other heterocyclic rings. This potency and wide applicability of the imidazole pharmacophore can be attributed to its hydrogen bond donor-acceptor capability, p–p stacking interactions, and coordination bonds with metals (e.g., Mg, Fe, and Zn) as a ligand, van der Waals, polarization, and hydrophobic forces. Imidazoles could interfere with DNA synthesis and then halt cell growth and division. Several imidazole-containing molecules have been reported to show cytotoxic activity against diverse cancer cell lines. 2,4,5-Trisubstituted and

1,2,4,5-tetrasubstituted imidazoles3 are present in compounds possessing versatile pharmacological activities such as p38 MAP kinase inhibitors, antitumor agents, B-Raf kinase inhibitors, antibacterial agents, cannabinoid receptor antagonists, anti-inflammatory agents, CSBP kinase inhibitors, and glucagon receptor antagonists [107].

1.12.1.3 Antitubercular activity

Tuberculosis has plagued humans throughout recorded and archaeological history, and is the leading cause from a single infectious agent currently. The emergency and widely spread of various forms of drug-resistant MTB pathogens, making the first-line anti-TB agents more and more ineffective. Therefore, it's imperative to develop new anti-TB agents with great potency against both drug-sensitive and -resistant TB. The exploration of heterocycles as anti-TB agents remains an intriguing scientific endeavour. Imidazoles are one of the most important, significant and abundant five-membered heterocycles, which are constituents of various natural and synthetic products. The favorable properties of imidazoles such as moderate dipole character, hydrogen bonding capability, rigidity and stability making them become indispensable units in medicinal chemistry applications. Several imidazole derivatives are under evaluation in clinical trials, and delamanid as the most emblematic example has already received approval for treatment of MDR-TB infected patients, indicating development of imidazole derivatives as novel anti-TB drugs active against both drug-sensitive and -resistant MTB pathogens are of critical importance [108].

1.12.1.4 Antifungal activity

In recent years, the frequency of opportunistic and pathogenic fungal infections has increased. The occurrence of these infections has increased since the early 1980s and is due to many factors, such as reckless use of antibiotics. Currently, the available antifungal agents

can be divided into four categories based on their mode of action, including azoles, polyenes, echinocandins, and antimetabolites. Clinically representative antifungal agents have certain limitations such as a narrow spectrum of activity, suboptimal pharmacokinetics, and susceptibility to drug resistance. Therefore, there is an urgent need to develop antifungal agents. 2-(substituteddithiocarbamoyl)-N-[4-((1H-imidazol-1-yl) methyl) phenyl] acetamide derivatives was designed and synthesized to combat the increasing incidence of drug-resistant fungal infections [109]. The synthesized compounds displayed promising antifungal activity compared to the standard drugs. In addition to this, molecular docking study of these synthesized imidazole derivatives demonstrates that they have a high affinity towards the active site of enzyme P450 cytochrome lanosterol 14a-demethylase, which provides a strong platform for new structure-based design efforts.

1.12.1.5 Anti-HIV activity

Human immunodeficiency virus (HIV) and hepatitis C virus (HCV) infect 40 million and 170 million people worldwide, respectively. There is no vaccine for either virus, but drug development is progressing at a rapid pace. At present, 24 drugs have been formally approved for the treatment of HIV infections. They belong to 7 different classes: NRTIs (nucleoside reverse transcriptase inhibitors), NtRTIs (nucleotide reverse transcriptase inhibitors), NNRTIs (non-nucleoside reverse transcriptase inhibitors), protease inhibitors, fusion inhibitors, CRIs (co-receptor inhibitors) and integrase inhibitors (INIs). The human immunodeficiency virus type 1 (HIV1) reverse transcriptase (RT) enzyme is the primary target for inhibiting HIV1 replication. RT can be inhibited by two classes of drugs, either nucleoside (or nucleotide) reverse transcriptase (N (t) RTI) inhibitors or non-nucleoside reverse transcriptase inhibitors (NNRTIs). HIV-1 NNRTIs have become key components in the combination regimens of anti-HIV therapy [110]. HIV-1 NNRTIs have become key

components in the combination regimens of anti-HIV therapy. To understanding the role of the five-membered heterocycles in the binding of the inhibitors to the RT and finding potent HIV replication inhibitors, a novel series of imidazole thioacetanilide (ITA) derivatives was designed and synthesized based on the general principle of bioisosterism in medicinal chemistry. A series of 2-(1-aryl-1H-imidazol-2-ylthio) acetamide [imidazole thioacetanilide (ITA)] derivatives were synthesized and evaluated as potent inhibitors of human immunodeficiency virus type-1 (HIV-1). All of the newly synthesized imidazole thioacetanilides were first evaluated for their anti-HIV activity [111]. The above study on different imidazole derivatives is an important class of heterocyclic compounds, showing promising results in most pharmacological activities., and also has fascinating results including antibacterial, anticancer, antitubercular, antifungal, analgesic, and anti-HIV activities. To date, imidazole nuclear modifications have been found to show promising biological activities. Motivated by the above data and in continuation of our previous reports in building novel biologically active molecules [112]. In the present study, we designed imidazole containing compounds and explored their potential through docking experiments for its interactions with isoforms of HDAC enzymes and synthesize the best candidature among them for its role in modulating histone modifying enzymes thereby demonstrate its anticancer potential in A549 cell line.

Design of imidazole-based derivatives

Fig. 23. A) The four different clinically tested HDAC inhibitors. These structures represent the most common pharmacophore cap group, zinc binding group (ZBG) and hydrophobic spacer; B) Design and synthesis of Imidazole Based Compounds.



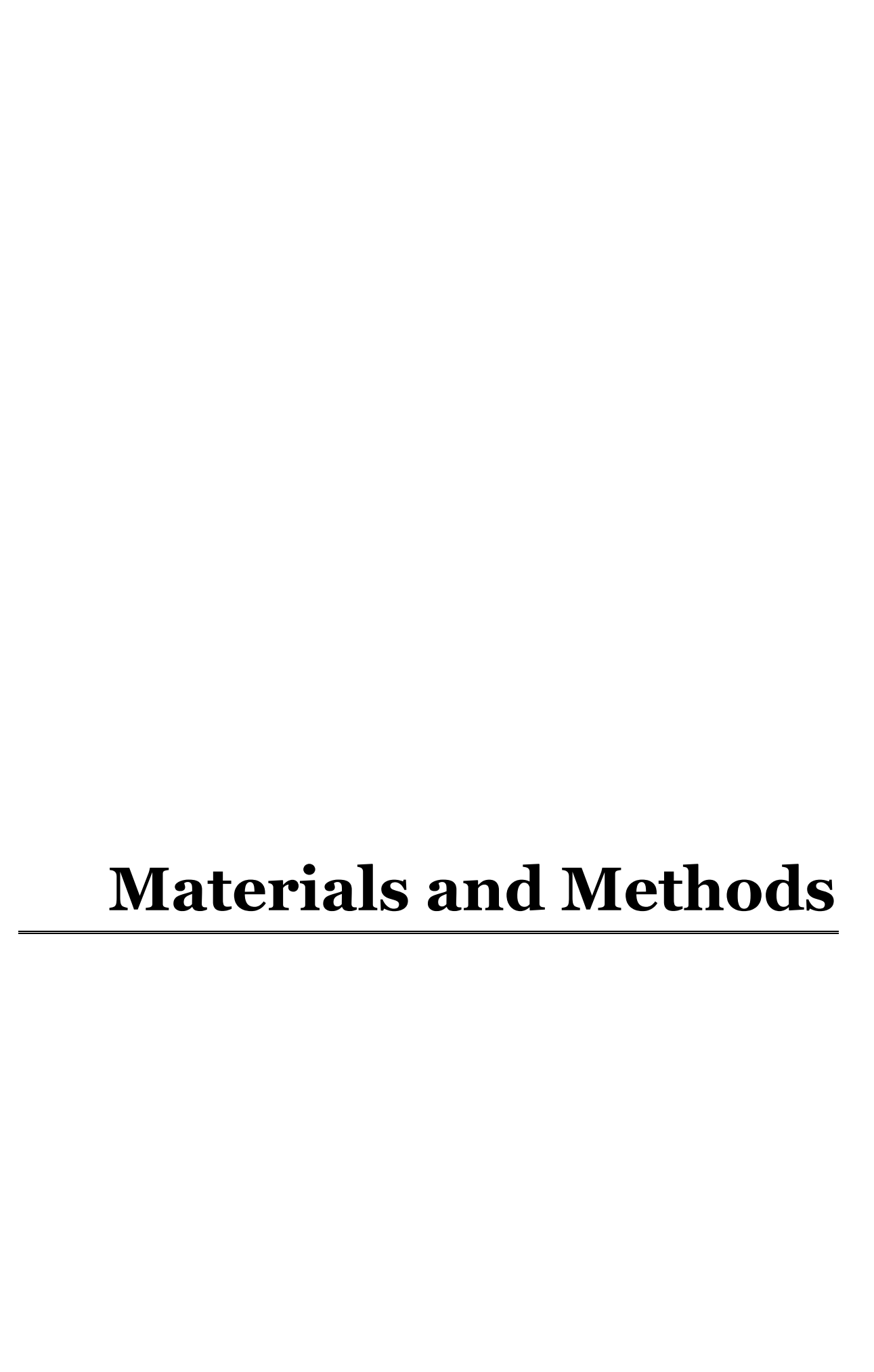
2.0 Aim and Objectives

Lung cancer is predominant in cancer and causes death in worldwide. Posttranslational modifications of histones play a crucial role in cancer development and progression by modulating gene transcription, chromatin remodelling, and nuclear architecture. Histone acetylation, a well-studied posttranslational histone modification, is controlled by the opposing activities of histone acetyltransferases (HATs) and histone deacetylases (HDACs). HDACs play crucial roles in cancer by deacetylating histone and nonhistone proteins, which are involved in the regulation of cell cycle, apoptosis, DNAdamage response, metastasis, angiogenesis, autophagy, and other cellular processes. HDACi has not only accelerated our understanding of HDAC functions and mechanism of actions, but also presented a promising new class of compounds for cancer treatment. To date, numerous synthetic or natural molecules that target classes I, II, and IV enzymes have been developed and characterized, although interest in the class III Sirtuin family is increasing. The rationale for targeting HDACs in cancer therapy is that altered HDAC expression and/or function is frequently observed in a variety of cancer types. Moreover, although the inhibition of HDACs may reactivate some tumor suppressors, they can also affect numerous other genes, the second-generation of HDACi have been developed with improved pharmacodynamics and pharmacokinetic values, given that these new agents possess similar specificity profiles as their parental compounds, it is unclear whether these newer agents will have improved and less toxic clinical outcomes. Currently, major efforts in therapeutic strategies are focused on developing selective inhibitors and studying combination therapies, with the aim of increasing potency against specific cancer types and overcoming drug toxicity and resistance. Based on these studies, we set out to discover new therapeutically efficacious HDACi. we designed imidazole containing compounds and

explored their potential through docking experiments for its interactions with isoforms of HDAC enzymes and synthesize the best candidature among them for its role in modulating histone modifying enzymes thereby demonstrate its anticancer potential in A549 cell line.

The present work proposed with specific following objectives:

- To designing of most frequent ring (imidazole) scaffolds in FDA approved drugs and their molecular target analysed in computer-aided drug designing tool (Maestro Schrödinger).
- 2. To synthesis and characterization of the selected Imidazole isoforms through their binding efficacy evaluation on docking analysis.
- 3. To evaluate the cytotoxicity assay of the Imidazole derivatives in lung cancer cell line (A549) while compared to control cell line (L132).
- 4. To investigate the effect of imidazole derivatives on the induction of histone acetylation in lung cancer cell lines using Reverse transcriptase and Immunoblotting techniques.
- To study the molecular mechanisms involved in the induction of cell cycle arrest by imidazole derivatives in lung cancer cell line.
- 6. To investigate the effects of compound on the PI3K/Akt/mTOR signalling pathway and cell migration detection via Matrix metalloproteinase (MMPs) in A549 cells.



3.0 Materials and Methods

3.1 Chemicals

Dulbecco's modified Eagle's medium, fetal bovine serum, 10X phosphate buffered saline (PBS), Antibiotic Antimycotic solution 100X, 3-(4,5-dimethyl-2-thiazolyl)- 2,5-diphenyl-2H-tetrazolium bromide (MTT), Dimethyl sulfoxide (DMSO), Acridine Orange (AO) and Ethidium Bromide (EB) 2', 7'- dichlorofluorescin diacetate (DCFHDA), Rhodamine-123, Hoechst 33,258 were purchased from HiMedia Laboratories, Mumbai, India. Trichostatin- A, Imidazole Acetyl H3 and H4, histone deacetylase (HDAC) antibody sampler kit and apoptosis antibody sampler kit were purchased from Cell Signalling Technology, (Danvers, MA, USA). Matrix metalloproteinase (MMPs) 2 and 9, p53, p21, caspase cascade pathway antibody sampler kit were purchased from Santa Cruz Biotechnology, Inc. (Dallas, TX, USA).

3.2 Procedure for the synthesis of ethyl (2, 5-diphenyl-1H-imidazole-4-yl) acetate

The reaction mixture was stirred at room temperature for 12 h. The reaction mixture was diluted with water and the organic layer was separated. The layer was washed with water, dried (anhydrous Na₂SO₄) and the solvent was removed under reduced pressure. The crude product C3 so obtained was purified by column chromatography (Silica gel, 100e200 mesh) using ethyl acetate/hexane (1:3). ethyl (2,5-diphenyl-1H-imidazole-4-yl)acetate (C3): Off-white semisolid; Yield: 107 mg (35%); IR (KBr): 3357 (NeH), 2976 (CeH), 1734 (C]O) cm1; ¹H NMR (400 MHz, CDCl₃): d 7.85 (d, J ¹/₄ 6.8 Hz, 2H), 7.55 (d, J ¹/₄ 7.2 Hz, 2H),7.41e7.30 (m, 7H), 4.18 (q, J ¹/₄ 7.2 Hz, 2H), 3.80 (s, 2H), 1.26 (t, J ¹/₄ 7.0 Hz, 3H) ppm; ¹³C NMR (100 MHz, CDCl₃): d 171.3, 146.0, 134.7, 132.2, 129.9, 128.74, 128.65, 128.6,

127.3, 127.2, 125.4, 61.3, 32.5, 14.1 ppm.; HRMS (ESI) calcd. for C₁₉H₁₈N₂O₂: 307.1441 [M \(\bar{b} \) H\(\bar{b} \)], found 307.1442.

3.3 Synthesis of 2-(1H-imidazol-1-yl)-N-(pyridin-2-yl) acetamide (2)

The required compound was synthesized in two steps from commercially available 2-amino pyridine as starting material and the synthetic route is described in Scheme 1. The acylation of 2-amino pyridine using chloroacetylchloride under basic condition at room temperature gave 2-chloro-N-(pyridine-2-yl)acetamide 1 in 77% yield. Nucleophilic displacement of chlorine in compound 1 carried out using imidazole in the presence of K₂CO₃ at 50°C furnished 2-(1H-imidazol-1-yl)-N-(pyridin-2-yl)acetamide 2 in 92% yield. The compounds were confirmed by melting point, IR, NMR, elemental analysis and HPLC.

3.4 2-Chloro-N-(pyridine-2-yl) acetamide (1)

To a stirred solution of 2-amino pyridine (1 mmol, 94 mg) in DCM (3 mL) was added triethyl amine (2 mmol, 0.3 mL). After 10 mins, chloroacetyl chloride (1.2 mmol, 0.1 mL) was carefully added drop wise to the reaction mixture at room temperature and continued the stirring for 5 h. Then, the reaction mixture was quenched with water and extracted with 2 X 10 mL dichloromethane. The organic layer was washed with brine solution and dried over Na₂SO₄. The crude product was purified by column chromatography using hexane: ethyl acetate (6:4) to get the compound 1. White solid; Yield: 77% (131 mg); Decomp.: 119-122 °C; $_{1}$ H NMR (500 MHz, CDCl₃): $_{2}$ S (ppm) 4.21 (s, 2H), 7.12 (m, 1H), 7.76 (m, 1H), 8.21 (d, J= 10.5 Hz, 1H), 8.33 (d, J = 5.5 Hz, 1H), 9.00 (s, 1H); $_{13}$ C NMR (125 MHz, CDCl₃): $_{2}$ S (ppm) 42.82, 114.09, 120.63, 138.79, 147.74, 150.35, 164.60; Elemental analysis Calcd for C7H7ClN2O: C, 49.28; H, 4.14; N, 16.42; found C, 50.05; H, 3.97; N, 16.52.

3.5 2-(1H-imidazol-1-yl)-N-(pyridin-2-yl) acetamide (2)

To the stirred solution of compound 1 (1 mmol, 170 mg) in THF (5 mL) was added imidazole (1 mmol, 70 mg) and K_2CO_3 (2 mmol, 280 mg). The reaction mixture was stirred for 3 h at 50 °C. After completion of the reaction, confirmed by TLC, the solvent was evaporated in vacuum. The reaction mixture was quenched with water and extracted using 2 x 10 mL of ethyl acetate. The organic layer was washed with brine solution and dried over Na_2SO_4 . The crude product was purified by column chromatography to get the target compound 2. White solid; Yield: 92% (185 mg); m. p.: 195-198 °C; ¹H NMR (500 MHz, DMSO-d6):): δ (ppm) 4.70 (s, 2H), 6.91 (s, 1H), 7.11-7.14 (m, 1H), 7.18 (s, 1H), 7.67 (s, 1H), 7.77-7.81 (m, 1H), 8.01-8.03 (m, 1H), 8.34 (t, 1H, J = 5 Hz), 10.88 (s, 1H); ¹³C NMR (125 MHz, DMSO-d6): δ (ppm) 54.4, 118.6, 124.93, 125.98, 133.06, 143.59, 153.33, 156.82, 171.86; Elemental analysis Calcd for $C_{10}H_{10}N_4O$: C, 59.40; H, 4.98; N, 27.71; found C, 59.23; H, 5.27; N, 27.91.

3.6 Characterization of synthesised compounds

3.7 Fourier transform infrared spectroscopy (FT-IR)

Fourier transform infrared spectroscopy (FT-IR) was recorded as KBr pellets (JASCO FT-IR 4600, Japan) in the range of 400-4000 cm⁻¹.

3.8 Nuclear Magnetic Resonance (NMR)

¹H and ¹³C NMR spectra were recorded on a 400 MHz (Bruker Advance-III, USA) instrument using TMS as an internal standard and CDCL₃ as a solvent at SAIF, Department of Chemistry, Bharathidasan University, Tiruchirappalli, Tamil Nadu.

3.9 High resolution mass spectra (ESI)

High resolution mass spectra (ESI), was recorded on a Q-TOF mass spectrometer (Agilent, USA). Indian Institute of Technology, Chennai, Tamil Nadu.

3.10 Mass Spectroscopy

Mass spectroscopy was recorded on JEOL GCMATE II with data system having high resolution, double focusing instrument.

3.11 High –performance liquid chromatography (HPLC)

High performance Liquid Chromatography (HPLC) was recorded on a JASCO LC 4000 HPLC instrument.

3.12 Melting Point

Melting Points were recorded with 'EI' melting point apparatus with a digital temperature controller.

3.13 Homology modeling and validation

The homology modeling of targeted proteins was performed by PRIME module (prime, version 4.1, Schrodinger, LLC, and New York-1). The geometry and energy profile were constructing by using PRIME. The structures was further validated by using Procheck, and ERRAT and Verify 3D to consider amino acid, and energy level of protein. By the assist of Ramachandran plot the phi and psi angles were analyzed for the backbone of 3D structure of proteins. Furthermore, the modeled structures energy criterion was compared with huge set of known protein structures [115].

3.14 Protein and Ligand preparation

The Ligand was prepared and minimization was done by LigPrep module of Schrodinger 2019-4.0 version. The structures of the designed compounds were C1 - C14 and Standard Known HDACi (TSA) was further processed by ligprep module of Schrödinger suite, which was produce a 1000 conformers in Pre-process (100-step) and Post-process (50) minimization steps. The conformers were filtered by virtual energy and best conformers were selected [116].

The 3D structure of human HDACs (PDB ID: 4BKX, 3MAX, 4A69, 2VQM, 3C5K, 3C10 and 1T64) family proteins obtained from Protein Data Bank. These targeted proteins were first imported in protein preparation wizard by adding hydrogen bonds and removal of hetero atoms form proteins. Then the prepared proteins does not contain any co-crystal ligand, so active site were predicted by using the Site map module of Maestro (version 2.3, 2009, Schrödinger, LLC, New York, USA) with default parameters (Anne Marie J et al. 2008). The possible binding sites were identified by various physical descriptors like size, degree of enclosure, degree of exposure, tightness, hydrophobic, hydrophilic, hydrogenbonding possibilities, and linking site points, which are more likely to be contributing to protein-ligand binding. After modification, structures were exposed to receptor grid generation process, to determine amino acid position of the targeted proteins [117, 118].

3.15 Molecular docking analysis

We performed the molecular docking studies by using GLIDE module of Schrödinger (version 2.3, 2009, Schrödinger, LLC, New York, USA). The prepared compounds were docked with the active site of HDACs family proteins Glide module under rigid-receptor with flexible-ligand conditions in extra-precision (XP) mode using standard protocols. The GLIDE docking workflow consists of three phases: high throughput virtual screening (HTVS), Standard Precision (SP), and extra-precision (XP). All the phases filter the top 10% of compounds and pull to the next phase. The top 10% of compounds are placed based on good scoring poses of the ligand molecules. The final XP phase identifies the top molecules, which have the stable binding pose and binding affinity. All the settings are kept as default and to produce the output with computed RMSD for all complex molecules with a good pose. Finally, the top hit compounds are selected based on the binding affinity and the numbers of interacting residues, the selected compound are further validated by computational studies [119, 120].

3.16 Molecular dynamics simulations (MDs)

Molecular dynamics (MDs) simulations were performed using the program Desmond [121]. Neutral territory method (midpoint method) [122] was adopted to efficiently exploit a high degree of computational parallelism. The OPLS 2005 force-field model was used to analyse amino acid interactions in protein and the simple point charge (SPC) method was used for the water model [123]. The equilibration of the system was passed out by default protocol provided in Desmond, which consists of a series of restrained minimizations and molecular dynamics simulations that are designed to slowly relax the system without deviating substantially from the initial protein coordinates. The initial coordinates for the MD calculations were taken from the modelled protein X-ray crystallographic structure of HDAC enzymes from PDP data base. The simple point charge (SPC)water molecules were added (theorthorhombic dimensions of each water box were 10 Å X 10 Å X 10 Å approximately, which confirmed the whole surfaces of the complexes to be covered), and the neutralization of system was carried out by adding Cl counter ions to balance the net charge of the system. After the construction of the solvent environment, each complex system was composed of about 34,942 atoms. Before equilibration and the long production MD simulations, the systems were minimized and pre-equilibrated using the default relaxation routine implemented in Desmond. The whole system was subjected to 300 K for 10ns of simulation of the protein-ligand complex. The structural changes and dynamic behaviour of the protein were analysed by calculating the RMSD and energy.

3.17 Cell culture

Cell lines were cultured in Dulbecco's modified Eagle's medium (DMEM) medium with 10% fetal calf serum (Hi Media Laboratories, Mumbai, India) supplemented with) 1% of antibiotic Antimycotic solution in a CO₂ incubator (5% CO₂) at 37 °C.

3.18 Cell viability assay

The potential cytotoxicity of the synthesized compound was determined by 3-(4, 5-dimethylthiazol-2-yl)-2, 5-diphenyl tetrazolium bromide (MTT) assay using the reported protocol with minor modifications [124]. A549 cells were cultured in a 96 well microtiter culture plate (10,000 cells per 100 mL) under characteristic culture conditions. The different concentrations of the C3 compound (10-100 mM) were added to the cell monolayer. Samples were incubated at 37°C for 24 h in the atmosphere of 5% CO₂ with 95% relative humidity. The assay was accomplished according to the manufacturer's protocol and the absorbance was read at 650 nm in an ELISA iMARKTM microplate reader (Bio-Rad, USA).

3.19 Morphological changes of the C3 compound in A549 cells

A549 cells were seeded in 6-well cultured plates (5 x 10⁴ cells/ mL) under characteristic culture conditions. After overnight incubation, cells were treated with three different concentrations of C3 compound including IC₅₀ concentration (60 mM), below (30 mM), and above (100 mM) IC₅₀ identified concentration and incubated to allow colony formation for 24 h. The colonies were fixed with ethanol/acetic solution (3:1). Finally, the plates were inspected in bright field inverted light microscope (Labomed TCM 400) at 40X magnification and the morphological changes of A549 cells were documented.

3.20 Colony formation inhibition assay

A549 cells at the exponential phase were plated into 6-well culture plates at a single -cell density (500 cells/well) and allowed to adhere for 24 h before treatment. Cells were incubated with culture medium containing compounds at their respective IC_{50} concentrations as follows, 50, 100, 150, 200 and 250 μ M. After 24 h, the medium was replaced with a fresh medium and cells were incubated for 1-7 days or 14 days [125]. Cells

were then washed with 1X PBS, fixed with 4% paraformaldehyde and stained with 0.5% methylene blue prepared in 10% ethanol for 30 min and rinsed with distilled water to remove excess dye. Plates were photographed with a digital camera.

3.21 DNA fragmentation assay

The fragmentation assay was performed as described previously with minor modifications [126]. Briefly, the cells were collected and washed with PBS. To the washed cells, 500 μL extraction buffer (10 mM Tris, pH 8.0; 10 mM EDTA, pH 8.0; 75 mM NaCl; 0.5 % SDS) was added and incubated at 37°C for 1 h, followed by the addition of 150 μg/mL proteinase K [Sigma-Aldrich, St. Louis, MO, USA]) and incubated at 55 °C for 1 h. After incubation, the sample was centrifuged at 12000 rpm for 20 min at 4°C. The supernatant was recovered for DNA precipitation by adding 2 volumes of 100% ethanol with 0.1 M NaCl. The precipitated DNA was washed with 70% ethanol and then treated with RNase for 60 mins. Finally, the pellet was dissolved in 50 μL of TE buffer and the sample was electrophoresed at 50 V in a 0.8 % agarose gel containing ethidium bromide.

3.22 HDAC Activity

This assay was performed using HDAC Activity Colorimetric Assay Kit (BioVision Incorporated, Catalog #K331-100, Milpitas, CA, U.S.A), according to the manufacture protocol. Lethal dosage concentrations of the 2-(1H-imidazole-1-yl) treated A549 cell lysate, control lysate and TSA treated cell lysate were used for quantifying the total HDAC. The entire samples in a triplicate manner were added to the 96-well plates and a final volume was made up to 85 μ L using deionized water. After that, 10 μ L of 10 X HDAC assay buffer and 5 μ L of the colorimetric substrate were added and incubated for 1 h at 37oC. Subsequently, 10 μ L of lysine developer was added and incubated for 30 mins at 37°C to

arrest the reaction. The absorbance was read at 400 nm using an ELISA plate reader. HDAC activity was expressed as relative optical density (OD) values per microgram of protein. TSA was used as a positive control.

3.23 Reverse transcription polymerase chain reaction (RT-PCR)

3.23.1 Total RNA Isolation

Total mRNA was isolated by using TRIzol reagent (Invitrogen, Green Island, NY, USA). Concisely, control cells (A549), 2-(1H-imidazol-1-yl)-N-(pyridin-2-yl)acetamide treated cells and positive control (TSA) cells washed with ice cold PBS twice. 1mL of TRIzol reagent was added into T-25 tissue culture plates lysed the cells directly in a culture plate after lysed cells collected into 2mL centrifuge tubes and added 0.2 mLof chloroform then vortex vigorously for 5 mins and incubated 20 mins at RT. After incubation, the samples were centrifuged 12, 000 rpm for 15 mins at 4°C and carefully removed the upper aqueous phase which contains total RNA in a new 1.5 mL centrifuge tubes. Total RNA was precipitated from the aqueous phase by using 0.5 mL of isopropyl alcohol were added, mixed gently by inverting the tubes and incubated 10 mins at RT. After incubation, the samples were centrifuged at 10, 000 rpm for 100 mins at 4°C and after centrifugation, removed the supernatant carefully and washed the RNA pellet by adding 1 mL of 75% ethanol, mixed gently by inverting the tubes again, centrifuged the tubes at 12,000 rpm for 5 mins at 4°C after centrifugation, removed all leftover ethanol and invert tubes allowed air dry RNA pellet for 10 mins. Dissolved RNA pellet by adding 50µL Nuclease free water and stored in-20°C freezer for further experiments.

3.23.2 RNA quantification and cDNA construction

Total RNA was quantified in the Eppendorf bio spectrophotometer. The samples A260/A280 ratio \leq 1.80 and the A260/A230 ratio \leq 0.5 only taken for cDNA synthesis, 2µg of RNA was used for cDNA construction. cDNA was constructed by using prime ScriptTM RT reagent kit (Catalogue number: RR037A – Takara Bio Inc, Japan). For 20µL of cDNA, 5X primeScript buffer-4.0µL; RT Enzyme - 1µL; 50µM Oligo dT primer - 10µL; Random 6 mers -1µL; RNA- 2 µg and Nuclease free water up to 13µL added all the reagents into 0.2µL PCR tube vortex gently. Incubated the RNA- primer mix under the following conditions: 37°C for 15 min, 85°C for 5 sec and final hold in 4°C in Takara PCR Thermal Cycler (Takara Bio Inc, japan). Synthesized cDNA was stored at -20°C for the further experiments.

3.23.3 RT-PCR

The mRNA expression levels were quantified through RT-PCR using EmeraldAmp GT PCR master mix (Catalogue number: RR310A – Takara Bio Inc, Japan) on the Takara PCR thermal cycler dice (Takara Bio Inc, Japan). For 10μL RT-PCR reaction, 2X PCR master mix - 5μL; cDNA – 1μL; Reverse Primer - 1μL; Forward Primer - 1μL; Nuclease free water - 2μL added all the reagents into PCR tubes and mix gently and incubated under following conditions: 35 cycles at 95°C for 30s, 60°C for 30s, and 72°C for 30s, Gene expression was determined for each gene of interest and normalized to a housekeeping gene (βactin) by running 2% agarose gel electrophoresis and gel documented using Gel Dock (Bio-Rad, USA). The intensities of the bands were quantified using Image J software (National Institute of Health, Bethesda, MD, USA). The sequence of the primer sets is given in the Table 3.

S.NO	Oligo name	Sequence	(5' 3')
		FORWARD	REVERSE
1.	HDAC1	CCTGAGGAGAGTGGCGATGA	GTTTGTCAGAGGAGCAGATCGA
2.	HDAC2	GCTCTCAACTGGCGGTTCAG	AGCCCAATTAACAGCCATATCAG
3.	HDAC3	CCCAGACTTCACACTTCATCCA	GGTCCAGATACTGGCGTGAGTT
4.	HDAC4	GACCTGACCGCCATTTGC	GGGAGAGGATCAAGCTCGTTT
5.	HDAC5	CAACGAGTCGGATGGGATGT	GGGATGCTGTGCAGAGAAGTC
6.	HDAC6	TGCCTCTGGGATGACAGCTT	CCTGGATCAGTTGCTCCTTGA
7.	HDAC7	AGCAGCTTTTTGCCTCCTGTT	TCTTGCGCAGAGGGAAGTG
8.	HDAC8	CGGCCAGACCGCAATG	CACATGCTTCAGATTCCCTTT
9.	HDAC 9	AGGCTCTCCTGCAGCATTTATT	AAGGGAACTCCACCAGCTACAA
10.	HDAC10	ATGACCCCAGCGTCCTTTACT	CGCAGGAAAGGCCAGAAG
11.	HDAC11	CCCCTTGGTCATGGGATTT	CATCCACACCAGTGCCTATAGC
12.	IL 6	CCAGAGCTGTGCAGATGAGT	AGTTGTCATGTCCTGCAGCC
13.	IL 8	ATG ACT TCC AAG CTG GCC GTG GCT	TCT CAG CCC TCT TCA AAA ACT TCT
14.	Cox-2	TACCCTCCTCAAGTCCCTGA	ACTGCTCATCACCCCATTCA
15.	P53	TGACACGCTTCCCTGGATTG	GCTGCCCTGGTAGGTTTTCT
16.	p21	ACCGAGGCACTCAGAGGAG	ATCTGTCATGCTGGTCTGCC
17.	TNF-α	CATCAGCCGCATCGCCGTCT	GGGTTCCGACCCTAAGCCCC
18.	Fas Ligand	ACATGAGGAACTCTAAGTATCC	AAAATTGACCAGAGAGAGC
19.	MMP-2	ACCTGGATGCCGTCGTGGAC	TGTGGCAGCACCAGGGCAGC
20.	MMP-9	GGTCCCCCACTGCTGGCCCTTCTACGGCC	GTCCTCAGGGCACTGCAGGATGTCATAGGT
21.	Caspase-8	CTTTCTGGGCACGTGAGGTT	CCTCCGCCAGAAAGGTACAG
22.	Caspase-3	CTGTGGCTGTGTATCCGTGG	CTGAGGTTTGCTGCATCGAC
23.	PIK3	GGCCACTGTGGTTGAATTGGGA	AGTGCAC-CTTTCAAGCCGCC
24.	AKT	CAAGTCCTTGCTTTCAGGGC	ATACCTGGTGTCAGTCTCCGA
24.	mTOR	AACCTCCTCCCAATGA	CAAGGTCATCCATGACAACTTTG
25.	GAPDH	CTCATGACCACAGTCCATGCCATC	CTGCTTCACCACCTTCTTGATGTC

Table. 3. List of RT-PCR primer sequences used in this study

3.24 Western blotting

A549 cells were treated with 2-(1H-imidazol-1-yl)-N-(pyridin-2-yl)acetamide lethal dosage value for 24 h. To prepare the whole cell lysate, the cells were harvested, and lysed with 1 mL of RIPA (Radio Immunoprecipitation Assay) lysis buffer (pH 7.4 + 0.1) containing 10 μ L of (200mM) PMSF, 10 μ L of (100mM) Sodium orthovandate and 10 μ L of protease inhibitor cocktail (Santa Cruz Biotechnology, Santa Cruz, CA, USA). The cells were collected form the plates by using cell scraper and added into micro centrifuge tubes,

then kept in ice for 15 min and vortexed for 5 min. After incubation, the cells were centrifuged at 12,000 rpm for 20 min at 4°C. The cleared supernatant was collected for further use. Isolated protein samples were stored at -20°C freezer until further experiments.

3.24.1 Protein estimation

Total protein concentration was measured by using Lowry's method (Lowry *et al.*, 1951). BSA (Bovine serum albumin) was used as a standard and measured the absorbance of standard and samples at 600 nm.

3.24.2 Separation of protein by SDS-gel electrophoresis and detection

The quantified protein (50µg per lane) was resuspended in 6 X protein loading buffer and separated by using 12% SDS-polyacrylamide gel electrophoresis (100V, 2.30h) and then were transferred onto a nitrocellulose membrane (150V for an 1.30h) (Bio-Rad, Hercules, CA, USA). The membranes were incubated at room temperature for 1 h with blocking buffer (freshly prepared 5% skimmed milk powder in TBS-T (20mM Tris, 136mM NaCl, 0.1% Tween 20, pH7.6) to block non-specific antibody binding. Primary monoclonal antibodies were used at 1; 1000 dilutions and were incubated overnight at 4°C. Membranes were washed with 3 times TBS-T and TBS. and then further incubated for 1 h at room temperature with a secondary antibody (Cell Technology), then the membranes were washed with TBS-T and TBS (3 times). Bands detected using the 200 µL of BCIP/NPT solution (Genei, USA) were visualized using Bio-Rad Gel doc XR plus (Bio-Rad, Hercules, USA) and band intensity were quantified using Image J Software (NIH).

3.25 Cell Cycle distribution analysis by flow cytometry

The effect of 2-(1H-imidazol-1-yl)-N-(pyridin-2-yl) acetamide on cell cycle flow cytometer is an important tool to detect DNA content analysis for cell cycle distribution was analysed by flow cytometer with PI staining as we previously described [127,128]. A549

cells were treated with 2-(1H-imidazol-1-yl)-N-(pyridin-2-yl) acetamide and TSA used as a positive control allowed to incubating for 24 h to access the effect of compound. The cells were collected, fixed in 75% ethanol, and resuspended in 50 µg/mL of PI solution. The treated cells were subjected to flow cytometer (FACS Calibur, Becton Dickinson) with standard filter setup, and the percentage of the cells in each cell cycle phase was analysed using Cell Quest Pro software (Becton Dickinson).

3.26 Measurement of Reactive Oxygen Species (ROS) Level

The intracellular ROS generation of cells can be investigated using the 2', 7', dichlorofluorescein-diaacetate (DCFH-DA) as well as established compound to detect and quantify intracellularly produced H₂O₂. DCFH-DA is transported across the cell membrane and deacetylate by esterases to form the non-fluorescent 2', 7', - dichlorofluorescin (DCF). This compound trapped inside the cells. After that, DCFH is converted to DCF through the action of peroxide in the presence of peroxidases. Then, the fluorescence intensity was measured in a fluorescence microscope. Approximately 5 x 10⁵ cells were seeded in a cell culture plate and allowed to attach overnight for appropriate characteristic conditions. At the end of incubation, the old media was replaced with fresh medium containing IC50 concentration of 2-(1H-imidazol-1-yl)-N-(pyridin-2-yl) acetamide and incubated for 24 h. After incubation, 0.5 mL of 10 mM of 2', 7'-dichlorfluorescein-diacetate (DCFH-DA) dye was used in the measurement of ROS generation and Rhodamine-123(10 mg/mL) dye was used to observe mitochondrial membrane potential in both control and treated A549 cells.

3.27 Mitochondrial membrane potential (ΔΨm)

Mitochondrial membrane potential ($\Delta\Psi$ m) is an early event in the process of ROS generation and cell death. During apoptosis the mitochondrial outer membrane becomes permeable, leading to the release of apoptogenic factors into the cytosol. Rhodamine-123 (RH-123) was first used to measure in intact cells both as a microscopic stain and by

cytofluorometry by monitoring the increase in fluorescence due to its electrophoretic accumulation in mitochondria. It is a cationic dye that can selectively enter into mitochondria and reversibly change colour from intense green to low. A549 cells 5 x 10⁵/mL were seeded in 6well tissue culture plates and incubated overnight for the cells to attach. After 24 h the old medium was replaced with fresh medium containing C3 Compound and incubated for 24 h respectively. Following treatment, cells were exposed to Rhodamine-123 dye (10 mg/mL) to observe mitochondrial membrane potential [129]. The dye was exposed to the cells for 10 min at room temperature and followed by 1X PBS wash and observed with EVOS® FLoid® Cell Imaging Station at a magnification of 20 (green filter: excitation 532/59 nm, emission 532/59 nm).

3.28 Nuclear damage by Hoechst staining

Hoechst is a bisbenzimide DNA intercalator that binds to the AT rich regions of dsDNA and it has two types of derivatives as Hoechst (33258 & 33342) dye. Hoechst 33528 fluorescence when binds to double stranded genomic DNA and it won't fluorescence when binds to short pieces of single-stranded DNA. The Hoechst dyes, are impermeable through the cell membranes of viable cells, and can be used as a fluorescent indicator of dead cells. Hoechst 33528 produced strong fluorescence after binding with nuclear in dead and living cells. A549 cells were seeded at 5 x 10⁵ cells/well in 6 well plate and allowed to attach overnight under characteristic conditions. After overnight incubation, the cells were treated with IC₅₀ concentrations of the 2-(1h-imidazol-1-yl)-n-(pyridin-2-yl) acetamide compound for 24 h respectively, and the treated cells were exposed with Hoechst 33528 at 2 mg/mL based on the manufacture protocol without any modifications [130] and observed under EVOS® FLoid® Cell Imaging Station at 20X magnification with the blue filter at excitation 390/40 nm and emission 446/ 33 nm.

3.29 Propidium iodide Staining

Propidium iodide is a popular red-fluorescent nuclear and chromosome counterstain. Since Propidium iodide is not permeant to live cells, it's commonly used to detect dead cells in a population. It binds to double stranded DNA by intercalating between base pairs and emits red fluorescence. It stains only to the dead cells and it induces apoptosis, from this it can be assessed easily after treatment. A549 cells were seeded at 5 x 10⁵ cells/well in 6 well plate and allowed to attach overnight under characteristic conditions. After overnight incubation, the cells were treated with IC₅₀ concentrations of the 2-(1h-imidazol-1-yl)-n-(pyridin-2-yl) acetamide compound for 24 h respectively. After incubation, stained by 50 μL/mL of propidium iodide incubated at 37°C with 5% CO₂ for 30 min and the changes in the cells were examined and photographed using 20 x objective under a fluorescence microscope.

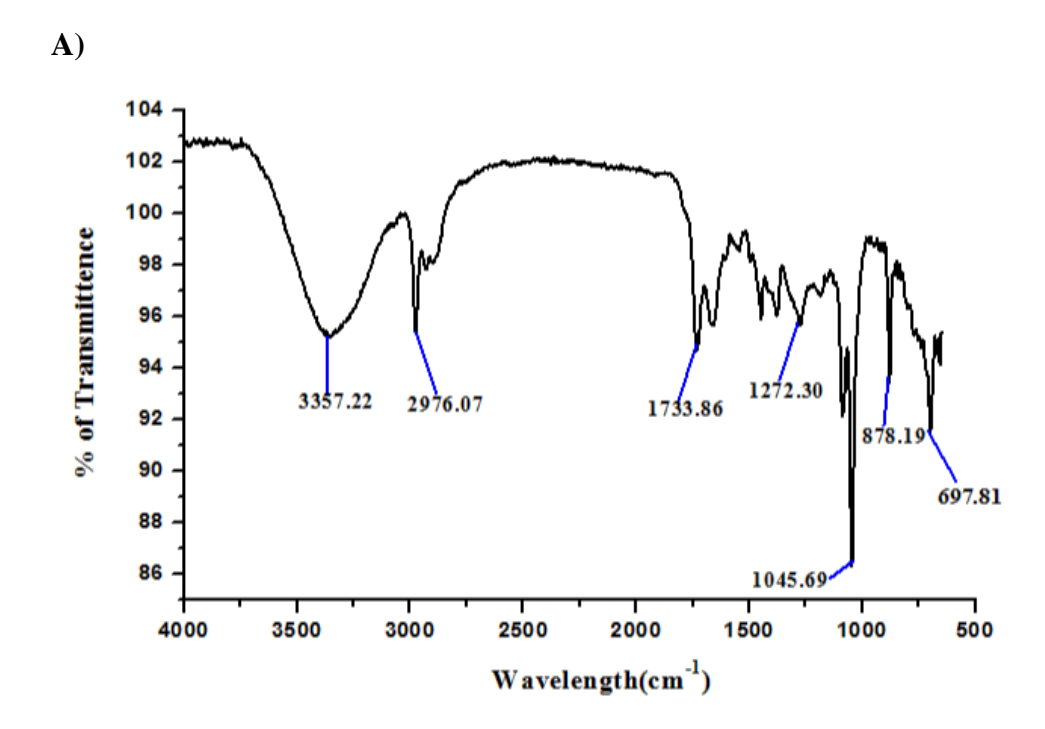
3.30 Statistical analysis

One-way ANOVA with Dunnett's post test was used for testing the mean value \pm SD using Graph pad prism software version 6.03 (La Jolla, CA). Values with P < 0.05 were considered significant.

Results

4.0 Results

4.1 Fourier transform infrared spectroscopy analysis of compounds



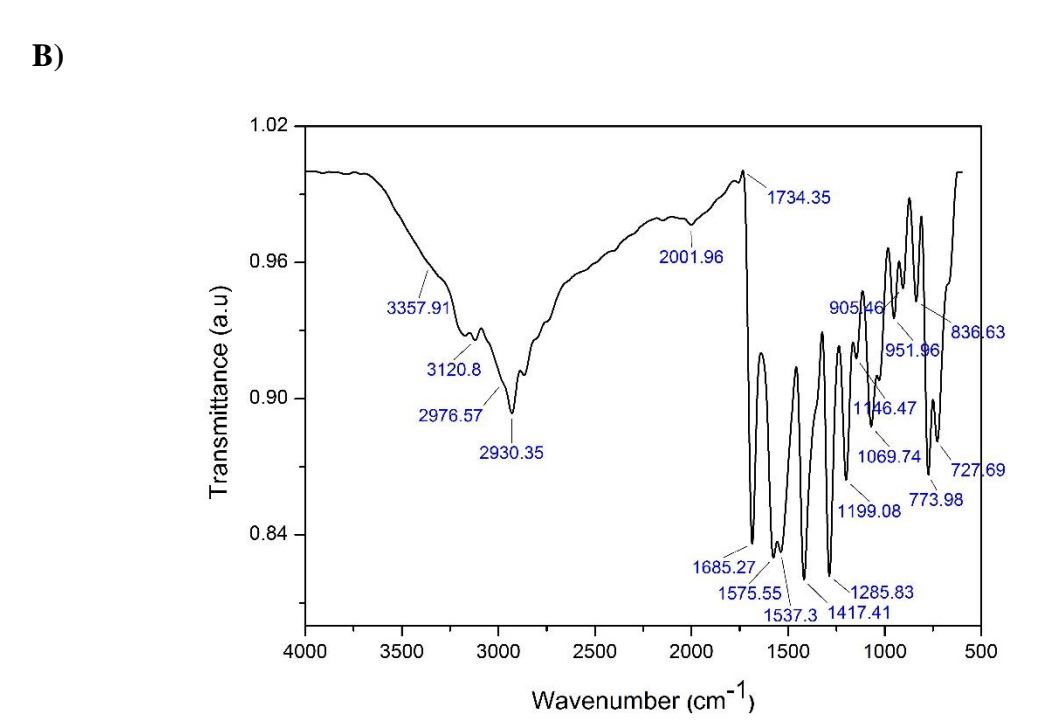


Fig.4.1 A) FTIR analysis of ethyl (2-phenyl-5-phenyl-1H-imidazole-4-yl) acetate and B) 2-(1H-imidazol-1-yl)-N-(pyridin-2-yl) acetamide

4.1.1 Nuclear magnetic resonance spectroscopy analysis of synthesised compounds

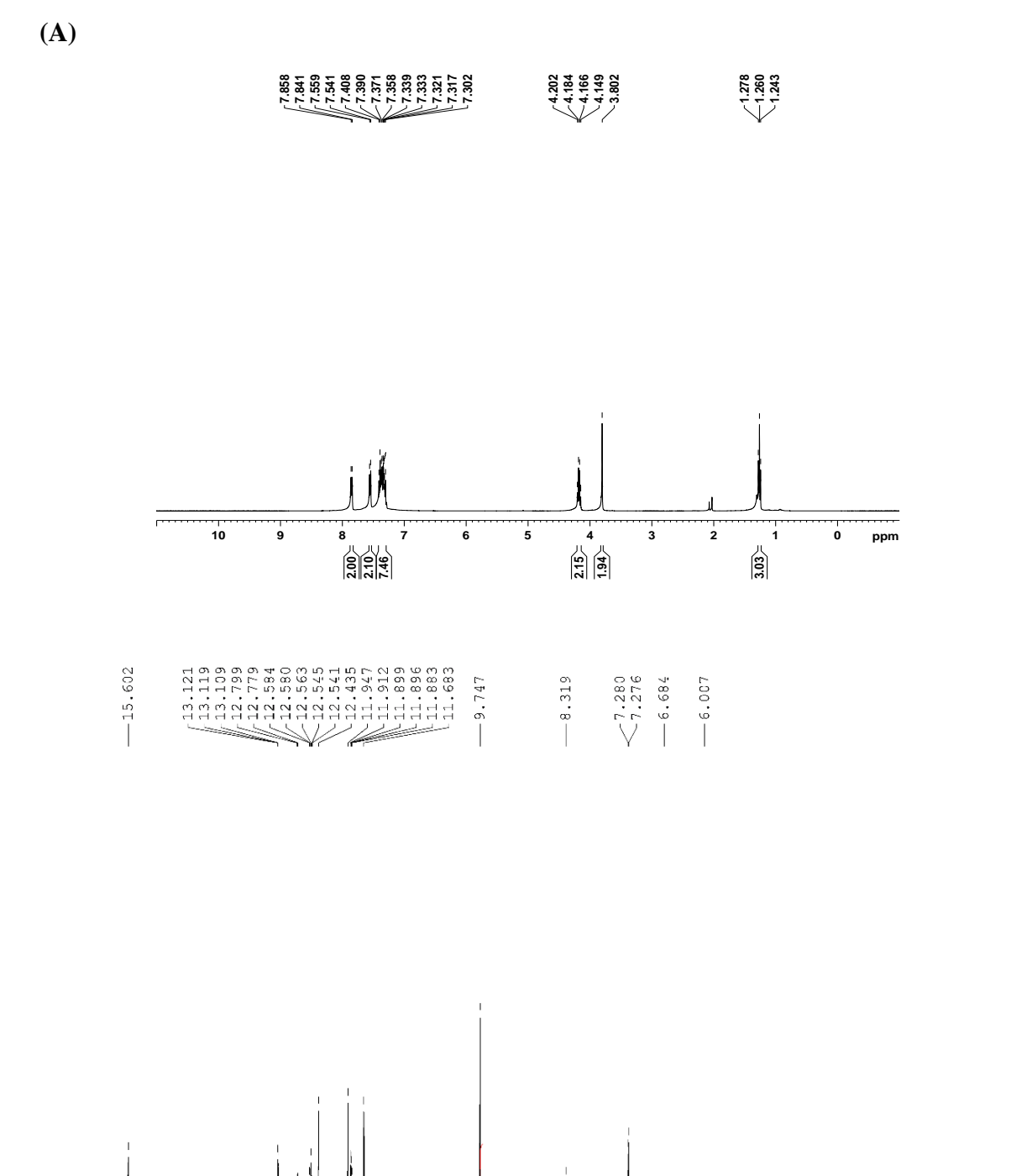


Fig. 4.1.1. A) ¹H NMR spectrum of (CDCl3, 400 MHz) of compound ethyl (2-phenyl-5-phenyl-1H-imidazole-4-yl) acetate and 2-(1H-imidazol-1-yl)-N-(pyridin-2-yl) acetamide

211

1.28

1.00

ppm

1.03 1.03 1.09 1.09 1.09

15

1.19



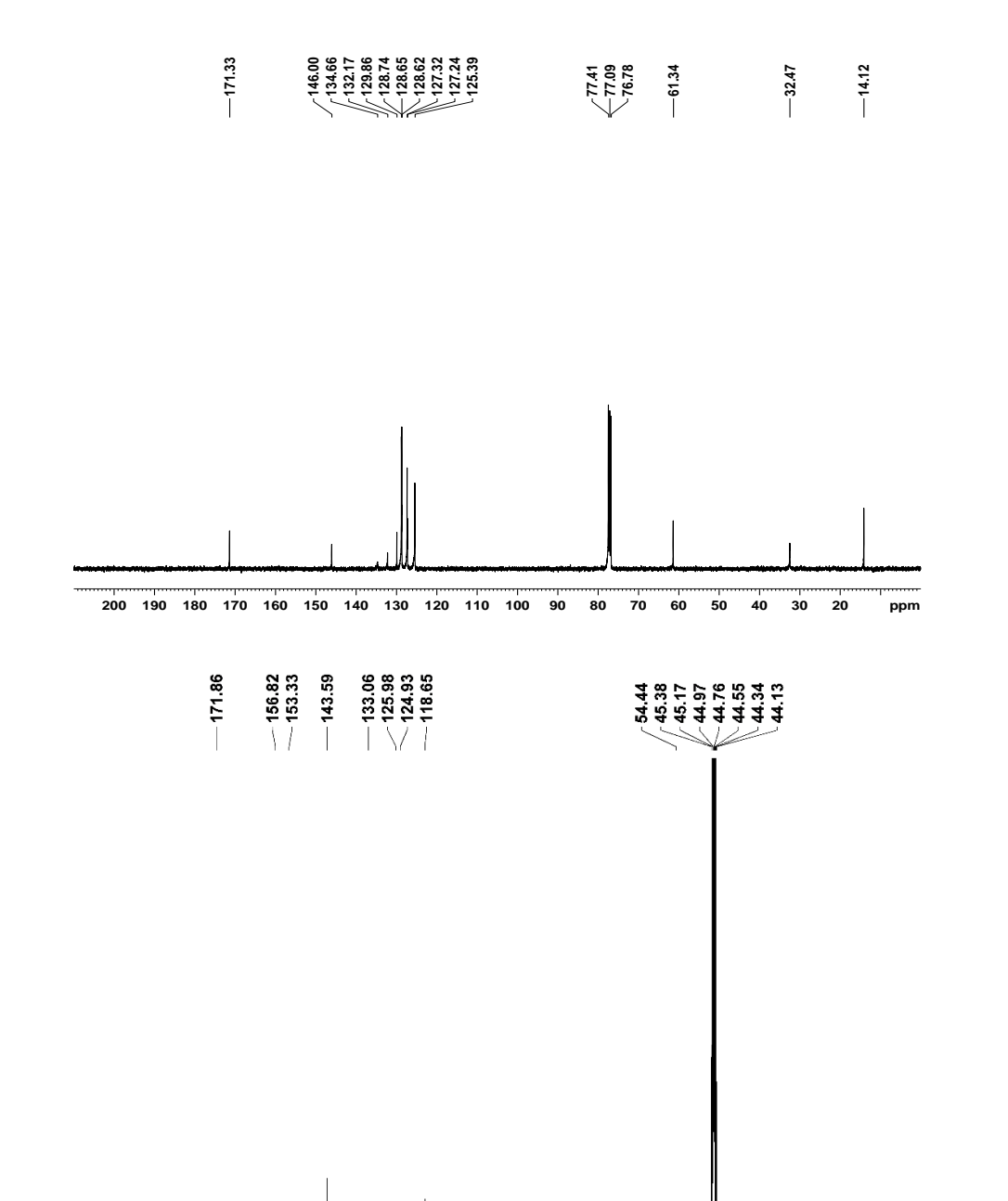


Fig. 4.1.1. B) ¹³C NMR spectrum of (CDCl3, 100 MHz) of compound ethyl (2-phenyl-5-phenyl-1H-imidazole-4-yl)acetate and 2-(1H-imidazol-1-yl)-N-(pyridin-2-yl)acetamide

4.1.2. High Resolution Mass Spectroscopy Analysis of Synthesised Compounds

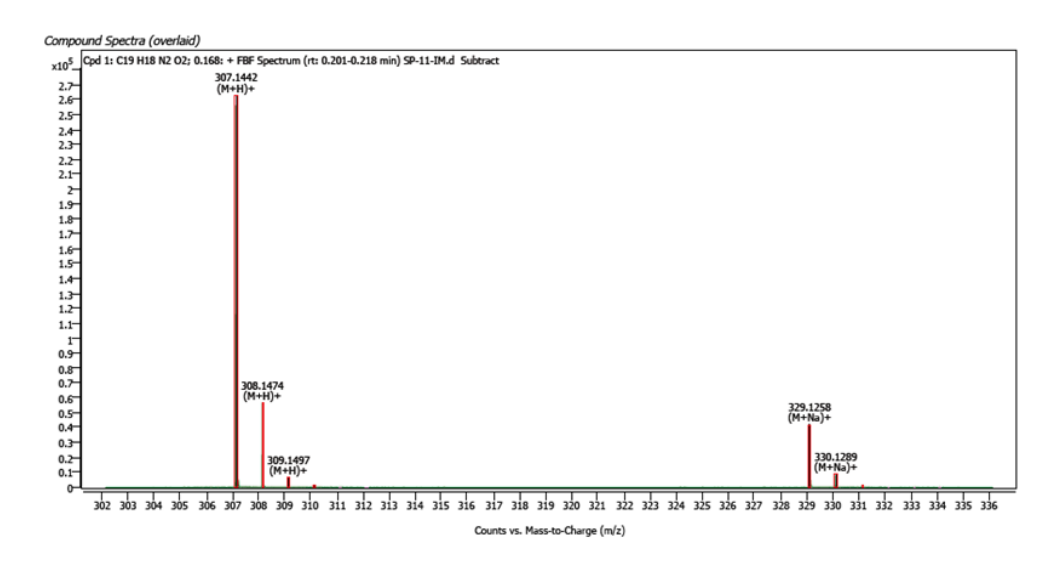
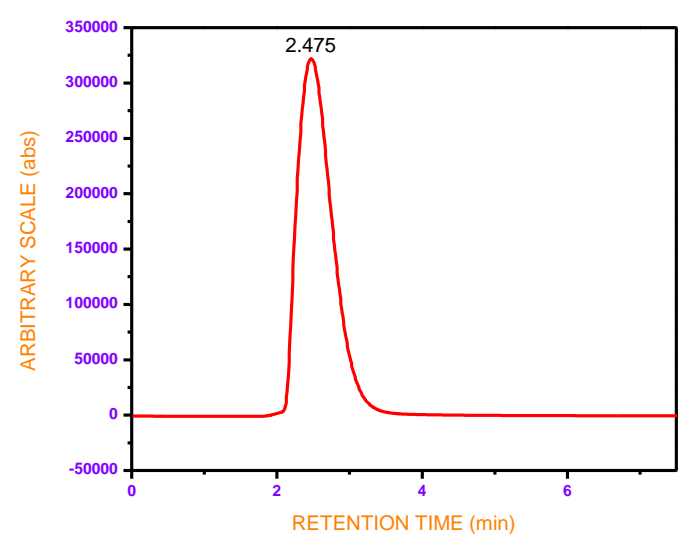


Fig. 4.1.2. High resolution mass spectra (ESI) of (2-phenyl-5-phenyl-1H-imidazole-4-yl) acetate were recorded on a Q-TOF mass spectrometer.

4.1.3. High performance liquid chromatography (HPLC) analysis of 2-(1H-imidazol-1-yl)-N-(pyridin-2-yl) acetamide compound



S.No.	Retention Time (min)	Peak Area	Peak Height	Peak Width	% Area
1	2.475	10903341.13	322378	0.535	100

Fig. 4.1.3. The high-performance liquid chromatography analysis of the synthesized compound 2-(1H-imidazol-1-yl)-N-(pyridin-2-yl) acetamide using silica gel (100-200 mesh) and methanol as eluent. The purity of the compound was found to be 100%.

4.1.4. Molecular docking validation of the synthesized compounds

The crystal structure of the human HDACs family proteins obtained from protein data bank i.e. HDAC 1 (4BKX), HDAC 2 (3MAX), HDAC 3 (4A69), HDAC 8 (3SFF), HDAC 4 (2VQM), HDAC 6 (3C5K), and HDAC 7 (3C10) were selected as the docking target. The designed structures of the compound were C1 - C14 and established HDACi (TSA) were further examined by the ligprep module of Schrödinger suite. The prepared compounds were docked with the active site of HDACs family proteins Glide module under rigid-receptor with flexible-ligand conditions in extra-precision (XP) mode using standard protocols. Protein files were done by the protein preparation wizard module.

S.no	Compound	HDAC 1	HDAC 2	HDAC 3	HDAC 8	HDAC 4	HDAC 6	HDAC 7
1.	C1	-3,423	-4.589	-5.266	-6.937	-3.491	-4.08	-3.586
2.	C2	-3.018	-5.00	-5.223	-4.355	-4.205	-4.165	-4.002
3.	СЗ	-3.149	-5.163	-4.885	-11.039	-5.004	-5.098	-5.163
4.	C4	-2.603	-5.098	-5.234	-9.021	-4.452	-4.902	-5.300
5.	C5	-2.744	-5.004	-6.053	-8.788	-4.771	-3.445	-3.362
6.	C6	-2.97	-2.756	-2.909	-5.39	-3.478	-3.21	-4.267
7.	C7	-3.042	-4.766	-3.007	-4.805	-3.395	-3.721	-04.411
8.	C8	-2.527	-4.237	-2.454	-5.367	-1.943	-3.262	-2.864
9.	C9	-3.387	-3.966	-2.747	-4.252	-2.208	-3.063	-1.203
10.	C10	-2.592	-3.769	-2.08	-3.988	-2.783	-1.282	-2.933
11.	C11	-2.904	-4.502	-3.494	-5.984	-3.477	-3.219	-1.587
12.	C12	-1.858	-4.484	-3.203	-6.858	-2.537	-3.809	-2.945
13.	C13	-2.502	-3.853	-2.684	-6.696	-3.014	-3.202	-1.74
14.	C14	-2.485	-5.173	-3.079	-5.717	-3.717	-2.996	-2.126

Table 4.1. Calculated the docking score of designed compounds.

S.no	Compound	HDAC 1	HDAC 2	HDAC 3	HDAC 8	HDAC 4	HDAC 6	HDAC 7
1.	TSA	-4.241	-2.768	-4.637	-9.322	-2,277	-4.114	-4.225
2.	SAHA	-1.817	-7.06	-3.500	-9.219	-4.388	-8.903	-5.069
3.	LBH 589.1	-4.207	-4.174	-3.905	-7.522	-3.409	-3.756	-6.782
4.	SCRIPTAID	-3.827	-5.294	-4.079	-6.782	-5.751	-3.976	-7.187
5.	BELINOSTAT	-3.484	-6.559	-3.145	-6.337	-2.179	-3.74	-3.576
6.	MS278.1	-2.991	-8.472	-4.025	-10.909	-4.512	-4.19	-7.605

Table 4.2. Docking Score for clinically tested standard Histone deacetylase inhibitor.

4.1.5 Molecular dynamics simulation (MDs) of ethyl (2, 5-diphenyl-1H-imidazole-4-yl) acetate (C3) compound

The molecular dynamics simulations were performed for HDAC enzyme-ligand complexes. The stability of protein-ligand complex was governed by RMSD analysis. The RMSD results of the HDAC family proteins and tested compound ligand complexes attained 0.2 nm to 0.4 nm deviation which manifested the C3 compounds have more stable in the HDAC family proteins. At the end of the 20 ns of time scale simulation, all the protein-ligand complexes were attaining their stable conformation. The hydrogen bond analysis of C3 compound and HDAC family proteins shows (Fig. 4.1.5). The hydrogen bond analysis showed the ethyl (2, 5-diphenyl-1H-imidazole-4-yl) acetate compound making hydrogen bond interaction with HDAC family proteins ranging from 1 to 8 hydrogen bonds. Finally, the dynamics results are well correlated with docking and in vitro studies and the compound ethyl (2, 5-diphenyl-1H-imidazole-4-yl) acetate were stable in HDAC family proteins.

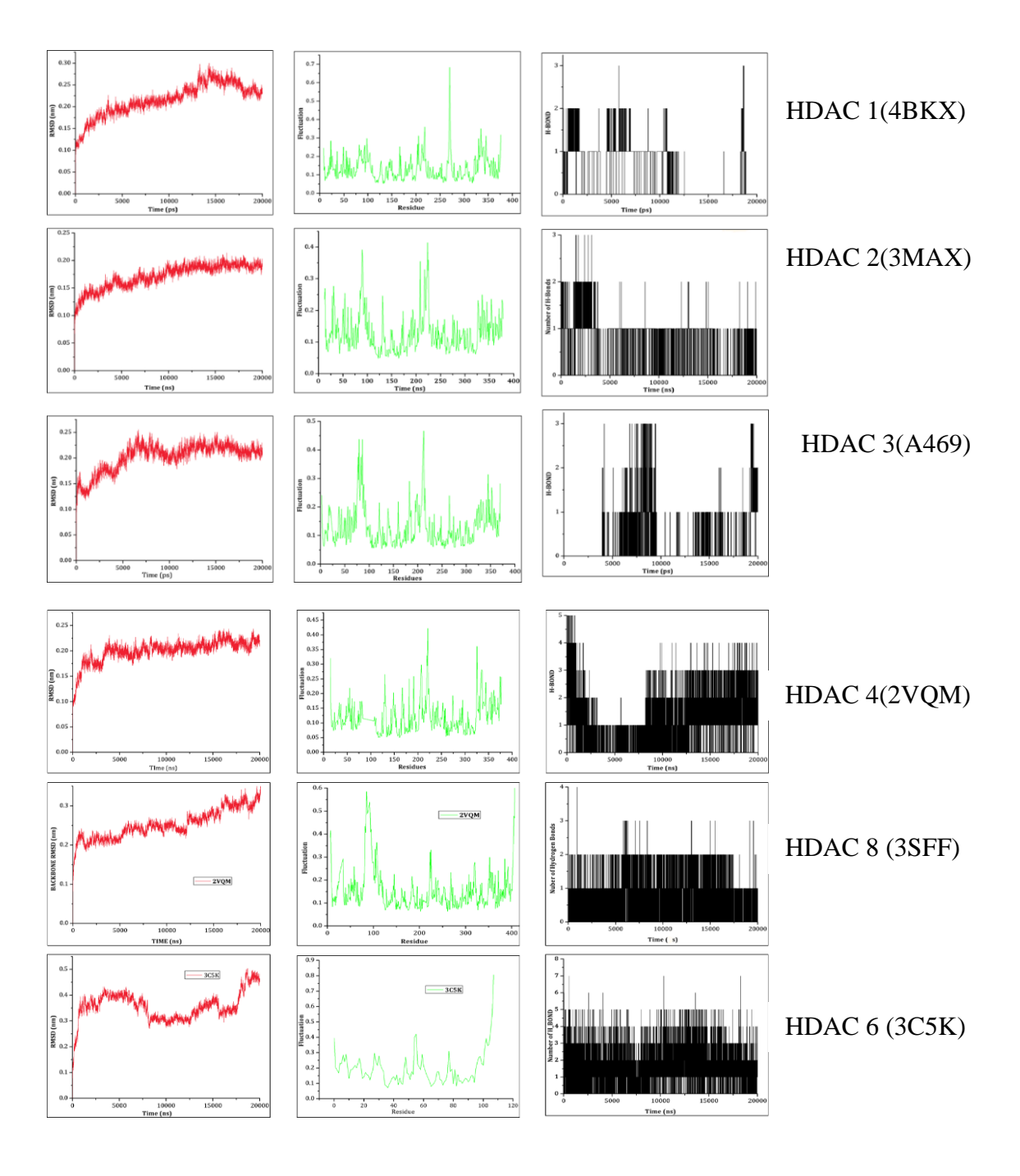


Fig 4.1.5. Root mean square deviations and total energy of protein e ligand complexes during 10 ns simulation time. The Red colours represent the backbone RMSD of protein stability. Green colours represent the RMSF of the protein residues. Black colours represent the hydrogen bond interaction of the protein-ligand complex. Figures generated by the program Gromacs 4.5.5 software.

Schematic representation of our second generation of newly designed compound

Vorinostat (SAHA)

Scheme 1: Design and Synthesis of 2-(1H-imidazol-1-yl)-N-(pyridin-2-yl) acetamide 1) TEA, DCM, RT, 5 h 2) Imidazole, K₂CO₃, THF, 50 °C, 3 h

4.1.6. Homology modelling and validation

The homology modelling of targeted proteins was performed by PRIME module (prime, version 4.1, Schrodinger, LLC, and New York-1). The geometry and energy profile were constructing by using PRIME. Furthermore, the structure was validated by using Procheck, and phi and psi torsions angles were analysed for the backbone of crystal structure of proteins, by the assist of Ramachandran plot as shown in (Fig.4.1.6). The modelled structures energy criterion was compared with huge set of known protein structures [131].

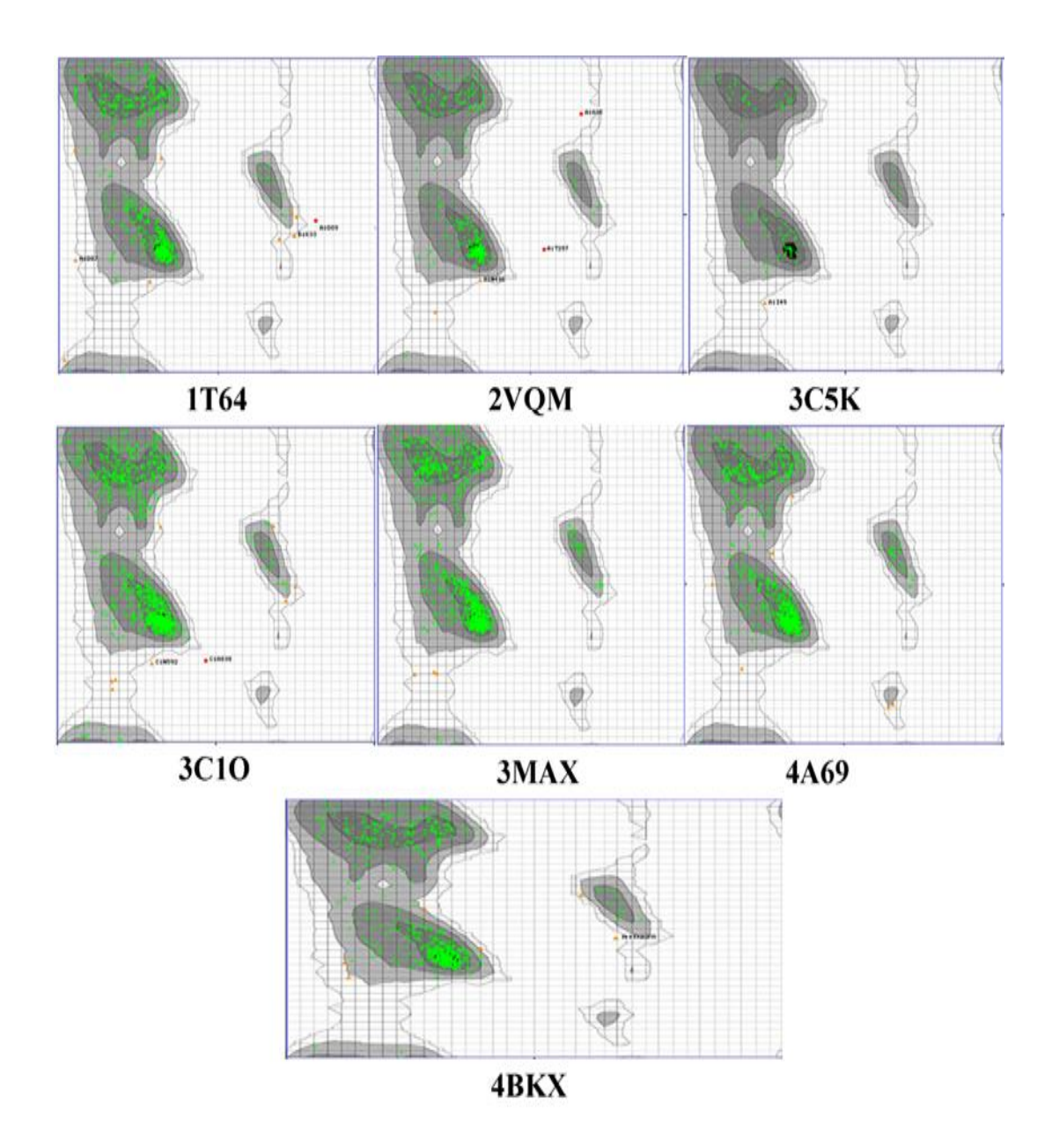


Fig. 4.1.6. The Ramachandran plot image of all PDB proteins. (Highly Preferred observations shown as GREEN, Preferred observations showed as BROWN, Questionable observations shown as RED).

PDB- ID	ERRAT	Verify 3D	PROCHECK
4A69	97.479	97.08% of the residues have averaged 3D-1D score >= 0.2	91.5% core region, 8.3% allowed region 0.2% generic, 0.0% disallowed region
1T64	91.4513	88.30% of the residues have averaged 3D-1D score >= 0.2	90.4% core region, 9.6% allowed region, 0.0% generic, 0.0% disallowed region
4BKX	93.6709	92.72% of the residues have averaged 3D-1D score >= 0.2	90.3% core region, 9.1% allowed region, 0.5% generic, 0.2% disallowed region
3MAX	94.3396	81.94% of the residues have averaged 3D-1D score >= 0.2	89.7% core region, 10.0% allowed region, 0.3% generic, 0.0% disallowed region
2VQM	90.5013	92.84% of the residues have averaged 3D-1D score >= 0.2	90.8% core region, 8.3% allowed region, 0.9% generic, 0.0% disallowed region
3C10	93.271	96.22% of the residues have averaged 3D-1D score >= 0.2	89.3% core region, 10.1% allowed region, 0.5% generic, 0.0% disallowed region
3C5K	81.8182	Fewer than 80% of the amino acids have scored >= 0.2 in the 3D/1D profile.	91.0% core region, 7.9% allowed region, 1.1% generic, 0.0% disallowed region.

Table 4.3. Calculated the amino acid and energy level of protein using ERRAT, and PROCHECK

4.1.7. Molecular docking analysis

Molecular docking used to estimate the stability of targeted proteins and ligand interactions. We docked in the active site of 1T64, 2VQM, 3C5K, 3C10, 3MAX, 4BKX, 4A69 proteins and the known HDACi TSA. Glide XP docking affirms that the identified our compounds were bound to the active site of targeted protein and precise many amino acid interactions. The synthesized compounds, 2-(1H-imidazol-1-yl)-N-(pyridin-2-yl) acetamide shared the common pharmacophore like SRM, Linker, CU and ZBG groups which is shared by the different classes including the FDA approved established classical HDACi. Our experimental data demonstrate that CU and ZBG group is vital for HDACi which is essential for a ligand to trigger chromatin remodelling by modulation of highly expressed HDAC enzymes as shown in (Fig.4.1.7). Finally, the tested compounds were

selected based on the binding affinity and the numbers of interacting residues. After that, the selected compounds were further validated by computational studies [132, 133].

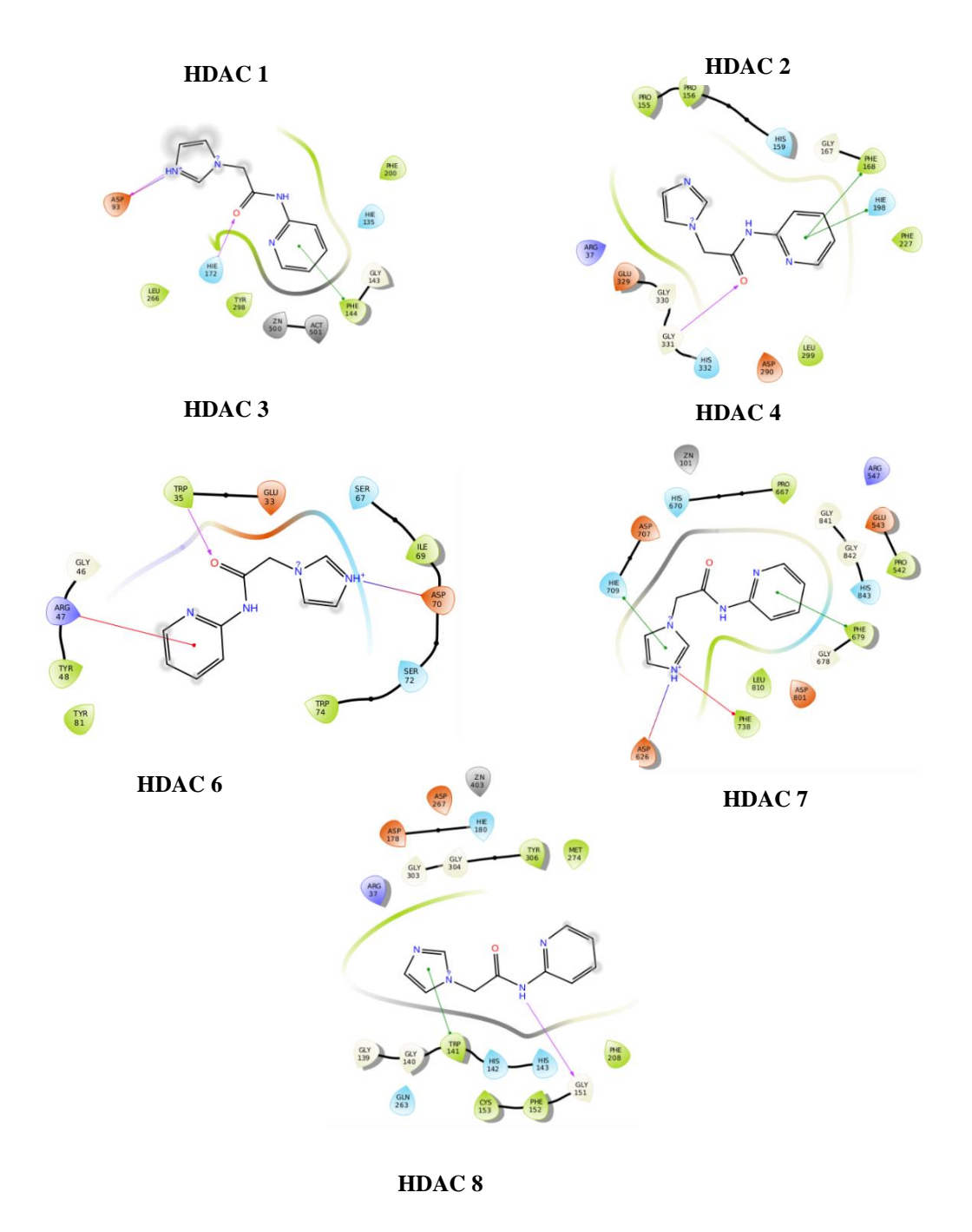


Fig. 4.1.7. 2D representation of the interactions of Compound C3 with the amino acid residues of HDACs (PDB ID): (a) HDAC 1 (4BKX); (b) HDAC 2 (3MAX); (c) HDAC 3 (4A69); (d) HDAC 8 (3SFF); (e) HDAC 4 (2VQM); (f) HDAC 6 (3C5K); (g) HDAC 7 (3C10). Pink colour represents the hydrogen bond interaction, green colour represents the pi-pi interaction, red colour represents the pie cation interaction, and red-with-blue combination represents the salt bridges.

4.1.8. DFT analysis and salvation energy calculation

Density functional theory was done through the Jaquar, version 7.8 (Schrödinger, LLC, New York, NY, 2015- 4. Hybrid DFT with Becke's three-parameter functional and the Lee– Yang–Parr correlation functional (B3LYP) (Becke, 1993; Lee, Yang, & Parr, 1988)-/-6-31G** basic set level (Binkley, Pople, & Hehre, 1980; Pietro et al., 1982) was used to completed the geometry optimization of the preferred ligands. The B3LYP hybrid functional is admired to evaluate the properties and reactions of organic molecules. Furthermore, the ligands molecular electrostatic potential map (MESP), frontier molecular orbitals (i.e. Highest Occupied Molecular Orbitals (HOMOs) and Lowest Unoccupied Molecular Orbitals (LUMOs), and HOMO–LUMO energy gap (HLG) were calculated using the jaguar model as shown in Table 4.4 and Fig. 4.1.8.

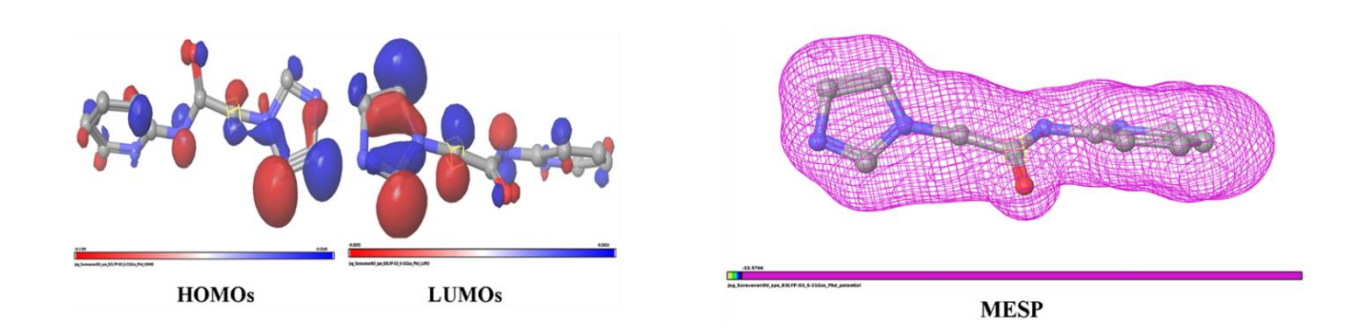


Fig. 4.1.8. MESP mapping of 2-(1H-imidazol-1-yl)-N-(pyridine -2-yl) acetamide compound

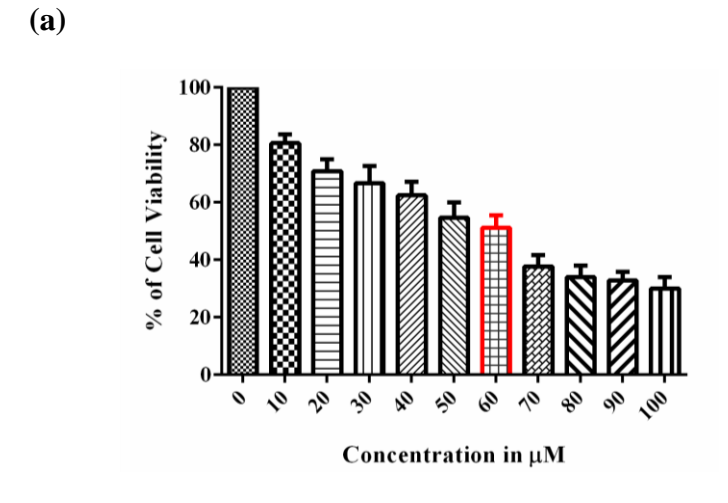
Compound	Solvation	HOMOs	LUMOs	MESP
	Energy(kcal/mol)	(kcal/mol)	(kcal/mol)	(kcal/mol)
2-(1H-imidazol-1-yl)-N- (pyridin-2-yl)acetamide	-6.48	-0.24704	-0.21127	-34.45

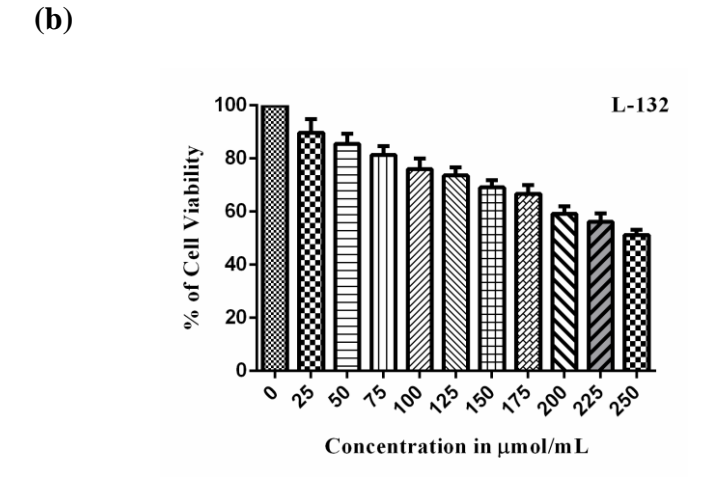
Table. 4.4. HOMO, LUMO, HLG and MESP ranges from lead molecules in DFT calculation.

4.2. Biological evaluation of the synthesized compounds

4.2.1. Cytotoxicity assay of compounds against in A549 cells using MTT

To evaluate the inhibitory effects of synthesized compounds on A549 cells and L-132 human normal lung epithelial cell lines, to determine the significant IC₅₀ values at the specific time points. We first aimed to determine the effect of ethyl (2-phenyl-5- phenyl-1H-imidazole-4-yl) acetate (C3) and 2-(1H-imidazol-1-yl)-N-(pyridin-2-yl) acetamide individually in A549 cells. Cell viability was determined by MTT assay and the results are shown in (Fig 4.2.1 (a)). Cell viability was significantly reduced in 12 and 24 h treatment. Almost 50% of cell death was observed at 60 µM concentration of C3 compound and it was fixed as IC₅₀ concentration. Treatment of the C3 compound decreased the cell viability of A549 lung cancer cells in a concentration dependent manner. From these results the IC₅₀ value of C3 compound were calculated as equal to 60 µM. (Fig 4.2.1 (b)) showed that 2-(1H-imidazol-1-yl)-N-(pyridin-2-yl)acetamide at 150 μM concentration near to 50% of cells only viable. As shown in (Fig 4.2.1 (c)) compounds suppressed the growth of normal lung epithelial cells L-132 in both dose and time dependent manner. The IC₅₀ was value of the treated compound was detected at 12, and 24h treatment. From these results, half maximal inhibitory concentration of 60 µM, 150 µM, and 225 µM. respectively. Hence, we selected these concentrations to maximize the effects of dose level to identify the action of the compounds.





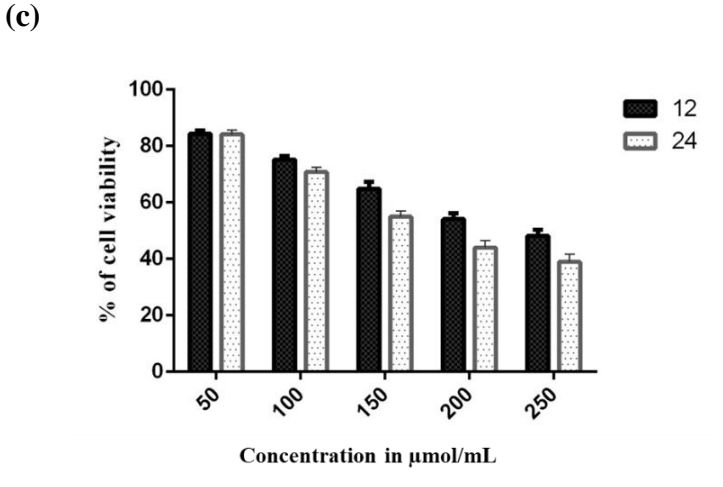


Fig 4.2.1. Cell viability was determined by using MTT in a time and dose-dependent manner for 12, 24, and 48 h. (a) ethyl (2-phenyl-5- phenyl-1H-imidazole-4-yl)acetate (C3), (b) 2-(1H-imidazol-1-yl)-N-(pyridin-2-yl) acetamide, and (c) Cross examination of 2-(1H-imidazol-1-yl)-N-(pyridin-2-yl) acetamide Compound treated in normal lung epithelial L-132 cells. All experiments were done in triplicates, and error bars represent the mean value ±SD.

The findings of the *in-vitro* cytotoxicity activities confirm the binding of the complexes to DNA, which consequently leads to cell death. Imidazole based heterocyclic compounds were designed to employ efficient inhibition of HDAC enzymes followed by synthetic methodologies in pure form was implemented and was tested for its inhibitory activity against HDAC enzymes. The structural features of the imidazole ring with desirable electron rich characteristics are beneficial for imidazole derivatives to readily bind with a variety of enzymes and receptors in the biological system. Molecular docking studies revealed that the binding interactions of the C3 compound had significant binding ability with the active site of the HDAC enzyme. But it exhibited the limited isoform efficacy. We believe that these results encourage synthesis of new and similar compounds (more selective, more active and non-toxic derivatives). In most of the structural activity relationship studies, to investigate the role of ZBG, a considerable effort was being used in searching for alternates to hydroxamic acid and to some extend the linker too. To better understand the SAR and discover novel HDACs inhibitor with high potency and good safety profiles. Our results indicate that 2-(1H-imidazol-1-yl)-N-(pyridin-2-yl) acetamide compounds effectively inhibit the proliferation of cells when compared than ethyl (2phenyl-5- phenyl-1H-imidazole-4-yl) acetate. In the present study, evidence of cytotoxicity induction was obtained for the compound. Further, we persisted in A549 cells.

4.2.2. Morphological changes of A549 cells treated with 2-(1H-imidazol-1-yl)-N-(pyridin-2- yl) acetamide compound using phase contrast microscopy

After the successful detection of the IC₅₀ concentration, Microscopic observations of A549 cells treated with 2-(1H-imidazol-1-yl)-N-(pyridin-2- yl) acetamide compound revealed significant morphological changes when compound used at higher concentrations (250 μ M/mL). A549 cells showed a loss of cell extensions, rounding up and detachment, apoptotic blebbing, and reduction in size as well as in cell density was observed when

compared to untreated A549 cells [Fig. 4.2.2]. These results revealed that the imidazole based 2-(1H-imidazol-1-yl)-N-(pyridin-2- yl) acetamide compound has potentially inhibited A549 cells when compared with L-132 normal human lung cells.

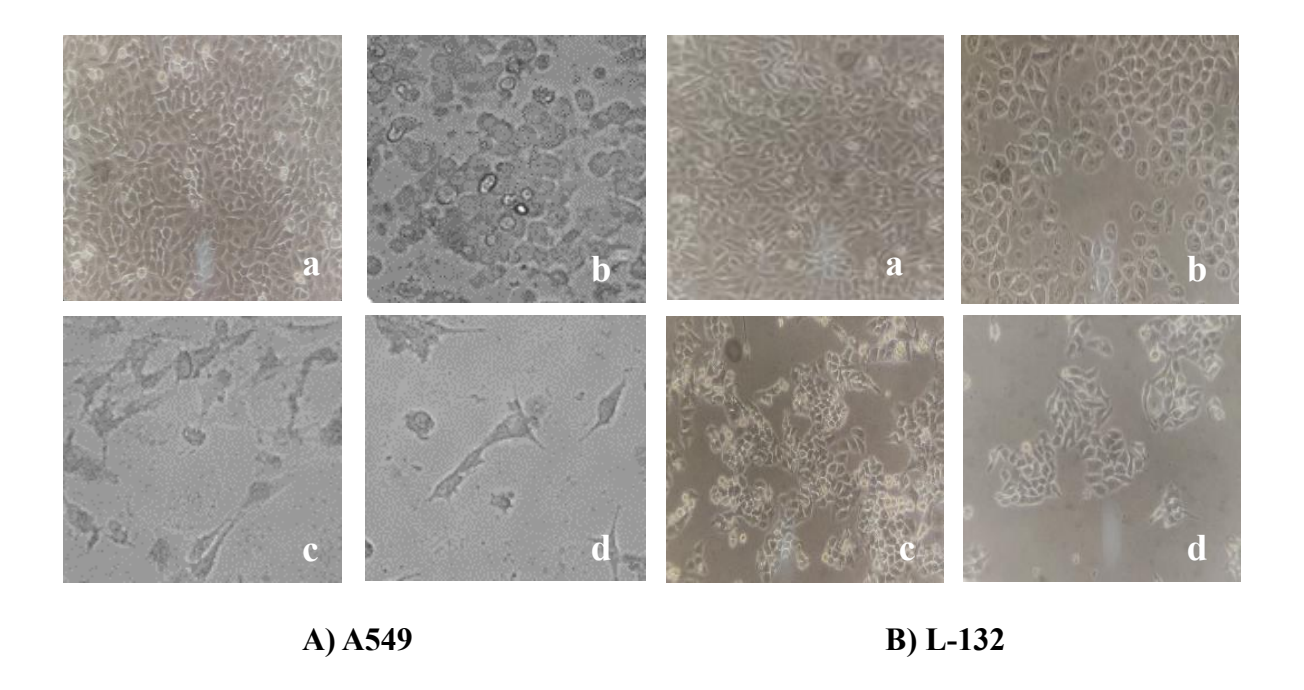


Fig 4.2.2 Effect of 2-(1H-imidazol-1-yl)-N-(pyridin-2- yl) acetamide on morphological changes in A549 and L-132cells detected by phase contrast microscopy.

4.2.3 Clonogenic (CFU) assay

Colony forming unit (CFU) assay was performed to assess the capacity of a single cell to form colonies under the influence of 2-(1H-imidazol-1-yl)-N-(pyridin-2- yl) acetamide compound. This assay is a means to measure the ability of each cell to undergo continuous proliferation [134]. Therefore, we assessed the effect of 2-(1H-imidazol-1-yl)-N-(pyridin-2- yl) acetamide on colony formation of living A549 cells. Cells were treated individually with various concentrations of in 2-(1H-imidazol-1-yl)-N-(pyridin-2- yl) acetamide compound. We were able to observe significant colony reduction in colonies 50 μ M, 100 μ M, 150 μ M, 200 μ M, 250 μ M (Fig. 4.2.3).

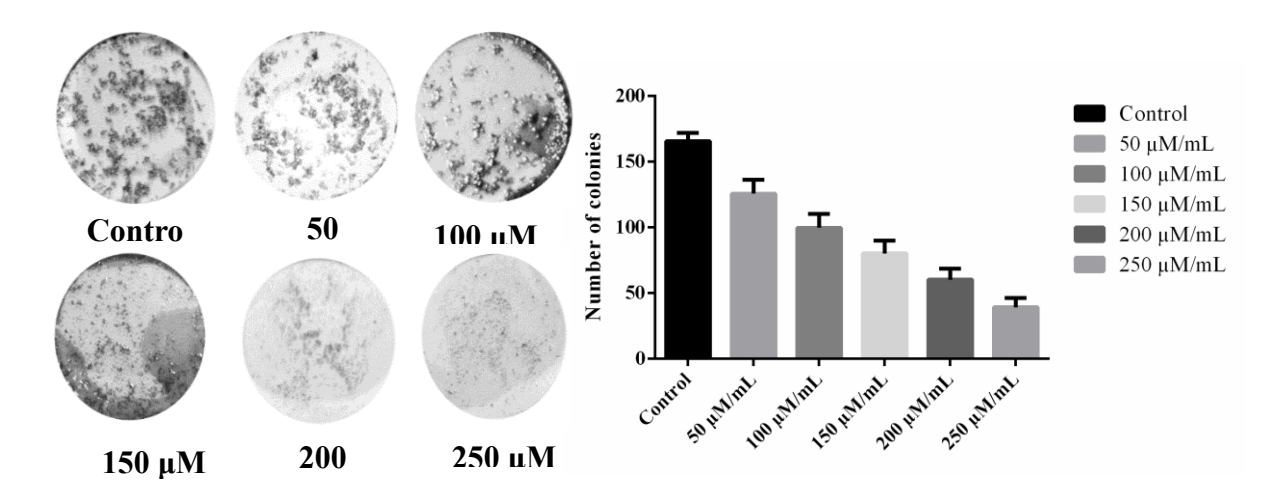


Fig 4.2.3 Colony Formation Unit Assay. Dosage-dependent CFU assay was performed for 2-(1H-imidazol-1-yl)-N-(pyridin-2- yl) acetamide compound with varied doses of drugs. We were able to observe significant reduction in colony formation and cell abundance.

4.2.4. DNA fragmentation assay

DNA fragmentation is accredited as the distinctive identification of apoptosis and was characterized by the breakdown of chromosomal DNA into oligonucleosomal fragments [135]. After Clonogenic assay, the apoptotic capability was analysed by performing the DNA fragmentation assay. Cells were treated with half maximal inhibitory concentration of the 2-(1H-imidazol-1-yl)-N-(pyridin-2- yl) acetamide compound in A549 and L-132 cells for 24 h and 48 h. From the results revealed that there was no changes observed in the control A549 cell line and normal human epithelial lung cells compared with treated cancer cells. As shown in Fig. 4.2.4 which substantiates the apoptotic potential of 2-(1H-imidazol-1-yl)-N-(pyridin-2-yl) acetamide compound against cancer.

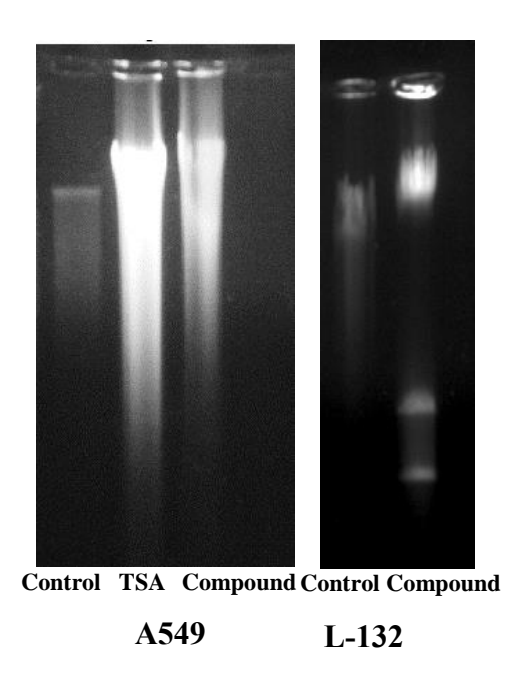


Fig 4.2.4. DNA fragmentation. DNA laddering pattern following treatment of A549 cells with 2-(1H-imidazol-1-yl)-N-(pyridin-2-yl) acetamide (150 μ M) and TSA (4.0 μ M) for 12 h and exhibiting the DNA cleavage of the treated compound in L-132 cells for 48 h. with 2-(1H-imidazol-1-yl)-N-(pyridin-2-yl) acetamide significantly increased the typical internucleosomal DNA cleavage as indicated by DNA laddering.

4.2.5. Histone deacetylase enzyme colorimetric activity in A549 cells

After the successful detection of DNA cleavage by DNA fragmentation assay, for checking the role of histone deacetylase regulation in A549 cells. We need to measure the total HDAC activity using IC₅₀ concentration of the 2-(1H-imidazol-1-yl)-N-(pyridin-2-yl) acetamide and TSA used as a positive control. TSA is a broad deacetylase inhibitor of most members of the HDAC family. Dynamic acetylation and deacetylation balance occur via HDAC and HAT activity. An elevation level HDAC activity is more important than a reduction of HAT activity [136]. In the present study, our data suggested that the tested compound are more potent than TSA in inhibiting HDAC activity (Fig 4.2.5). The acetamide derivatives containing imidazole compound have been reported to exhibit higher enzyme inhibitory actives than others. The HDAC activity of 2-(1H-imidazol-1-yl)-N-(pyridin-2-yl)

acetamide treated cells was significantly decreased in comparison to standard HDAC inhibitor TSA treated and control A549 cells.

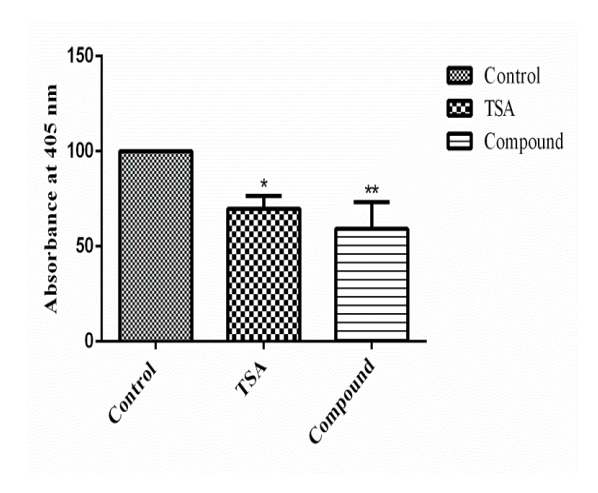


Fig 4.2.5. To determine the inhibitory mechanism of the tested compound on histone deacetylase activity.

4.2.6. Effect of 2-(1H-imidazol-1-yl)-N-(pyridin-2-yl) acetamide regulating various classes of HDACs

The total HDAC colorimetric assay result gave the sign that 2-(1H-imidazol-1-yl)-N-(pyridin-2-yl) acetamide compound significantly arrested the HDAC activity and could be a strong HDACi. Further, we checked the different classes of HDAC mRNA and protein expressions after the treatment with tested compound. The result showed that 2-(1H-imidazol-1-yl)-N-(pyridin-2-yl) acetamide treated cells reduced the mRNA expression of all classes of zinc dependent histone deacetylase family Classes I, II and IV. Class I HDACs (1, 2, 3 and 8) and class II HDACs (4-7, 9 and 10) are reported to have crucial roles in tumorigenesis. However, the subtypes of classes I and II were strongly reduced the by 2-(1H-imidazol-1-yl)-N-(pyridin-2-yl) acetamide compound compare than class IV HDACs as shown in (Fig 4.2.6 (A-D)). From the results revealed that strong inhibition of class I and II HDACs and moderate inhibition of class IV HDACs by tested compound might be the possible mechanism for antineoplastic activity. The results were intensely supported by the

protein expression of Class I and II HDACs (Fig 4.2.6 (E)). The downregulation of mRNA and protein expressions of 2-(1H-imidazol-1-yl)-N-(pyridin-2-yl) acetamide compound were comparable to the standard HDAC inhibitor TSA.

A)

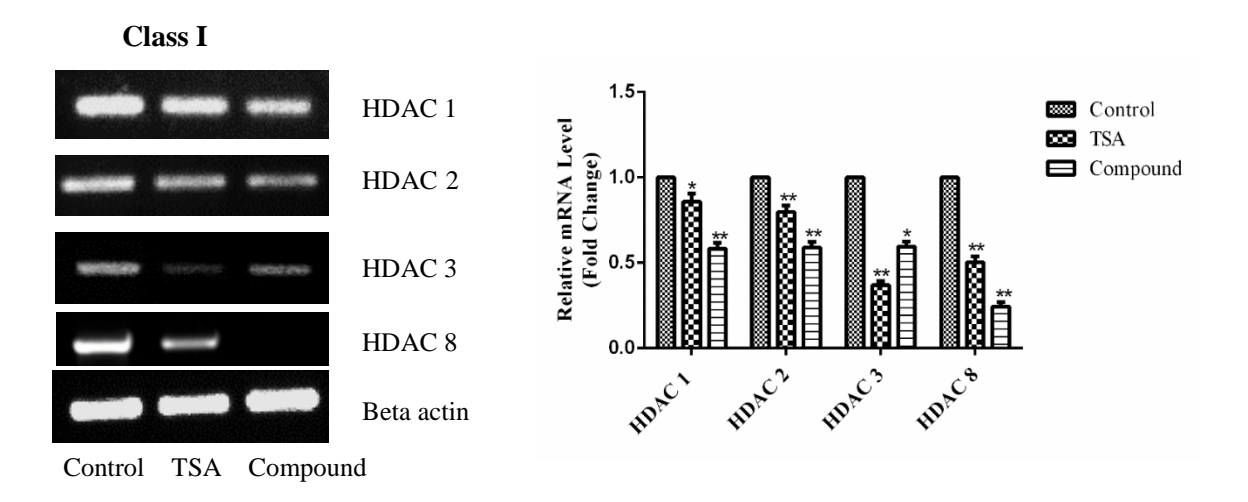
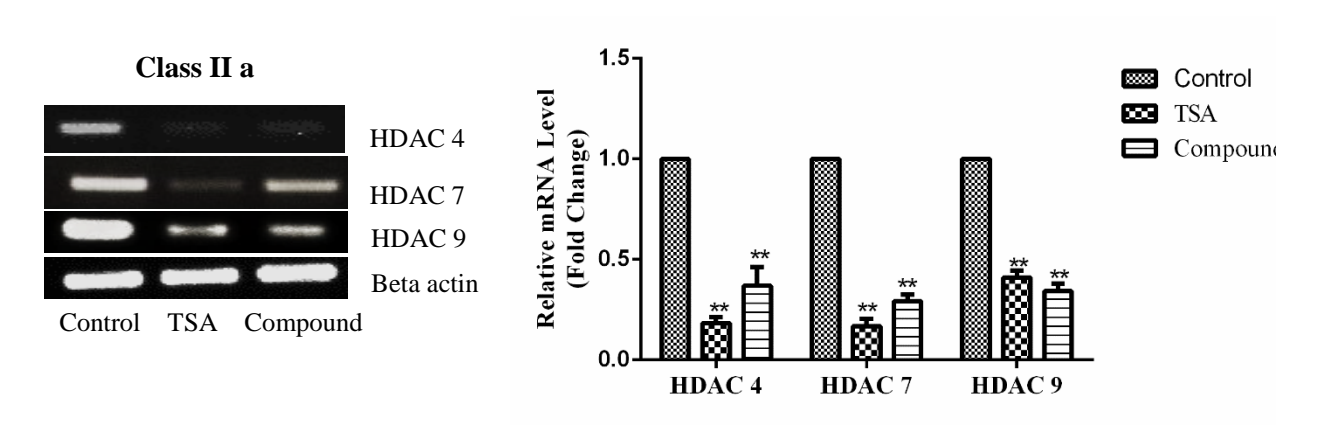
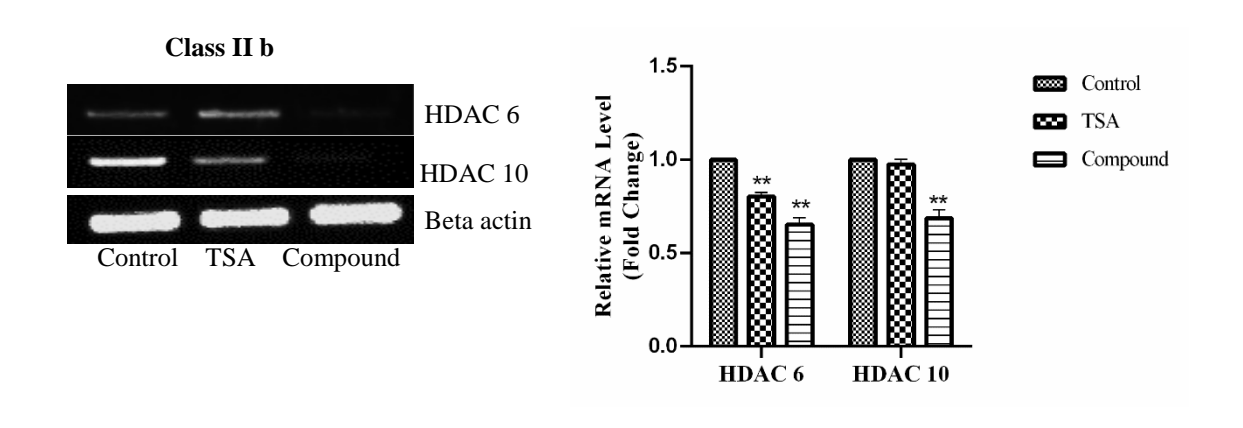


Fig 4.2.6. Effect of 2-(1H-imidazol-1-yl)-N-(pyridin-2- yl) acetamide and TSA in the inhibition of different classes of HDACs in A549 cells. **A)** mRNA expression of Class –I Histone deacetylase enzyme (HDACs 1, 2, 3, and 8) by RT-PCR. β actin served as an internal control.

B)



C)



D)

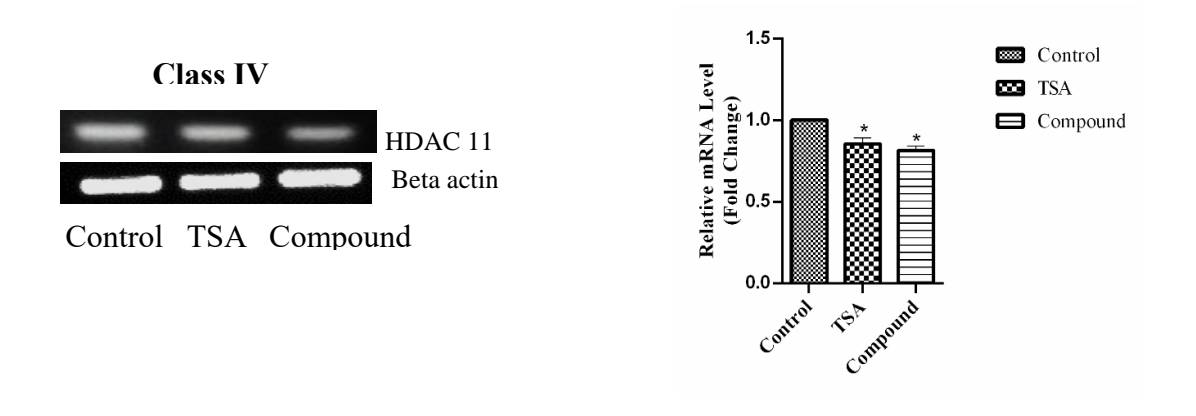
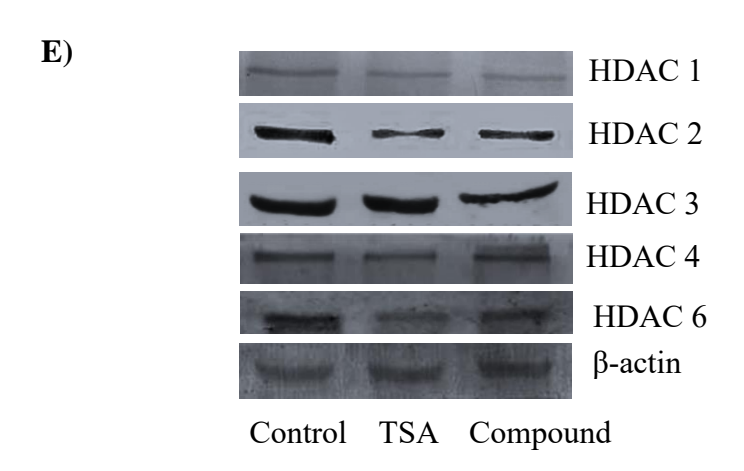


Fig 4.2.6. B) Total mRNA expression of Class II- a (4, 7, and 9), Class II -b (6, and 10), and C) Class IV (11) by RT-PCR. β -actin was used as an internal control. (*P < 0.05 and **P < 0.01).



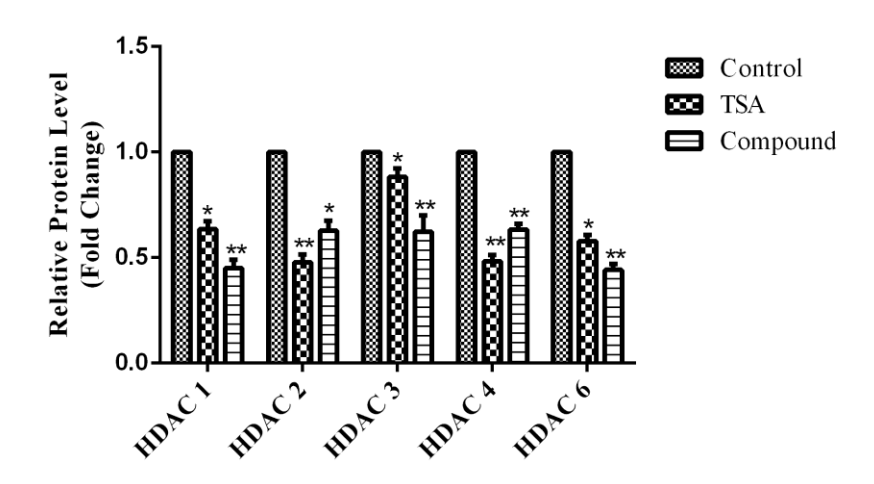


Fig. 4.2.6. E) Western blotting analysis of histone deacetylase 1, 2, 3, 4, and 6 protein expression. β -actin was used as an internal control. Data represent mean values \pm SD. (*P < 0.05 and **P < 0.01).

4.2.7. 2-(1H-imidazol-1-yl)-N-(pyridin-2-yl) acetamide increase the acetylation State of Histone H3 and H4

Histone acetylation appears to play an important role in transcriptional regulation. The genetic special effects of histone deacetylase inhibitors are thought to be associated in part with modifications of the acetylation state of histone. In general, increased levels of histone acetylation (hyperacetylation) are associated with the increased transcriptional activity, whereas decreased levels of acetylation (hypo acetylation) are associated with the repression of gene expression [137]. In this study we have examine the effects of 2-(1H-

imidazol-1-yl)-N-(pyridin-2-yl) acetamide and TSA on the acetylation of histone H3 and H4 proteins when compared to control A549 cells. Western blot analysis of isolated histones showed the acetylated forms of histones H3 and H4.

Our results suggested that in acetylated histones H3 expression was significantly increased when compared to control cells. Whereas tested compound exhibited increased expression compared to standard drugs. Histone H4 expression in 2-(1H-imidazol-1-yl)-N-(pyridin-2-yl) acetamide highly expressed when compared to standard drugs as well as to the control A549 cells. Hyperacetylation of histones H3 and H4 was observed following tested compound and TSA treatments. Interestingly, hyperacetylation protein expression was higher in 2-(1H-imidazol-1-yl)-N-(pyridin-2-yl) acetamide compound than TSA-treated A549 cells (Fig 4.2.7). Thus, our results clearly revealed that 2-(1H-imidazol-1-yl)-N-(pyridin-2-yl) acetamide induced the activity of acetylated histones.

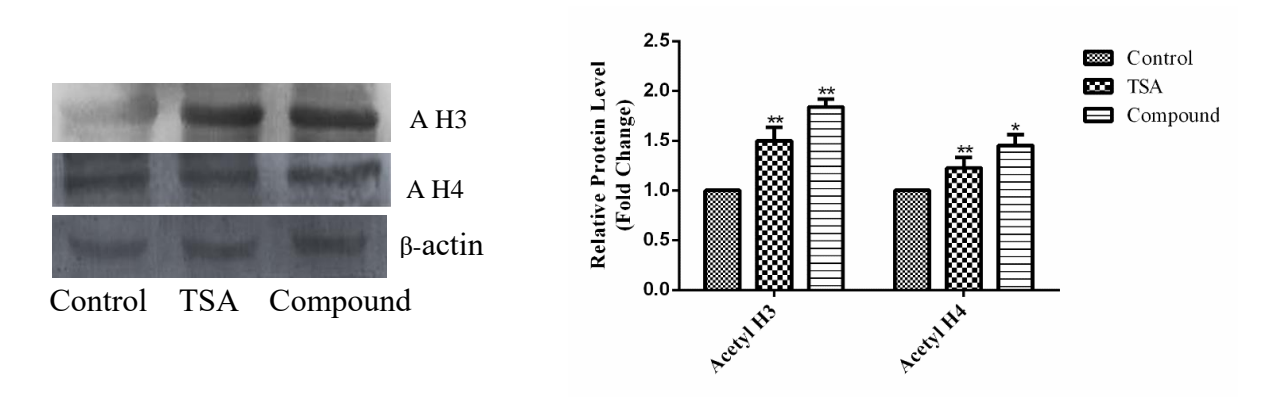


Fig 4.2.7. Western blot analysis of hyperacetylation in acetyl histones H3 and H4 in A549 cells and densitometry analysis of hyperacetylation. Protein bands were normalized to β-actin. Data represent mean values \pm SD. (*P < 0.05 and **P < 0.01).

4.2.8 Effect of tested compound on the expression of p53 and p21 in A549 cells

Alterations in the tumour suppressor gene p53 lead to impaired cell cycle control, allowing for the development and growth of tumours. The p53 protein mediates cell cycle

arrest and apoptosis in response to chemical- or radiation induced DNA damage by modulating the expression of the target genes involved in these processes. Indeed, absence of functional p53 leads to defects in these pathways such that subsequent cell growth arrest and death are impaired, further allowing development and growth of tumours. Mutation of the tumour suppressor gene p53 is the most frequent genetic alteration observed in human cancer [138]. On the other hand, p21 was reported to be specifically cleaved by CASP3-like caspase, which leads to activation of CDK2, and then activates downstream caspase leading to programmed cell death [139]. p21 is regulated by both p53-dependent and p53independent mechanisms, but the p53-dependent p21 pathway plays a critical role in cell cycle arrest and prevents cellular DNA synthesis in response to DNA damage [140, 141]. p21 can interact with proliferating cell nuclear antigen (PCNA), a DNA polymerase accessory factor, and act as a regulatory role in S phase DNA replication and DNA damage repair [142]. p21 (also known as p21WAF1/CIP1) is a member of the Cip/Kip family of cyclin-dependent kinase inhibitors, and the expression of p21 is tightly regulated at the transcriptional and post-transcriptional levels [143]. As shown in Fig. 4.2.8. A and B, the gene expression of p53 and p21 were significantly upregulated by treatment with the test compound.

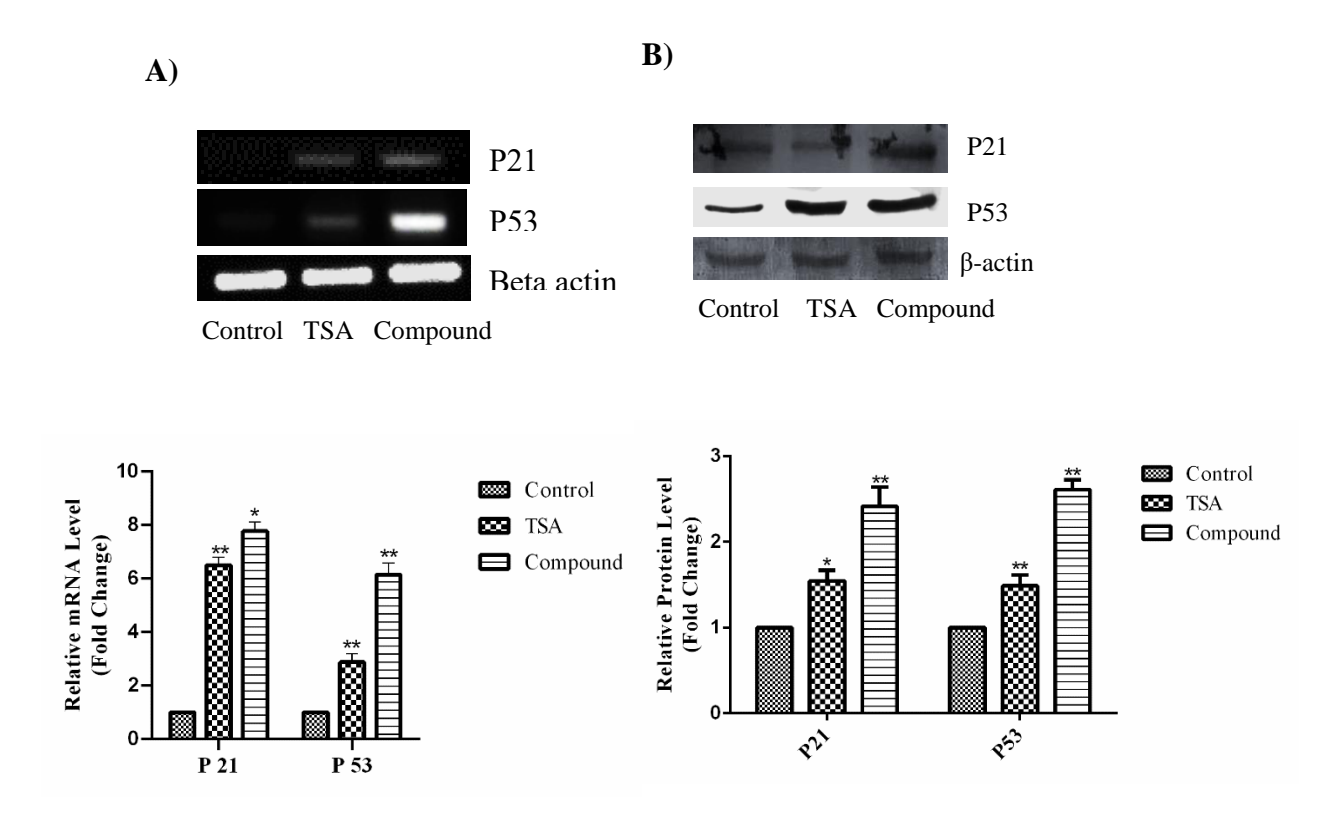


Fig 4.2.8. A) p53, p21 mRNA expression in A549 cells detected by RT-PCR. B) Western blot analysis of protein levels and the fold increase in A549 cells after exposure to the tested compound. Protein bands were normalized to β-actin. *P < 0.05 and **P < 0.01.

4.2.9. Induction of cell cycle arrest by 2-(1H-imidazol-1-yl)-N-(pyridin-2-yl) acetamide in A549 cells

Cell cycle is a cyclic process of cell division. Induction of cell cycle arrest may be a strategy for cancer therapy. In order to establish the ability of tested compound and TSA to induce apoptosis was related to cell cycle arrest, the cell cycle distribution of A549 cells was determined by flow cytometer after treatment for 24 h. To discover the inhibition of A549 cell growth arrest observation linked with cell cycle arrest. We treated with TSA as a positive control and 2-(1H-imidazol-1-yl)-N-(pyridin-2-yl) acetamide. Form the results suggested that the proportion of cells at G2-M phase were increased in the tested compound

as shown in Fig. 4.2.9. Furthermore, the proportions of sub-Go/G1 phase were increased by 2-(1H-imidazol-1-yl)-N-(pyridin-2-yl) acetamide and TSA

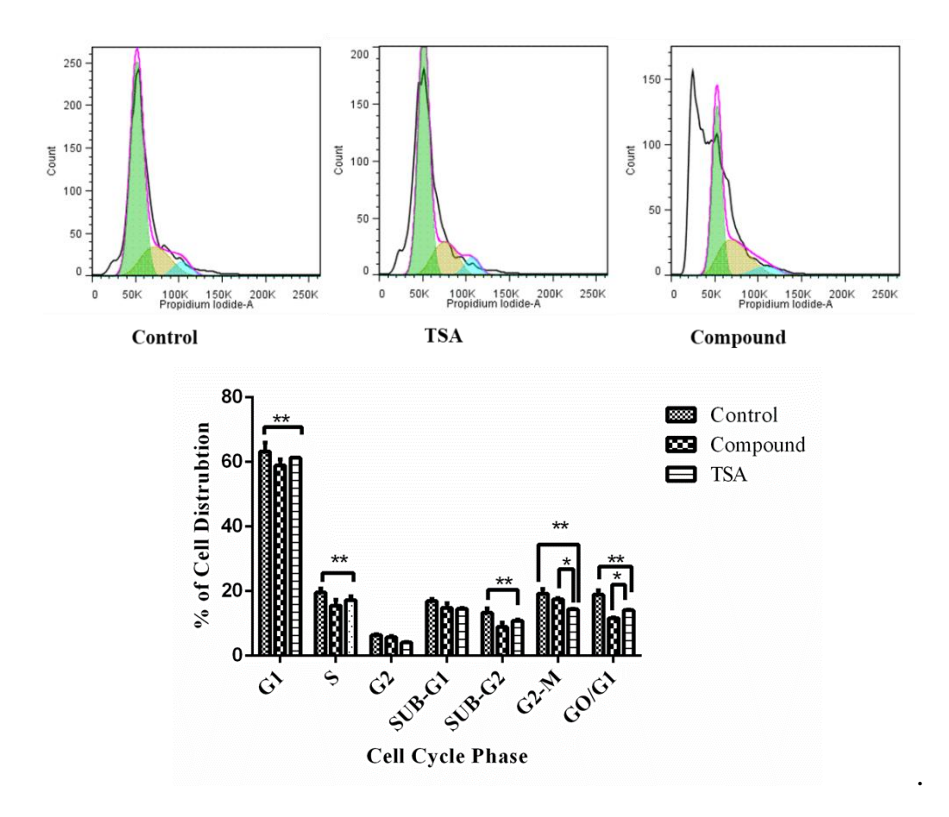


Fig. 4.2.9. Effect of tested compound on cell cycle analysis in A549 cells. The cell cycle profile was measured by flow cytometry. Bar chart displaying in the percentage of cells in each phase (*P 0.01).

4.2.10. Effect of 2-(1H-imidazol-1-yl)-N-(pyridin-2-yl) acetamide inhibits Tumour necrosis factor (TNF-α) mediated Cyclooxygenase (COX-2) expression

The characteristics of cancer cells, such as invasiveness are affected by the tumour microenvironment. Several studies have shown that interleukin (IL)-6 and tumour necrosis factor (TNF)-α regulate the proliferation of lung cancer. (TNF-α) is a major cytokine involved in inflammation and immunity [144]. Interleukin-8 is a potent angiogenic factor in several cancers including NSCLC and is associated with metastasis. Elevated IL-8 is correlated with angiogenesis, tumour progression and poor survival in NSCLC [145]. COX-2 is responsible for play a critical role in tumour growth, because they reduce apoptotic cell

death, stimulate angiogenesis and inflammation. Inflammatory cytokines can contribute to the high level of the COX-2 expression in inflamed cells and tissue. We investigated the effect of 2-(1H-imidazol-1-yl)-N-(pyridin-2-yl) acetamide on TNF- α , IL-6, IL-8, and its target gene COX-2 mRNA expression in A549 cells. An exposure of cells the tested compound diminished the expression of COX-2 and TNF- α mRNA gene (Fig.4.2.10). These results suggested that the tested compound possesses an inhibitory effect on the COX-2 activation pathway. And the decreased level of inflammatory cytokines (TNF- α , IL-6, IL-8) indicates the inhibition of cell growth and angiogenesis.

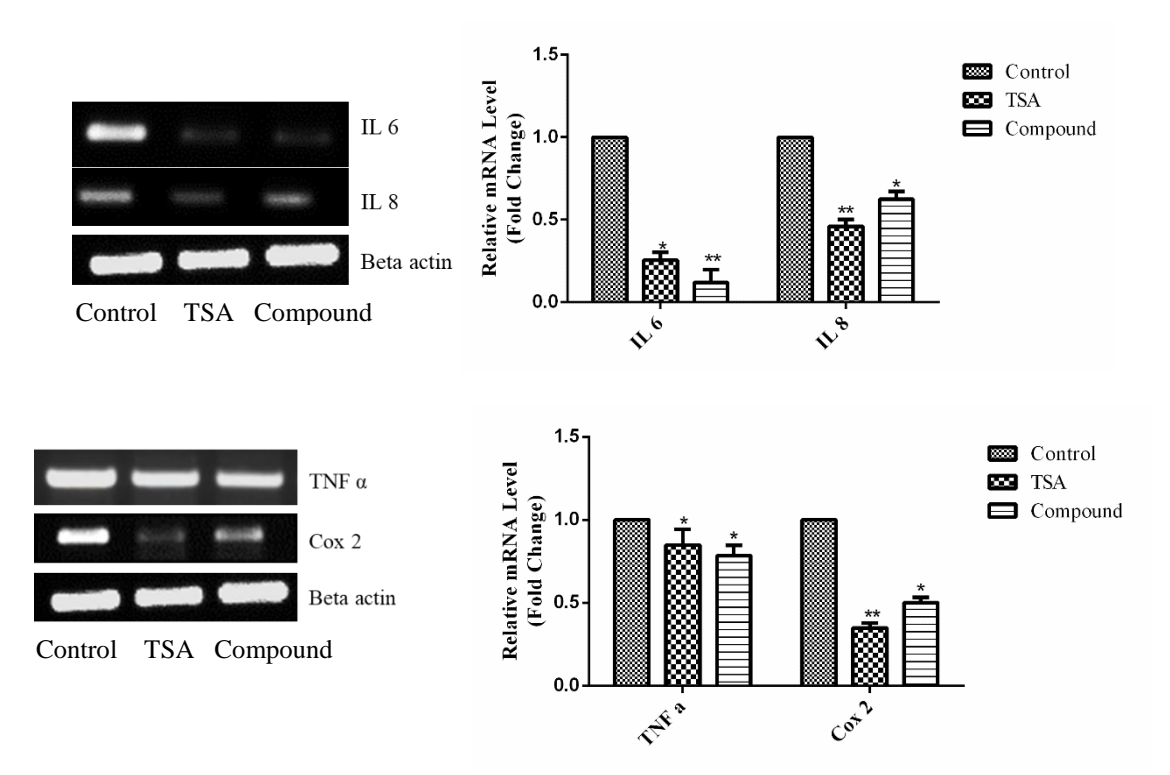


Fig 4.2.10. mRNA expression of inflammatory cytokine (TNF- α , IL-6, IL-8) and COX-2 in A549 cells on treated with the tested compound at their respective IC50 values. Data represents mean values \pm SD. *P < 0.05 and **P < 0.01.

4.2.11. 2-(1H-imidazol-1-yl)-N-(pyridin-2-yl) acetamide triggers the apoptotic regulating proteins.

Caspase plays a central role in most apoptotic death is due to responsible for disturb the cellular mechanism of DNA repair and regulation. Now we determine the gene expression of Fas L, caspase-3 and caspase-8 which are significantly induced exposure of tested compound and TSA, treatment as shown in (Fig. 4.2.11 (A)). Further, we analysed the protein expression of cytochrome-c, caspase-3. 8 and 9. As shown in (Fig. 4.2.11 (B)). The 2-(1H-imidazol-1-yl)-N-(pyridin-2-yl) acetamide treatment resulted in a significant increase expression of cytochrome-c to disturb the mitochondria it leads to apoptosis. Furthermore, the substantial release of cytochrome-c mediated the activation of caspase 8, 9 and 3) was observed in the 2-(1H-imidazol-1-yl)-N-(pyridin-2-yl) acetamide treated cells when compared to TSA and untreated A549 cells. These results strongly suggested that the tested compound induce apoptosis through caspase cascade activation pathway.

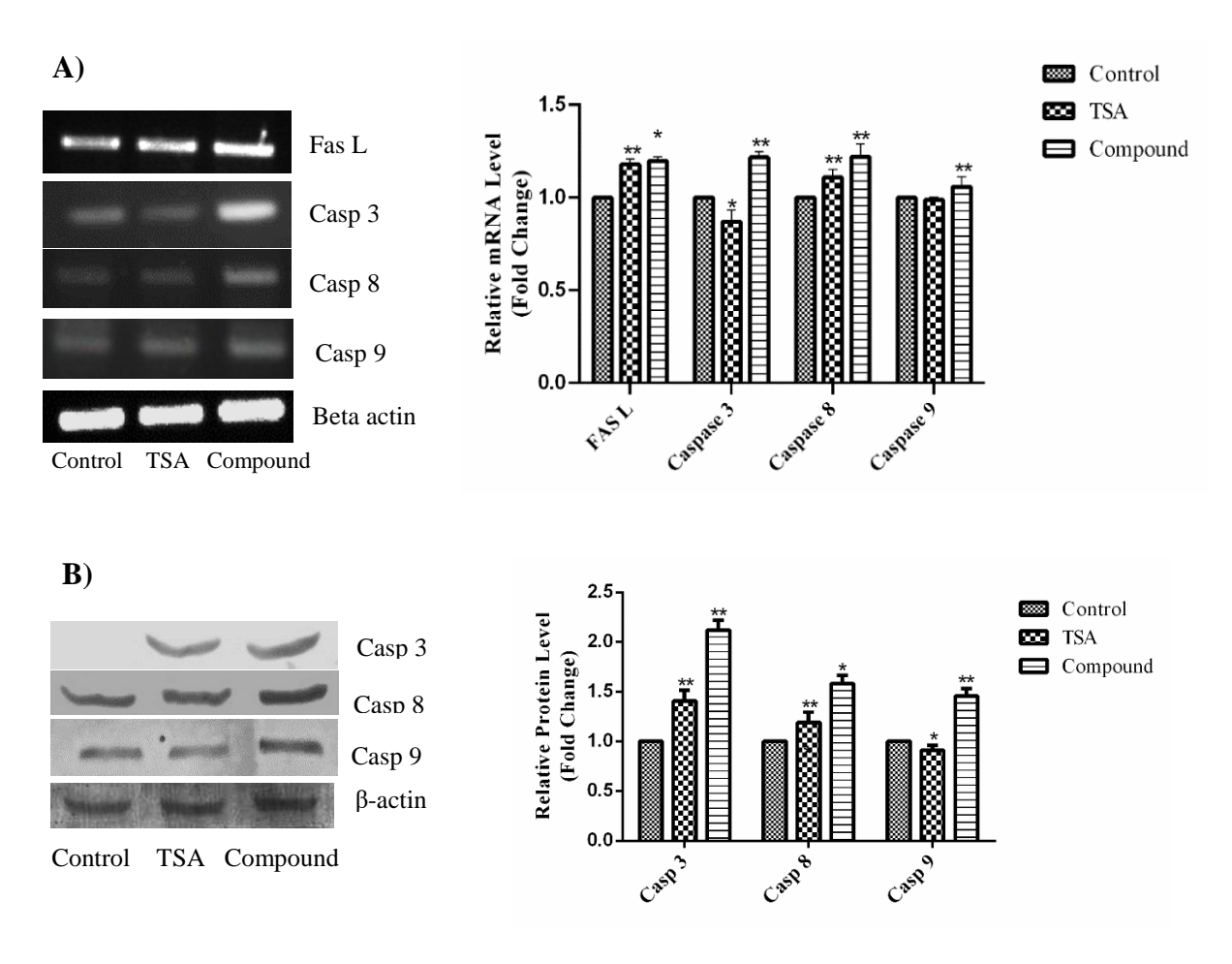


Fig 4.2.11. A) Fas Ligand, Caspase 3, 8, 9 and β-actin. mRNA expression in A549 cells detected by RT-PCR. **B**) Western blot analysis of Caspase 3, 8 and 9. Protein bands were normalized to β-actin. *P < 0.05 and **P < 0.01.

4.2.12. Effect of tested compound on pro-apoptotic proteins Bax and Anti-apoptotic proteins Bcl-2 in A549 cells.

Apoptotic proteins and pro-apoptotic proteins are mainly involved in the regulation of the both intrinsic and extrinsic/mitochondria mediated pathway. We investigated the contribution of Bax and Bcl-2 proteins to 2-(1H-imidazol-1-yl)-N-(pyridin-2-yl) acetamide compound induced apoptosis in A549 cells. The ratio of apoptotic proteins is crucial for the induction of apoptosis because it determines whether cell will undergo apoptosis.

To investigate the mitochondria mediated apoptotic events involved in the tested compound induce apoptosis, we first analysed the changes in the level of the pro-apoptotic proteins Bax and anti-apoptotic protein Bcl-2. The results of the western blot analysis showed that the treatment of tested compound in A549 cells shows that reduction levels of anti-apoptotic proteins of the Bcl-2 family, compared to standard inhibitor TSA and control cells. At the same time, the level of pro-apoptotic proteins Bax increases both treated and TSA when compared to untreated cells (Fig 4.2.12). These results suggested that the tested compound has ability to alter the levels of pro-apoptotic and anti-apoptotic proteins.

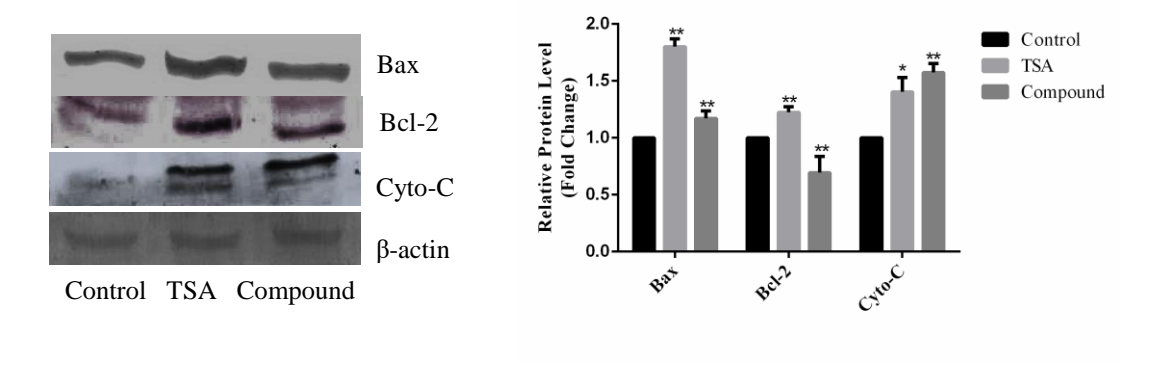


Fig 4.2.12. Western blot analysis of Pro-apoptotic, anti-apoptotic and Cytochrome- C. Protein bands were normalized to β-actin. *P < 0.05 and **P < 0.01.

4.2.13 2-(1H-imidazol-1-yl)-N-(pyridin-2-yl) acetamide induce downregulation of MMP2 and MMP 9 expression in A549 cells

Mitochondria membrane potential MMPs is one of the major roles in cancer progression, which allows cancer cells to migrate out of primary tumour to form metastases. Especially, MMP-2 and MMP-9 are thought to a play key role in degradation of type IV collagen and gelatin, the two main components of extra cellular matrices. In the present investigation, we studied the effect of tested compound on the expression of MMP-2, 9 in A549 cells. To confirm the role of MMPs gene expression by RT-PCR and western blot analysis. The influence of 2-(1H-imidazol-1-yl)-N-(pyridin-2-yl) acetamide compound on the expression of mRNA was well understood with downregulation of MMP-2 and MMP-9 genes compared to control cells (Fig. 4.2.13 (A)). To further confirm the role of MMP-2, 9 proteins expression in A549 treated cells (Fig. 4.2.13 (B)). The expression of active MMP-2 and MMP-9 proteins were significantly decreased in 2-(1H-imidazol-1-yl)-N-(pyridin-2-yl) acetamide treated A549 cells. In order to illustrate the mechanism underlying the suppression of both migration and invasion by the tested compound in A549 cells as shown in (Fig.4.2.13 (C)).

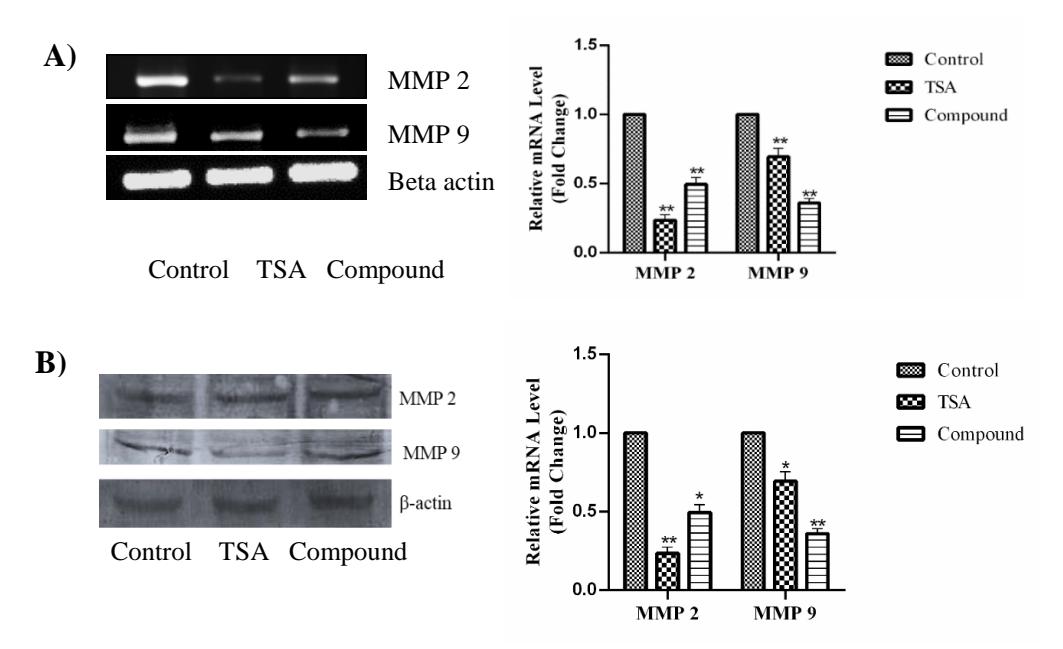


Fig. 4.2.13 A) Effect of 2-(1H-imidazol-1-yl)-N-(pyridin-2-yl) acetamide and TSA on MMP-2 and MMP-9 mRNA expression in A549 cells by RT-PCR. **B)** Cell lysate of A549 cells were harvested 24 h after indicated treatment and analysed for MMP-2 and MMP-9 by western blotting. β- actin served as an internal control. *P < 0.05 and **P < 0.01.

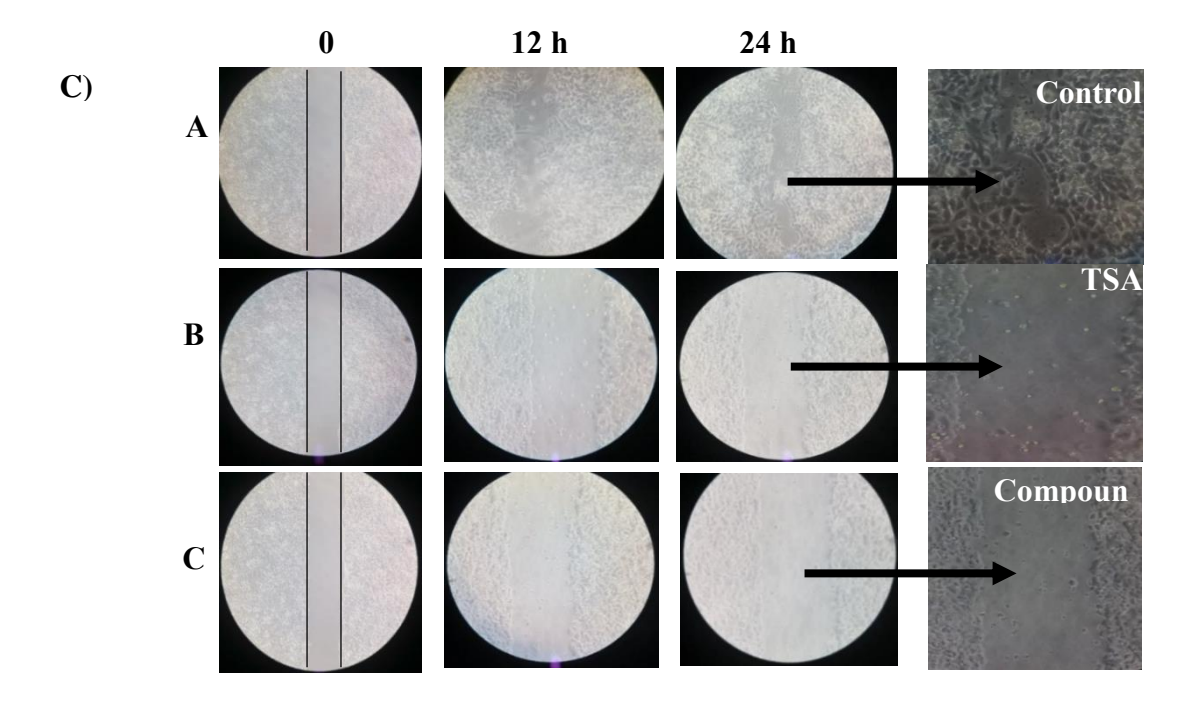


Fig. 4.2.13 C) Analysis of cell migrating ability after treatment of 2-(1H-imidazol-1-yl)-N-(pyridin-2-yl) acetamide and TSA in A549 cells. Pictures were viewed by Phase contrast microscopy after 24 hours. A) Untreated cells, B) TSA (4.0 μ M) C) treated with tested compound (150 μ M).

4.2.14 2-(1H-imidazol-1-yl)-N-(pyridin-2-yl) acetamide induces excessive ROS accumulation induced apoptosis by increasing oxidative stress and altering mitochondrial functions

The excessive accumulation of ROS levels in cancer cells induces oxidative stress and alters the mitochondrial functions and this is known to play a major role in apoptotic stimulation. To study the relationship between cytotoxicity and generation of ROS level, A549 cells were exposed to (150 µM) concentrations of tested compound, it had been detected with intracellular ROS indicator DCFHDA. In the presence of endogenously generated ROS, DCFH-DA is oxidised to release the fluorophore DCF. After 24 h treatment, ROS generation was gradually increased when compared to the untreated cells. From this result revealed that lower DCF fluorescence intensity was detected with untreated cells when compared to the treated cells. Recent work proved that exposure of tested compound induce a mitochondrial-dependent ROS response that significantly enhances the cytotoxic effect caused by nuclear DNA damage in cancer cells. The sensitization of the outer layer mitochondrial membrane is an important process to initiate apoptosis of A549 cells. Rhodamine 123 staining method was used to evaluate mitochondria membrane potential (ΔΨm) in treated and control. After 24 h treatment A549 cells were decreased as shown in (Fig. 4.2.14 A) the uptake of Rhodamine 123. Results of the present study indicated that the C3 compound had induced apoptosis through an elevated level of ROS generation and alter the mitochondria membrane potential. We conclude from experimental data clearly emphasize enhanced generation of ROS and down regulation of ΔΨm in cancer cells is a key pathway of apoptosis development that leads to cancer cell viability (Fig. 4.2.14 B). Further, the mechanism of cell death induced by the tested compound were studied by observing the apoptotic changes in the form of chromatin condensation and apoptotic bodies. The stimulation of apoptosis has been considered as a standard and the best strategy in anticancer therapy [144], Propidium iodide (PI) is a small fluorescent molecule that binds to DNA but cannot passively traverse into cells that possess an intact plasma membrane. PI exclusion can be used to discriminate dead cells, in which plasma membranes become permeable regardless of the mechanism of death, from live cells with intact membranes. However, apoptotic cells can be distinguished from necrotic cells by co-staining with propidium iodide (PI) because PI enters necrotic cells but is excluded from apoptotic cells as shown in Fig. 4.2.14 C.

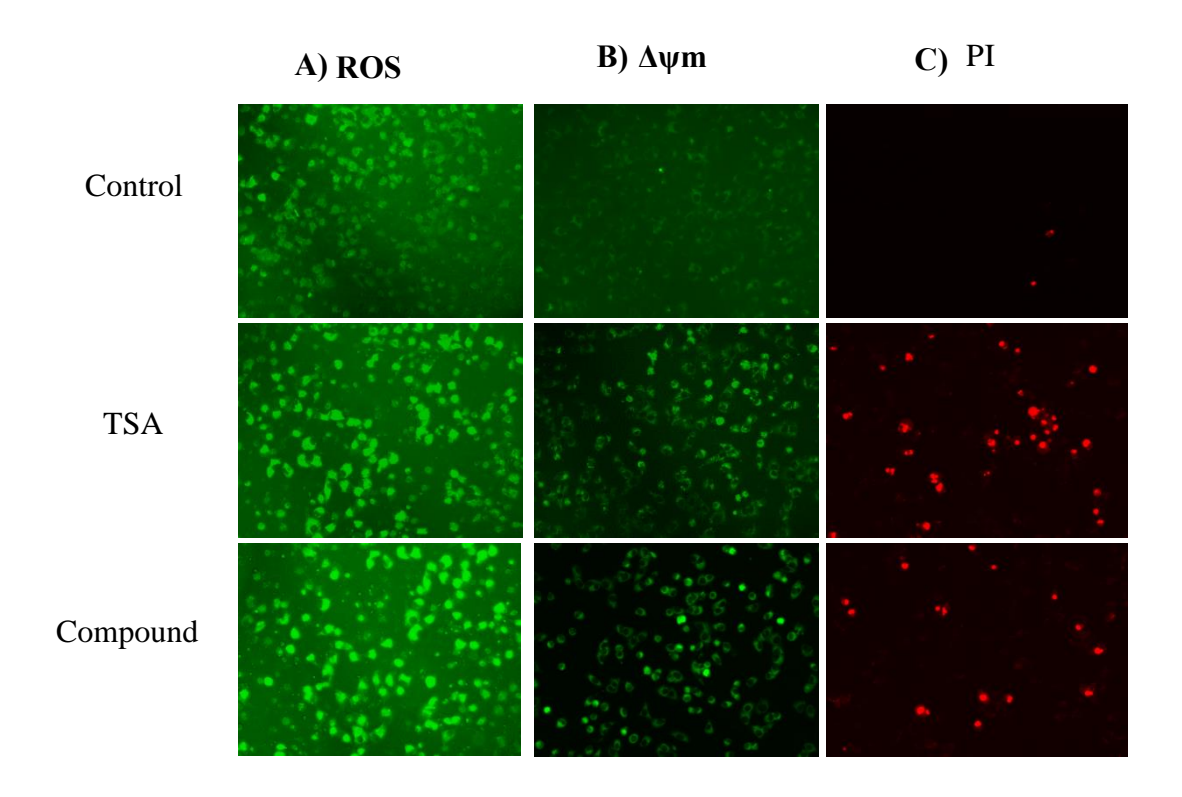


Fig. 4.2.14 Fluorescence microscopy analysis of A549 cells. A) ROS generation of tested compound induced apoptosis through DCFH-DA staining. **B)** Rhodamine-123 staining was used to detect the loss of mitochondrial membrane potential when exposed to IC₅₀ doses of the tested compound as compared to control. **C)** Propidium iodide (PI) was used to detect necrotic cells or late apoptotic cells.

4.2.15 Role of Phosphoinositide 3-kinase (PI3K)/Akt signalling in A549 cells.

The PI3K/Akt signalling pathway is activated and negatively regulates autophagy by inhibiting mTOR expression in cancer cells. Therefore, it is crucial to consider in target specific cancer treatment. On activation of PI3Ks, phosphatidylinositol (3, 4)-bisphosphate

converts to phosphatidylinositol (3, 4, 5)-triphosphate and engage Akt to cell membrane [144]. PI3Ks channel signal from cell surface is carried toward cytoplasm by generation of second messengers, phosphorylated phosphatidylinositol which successively phosphorylate downstream substrate and in the end event in proliferation, cell survival, and promote normal cell growth [145]. Aberrant activation of PI3K signalling pathway aid tumor angiogenesis and carcinogenesis [146]. Thus, PI3K is a crucial target for different cancer types and phytochemicals targeting PI3K can be a novel and promising therapy for cancer. From the results revealed that the tested compound has ability to inhibit the differentiation, cell proliferation, and angiogenesis through PI3K/Akt/Mtor signalling pathway as shown in Fig. 4.2.15.

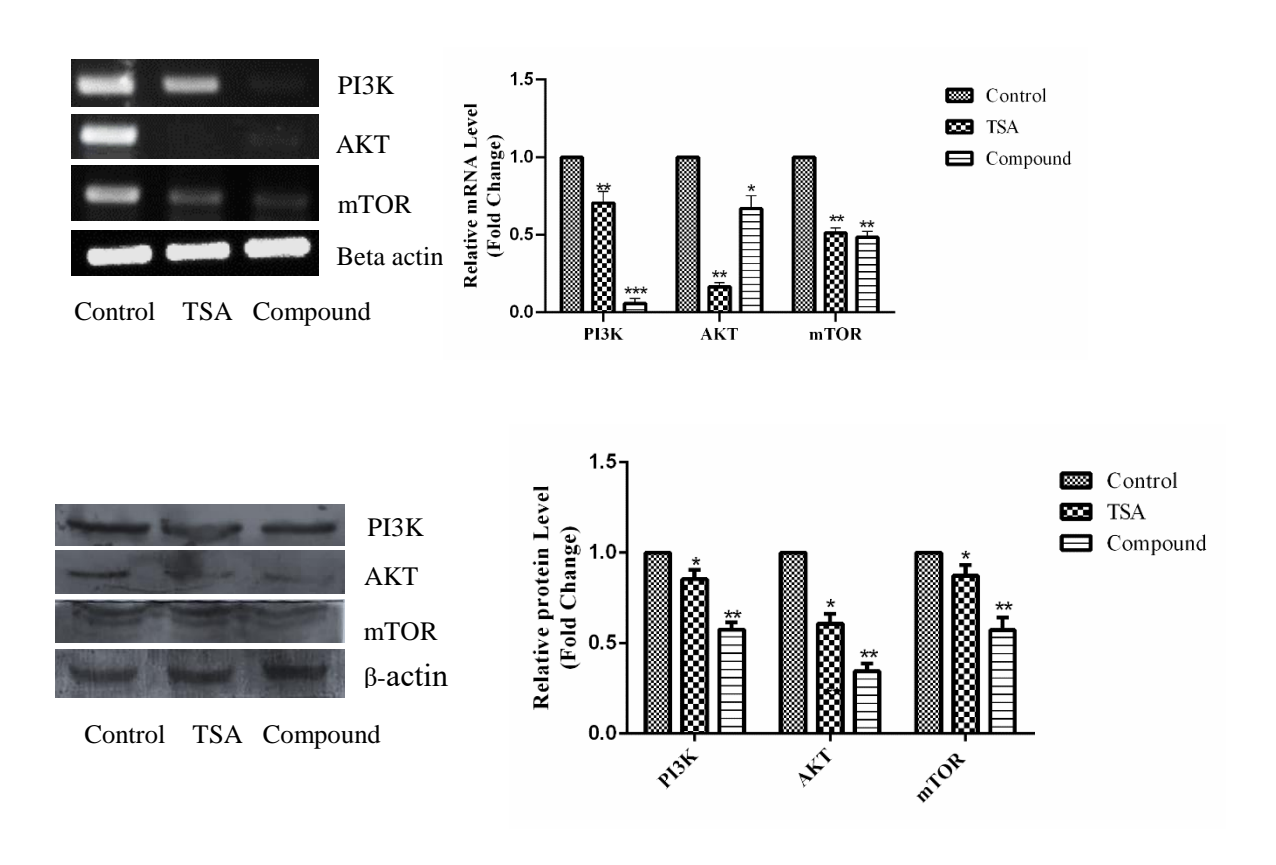


Fig 4.2.15. Effect of 2-(1H-imidazol-1-yl)-N-(pyridin-2-yl) acetamide targeting down regulation of PI3K/Akt/mTOR signalling pathway in A549 cells. mRNA expression were analysed by RT-PCR and protein expression of cell lysate were analysed by western blot analysis. *P < 0.05 and **P < 0.01

Discussion

5.0 Discussion

Cancer is one of the top most leading cause of death worldwide, 19.3 million cases and 10 million cancer deaths in 2020 (Globocan 2020) for an estimated 11.2 million deaths by 2021. International Agency for Research on Cancer (IARC) estimates that globally, 1 in 5 people develop cancer during their lifetime, and 1 in 8 men and 1 in 11 women die from the disease. The global cancer burden is expected to be 28.4 million cases in 2040, a 47% rise from 2020, with a larger increase in transitioning (64% to 95%) versus transitioned (32% to 56%) countries due to demographic changes, although this may be further exacerbated by increasing risk factors associated with globalization and a growing economy [147].

Lung cancer is the second most commonly diagnosed cancer and the leading cause of cancer death in 2020, representing approximately one in 10 (11.4%) cancers diagnosed and one in 5 (18.0%) deaths, with an estimated 2.2 million new cancer cases and 1.8 million deaths, followed by colorectal (9.4%), liver (8.3%), stomach (7.7%), and female breast (6.9%) cancers [148]. More than 80% of lung cancer cases due to non-small cell lung cancer and it is the most common kind of lung cancer with the subtypes of squamous cell carcinoma, adenocarcinoma and large cell carcinoma.

Epigenetic programming is vital in mammalian development, and stable inheritance of epigenetic settings is essential for the maintenance of tissue and cell type specific functions. Major epigenetic mechanisms include DNA methylation, post-translational modification of histones and RNA associated gene silencing mechanism [148]. Epigenetic changes can prompt abnormal genes expressions that regulate cell proliferation, differentiation and apoptosis and increase the potential of cellular transformation.

Modifications of histone are connected with both gene silencing and activation, depending on the nature of the modification and the specific amino acid modified. The acetylation status of core histones plays a crucial role in regulating gene transcription through the modulation chromatin condensation. The acetylation status of histone is governed by two opposite enzymatic activates, histone acetyltransferases (HAT) and histone deacetylases (HDACs). Besides histones, HATs and HDACs also target non-histone proteins including variety of transcription factors, cell cycle proteins and in doing so have major impact on the control of cell fate. The inactivation of HATs and aberrant HDACs activity are closely associated with the development of the transformed state of human tumors, due to transcriptional repression of tumor suppressor genes and activation of oncogenes.

Given these insight into the function of HDACs, it is not surprising that HDAC inhibitors (HDIs) are emerging as promising new agents for cancer therapy. HDIs are a new class of antineoplastic agents which were originally recognized by their capacity to reverse the transformed phenotype. Their anticancer activities were observed in pre-clinical studies of a broad range of different cancer cell lines both invitro and invivo. By blocking the activity of HDACs, HDIs restore the expression of some tumor suppressor genes, induce cell differentiation, growth arrest and apoptosis of tumors cells. HDIs are preferentially cytotoxicity for tumor cells, whereas normal cells are 10-fold for more resistant.

Besides, many HDIs have been enhance their anticancer activity while combine with the large number of traditional chemotherapeutic drugs such as vincristine and epotoside, DNA methyltransferases inhibitors and also other therapeutic regimens such as TRAIL. Several HDIs are currently in clinical trials as single agent or in combination with other therapeutic agents for treatment of both solid and hematologic malignancies. HDIs were identified, mainly, based on their ability to change the behaviour of transformed cells in culture, exhibiting potent antitumor activity in human xenografts model, suggesting their

usefulness as novel anticancer agents. HDIs consist of several different class of chemical families like short chain fatty acids, including sodium n-butyrate and valproic acid; organic hydroxamic acids, including Trichostatin A (TSA), and Suberoylanilide hydroxamic acid (SAHA); cyclic tetrapeptides, including trapoxin (TPX), depsipeptide; and the benzamides, including CI-994, MS-275.

The current generation of HDIs mediates a wide variety of intrinsic effects on cell growth and survival which can be broadly divided into two categories: transcriptional effects and non-transcriptional effects.

Imidazoles are well known heterocyclic compounds and have an important feature of a variety of medicinal agents. The high therapeutic properties of the imidazole related drugs have encouraged the medicinal chemists to synthesize a large number of novel chemotherapeutic agents. The structural features of the imidazole ring with desirable electron rich characteristics are beneficial for imidazole derivatives to readily bind with a variety of enzymes and receptors in the biological system. Synthesis of imidazole containing compounds by multicomponent reaction and their anti-cancer potential of against the panel of National Cancer Institute 60 cancer cell line panel. 2,20-(2- (3-(cyclopentyloxy)-4methoxyphenyl)-1-isobutyl-1H-imidazole- 4,5- diyl)dipyridine imidazole derivative is shown to have antiproliferative activity in A549 epithelial cancer cells by affecting proliferation, migration, anchorage independent growth, and by inducing cell cycle arrest in the G2/M Phase plus the activation of apoptosis. In recent years, applications of imidazole derivatives in medicinal chemistry have achieved remarkable progress in cancer. But there is no sufficient work to prove imidazole having HDAC inhibition property to inhibit HDACs in non-small cell lung cancer cells. Based on these observations, we designed and synthesized imidazole containing HDACi specific blocker molecule to inhibit HDACs enzymes with general pharmacophore of established HDACi that follows the schematic of CAP- Spacer- ZBG. In recent years, the impact of molecular dynamics (MDs) simulations in molecular biology and drug discovery has expanded dramatically. These simulations can capture a wide variety of important bimolecular processes, including conformational change, ligand binding and protein folding, revealing the positions of all of the atoms at femtosecond temporal resolution. Motivated by the above data and in continuation of our previous reports in building novel biologically active molecules in the present study, we designed imidazole containing compounds and explored their potential through docking experiments for its interactions with isoforms of HDAC enzymes and synthesize the best candidature among them for its role in modulating histone modifying enzymes thereby demonstrate its anticancer potential in A549 cell line.

The salient features of the following results:

In the present investigation, we inaugurate for the first time that imidazole containing acetamide derivatives form aminopyridine downregulates HDACs in the A549 cell line. Initially, we performed the molecular docking studies by using GLIDE (Schrödinger). The accuracy of the protein–ligand interaction and the energy was examined using Glide extra-precision docking protocol. Molecular docking studies revealed that the binding interactions of the 2-(1H-imidazol-1-yl)-N-(pyridin-2-yl) acetamide compound had significant binding ability with the active site of the HDAC enzyme, thus forming hydrogen bonding interactions and metal coordinates of HDAC family proteins. In insilico prediction exhibiting the tested compound having a high binding affinity with the HDAC family, suggesting the potential role of 2-(1H-imidazol-1-yl)-N-(pyridin-2-yl) acetamide compound in epigenetic modulation. The above results were followed by other molecular biochemical experimental studies.

The anti-cancer effect of imidazole derivatives has been well documented in many different types of human cancers [148]. In the present study, we found that 2-(1H-imidazol-

1-yl)-N-(pyridin-2-yl) acetamide inhibits the growth of A549 NSCLC cells by decrease in cell viability, as determined by the MTT assay in A549 cell line (Fig. 4.2.1). The cytotoxicity assay revealed that the tested compound were found to cause DNA damage and cell death in a dose dependent manner. The cells were treated with different concentrations $50 \mu M$, $100 \mu M$, $150 \mu M$, $200 \mu M$ and $250 \mu M$ for determining the IC₅₀.

Apoptosis is a crucial phenomenon in the cytotoxic mechanism of many anticancer drugs. In the current study, a change in the cell morphology was observed in 2-(1H-imidazol-1-yl)-N-(pyridin-2-yl) acetamide treated A549 cells including cell shrinkage, elongation, reduced cell density and appearance of many mitotic cells (spherical shape) (Fig. 4.2.2). The morphological changes positively indicated that A549 cells undergo apoptotic mode of cell death during 2-(1H-imidazol-1-yl)-N-(pyridin-2-yl) acetamide treatment, which may be mediated through mitotic arrest.

Further confirmed that the morphological effect of 2-(1H-imidazol-1-yl)-N-(pyridin-2-yl) acetamide is accompanied by the presence of nuclear condensation, irregular morphology of nucleus and fragmentation of nuclei. Clonogenic assay or colony formation assay is an in vitro cell survival assay based on the ability of a single cell to grow into a colony. The assay essentially tests every cell in the population for its ability to undergo "unlimited" division. Clonogenic assay is the method used to determine cell reproductive death after treatment with ionizing radiation, but can also be used to determine the effectiveness of other cytotoxic agents [149]. Dose-dependent colony formation unit (CFU) assay revealed significant reduction in colonies at their respective IC₅₀ values suggesting lower doses of these drugs to be even more effective on A549 proliferation (Fig. 4.2.3). Control cells proliferated in huge numbers; hence they could not be counted as colonies (TNTC—too numerous to count). DNA fragmentation was also demonstrated in agarose gel

electrophoresis (Fig. 4.2.4). Ladder pattern of low molecular weight DNA (Oligonucleosomal size fragments) is the unique biochemical feature in late apoptotic cells.

After validation, to finding the HDACs function as transcriptional repressors and corepressors has ushered a surge of interest in this subject, and reports of genes that are regulated by HDACs are continuously expanding. HDACs also play a key biological role in regulating histones and chromatin cross talk. The best studied examples of histone modification cross talk occurs between acetylation and methylation [150]. Particularly H3 and H4, are subjected to PTM including methylation and acetylation, many of these modifications are associated with distinct transcription states [151]. We extend our study to include the detailed analysis of histone modifications in the tested compound. Histone H3 and H4 have a relatively higher enrichment of histone modifications. In our results showed that inhibition of HDAC activity induced hyperacetylation state of histone H3 and H4 as shown in Fig. 4.2.7 therefore, showing acetyl histones H3 and H4 as target molecules for HDIs. After the successful detection of total HDAC activity, to detect 2-(1H-imidazol-1yl)-N-(pyridin-2-yl) acetamide induced mRNA expression of HDACs Class I (1, 2, 3, and 8), Class II-A (4, 7, and 9), Class II-B (6 and 10) and Class IV (11). The results suggested that string inhibition of class I and II HDACs and moderate inhibition of class IV by 2-(1Himidazol-1-yl)-N-(pyridin-2-yl) acetamide compound might be the possible mechanism for antineoplastic activity. The results were intensely supported by the protein expression of class I and II HDACs as shown in Fig. 4.2.6. The tested compound downregulated HDAC mRNA and protein expressions were comparable to standard HDIs TSA.

We inspected Mitochondrial membrane potential ($\Delta\Psi m$) is an early event in the process of enhanced ROS generation and cell death. The low level of ROS generation in the cancer cells is essential for their physiological functions involved in the cancer cell proliferation, differentiation, cell cycle progression, invasion, and migration. As well as the

elevated level of ROS in the cancer cell affects the normal function and leads to cell death [153]. The effect of tested compound on ROS generation of NSCLC cells was investigated using DCFH-DA staining. After 24 h treatment, ROS generation was gradually increased when compared to the untreated cells. As shown in (Fig. 4.2.14A). From this result revealed that lower DCF fluorescence intensity was detected with untreated cells when compared to the treated cells. Rhodamine 123 staining method was used to evaluate mitochondria membrane potential ($\Delta\Psi$ m) in treated and control. After 24 h treatment A549 cells were decreased as shown in (Fig. 4.2.14B) the uptake of Rhodamine 123. Results of the present study indicated that the C3 compound had induced apoptosis through an elevated level of ROS generation and alter the mitochondria membrane potential. We conclude from experimental data clearly emphasize enhanced generation of ROS and down regulation of ($\Delta\Psi$ m) in cancer cells is a key pathway of apoptosis development that leads to cancer cell viability. There are convincing evidence that ROS may contribute to cytochrome C release due to disruption of the mitochondrial membrane potential.

Mitochondria are found to be a crucial factor in the regulation of apoptosis and the loss of $\Delta\Psi m$ has become a mechanism of interest in drug research. A loss in the $\Delta\Psi m$ leads to the translocation of proapoptotic Bax to mitochondria and induce the p53 mediated apoptosis through the release of Cytochrome C from the mitochondria to the cytosol [155]. The instability of the mitochondrial membrane results in the release of cytochrome c, which binds to apoptotic activating factor-1 (APAF-1) and activates casapase-9, leading to the activation of caspase-3. Caspase-3 is the most potent caspase with many substrates. Mitochondrial membrane permeability is regulated by a family of proto-oncogenes. The Bcl-2 family of proto-oncogenes is antiapoptotic (Bcl-2) or proapoptotic (Bad, Bax) [156]. The antiapoptotic protein Bcl-2, inhibits the ability of Bax to increase membrane potential [157]. The Bcl-2 family is most notable for their regulation of apoptosis, a form of

programmed cell death, at the mitochondrion. The Bcl-2 family proteins consists of members that either promote or inhibit apoptosis, and control apoptosis by governing mitochondrial outer membrane permeabilization (MOMP), which is a key step in the intrinsic pathway of apoptosis. Various apoptotic stimuli induce expression and/or activation of specific BH3-only family members, which translocate to the mitochondria and initiate Bax/Bak-dependent apoptosis [158, 159]. We analysed the antiapoptotic Bcl-2 and proapoptotic Bax gene and protein by RTPCR and western blotting. The BcL2 gene is gradually decreased in 2-(1H-imidazol-1-yl)-N-(pyridin-2-yl) acetamide treated when compared to untreated cells, and the other hand, Bax gene is significantly increased is treated with tested compound when compared to control of A549 cells (Fig. 4.2.12). Additionally, theses apoptotic proteins may be responsible for the concomitant execution phase of apoptosis observed in these cells, to disturb the mitochondrial membrane Together, these results initiate the p53 dependent intrinsic signalling apoptosis pathway. We found that the treatment of A549 cells with berberine leads to the Caspase activation. As the levels of cytochrome c increase in cytosol, to activate the Caspase -3, 8 and Caspase-9 and cleaved Caspase 3, 8, and 9 it will leads to induction of apoptosis. These results strongly suggested that identify a mechanism of positive apoptosis control that operates directly at the level of an essential initiator Caspase in the extrinsic pathway.

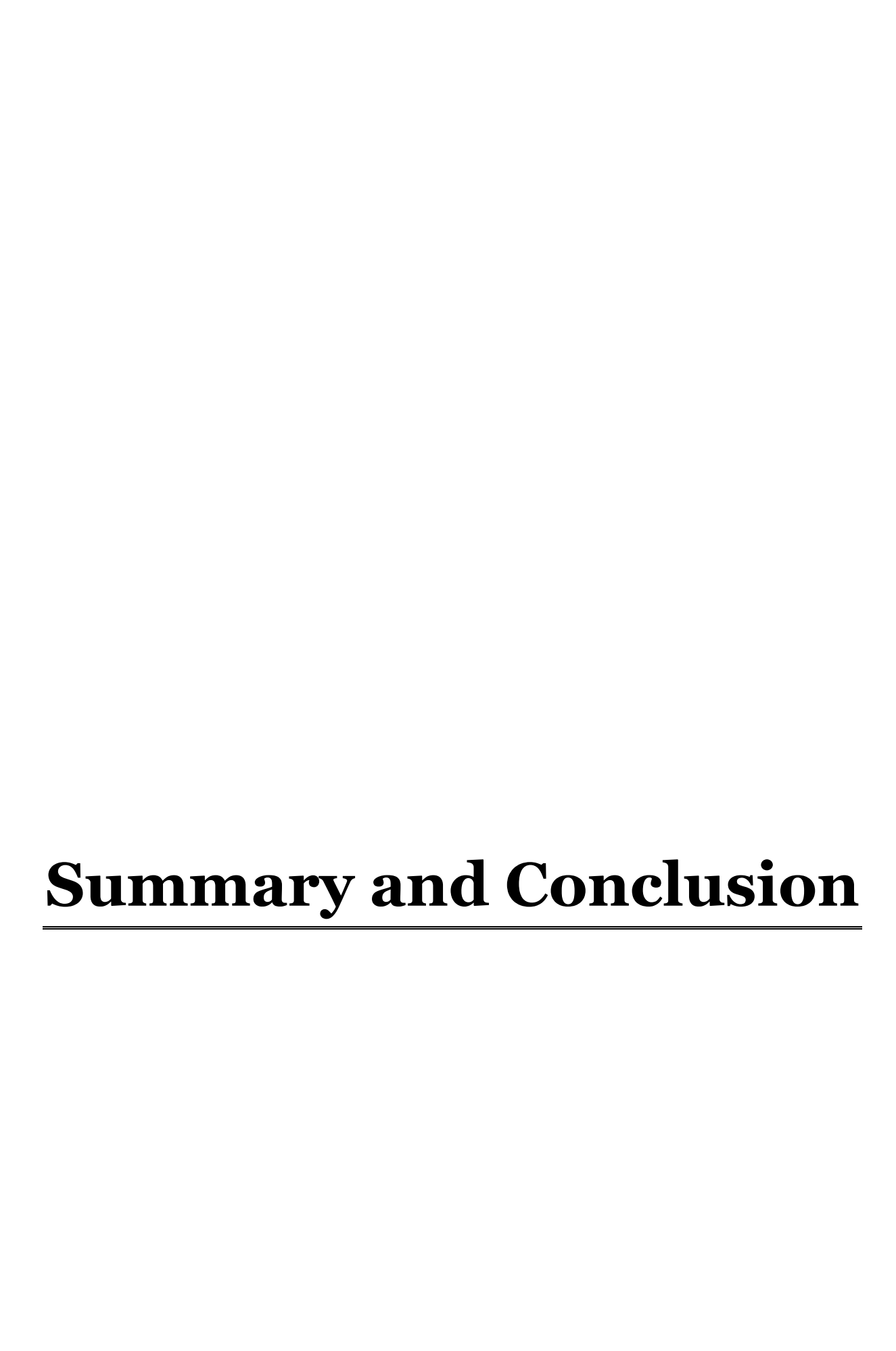
Additionally, there is considerable evidence that MMP-2 and MMP-9 are associated with tumor invasion and metastasis. Increased histone acetylation by HDIs inhibitors in the promoter region is the suppressor of invasion and metastasis, including metalloproteinases in carcinogenesis. The downregulation of HDAC blocked cancer cell invasion and migration through MMP [162]. In this study (Fig. 4.2.13), HDAC down regulation by 2-(1H-imidazol-1-yl)-N-(pyridin-2-yl) acetamide compound resulted in a decrease in MMP-2 and MMP-9

mRNA and protein levels. The fluorescence microscopic studies also correlate that inhibit expression of MMP-2 and MMP-9 in A549 cells.

As well as, p53 and p21 play a pivotal role in multi-cellular organisms to mediate a variety of anti-proliferative processes. p21 has been assigned a major role in the growth arrest after DNA damage and is thought to be a key mediator of p53 tumor suppressor function, to control the number and behaviour of cells in a particular tissue within an organism. We inspected the effect of 2-(1H-imidazol-1-yl)-N-(pyridin-2-yl) acetamide on p53 and p21 mRNA and protein expression studies. The alterations in p53 and p21 mRNA expression levels in response to the tested compound and standard HDIs TSA were observed the increase the levels of Cyclin-cdk inhibitors P21 and tumor suppressor protein p53 pathway thereby induce cell cycle arrest and inhibit cell proliferation. Our results showed that increased mRNA and protein expression of p21 and p53 in A549 cells (Fig. 4.2.8), upregulation of p21 and p53- independent arrest in G2/M phase [160]. Consequence, HDIs can also induce hyperacetylation of p53 and trigger transactivation-dependent apoptosis. Activated p53 triggers cell cycle arrest and apoptosis by inducing transcription of numerous cell cycle regulators and proapoptotic genes.

We further extended our studies to understand the impact of epigenetic modulation by 2-(1H-imidazol-1-yl)-N-(pyridin-2-yl) acetamide compound on cell cycle and apoptosis regulating proteins. Histone acetylation is regulated in the S phase, and its interruption activates cell cycle arrest within the G2/M phase. The G2/M phase is related to HDAC inhibitor- mediated hyperacetylation of the centromere, permitting the release of heterochromatin protein, resulting in atypical chromosomal segregation and nuclear damage, as shown in Fig. 4.2.9 [161] Therefore, it is possible that deregulated histone acetylation during the S phase associated with sub-G0/G1 cell cycle arrest may be necessary for tested compound induced cell death.

PI3K/Akt/mTOR pathway plays an important role in regulating cell cycle, cell apoptosis and autophagy [162]. Negative regulation of PI3K-AKT pathway can regulate different cell functions, based on their target protein. To investigate whether the effects of 2-(1H-imidazol-1-yl)-N-(pyridin-2-yl) acetamide on A549 cells is related to this pathway, we examined the activity of 2-(1H-imidazol-1-yl)-N-(pyridin-2-yl) acetamide on the representative signal proteins in the pathway. As shown in (Fig. 4.2.15). AKT enhances the survival of cells by blocking the function of proapoptotic proteins and processes. From the results suggested that the 2-(1H-imidazol-1-yl)-N-(pyridin-2-yl) acetamide compound which may be the key mechanism for its anticancer activity.



6.0 Summary and Conclusion

HDACs are most promising targets for cancer treatment, which attracted excessive attention in the HDAC function exploration and inhibitor development. Imidazole based heterocyclic compounds were designed to pay efficient inhibition of HDACs enzymes followed by synthetic methodologies in pure form was executed and was tested for their inhibitory activity against HDAC enzymes. In this study, we initiate for the first-time dual inhibition of synthesized compound (2-(1H-imidazol-1-yl)-N-(pyridin-2-yl) acetamide) down regulates HDACs enzyme by targeting PI3K/Akt signalling pathway in the A549 cell line.

First, the docking studies provided valuable data, which allowed the interaction of HDACs enzyme and they exactly fit into active site region and the ligand formed more hydrogen bond interactions, which are promising tools for the discovery of new active inhibitors useful as pharmacological agents. The cytotoxicity assay revealed that the synthesized compound found to cause DNA damage and cell death in a dose dependent manner for determining the half maximal inhibitory concentration (IC₅₀). Further, HDAC enzyme colorimetric assay determined, and the results were good HDACi activity compared than standard histone deacetylase inhibitor TSA in A549 cells, which was accompanied by histone hyperacetylation, suggesting that inhibitory modulation of HDACs classes. This phenomenon was further confirmed by gene expression and western blotting, speculating the altered expression of class I and class II HDACs upon 2-(1H-imidazol-1-yl)-N-(pyridin-2-yl) acetamide has ability to inhibit the cell proliferation. We further extended our studies to understand the impact of epigenetic modulation by 2-(1H-imidazol-1-yl)-N-(pyridin-2-yl) acetamide on cell cycle and apoptosis regulating proteins. Histone acetylation is

regulated in the S phase, and its interruption activates cell cycle arrest within the G2/M phase. Therefore, it is possible that deregulated histone acetylation during the S phase associated with sub-G0/G1 cell cycle arrest.

We observed the increase of the levels of the cyclin-cdk inhibitors p21 and tumor suppressor proteins p53 after co-treatment. From the present study, suggested that the synthesized compound and TSA induces p21 expression through p53 pathways thereby induces cell cycle arrest and inhibit cell proliferation. Henceforward, further studies were carried out the cells treated with A549 cells, the anti-inflammatory property of synthesized compound the downregulation of mRNA expression of inflammatory cytokines (TNF- α , IL-6, IL-8, and Cox-2) and indicates that synthesized compound has a good anti-inflammatory property might suppress the tumour development. The 2-(1H-imidazol-1-yl)-N-(pyridin-2-yl) acetamide treatment is to enhance the ROS generation, altered $\Delta \psi m$, and activates apoptosis mitochondria mediated cell death.

In our study, we confirmed the caspase activation of synthesized compound treated in A549 cells; increased expression of caspase-3 and caspase-8 mRNA, protein expression of caspase-3, 8 and caspase-9. Further activation of pro and anti-apoptotic proteins like Bax and Bcl-2. 2-(1H-imidazol-1-yl)-N-(pyridin-2-yl) acetamide compound induces Bax activation in A549 cells, which disturbs the loss of mitochondria membrane potential (Δψm), thereby allowing for the p53-pathway-mediated release of cytochrome c to cytosol. This event leads to the subsequent activation of caspase-signalling pathway results in apoptosis. In the present investigation, we found that MMP-2 and MMP-9 mRNA and protein expression decreased on treatment with 2-(1H-imidazol-1-yl)-N-(pyridin-2-yl) acetamide compound inhibit secretion of MMP-2, 9 by A549 cells and thereby reduce the potential for metastasis

In conclusion, 2-(1H-imidazol-1-yl)-N-(pyridin-2-yl) acetamide compound showed potent activities on human NSCLC A549 cells and its weak cytotoxicity on normal cell lines might become a promising drug candidate for NSCLC cancer therapy in the future. We provide mechanistic evidence that our second generation of acetamide compound 2-(1H-imidazol-1-yl)-N-(pyridin-2-yl) acetamide compound induced apoptosis in A549 cells is mediated through HDAC inhibition by PI3K/Akt signalling and activation of hyperacetylation in a lung cancer cell line. Conversely, we realize that it is necessary to exhibit favourable in vivo antitumor activity for 2-(1H-imidazol-1-yl)-N-(pyridin-2-yl) acetamide compound to become a drug candidate, which remains unclear and will be investigated in our next work.

References

References

- 1. Hamidpour, Rafie, et al. "Sage: The functional novel natural medicine for preventing and curing chronic illnesses." International Journal of Case Reports and Images 4.12 (2013): 671-677.Magee JA (2012)
- 2. Magee, Jeffrey A., Elena Piskounova, and Sean J. Morrison. "Cancer stem cells: impact, heterogeneity, and uncertainty." *Cancer cell* 21.3 (2012): 283-296.
- 3. Lodish, Harvey, et al. "Proto-oncogenes and tumor-suppressor genes." Molecular cell biology 4 (2000): Section.Cooper GM (2000)
- 4. Yoon, Paula W., et al. "Public health impact of genetic tests at the end of the 20th century." Genetics in Medicine 3.6 (2001): 405-410.
- 5. Plummer, Martyn, et al. "Global burden of cancers attributable to infections in 2012: a synthetic analysis." The Lancet Global Health 4.9 (2016): e609-e616.
- 6. Chial, Heidi. "Proto-oncogenes to oncogenes to cancer." Nature education 1.1 (2008): 33.
- 7. Chow, A. Y. "Cell cycle control by oncogenes and tumor suppressors: driving the transformation of normal cells into cancerous cells." *Nature Education* 3.9 (2010): 7.
- 8. DeBerardinis, Ralph J., et al. "The biology of cancer: metabolic reprogramming fuels cell growth and proliferation." *Cell metabolism* 7.1 (2008): 11-20. [7]
- 9. Bunz, Fred. *Principles of cancer genetics*. Vol. 1. New York, NY, USA:: Springer, 2008.
- 10. Massoud, Tarik F., et al. "Reporter gene imaging of protein–protein interactions in living subjects." *Current opinion in biotechnology* 18.1 (2007): 31-37.
- 11. Massoud, Tarik F., Ramasamy Paulmurugan, and Sanjiv S. Gambhir. "Molecular imaging of homodimeric protein–protein interactions in living subjects." *The FASEB journal* 18.10 (2004): 1105-1107.
- 12. Paulmurugan, Ramasamy, et al. "Molecular imaging of drug-modulated protein-protein interactions in living subjects." *Cancer research* 64.6 (2004): 2113-2119.
- 13. https://gco.iarc.fr/today/data/factsheets/populations/356-india-fact-sheets.pdfAlberg AJ (2005)

- 14. Baba, Alecsandru Ioan, and Cornel Cătoi. Comparative oncology. Bucharest: Publishing House of the Romanian Academy, 2007.
- 15. Plummer, Martyn, et al. "Global burden of cancers attributable to infections in 2012: a synthetic analysis." The Lancet Global Health 4.9 (2016): e609-e616.
- 16. Alberg, Anthony J., Malcolm V. Brock, and Jonathan M. Samet. "Epidemiology of lung cancer: looking to the future." Journal of Clinical Oncology 23.14 (2005): 3175-3185.
- 17. Curado, Maria-Paula, et al. Cancer incidence in five continents, Volume IX. IARC Press, International Agency for Research on Cancer, 2007.
- 18. Hashibe, Mia, et al. "Marijuana use and the risk of lung and upper aerodigestive tract cancers: results of a population-based case-control study." Cancer Epidemiology and Prevention Biomarkers 15.10 (2006): 1829-1834.
- 19. Colby TV. Tumors of the lower respiratory tract. Atlas tumor pathol. 1995;309-17
- 20. Nicholson, Siobhan A., et al. "Small cell lung carcinoma (SCLC): a clinicopathologic study of 100 cases with surgical specimens." The American journal of surgical pathology 26.9 (2002): 1184-1197.
- 21. Schrump DS, Carter D, Kelsey CR, Marks LB, Giaccone G. Non-small cell lung cancer. In: DeVita VT, Lawrence TS, Rosenberg SA, eds. DeVita, Hellman, and Rosenberg's Cancer: Principles and Practice of Oncology. 9th ed. Philadelphia, Pa: Lippincott Williams & Wilkins; 2011:799–847.
- 22. Krug LM, Pietanza C, Kris MG, Rosenzweig K, Travis WD. Small cell and other neuroendocrine tumors of the lung. In: DeVita VT, Lawrence TS, Rosenberg SA, eds. DeVita, Hellman, and Rosenberg's Cancer: Principles and Practice of Oncology. 9th ed. Philadelphia, Pa: Lippincott Williams & Wilkins; 2011: 848–870.
- 23. Krishnamurthy, A., et al. "The relevance of" Nonsmoking-associated lung cancer" in India: A single-centre experience." Indian journal of cancer 49.1 (2012): 82.
- 24. Ramshankar, Vijayalakshmi, and Arvind Krishnamurthy. "Lung cancer detection by screening-presenting circulating miRNAs as a promising next generation biomarker breakthrough." Asian Pacific Journal of Cancer Prevention 14.4 (2013): 2167-2172.
- 25. Ferlay J, Soerjomataram I, Ervik M, Dikshit R, Eser S, Mathers C, Rebelo M, Parkin DM, Forman D, Bray, F. GLOBOCAN 2012 v1.0, Cancer Incidence and Mortality Worldwide: IARC CancerBase No. 11 [Internet].Lyon, France: International Agency for Research on Cancer; 2013.

- Dube Sr, Asman K., A. Malarcher, and R. Carabollo. "Office on Smoking and Health, National Center For Chronic Disease Prevention And Health Promotion.: Cigarette Smoking Among Adults And Trends In Smoking Cessation—United States 2008." Mmwr Weekly 58 (2009): 1227-1232.
- 27. Siegel, Rebecca, et al. "Cancer treatment and survivorship statistics, 2012." CA: a cancer journal for clinicians 62.4 (2012): 220-241.
- 28. Molina, Julian R., et al. "Non-small cell lung cancer: epidemiology, risk factors, treatment, and survivorship." Mayo Clinic Proceedings. Vol. 83. No. 5. Elsevier, 2008.
- 29. Cho, Kwangjae, et al. "Therapeutic nanoparticles for drug delivery in cancer." Clinical cancer research 14.5 (2008): 1310-1316.
- 30. Luger, Karolin, et al. "Crystal structure of the nucleosome core particle at 2.8 Å resolution." *Nature* 389.6648 (1997): 251-260.
- 31. Jones, Peter A., and Stephen B. Baylin. "The epigenomics of cancer." *Cell* 128.4 (2007): 683-692.
- 32. Bernstein, Bradley E., Alexander Meissner, and Eric S. Lander. "The mammalian epigenome." *Cell* 128.4 (2007): 669-681.
- 33. Suzuki, Miho M., and Adrian Bird. "DNA methylation landscapes: provocative insights from epigenomics." *Nature Reviews Genetics* 9.6 (2008): 465-476.
- 34. Kouzarides, Tony. "Chromatin modifications and their function." *Cell* 128.4 (2007): 693-705.
- 35. Zhang, Baohong, et al. "microRNAs as oncogenes and tumor suppressors." *Developmental biology* 302.1 (2007): 1-12.
- 36. Jiang, Cizhong, and B. Franklin Pugh. "Nucleosome positioning and gene regulation: advances through genomics." Nature Reviews Genetics 10.3 (2009): 161-172.
- 37. Sharma, Shikhar, Theresa K. Kelly, and Peter A. Jones. "Epigenetics in cancer." *Carcinogenesis* 31.1 (2010): 27-36.
- 38. Egger, Gerda, et al. "Epigenetics in human disease and prospects for epigenetic therapy." Nature 429.6990 (2004): 457-463.
- 39. Jones, Peter A., and Stephen B. Baylin. "The fundamental role of epigenetic events in cancer." Nature reviews genetics 3.6 (2002): 415-428.

- 40. Jones, Peter A., and Stephen B. Baylin. "The epigenomics of cancer." *Cell* 128.4 (2007): 683-692.
- 41. Jones, Peter A., and Peter W. Laird. "Cancer-epigenetics comes of age." *Nature genetics* 21.2 (1999): 163-167.
- 42. Feinberg, Andrew P., Rolf Ohlsson, and Steven Henikoff. "The epigenetic progenitor origin of human cancer." Nature reviews genetics 7.1 (2006): 21-33.
- 43. Jones, Peter A., and Robert Martienssen. "A blueprint for a human epigenome project: the AACR human epigenome workshop." Cancer research 65.24 (2005): 11241-11246.
- 44. Bannister, Andrew J., and Tony Kouzarides. "Regulation of chromatin by histone modifications." *Cell research* 21.3 (2011): 381-395.
- 45. Jenuwein, Thomas, and C. David Allis. "Translating the histone code." *Science* 293.5532 (2001): 1074-1080.
- 46. Weckwerth, Wolfram, ed. Metabolomics: methods and protocols. Vol. 358. Springer Science & Business Media, 2007.
- 47. Rossetto, Dorine, Nikita Avvakumov, and Jacques Côté. "Histone phosphorylation: a chromatin modification involved in diverse nuclear events." *Epigenetics* 7.10 (2012): 1098-1108.
- 48. Morris, J. R. "Genes, genetics, and epigenetics: a correspondence." Science 293.5532 (2001): 1103-1105.
- 49. Rossetto, Dorine, Nikita Avvakumov, and Jacques Côté. "Histone phosphorylation: a chromatin modification involved in diverse nuclear events." Epigenetics 7.10 (2012): 1098-1108.
- 50. Cao, Jian, and Qin Yan. "Histone ubiquitination and deubiquitination in transcription, DNA damage response, and cancer." Frontiers in oncology 2 (2012): 26.
- 51. Liu, Hui-wen, et al. "Chromatin modification by SUMO-1 stimulates the promoters of translation machinery genes." Nucleic acids research 40.20 (2012): 10172-10186.

- 52. Feinberg, Andrew P., and Bert Vogelstein. "Hypomethylation distinguishes genes of some human cancers from their normal counterparts." Nature 301.5895 (1983): 89-92.
- 53. Riggs, Arthur D., and Peter A. Jones. "5-methylcytosine, gene regulation, and cancer." *Advances in cancer research*. Vol. 40. Academic Press, 1983. 1-30.
- 54. Rodriguez, Jairo, et al. "Chromosomal instability correlates with genome-wide DNA demethylation in human primary colorectal cancers." *Cancer research* 66.17 (2006): 8462-9468.
- 55. Eden, Amir, et al. "Chromosomal instability and tumors promoted by DNA hypomethylation." Science 300.5618 (2003): 455-455.
- 56. Howard, G., et al. "Activation and transposition of endogenous retroviral elements in hypomethylation induced tumors in mice." *Oncogene* 27.3 (2008): 404-408.
- 57. Fraga, Mario F., et al. "Loss of acetylation at Lys16 and trimethylation at Lys20 of histone H4 is a common hallmark of human cancer." Nature genetics 37.4 (2005): 391-400.
- 58. Halkidou, Kalipso, et al. "Upregulation and nuclear recruitment of HDAC1 in hormone refractory prostate cancer." The Prostate 59.2 (2004): 177-189.
- 59. Song, Jaehwi, et al. "Increased expression of histone deacetylase 2 is found in human gastric cancer." Apmis 113.4 (2005): 264-268.
- 60. Nguyen, Carvell T., et al. "Histone H3-lysine 9 methylation is associated with aberrant gene silencing in cancer cells and is rapidly reversed by 5-aza-2'-deoxycytidine." Cancer research 62.22 (2002): 6456-6461.
- 61. Valk-Lingbeek, Merel E., Sophia WM Bruggeman, and Maarten van Lohuizen. "Stem cells and cancer: the polycomb connection." Cell 118.4 (2004): 409-418.
- 62. Timmermann, S., et al. "Histone acetylation and disease." Cellular and Molecular Life Sciences CMLS 58.5-6 (2001): 728-736.
- 63. Cohen, Idan, et al. "Histone modifiers in cancer: friends or foes?." Genes & cancer 2.6 (2011): 631-647.
- 64. Barneda-Zahonero, Bruna, and Maribel Parra. "Histone deacetylases and cancer." Molecular oncology 6.6 (2012): 579-589.

- 65. Minucci, Saverio, and Pier Giuseppe Pelicci. "Histone deacetylase inhibitors and the promise of epigenetic (and more) treatments for cancer." Nature Reviews Cancer 6.1 (2006): 38-51.
- 66. Suzuki, Takeshi, et al. "Roles of histone methyl-modifying enzymes in development and progression of cancer." Cancer science 104.7 (2013): 795-800.
- 67. Marchion, Douglas, and Pamela Münster. "Development of histone deacetylase inhibitors for cancer treatment." Expert review of anticancer therapy 7.4 (2007): 583-598.
- 68. Mottamal, Madhusoodanan, et al. "Histone deacetylase inhibitors in clinical studies as templates for new anticancer agents." Molecules 20.3 (2015): 3898-3941.
- 69. Bardhan, Kankana, and Kebin Liu. "Epigenetics and colorectal cancer pathogenesis." Cancers 5.2 (2013): 676-713.
- 70. Santos-Rosa, Helena, and Carlos Caldas. "Chromatin modifier enzymes, the histone code and cancer." European journal of cancer 41.16 (2005): 2381-2402.
- 71. Yang, Xiang-Jiao, and Edward Seto. "Collaborative spirit of histone deacetylases in regulating chromatin structure and gene expression." Current opinion in genetics & development 13.2 (2003): 143-153.
- 72. Ruijter, Annemieke JM de, et al. "Histone deacetylases (HDACs): characterization of the classical HDAC family." Biochemical Journal 370.3 (2003): 737-749.
- 73. Thiagalingam, S. A. M., et al. "Histone deacetylases: unique players in shaping the epigenetic histone code." Annals of the New York Academy of Sciences 983.1 (2003): 84-100.
- 74. Legube, Gaëlle, and Didier Trouche. "Regulating histone acetyltransferases and deacetylases." EMBO reports 4.10 (2003): 944-947.
- 75. Glozak, M. A., and E. Seto. "Histone deacetylases and cancer." Oncogene 26.37 (2007): 5420-5432.
- 76. Johnstone, Ricky W. "Histone-deacetylase inhibitors: novel drugs for the treatment of cancer." Nature reviews Drug discovery 1.4 (2002): 287-299.
- 77. Nakagawa, Masamune, et al. "Expression profile of class I histone deacetylases in human cancer tissues." Oncology reports 18.4 (2007): 769-774.

- 78. Marquard, L., et al. "Prognostic significance of the therapeutic targets histone deacetylase 1, 2, 6 and acetylated histone H4 in cutaneous T-cell lymphoma." Histopathology 53.3 (2008): 267-277.
- 79. Bolden, Jessica E., Melissa J. Peart, and Ricky W. Johnstone. "Anticancer activities of histone deacetylase inhibitors." Nature reviews Drug discovery 5.9 (2006): 769-784.
- 80. Marks, Paul A., et al. "Histone deacetylase inhibitors as new cancer drugs." Current opinion in oncology 13.6 (2001): 477-483.
- 81. Glaser, Keith B. "HDAC inhibitors: clinical update and mechanism-based potential." Biochemical pharmacology 74.5 (2007): 659-671.
- 82. Lindemann, Ralph K., Brian Gabrielli, and Ricky W. Johnstone. "Histone-deacetylase inhibitors for the treatment of cancer." Cell cycle 3.6 (2004): 777-786.
- 83. Pan, L. N., Jun Lu, and Baiqu Huang. "HDAC inhibitors: a potential new category of anti-tumor agents." Cell Mol Immunol 4.5 (2007): 337-343.
- 84. Ungerstedt, J. S., et al. "Role of thioredoxin in the response of normal and transformed cells to histone deacetylase inhibitors." Proceedings of the National Academy of Sciences 102.3 (2005): 673-678.
- 85. Hasima, Noor, and Bharat B. Aggarwal. "Cancer-linked targets modulated by curcumin." International journal of biochemistry and molecular biology 3.4 (2012): 328.
- 86. Leonard, John P., Richard R. Furman, and Morton Coleman. "Proteasome inhibition with bortezomib: A new therapeutic strategy for non-Hodgkin's lymphoma." International journal of cancer 119.5 (2006): 971-979.
- 87. Piekarz, Richard L., Dan L. Sackett, and Susan E. Bates. "Histone deacetylase inhibitors and demethylating agents: clinical development of histone deacetylase inhibitors for cancer therapy." The Cancer Journal 13.1 (2007): 30-39.
- 88. Thurn, K. Ted, et al. "Rational therapeutic combinations with histone deacetylase inhibitors for the treatment of cancer." Future oncology 7.2 (2011): 263-283.
- 89. Lindemann, Ralph K., et al. "Analysis of the apoptotic and therapeutic activities of histone deacetylase inhibitors by using a mouse model of B cell lymphoma." Proceedings of the National Academy of Sciences 104.19 (2007): 8071-8076.

- 90. Miller, Thomas A., David J. Witter, and Sandro Belvedere. "Histone deacetylase inhibitors." Journal of medicinal chemistry 46.24 (2003): 5097-5116.
- 91. Yoshida, Minoru, et al. "Potent and specific inhibition of mammalian histone deacetylase both in vivo and in vitro by trichostatin A." Journal of Biological Chemistry 265.28 (1990): 17174-17179.
- 92. Nakajima, Hidenori, et al. "FR901228, a potent antitumor antibiotic, is a novel histone deacetylase inhibitor." Experimental cell research 241.1 (1998): 126-133.
- 93. Zahnow, C. A., et al. "Inhibitors of DNA methylation, histone deacetylation, and histone demethylation: a perfect combination for cancer therapy." Advances in cancer research. Vol. 130. Academic Press, 2016. 55-111.
- 94. New, Maria, Heidi Olzscha, and Nicholas B. La Thangue. "HDAC inhibitor-based therapies: can we interpret the code?." Molecular oncology 6.6 (2012): 637-656.
- 95. Qiu, Tianzhu, et al. "Effects of treatment with histone deacetylase inhibitors in solid tumors: a review based on 30 clinical trials." Future oncology 9.2 (2013): 255-269.
- 96. Wang, Yunfei, et al. "Identification of histone deacetylase inhibitors with benzoylhydrazide scaffold that selectively inhibit class I histone deacetylases." Chemistry & biology 22.2 (2015): 273-284.
- 97. Anderson, Amy C. "The process of structure-based drug design." Chemistry & biology 10.9 (2003): 787-797.
- 98. Khan, Mohemmed Faraz, et al. "Pharmacophore modeling, 3D-QSAR, docking study and ADME prediction of acyl 1, 3, 4-thiadiazole amides and sulfonamides as antitubulin agents." Arabian Journal of Chemistry 12.8 (2019): 5000-5018.
- 99. Verma, Rajeshwar P. "Cytotoxicity of heterocyclic compounds against various cancer cells: a quantitative structure–activity relationship study." *Bioactive Heterocycles III.* Springer, Berlin, Heidelberg, 2007. 53-86.
- 100. Martins, Pedro, et al. "Heterocyclic anticancer compounds: recent advances and the paradigm shift towards the use of nanomedicine's tool box." *Molecules* 20.9 (2015): 16852-16891.
- 101. Research, C. For D.E and new drugs at FDA: CDER's new molecular entities and new therapeutic biological products, Available online: http://www.fda.gov.

- Drugs/Development Approval process/Drug Innovation/default.htm. (Accessed 1 June 2015).
- 102. Sharma, Gangavaram VM, et al. "Imidazole derivatives show anticancer potential by inducing apoptosis and cellular senescence." MedChemComm 5.11 (2014): 1751-1760.
- 103. A. Kleeman, J. Engel, B. Kutscher, and D. Reichert, Pharmaceutical Substances: Syntheses, Patents, Applications of the Most Relevant APIs, Thieme Medical, New York, NY, USA, 3rd edition, 1999.
- 104. Debus, H. "Ueber die einwirkung des ammoniaks auf glyoxal, Annalen der Chemie und

Pharmacie, 107, 199–208." (1858).

- 105. H. Singh and V. K. Kapoor, Medicinal and Pharmaceutical Chemistry, vol. 2, Vallabh
 - Prakashan, Delhi, India, 2008 Kleemann, Axel. "Pharmaceutical substancessynthese, patents, applications." (1999).
- 106. Jain, Abhishek K., et al. "Synthesis and antibacterial evaluation of 2–substituted–4, 5–diphenyl–N–alkyl imidazole derivatives." Asian Pacific Journal of Tropical Medicine 3.6 (2010): 471-474.
- 107. Sharma, Gangavaram VM, et al. "Imidazole derivatives show anticancer potential by inducing apoptosis and cellular senescence." MedChemComm 5.11 (2014): 1751-1760.
- 108. Fan, Yi-Lei, et al. "Recent advances of imidazole-containing derivatives as antitubercular agents." European journal of medicinal chemistry 150 (2018): 347-365.
- 109. Altındağ, Firuze Diyar, et al. "Novel imidazole derivatives as antifungal agents: Synthesis, biological evaluation, ADME prediction and molecular docking studies." Phosphorus, Sulfur, and Silicon and the Related Elements (2019).

- 110. De Clercq, Erik. "The design of drugs for HIV and HCV." Nature reviews Drug discovery 6.12 (2007): 1001-1018.
- 111. Zhan, Peng, et al. "Synthesis and biological evaluation of imidazole thioacetanilides as novel non-nucleoside HIV-1 reverse transcriptase inhibitors." Bioorganic & medicinal chemistry 17.16 (2009): 5775-5781.
- 112. Kao, Hung-Ying, et al. "Isolation and characterization of mammalian HDAC10, a novel histone deacetylase." Journal of Biological Chemistry 277.1 (2002): 187-193.
- 113. Zhou, Xianbo, et al. "Identification of a transcriptional repressor related to the noncatalytic domain of histone deacetylases 4 and 5." Proceedings of the National Academy of Sciences 97.3 (2000): 1056-1061.
- 114. Harder, Edward, et al. "OPLS3: a force field providing broad coverage of drug-like small molecules and proteins." Journal of chemical theory and computation 12.1 (2016): 281-296.
- 115. Rodriguez, Rolando, et al. "Homology modeling, model and software evaluation: three related resources." Bioinformatics (Oxford, England) 14.6 (1998): 523-528.
- 116. Jayaraj, John Marshal, et al. "In silico identification and screening of CYP24A1 inhibitors: 3D QSAR pharmacophore mapping and molecular dynamics analysis." Journal of Biomolecular Structure and Dynamics 37.7 (2019): 1700-1714.
- 117. Singh, Kh Dhanachandra, et al. "Structure-based drug discovery of ApoE4 inhibitors from the plant compounds." Medicinal Chemistry Research 21.6 (2012): 825-833.
- 118. Sastry, G. Madhavi, et al. "Protein and ligand preparation: parameters, protocols, and influence on virtual screening enrichments." Journal of computer-aided molecular design 27.3 (2013): 221-234.
- 119. Haribabu, J., et al. "Isatin based thiosemicarbazone derivatives as potential bioactive agents: Anti-oxidant and molecular docking studies." Journal of Molecular Structure 1110 (2016): 185-195.
- 120. Ummanni R, Teller S, Junker H, et al (2008) Altered expression of tumor protein D52 regulates apoptosis and migration of prostate cancer cells. FEBS J 275:5703–5713. https://doi.org/10.1111/j.1742-4658.2008.06697.x.
- 121. Bowers, Kevin J., et al. "Scalable algorithms for molecular dynamics simulations on commodity clusters." SC'06: Proceedings of the 2006 ACM/IEEE Conference on Supercomputing. IEEE, 2006.

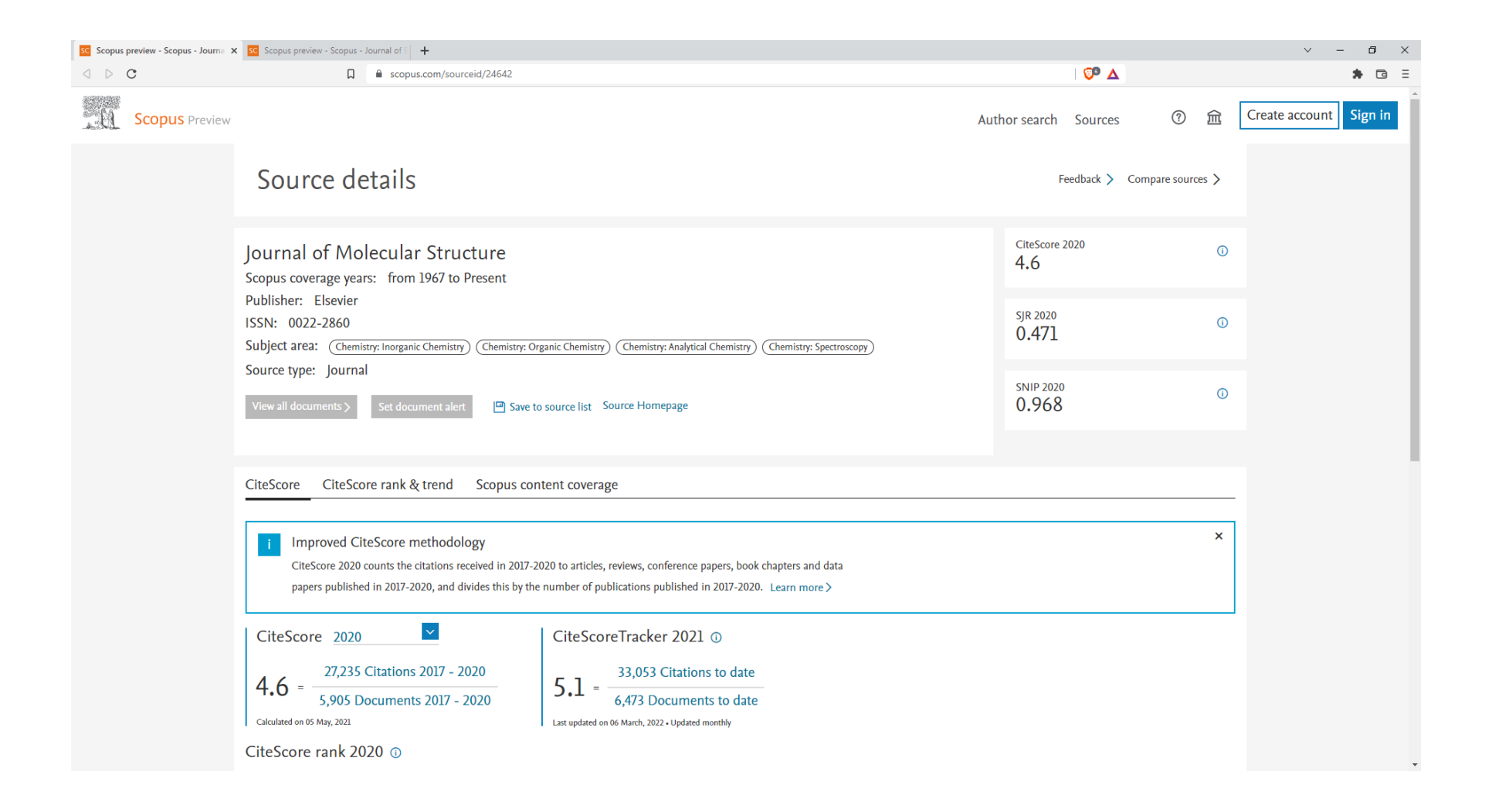
- 122. Bowers, Kevin J., Ron O. Dror, and David E. Shaw. "The midpoint method for parallelization of particle simulations." The Journal of chemical physics 124.18 (2006): 184109.
- 123. Kaminski, George A., et al. "Evaluation and reparametrization of the OPLS-AA force field for proteins via comparison with accurate quantum chemical calculations on peptides." The Journal of Physical Chemistry B 105.28 (2001): 6474-6487.
- 124. Ummanni, Ramesh, et al. "Altered expression of tumor protein D52 regulates apoptosis and migration of prostate cancer cells." The FEBS journal 275.22 (2008): 5703-5713.
- 125. Hartmann, Laura, et al. "Photon versus carbon ion irradiation: immunomodulatory effects exerted on murine tumor cell lines." Scientific reports 10.1 (2020): 1-13.
- 126. Chen, Chiung-Ju, et al. "Ursolic acid induces apoptotic cell death through AIF and endo G release through a mitochondria-dependent pathway in NCI-H292 human lung cancer cells in vitro." in vivo 33.2 (2019): 383-391.
- 127. Huang, An-Cheng, et al. "Casticin induces DNA damage and impairs DNA repair in human bladder cancer TSGH-8301 cells." Anticancer research 39.4 (2019): 1839-1847.
- 128. Jin, Meihua, et al. "Antiproliferative effect of aaptamine on human chronic myeloid leukemia K562 cells." International Journal of Molecular Sciences 12.11 (2011): 7352-7359.
- 129. Baracca, Alessandra, et al. "Rhodamine 123 as a probe of mitochondrial membrane potential: evaluation of proton flux through F0 during ATP synthesis." Biochimica et biophysica acta (BBA)-bioenergetics 1606.1-3 (2003): 137-146.
- 130. Combaret, Valérie, et al. "Effect of bortezomib on human neuroblastoma: analysis of molecular mechanisms involved in cytotoxicity." Molecular cancer 7.1 (2008): 1-12.
- 131. Jayaraj, John Marshal, et al. "Structural insights on Vitamin D receptor and screening of new potent agonist molecules: Structure and ligand-based approach." Journal of Biomolecular Structure and Dynamics 39.11 (2021): 4148-4159.
- 132. Haribabu, J., et al. "Isatin based thiosemicarbazone derivatives as potential bioactive agents: Anti-oxidant and molecular docking studies." Journal of Molecular Structure 1110 (2016): 185-195.

- 133. Zhou, Xianbo, et al. "Identification of a transcriptional repressor related to the noncatalytic domain of histone deacetylases 4 and 5." Proceedings of the National Academy of Sciences 97.3 (2000): 1056-1061.
- 134. Franken, Nicolaas AP, et al. "Clonogenic assay of cells in vitro." Nature protocols 1.5 (2006): 2315-2319.
- 135. Moyo, Batanai, and Stanley Mukanganyama. "Antiproliferative activity of T. welwitschii extract on Jurkat T cells in vitro." BioMed research international 2015 (2015).
- 136. Sonnemann, Jürgen, et al. "Increased activity of histone deacetylases in childhood acute lymphoblastic leukaemia and acute myeloid leukaemia: support for histone deacetylase inhibitors as antileukaemic agents." British journal of haematology 158.5 (2012): 664-666.
- 137. Banerjee, Hirendra Nath, and Mukesh Verma. "Epigenetic mechanisms in cancer." Biomarkers in medicine 3.4 (2009): 397-410.
- 138. Levine, Arnold J. "p53, the cellular gatekeeper for growth and division." cell 88.3 (1997): 323-331.
- 139. Fujino, Michihiro, et al. "Prognostic significance of p53 and ras p21 expression in nonsmall cell lung cancer." Cancer 76.12 (1995): 2457-2463.
- 140. Giono, Luciana E., and James J. Manfredi. "The p53 tumor suppressor participates in multiple cell cycle checkpoints." Journal of cellular physiology 209.1 (2006): 13-20.
- 141. Abbas, Tarek, and Anindya Dutta. "p21 in cancer: intricate networks and multiple activities." Nature Reviews Cancer 9.6 (2009): 400-414.
- 142. Waga, Shou, et al. "The p21 inhibitor of cyclin-dependent kinases controls DNA replication by interaction with PCNA." Nature 369.6481 (1994): 574-578.
- 143. Yi, C., et al. "MiR-663, a microRNA targeting p21 WAF1/CIP1, promotes the proliferation and tumorigenesis of nasopharyngeal carcinoma." Oncogene 31.41 (2012): 4421-4433.
- 144. Yap, Timothy A., et al. "Targeting the PI3K–AKT–mTOR pathway: progress, pitfalls, and promises." Current opinion in pharmacology 8.4 (2008): 393-412.

- 145. Burris, Howard A. "Overcoming acquired resistance to anticancer therapy: focus on the PI3K/AKT/mTOR pathway." Cancer chemotherapy and pharmacology 71.4 (2013): 829-842.
- 146. Patel, Shreyaskumar. "Exploring novel therapeutic targets in GIST: focus on the PI3K/Akt/mTOR pathway." Current oncology reports 15.4 (2013): 386-395.
- 147. Sung, Hyuna, et al. "Global cancer statistics 2020: GLOBOCAN estimates of incidence and mortality worldwide for 36 cancers in 185 countries." CA: a cancer journal for clinicians 71.3 (2021): 209-249.
- 148. Sharma, Pankaj, et al. "Imidazoles as Potential Anticancer Agents: An Update on Recent Studies." Molecules 26.14 (2021): 4213.
- 149. Franken, Nicolaas AP, et al. "Clonogenic assay of cells in vitro." Nature protocols 1.5 (2006): 2315-2319.
- 150. Fischle, Wolfgang, Yanming Wang, and C. David Allis. "Histone and chromatin cross-talk." Current opinion in cell biology 15.2 (2003): 172-183.
- 151. Zhang, Hong Ping, et al. "Association between histone hyperacetylation status in memory T lymphocytes and allergen-induced eosinophilic airway inflammation." Respirology 21.5 (2016): 850-857.
- 152. Khan, Musa, et al. "Berberine and a Berberis lycium extract inactivate Cdc25A and induce α-tubulin acetylation that correlate with HL-60 cell cycle inhibition and apoptosis." Mutation Research/Fundamental and Molecular Mechanisms of Mutagenesis 683.1-2 (2010): 123-130.
- 153. Redza-Dutordoir, Maureen, and Diana A. Averill-Bates. "Activation of apoptosis signalling pathways by reactive oxygen species." Biochimica et Biophysica Acta (BBA)-Molecular Cell Research 1863.12 (2016): 2977-2992.
- 154. Zorov, Dmitry B., Magdalena Juhaszova, and Steven J. Sollott. "Mitochondrial reactive oxygen species (ROS) and ROS-induced ROS release." Physiological reviews 94.3 (2014): 909-950.
- 155. Cao, Rui, et al. "Silencing of HJURP induces dysregulation of cell cycle and ROS metabolism in bladder cancer cells via PPARγ-SIRT1 feedback loop." Journal of Cancer 8.12 (2017): 2282.

- 156. Nguyen, Christopher, and Siyaram Pandey. "Exploiting mitochondrial vulnerabilities to trigger apoptosis selectively in cancer cells." Cancers 11.7 (2019): 916.
- 157. Campbell, Kirsteen J., and Stephen WG Tait. "Targeting BCL-2 regulated apoptosis in cancer." Open biology 8.5 (2018): 180002.
- 158. Roufayel, R. (2016). Regulation of stressed-induced cell death by the Bcl-2 family of apoptotic proteins. Molecular membrane biology, 33(6-8), 89-99.
- 159. Kleih, Markus, et al. "Direct impact of cisplatin on mitochondria induces ROS production that dictates cell fate of ovarian cancer cells." Cell death & disease 10.11 (2019): 1-12.
- 160. Liu, Zhaojian, et al. "Berberine induces p53-dependent cell cycle arrest and apoptosis of human osteosarcoma cells by inflicting DNA damage." Mutation Research/Fundamental and Molecular Mechanisms of Mutagenesis 662.1-2 (2009): 75-83.
- 161. Wang, Feng, et al. "HDAC inhibitor trichostatin A suppresses esophageal squamous cell carcinoma metastasis through HADC2 reduced MMP-2/9." Clinical and Investigative Medicine (2013): E87-E94.
- 162. Vinodhkumar, Radhakrishnan, et al. "Depsipeptide a histone deacetlyase inhibitor down regulates levels of matrix metalloproteinases 2 and 9 mRNA and protein expressions in lung cancer cells (A549)." Chemico-biological interactions 165.3 (2007): 220-229.

Publications

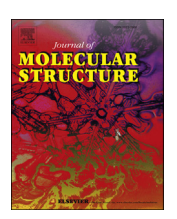


FISEVIER

Contents lists available at ScienceDirect

Journal of Molecular Structure

journal homepage: http://www.elsevier.com/locate/molstruc



Design and synthesis of imidazole based zinc binding groups as novel small molecule inhibitors targeting Histone deacetylase enzymes in lung cancer



Saravanan Kandasamy ^a, Prabhu Subramani ^a, Kannupal Srinivasan ^{b, **}, John marshal Jayaraj ^c, Gunasekaran Prasanth ^d, Karthikeyan Muthusamy ^c, Venkatachalam Rajakannan ^d, Ravikumar Vilwanathan ^{a, *}

- ^a Department of Biochemistry, School of Life Sciences, Bharathidasan University, Tiruchirappalli, 620 024, Tamil Nadu, India
- ^b School of Chemistry, Bharathidasan University, Tiruchirappalli, 620 024, Tamil Nadu, India
- ^c Department of Bioinformatics, Alagappa University, Karaikudi, Tamil Nadu, India
- d Centre of Advanced Study in Crystallography and Biophysics, University of Madras, Guindy Campus, Chennai, Tamilnadu, India, 600025

ARTICLE INFO

Article history: Received 2 February 2020 Received in revised form 21 March 2020 Accepted 31 March 2020 Available online 6 April 2020

Keywords:
Epigenetics
Histone deacetylase
HDACi
Imidazole
Pharmacophore
Zinc binding group (ZBG)

ABSTRACT

Histone deacetylase enzymes are involved in the remodelling of chromatin and have a pivotal role in balancing acetylation and deacetylation status of chromatin eventually ensures the epigenetic regulation of gene expression. Its aberrant activity was reported in several forms of cancer considering it as a potential target for cancer treatment. Histone deacetylase inhibitors emerged as new class of antineoplastic drugs. Recent developments in understanding the mechanism of interaction between drug and targeted molecule encourages rational development of new class of HDAC inhibitors directing global or gene specific histone acetylation. In the present study, we designed 14 imidazole based derivatives abiding the common pharmacophore structure like CAP, Spacer, and Zinc binding group (ZBG) shared among the established HDAC inhibitors and was explored for its epigenetic modulator candidature targeting histone modifying enzymes through docking experiments, Among them the compound ethyl (2,5-diphenyl-1Himidazole-4-yl)acetate (C3) was tightly bound to the isoforms of the HDAC enzymes at their receptor regions with high binding score. C3 was synthesized and have been characterized experimentally by IR and NMR techniques. The C3 inhibit cell proliferation of A549 lung cancer cell by inducing cytotoxicity and increased levels of ROS generation by disrupting mitochondrial permeability as evidenced from deflection in $(\Delta \psi m)$. From this study we revealed that C3 a novel imidazole derivative inhibit highly expressed HDAC enzyme in non-small cell lung cancer cell lines by chromatin remodelling. Further findings may validate the identified compound C3 as an effective epigenetic modulator.

© 2020 Elsevier B.V. All rights reserved.

1. Introduction

In the past 15 years, epigenetic modifications of genomic DNA have been intensifying as a field of study for cancer therapy. Epigenetic modifications are heritable changes that can alter the gene expression at the transcriptional level without any significant

E-mail addresses: srinivasank@bdu.ac.in (K. Srinivasan), ravikumarbdu@gmail.com (R. Vilwanathan).

changes in the DNA sequence [1]. Majorly, three epigenetic machineries are known to be related to cancer such as altered histone acetylations, DNA methylations and misregulated microRNA (miRNA) expression. Acetylation and deacetylation of histones by histone acetyltransferases (HATs) and histonedeacetylases (HDACs) is one of the most widely studied post-translational modifications as it is critical for the dynamic regulation of gene transcription process including cellular proliferation, differentiation and apoptosis [2]. HATs and HDACs are two important families of enzymes that regulate transcription. Particularly, HDACs have been found to overexpressed, thereby modifying the chromatin structure by deacetylating the lysine residues of histone and non-histone proteins, leading to aberrant expression of oncogenic

^{*} Corresponding author. Department of Biochemistry, School of Life Sciences, Bharathidasan University, Tiruchirappalli, 620024.

^{**} Corresponding author. School of Chemistry, Bharathidasan University, Tiruchirappalli, 620024.

transcription factors in cancer cells. To date, many histone and non-histone proteins have been identified as acetylation targets with direct involvement in tumorigenesis, contributing to the growing effort to control their regulations [2]. HDACs are divided into four classes based on homology and structure. Classes I, II and IV comprise Zn2+-dependent HDACs, whereas class III is made up of the NAD-dependent sirtuins. Class I HDACs (1, 2, 3 and 8) and class II HDACs (4–7, 9 and 10) are reported to have crucial roles in tumorigenesis. HDAC inhibitors (HDACi) were originally designed to target and inhibit HDACs, but they have a similar net effect to that of HATs, facilitating open chromatin structures that enhance transcription levels. The main function of HDACi is to prevent the subtraction of acetyl groups from lysine tails of histone proteins by blocking the active site of zinc-dependent HDAC enzymes.

HDAC inhibitors are classified into different chemical classes namely, hydroxamic acids, cyclic peptides, aliphatic fatty acids and benzamides [3,4]. Most of the HDAC inhibitors have three common pharmacophore features such as cap group, zinc binding group (ZBG) and hydrophobic spacer [5]. Recent developments indicate HDAC inhibition relies on the chelation of zinc from its core active site, thereby disturbing the substrate coordination [6]. To date, more than 20 HDACi have been used in the treatment of cancers. Only a few HDAC inhibitors like romidepsin, vorinostat, belinostat and panobinostat are approved by the U.S. Food and Drug Administration (FDA) for cancer treatment [7,8]. Based on these studies, we set out to discover new therapeutically efficacious HDACi. Molecular modelling – based rational drug design to play an important role in identifying potential inhibitors. Synthetic chemistry is also used to design new compounds or improving the efficacy or safety of readily used drugs in cancer therapy.

Heterocyclic molecules are well known to play a pivotal role in health care and pharmaceutical drug design [9]. A number of heterocyclic compounds are available and approved by FDA as anticancer drugs such as Lynparza® (Olaparib), Zydelig® (Idelalisib), Zycadia® (Ceritinib), Farydak® (Panobinostat), Lenvima® (Lenvatinib) and Ibrance® (Palbociclib). Full description of all currently investigated compounds is an unfeasible task, and here in the examples depicted and addressed are based upon the most frequent ring scaffolds in FDA approved drugs [10]. Innovativeness and categorization of heterocyclic drugs were addressed by taking previously approved therapies and their perspective molecular drugs by assessing internal FDA databases and listed drugs from the centre for drug evaluation and research (CDER) into account (Research, C. for D.E. and New Drugs at FDA 2015) [11]. Imidazoles are well known heterocyclic compounds and have an important feature of a variety of medicinal agents. The high therapeutic properties of the imidazole related drugs have encouraged the medicinal chemists to synthesize a large number of novel chemotherapeutic agents. The structural features of the imidazole ring with desirable electron rich characteristics are beneficial for imidazole derivatives to readily bind with a variety of enzymes and receptors in the biological system. The imidazole derivatives readily bind with a variety of enzymes and proteins molecules and receptors compared with other heterocyclic rings [12]. This potency and wide applicability of the imidazole pharmacophore can be attributed to its hydrogen bond donor-acceptor capability, π - π stacking interactions, co-ordination bonds with metals (e.g. Mg, Fe, and Zn) as ligands, van der Waals, polarization and hydrophobic forces. Synthesis of imidazole containing compounds by multicomponent reaction and their anti-cancer potential of against the panel of National Cancer Institute 60 cancer cell line panel. 2,2'-(2-(3-(cyclopentyloxy)-4-methoxyphenyl)-1-isobutyl-1H-imidazole-4,5- diyl)dipyridine imidazole derivative is shown to have antiproliferative activity in A549 epithelial cancer cells by affecting proliferation, migration, anchorage independent growth, and by inducing cell cycle arrest in the G2/M Phase plus the activation of apoptosis [12]. 2, 4, 5-Trisubstituted and 1, 2, 4, 5tetrasubstitutedimidazoles are present in compounds possessing versatile pharmacological activities such as p38 MAP kinase inhibitors. B-Raf kinase inhibitors, cannabinoid receptor antagonists. CSBP kinase inhibitors and glucagon receptor antagonists. In recent years, applications of imidazole derivatives in medicinal chemistry have achieved remarkable progress in cancer. But there is no sufficient work to prove imidazole having HDAC inhibition property to inhibit HDACs in non-small cell lung cancer cells. Based on these observations, we designed and synthesized imidazole containing HDACi specific blocker molecule to inhibit HDACs enzymes with general pharmacophore of established HDACi that follows the schematic of CAP- Spacer- ZBG. In recent years, the impact of molecular dynamics (MDs) simulations in molecular biology and drug discovery has expanded dramatically. These simulations can capture a wide variety of important bimolecular processes, including conformational change, ligand binding and protein folding, revealing the positions of all of the atoms at femtosecond temporal resolution [13]. Scheme 1

Motivated by the above data and in continuation of our previous reports in building novel biologically active molecules [14], in the present study, we designed imidazole containing compounds and explored their potential through docking experiments for its interactions with isoforms of HDAC enzymes and synthesize the best candidature among them for its role in modulating histone modifying enzymes thereby demonstrate its anticancer potential in A549 cell line.

2. Experimental details

2.1. General remarks

The IR spectrum was recorded on a FT-IR spectrometer (JASCO FT-IR 4600, Japan). The ¹H and ¹³C NMR spectra were recorded on a 400 MHz NMR spectrometer (Bruker Avance-III, USA). High resolution mass spectra (ESI) were recorded on a Q-TOF mass spectrometer (Agilent, USA). Silica gel (100–200 mesh) was used for column chromatography. Diethyl 2-(2-oxo-2-phenylethylidene) malonate required for the synthesis of C3 was prepared as per literature report [14]. Benzamidine hydrochloride was commercially purchased from Sigma-Aldrich.

2.2. Design of imidazole based derivatives

We designed 14 imidazole based derivatives which can possibly interact with the isoforms of HDAC enzymes. We designed these 14 compounds by considering the fulfilment of common

Synthesis of ethyl (2-phenyl-5-phenyl-1*H*-imidazol-4-yl)acetate

3

pharmacophore like CAP- Spacer- ZBG. Which was shared by the established HDAC inhibitors (Fig. 1).

2.3. Procedure for the synthesis of C3

The reaction mixture was stirred at room temperature for 12 h. The reaction mixture was diluted with water and the organic layer was separated. The layer was washed with water, dried (anhydrous Na₂SO₄) and the solvent was removed under reduced pressure. The crude product C3 so obtained was purified by column chromatography (Silica gel, 100–200 mesh) using ethyl acetate/hexane (1:3).

ethyl (2,5-diphenyl-1*H***-imidazole-4-yl)acetate (C3):** Off-white semisolid; Yield: 107 mg (35%); IR (KBr): 3357 (N–H), 2976 (C–H), 1734 (C=O) cm⁻¹; ¹H NMR (400 MHz, CDCl₃): δ 7.85 (d, J = 6.8 Hz, 2H), 7.55 (d, J = 7.2 Hz, 2H), 7.41–7.30 (m, 7H), 4.18 (q, J = 7.2 Hz, 2H),

3.80 (s, 2H), 1.26 (t, J=7.0 Hz, 3H) ppm; 13 C NMR (100 MHz, CDCl₃): δ 171.3, 146.0, 134.7, 132.2, 129.9, 128.74, 128.65, 128.6, 127.3, 127.2, 125.4, 61.3, 32.5, 14.1 ppm.; HRMS (ESI) calcd. for $C_{19}H_{18}N_2O_2$: 307.1441 [M + H⁺], found 307.1442.

3. Computational details

3.1. Molecular docking analysis for active site predictions

The crystal structure of the human HDACs family proteins obtained from protein data bank i.e. HDAC 1 (4BKX), HDAC 2 (3MAX), HDAC 3 (4A69), HDAC 8 (3SFF), HDAC 4 (2VQM), HDAC 6 (3C5K), and HDAC 7 (3C10) were selected as the docking target [15,16]. Removal of hetero atoms and adding of hydrogen bonds from their protein files were done by the protein preparation wizard module

Fig. 1. A) The four different clinically tested HDAC inhibitors. These structures represent the most common pharmacophore cap group, zinc binding group (ZBG) and hydrophobic spacer; B) Structure of designed imidazole derivatives.

applied from the Schrödinger suite, charted by their minimization using optimized potentials for liquid simulations (OPLS-2005) force field. Later, structures were exposed to the receptor grid generation process. The designed structures of the compound were C1 — C14 and established HDACi (TSA) were further examined by the ligprep module of Schrödinger suite. The synthesized compounds bond order and their charges were properly designated. Furthermore, optimized potentials for liquid simulations (OPLS-3) force field has been used to minimize the energy of synthesized compounds by using default setting [17]. The prepared compounds were docked with the active site of HDACs family proteins Glide module under rigid-receptor with flexible-ligand conditions in extra-precision (XP) mode using standard protocols.

3.2. Molecular dynamics simulations (MDs)

Molecular dynamics (MDs) simulations were performed using the program Desmond [18]. Neutral territory method (midpoint method) [19] was adopted to efficiently exploit a high degree of computational parallelism. The OPLS 2005 force-field model was used to analyse amino acid interactions in protein [20] and the simple point charge (SPC) method was used for the water model [21]. The equilibration of the system was passed out by default protocol provided in Desmond, which consists of a series of restrained minimizations and molecular dynamics simulations that are designed to slowly relax the system without deviating substantially from the initial protein coordinates. The initial coordinates for the MD calculations were taken from the modelled protein X-ray crystallographic structure of HDAC enzymes from PDP data base. The simple point charge (SPC) water molecules were added (theorthorhombic dimensions of each water box were 10 Å X 10 Å X 10 Å approximately, which confirmed the whole surfaces of the complexes to be covered), and the neutralization of system was carried out by adding Cl⁻ counter ions to balance the net charge of the system. After the construction of the solvent environment, each complex system was composed of about 34,942 atoms. Before equilibration and the long production MD simulations, the systems were minimized and pre-equilibrated using the default relaxation routine implemented in Desmond. The whole system was subjected to 300 K for 10ns of simulation of the protein-ligand complex. The structural changes and dynamic behaviour of the protein were analysed by calculating the RMSD and energy.

4. Evaluation of C3 in A549 cell lines

4.1. Reagents

Dulbecco's modified Eagle's medium, fetal bovine serum, 10X phosphate buffered saline (PBS), Antibiotic Antimycotic solution 100X, 3-(4,5-dimethyl-2-thiazolyl)- 2,5-diphenyl-2H-tetrazolium bromide (MTT), Dimethyl sulfoxide (DMSO), Acridine Orange (AO) and Ethidium Bromide (EB) were purchased from Hi Media Laboratories, Mumbai, India. 2′, 7′- dichlorofluorescin diacetate (DCFH-DA) for ROS detection, Rhodamine-123 mitochondrial specific fluorescent dye and Hoechst 33,258 dye (nuclear staining) were purchased from Sigma-Aldrich (Bangalore, India) was used in this study.

4.2. Cell culture

Cell lines were cultured in Dulbecco's modified Eagle's medium (DMEM) medium with 10% fetal calf serum (Hi Media Laboratories, Mumbai, India) supplemented with) 1% of antibiotic Antimycotic solution in a CO_2 incubator (5% CO_2) at 37 °C.

4.3. Cell viability assay

The potential cytotoxicity of the C3 was determined by 3-(4, 5-dimethylthiazol-2-yl)-2, 5-diphenyl tetrazolium bromide (MTT) assay using the reported protocol with minor modifications [22]. A549 cells were cultured in a 96 well microtiter culture plate (10,000 cells per 100 μ L) under characteristic culture conditions. The different concentrations of the C3 compound (10–100 μ M) were added to the cell monolayer. Samples were incubated at 37 °C for 24 h in the atmosphere of 5% CO2 with 95% relative humidity. The assay was accomplished according to the manufacturer's protocol and the absorbance was read at 650 nm in an ELISA iMARKTM microplate reader (Bio-Rad, USA).

4.4. Morphological changes of the C3 compound in A549 cells

A549 cells were seeded in 6-well cultured plates (5×10^4 cells/mL) under characteristic culture conditions. After overnight incubation, cells were treated with three different concentrations of C3 compound including IC₅₀ concentration ($60~\mu M$), below ($30~\mu M$), and above ($100~\mu M$) IC₅₀ identified concentration and incubated to allow colony formation for 24 h. The colonies were fixed with ethanol/acetic solution (3:1). Finally, the plates were inspected in bright field inverted light microscope (Labomed TCM 400) at 40X magnification and the morphological changes of A549 cells were documented [23].

4.5. Cytotoxicity assay using (AO/EB) staining

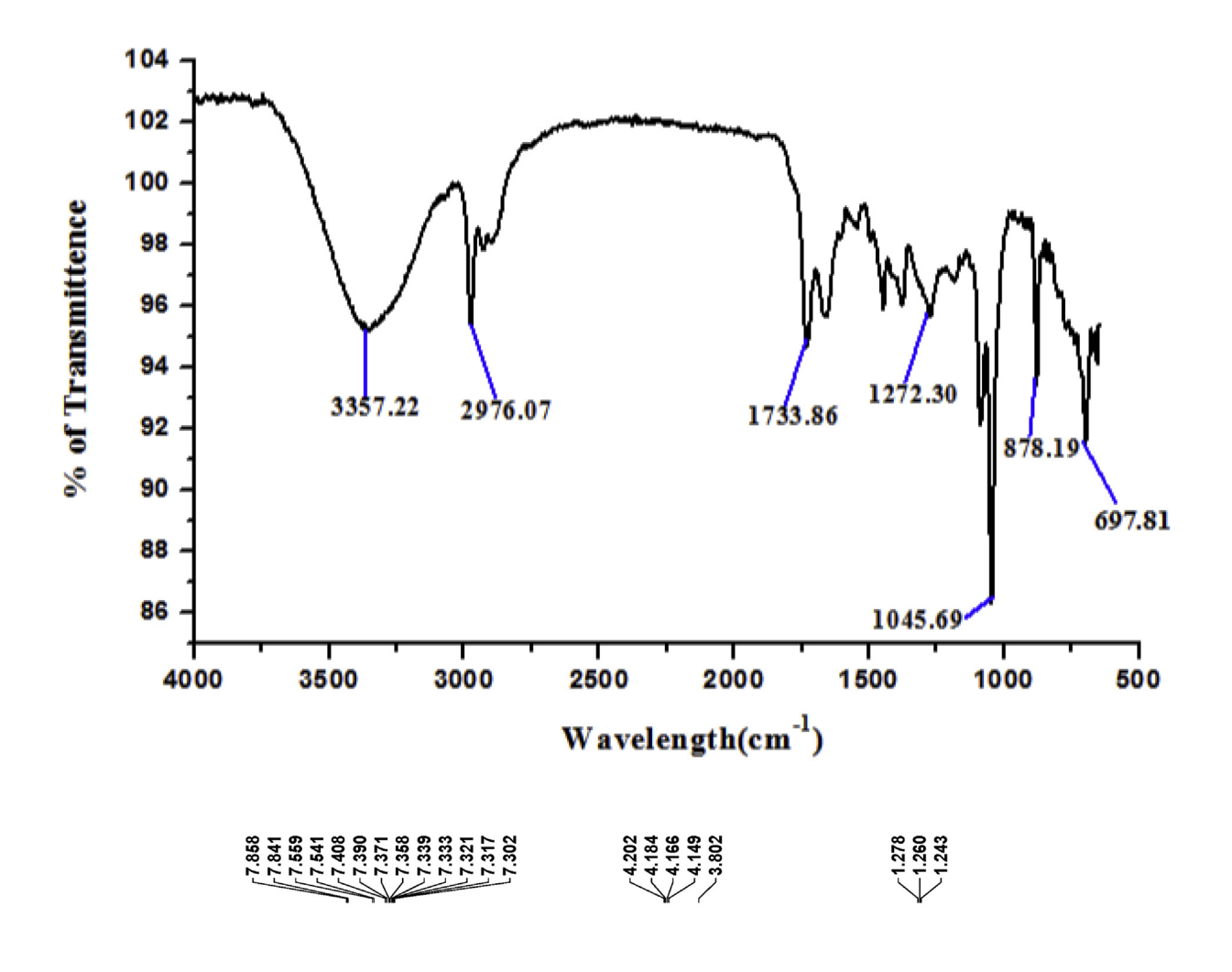
This assay was performed as described previously without any modifications [24]. Approximately 5×10^5 cells/mL were seeded in 6-well tissue culture plates and allowed to attach overnight. Next day, the attached cells were washed with 1X Phosphate Buffered Saline (PBS) and treated with IC50 concentration of C3 Compound (60 μ M) for 24 h and untreated cells were used as a control. After that, A549 cells were stained with (50 μ g/mL in 1X PBS) AO/EB for 5 min. The excess stained cells were washed using 1X PBS. Cells of the images were visualized by fluorescence microscope (EVOS® FLoid® Cell Imaging Station) Thermo Fisher Scientific, Bangalore, India) at 40X magnification with an excitation filter. AO (excitation 532/59 nm, emission 532/59 nm) and EtBr (excitation 646/68 nm, emission 646/68 nm).

4.6. Hoechst staining to detect nuclear damage

A549 cells were seeded at 5×10^5 cells/well in 6 well plate and allowed to attach overnight under characteristic conditions. After overnight incubation, the cells were treated with IC₅₀ concentrations of the C3 compound for 24 h respectively, and the treated cells were exposed with Hoechst 33,258 at 2 μ g/mL based on the manufacture protocol without any modifications [25] and observed under EVOS® FLoid® Cell Imaging Station at 20X magnification with the blue filter at excitation 390/40 nm and emission 446/33 nm.

4.7. Measurement of ROS generation by DCFH-DA staining method

2', 7'-dichlorfluorescein-diacetate (DCFH-DA) staining method was used in the measurement of ROS generation in both control and treated A549 cells [26]. A549 cells were seeded in 6-well tissue culture plates at 5×10^4 cells/mL and allowed to attach overnight. After overnight incubation, the medium was removed and replaced with fresh medium containing 10% FBS and supplemented with IC50concentration of C3 compound and incubated for 24 h. After



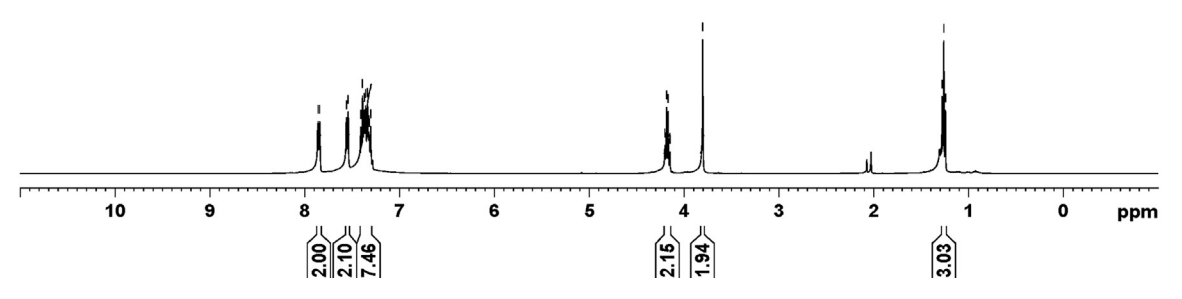


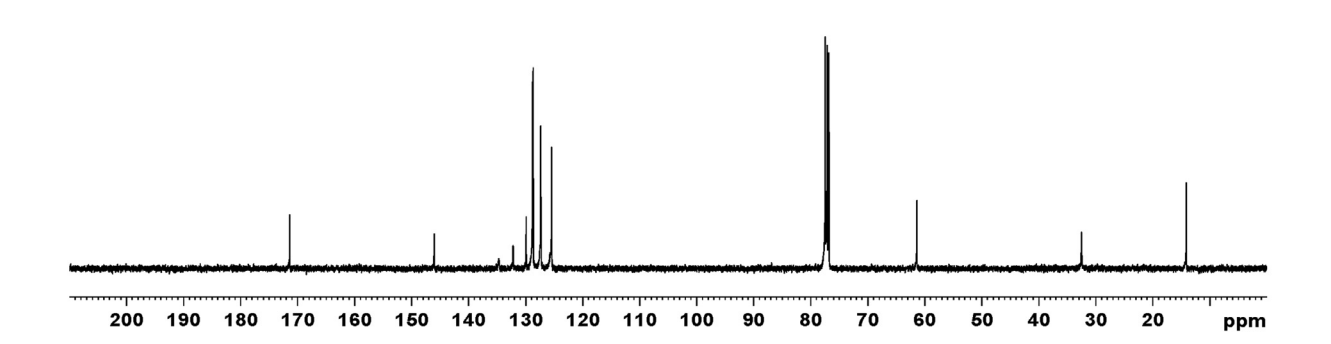
Fig. 2. IR, NMR and HRMS spectra of compound C3: 2.1) IR spectrum of compound C3, **2.2**) ¹H NMR spectrum of (CDCl₃, 400 MHz) of compound C3, **2.3**) ¹³C NMR spectrum of (CDCl₃, 100 MHz) of compound C3, **2.4**) HRMS spectrum of compound C3.

treatment, cells were washed with 1XPBS and subsequently stained with 0.5 mL of 10 mM of DCFH-DA dye for 10 min. Excess dye was removed with 1XPBS and samples were observed at 20X magnification with a green filter (EVOS®FLoid®Cell Imaging Station, excitation 532/59 nm, emission 532/59 nm).

4.8. Assessment of mitochondrial membrane potential ($\Delta \psi m$) using Rhodamine-123

A549 cells $5\times10^5/mL$ were seeded in 6 well tissue culture plates and incubated overnight for the cells to attach. After 24 h the old





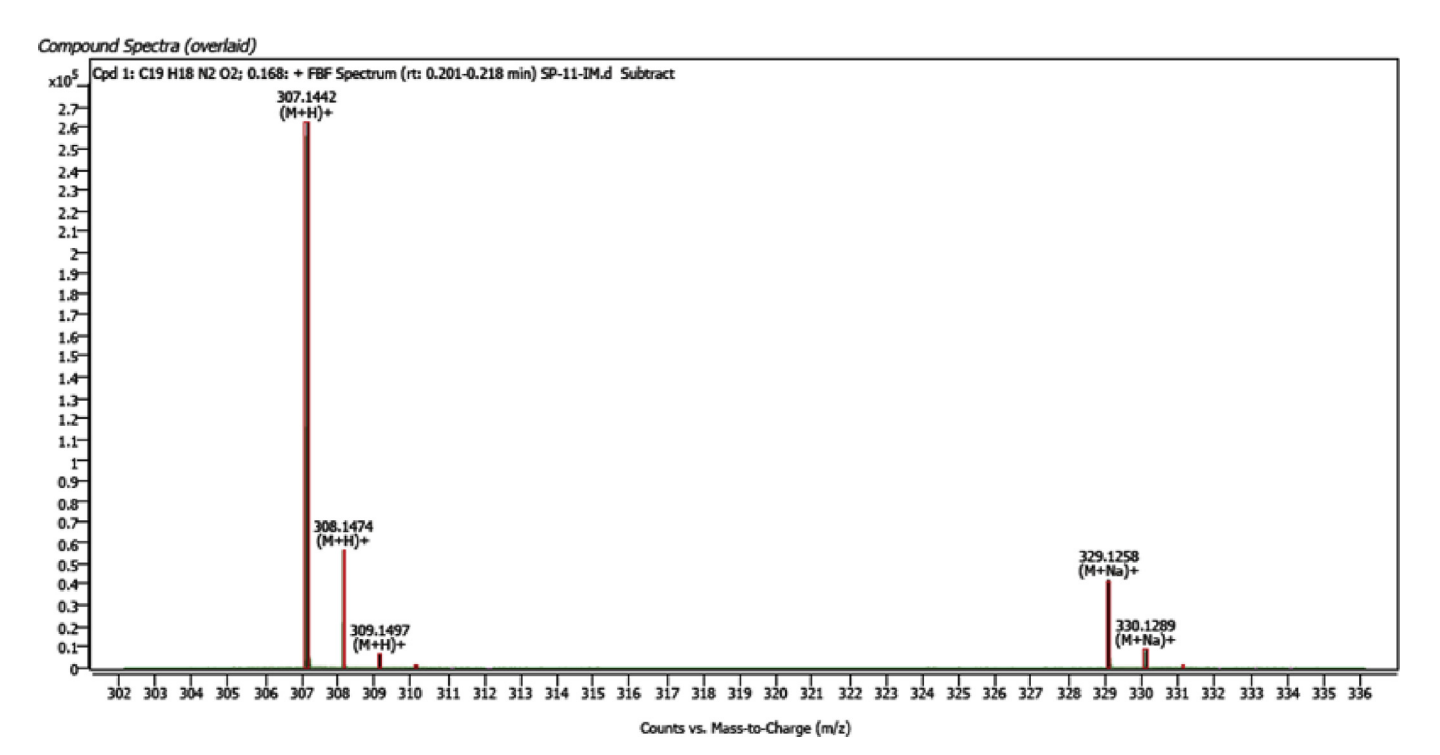


Fig. 2. (continued).

medium was replaced with fresh medium containing C3 Compound and incubated for 24 h respectively. Following treatment, cells were exposed to Rhodamine-123 dye (10 μ g/mL) to observe mitochondrial membrane potential [27]. The dye was exposed to the cells for 10 min at room temperature and followed by 1X PBS wash and observed with EVOS® FLoid® Cell Imaging Station at a magnification of $20\times$ (green filter: excitation 532/59 nm, emission 532/59 nm).

4.9. Statistical analysis

One way ANOVA with Dunnett's posttest was used for testing the mean value \pm SD using Graphpad prism software version 6.03 (La Jolla, CA). Values with P < 0.05 were considered significant.

5. Results and discussion

5.1. Characterization of compound C3 by IR, NMR and HRMS

The structure of compound 3 was unequivocally supported by its IR, ¹H NMR and ¹³C NMR spectra and high resolution mass spectrum (HRMS) (Fig. 2). The IR spectrum of 3showed three characteristic stretching absorptions at 3357, 2976 and 1734 cm⁻¹ corresponding to imidazole N-H, aromatic C-H and ester C=O groups, respectively. The ¹H NMR spectrum of **3** displayed a threeproton triplet at δ 1.26 (J=7.0 Hz) for the ester methyl protons, a two-proton singlet at $\delta 3.80$ for the methylene protons attached to the imidazole ring and a two-proton quartet at $\delta 4.18$ (J = 7.2 Hz) for the ester methylene protons in addition to signals for eleven aromatic and imidazole nitrogen protons in region of δ 7.30–7.86. The ¹³C NMR spectrum of **3** showed the ester methyl carbon at δ 14.1. the methylene carbon attached to the imidazole ring at δ 32.5, the ester methylene carbon at δ 61.3 and the ester carbonyl carbon at δ 171.3 in addition to signals for aromatic carbons. The HRMS of **3** showed a peak at m/z307.1442 corresponding to the [M + H⁺] ion (M = Molecular weight).

5.2. In- silico docking analyses of designed compounds on HDAC enzymes of class I and II

The designed compounds and the known HDACi (Table 2) were docked to the active site of the HDAC family proteins. Molecular docking studies on the test compounds and known inhibitors with respect to the HDACs family protein show that compound C3 has attractive binding energy compared to the known inhibitor (TSA) and other synthesized compounds. Table 1 shows that compound C3 has high scores for the HDACs 1, 2, 3, 8, 4, 6, & 7 proteins when compare to standard HDACi (TSA) used as a positive control. The oxygen atom of ethyl acetate moiety makes hydrogen bond interaction with Tyr 14 and Lys 123 residues of HDAC1 protein. In HDAC 2 protein Hie 183 residues forms hydrogen bond interaction with oxygen atom of ethyl acetate moiety. Lys 159, Lys474 and Lys475 residues interacted with ethyl acetate moiety and also Lys 159 interacted with 1-H imidazole region. Hie 198 residue of HDAC 4 and HDAC 6 protein residues Arg 47 and Tyr 76 makes hydrogen bond interaction with ethyl acetate moiety. 2, 5-diphenyl region of compound 3 makes Pi-Pi interaction with Phe 155 residue of HDAC 2, Tyr 306 of HDAC 8, His 159 of HDAC 4 and Tyr 35 and 48 residue of HDAC 6. Based on the docking study, compound C3 has more binding energy (Fig. 3) are responsible for inhibition of the HDAC family proteins. The designed compounds, ethyl (2-phenyl-5phenyl-1H-imidazole-4-yl)acetate shared the common pharmacophore like SRM, Linker, CU and ZBG groups which is shared by the different classes including the FDA approved established classical HDACi. Our experimental data demonstrate that CU and ZBG group is vital for HDACi which is essential for a ligand to trigger chromatin remodelling by modulation of highly expressed HDAC enzymes.

5.3. Molecular dynamics simulation (MDs) of C3 compound

The molecular dynamics simulations were performed for HDAC enzyme-ligand complexes. We used Gromacs 4.5.5 software for all the molecular dynamics simulation protocol [28]. The stability of protein-ligand complex was governed by RMSD analysis. The RMSD

Table 1	
Calculated the docking score of designed con	npounds.

S.no	Compound	HDAC 1	HDAC 2	HDAC 3	HDAC 8	HDAC 4	HDAC 6	HDAC 7
1.	C1	-3423	-4.589	-5.266	-6.937	-3.491	-4.08	-3.586
2.	C2	-3.018	-5.00	-5.223	-4.355	-4.205	-4.165	-4.002
3.	C3	-3.149	-5.163	-4.885	-11.039	-5.004	-5.098	-5.163
4.	C4	-2.603	-5.098	-5.234	-9.021	-4.452	-4.902	-5.300
5.	C5	-2.744	-5.004	-6.053	-8.788	-4.771	-3.445	-3.362
6.	C6	-2.97	-2.756	-2.909	-5.39	-3.478	-3.21	-4.267
7.	C7	-3.042	-4.766	-3.007	-4.805	-3.395	-3.721	-04.411
8.	C8	-2.527	-4.237	-2.454	-5.367	-1.943	-3.262	-2.864
9.	C9	-3.387	-3.966	-2.747	-4.252	-2.208	-3.063	-1.203
10.	C10	-2.592	-3.769	-2.08	-3.988	-2.783	-1.282	-2.933
11.	C11	-2.904	-4.502	-3.494	-5.984	-3.477	-3.219	-1.587
12.	C12	-1.858	-4.484	-3.203	-6.858	-2.537	-3.809	-2.945
13.	C13	-2.502	-3.853	-2.684	-6.696	-3.014	-3.202	-1.74
14.	C14	-2.485	-5.173	-3.079	-5.717	-3.717	-2.996	-2.126

 Table 2

 Docking Score for Clinically tested standard Histone deacetylase inhibitor.

S.no	Compound	HDAC 1	HDAC 2	HDAC 3	HDAC 8	HDAC 4	HDAC 6	HDAC 7
1.	TSA	-4.241	-2.768	-4.637	-9.322	-2277	-4.114	-4.225
2.	SAHA	-1.817	-7.06	-3.500	-9.219	-4.388	-8.903	-5.069
3.	LBH 589.1	-4.207	-4.174	-3.905	-7.522	-3.409	-3.756	-6.782
4.	SCRIPTAID	-3.827	-5.294	-4.079	-6.782	-5.751	-3.976	-7.187
5.	BELINOSTAT	-3.484	-6.559	-3.145	-6.337	-2.179	-3.74	-3.576
6.	MS278.1	-2.991	-8.472	-4.025	-10.909	-4.512	-4.19	-7.605

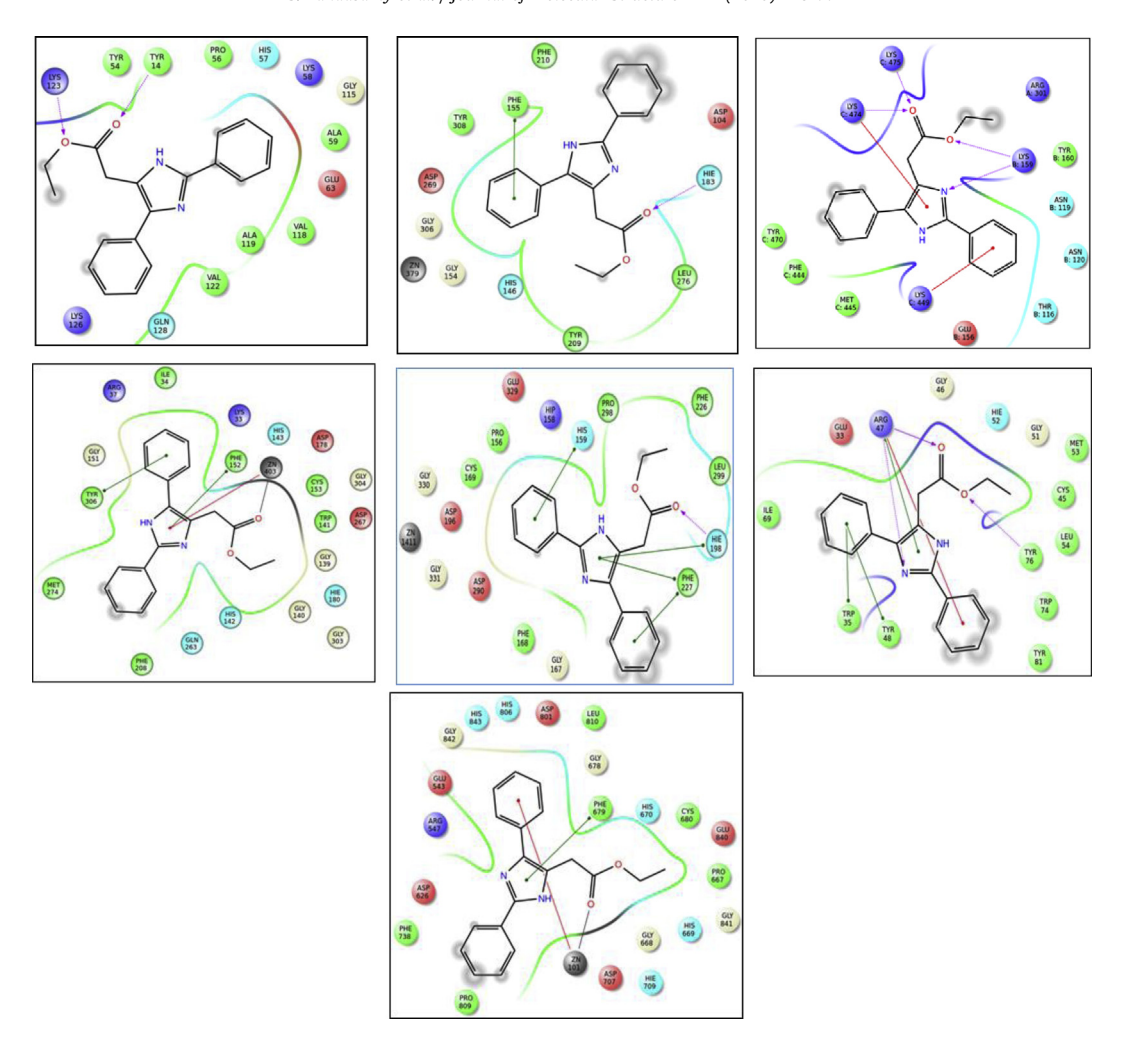


Fig. 3. 2D representation of the interactions of Compound C3 with the amino acid residues of HDACs (PDB ID): (a) HDAC 1 (4BKX); (b) HDAC 2 (3MAX); (c) HDAC 3 (4A69); (d) HDAC 8 (3SFF); (e) HDAC 4 (2VQM); (f) HDAC 6 (3C5K); (g) HDAC 7 (3C10). Pink colour represents the hydrogen bond interaction, green colour represents the pi—pi interaction, red colour represents the pi—cation interaction, and red-with-blue combination represents the salt bridges.

results of the HDAC family proteins and C3 ligand complexes attained 0.2 nm to 0.4 nm deviation which manifested the C3 compounds have more stable in the HDAC family proteins. At the end of the 20 ns of time scale simulation, all the protein-ligand complexes were attain their stable conformation. The hydrogen bond analysis of C3 compound and HDAC family proteins shows (Fig. 4). The hydrogen bond analysis showed the C3 compound making hydrogen bond interaction with HDAC family proteins ranging from 1 to 8 hydrogen bonds. Finally, the dynamics results are well correlated with docking and *in vitro* studies and the compound C3 were stable in HDAC family proteins.

5.4. Cytotoxicity assay of the C3 compound using MTT

To evaluate the inhibitory effects of C3 compound on the cancer cells, cells were treated with increasing concentrations (10–100 μM) of C3 in A549 lung cancer cells for 24 h and MTT assay was performed. As shown in (Fig. 5), almost 50% of cell death was observed at 60 μM concentration of C3 compound and it was fixed

as IC_{50} concentration. Treatment of the C3 compound decreased the cell viability of A549 lung cancer cells in a concentration-dependent manner. A significant dose-dependent inhibition of cancer cell proliferation and reduced cell viability were observed in A549 cells. These results suggest that C3 compound reduced cell viability and inhibit the anchorage independent growth of lung cancer cells.

5.5. Morphological changes of A549 cells treated with C3 compound using phase contrast microscopy

Microscopic observations of A549 cells treated with C3 compound revealed significant morphological changes when compound used at higher concentrations. A549 cells showed a loss of cell extensions, rounding up and detachment, apoptotic blebbing, and reduction in size as well as in cell density was observed when compared to untreated A549 cells (Fig. 6). These results revealed that the imidazole based C3 compound has potentially inhibited A549 cells.

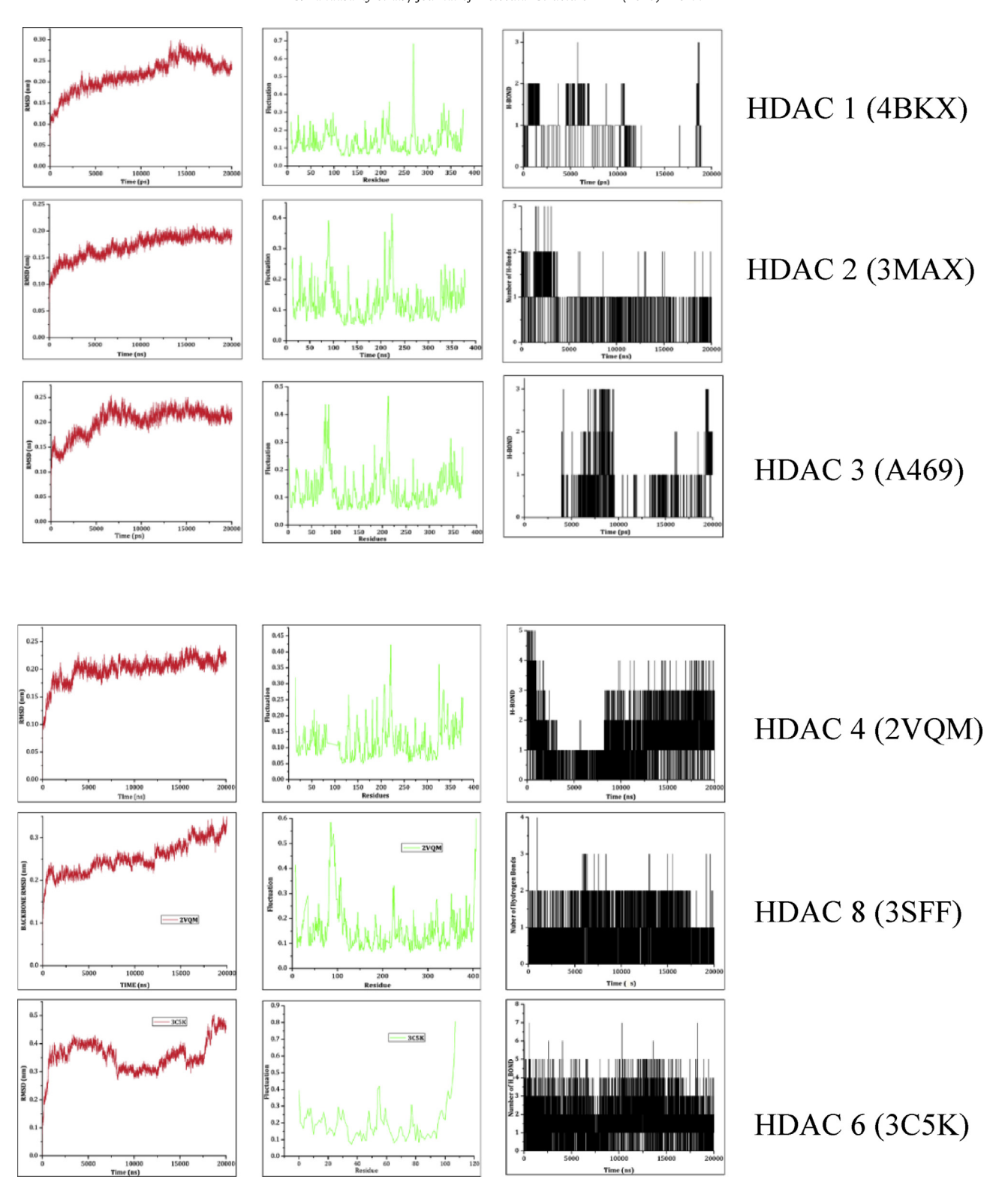


Fig. 4. Root mean square deviations and total energy of protein — ligand complexes during 10 ns simulation time. The Red colours represent the backbone RMSD of protein stability. Green colours represent the RMSF of the protein residues. Black colours represent the hydrogen bond interaction of the protein-ligand complex. Figures generated by the program Gromacs 4.5.5 software.

5.6. Effect of C3 compound on nuclear damage and induction of apoptosis

A549 cells were treated with IC_{50} concentration of C3 compound

stained with AO/EB. Dual staining of A549 cells was observed under a fluorescence microscope and detected the various stages of apoptosis. AO stains with both viable and dead cells produce green fluorescence, whereas EB emits red or orange fluorescence only in

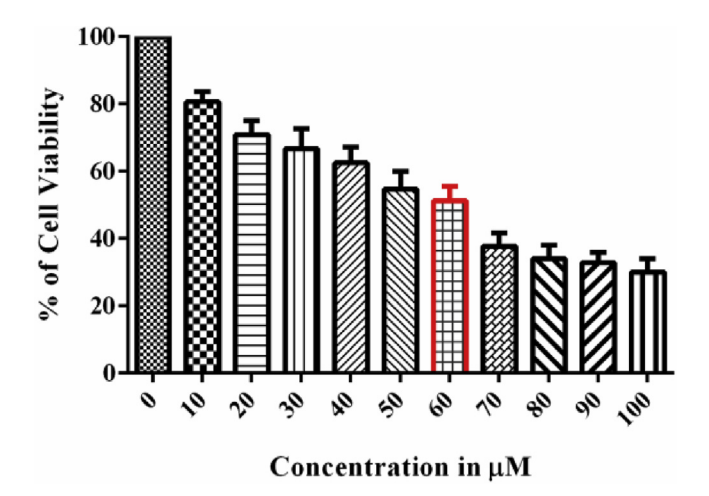


Fig. 5. Cell viability was analysed by the MTT assay. A549 cells were treated with C3 compound at indicated the IC50 value. Dose dependent inhibition of cell growth was observed after 24 h treatment

non-viable cells. Cells were treated with IC_{50} (60 μ M) of C3 compound revealed clear signs of apoptosis as shown in (Fig. 7A). The orange-red colour indicated necrotic bodies. Early stage apoptotic

cells were marked by green colour was detected and late stage apoptotic bodies were detected by orange colour. There was no significant apoptosis detected in the untreated cells. Further, we performed Hoechst 33,258 staining to investigate the nuclear morphological changes of C3 compound treatment on A549 cells. Hoechst 33.258 fluorescence stain is used to label DNA, live cells nuclei will be stained with uniformly light blue and apoptotic cells nuclei will be stained with bright blue because of chromatin condensation. After treatment with C3 compound, the A549 cells showed the characteristic morphological changes of apoptosis, including shrinking of the cytoplasm and nuclear fragmentation with an intact cell membrane and contracted nucleus. Bright blue colour was observed because of chromatin condensation and membrane blebbing as shown in (Fig. 7B). Our experimental data revealed that the C3 compound had induced apoptosis to contribute to the antitumor effect.

5.7. C3 induces excessive ROS accumulation induced apoptosis by increasing oxidative stress and altering mitochondrial functions

The excessive accumulation of ROS levels in cancer cells induces oxidative stress and alters the mitochondrial functions and this is known to play a major role in apoptotic stimulation. To study the relationship between cytotoxicity and generation of ROS level,

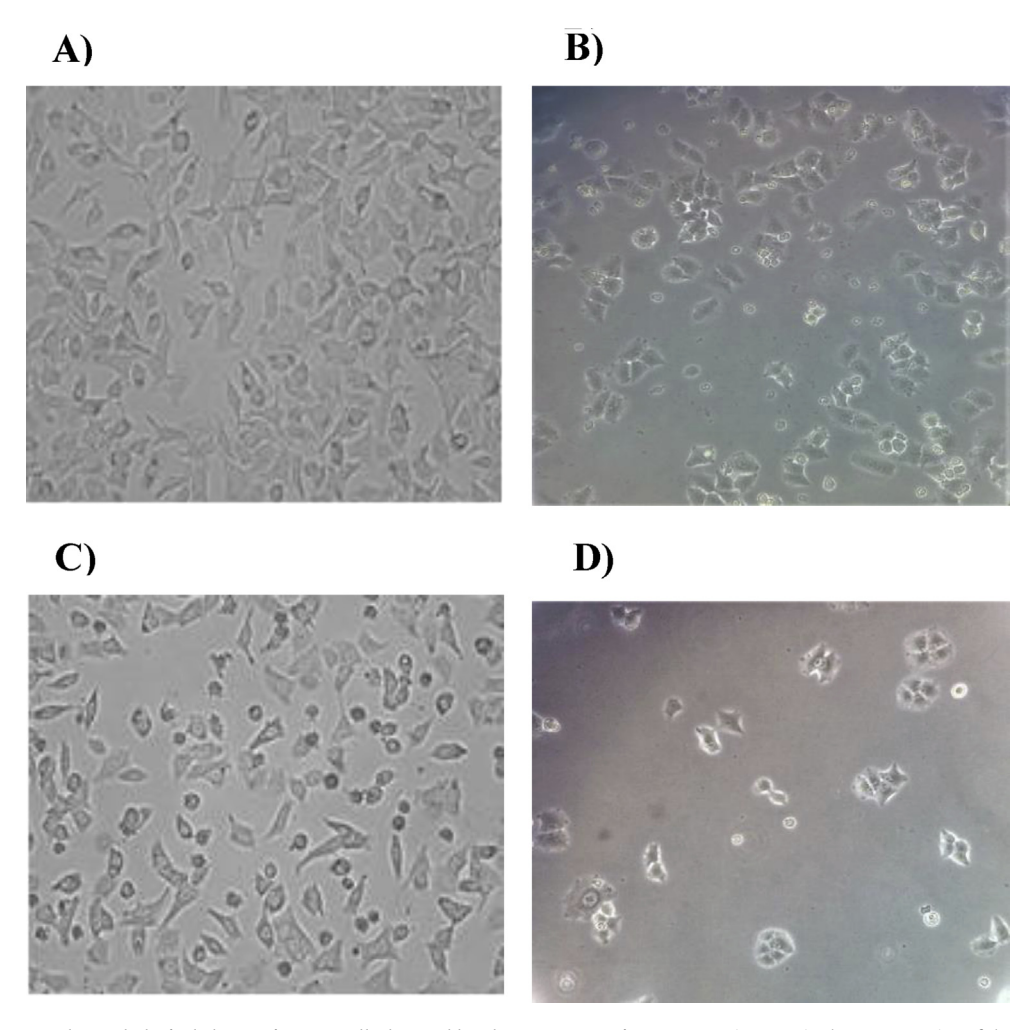


Fig. 6. Effect on C3 compound morphological changes in A549 cells detected by phase contrast microscopy. An increase in the concentration of the C3 compound affects the outer surface of the cells, membrane blebbing, and damage in A549 cells (b-d) than control cells. a) Control; b) below concentration of 30 μM/mL; c) IC₅₀ concentration of 60 μM/mL respective values; d) higher concentration of 100 μM/mL.

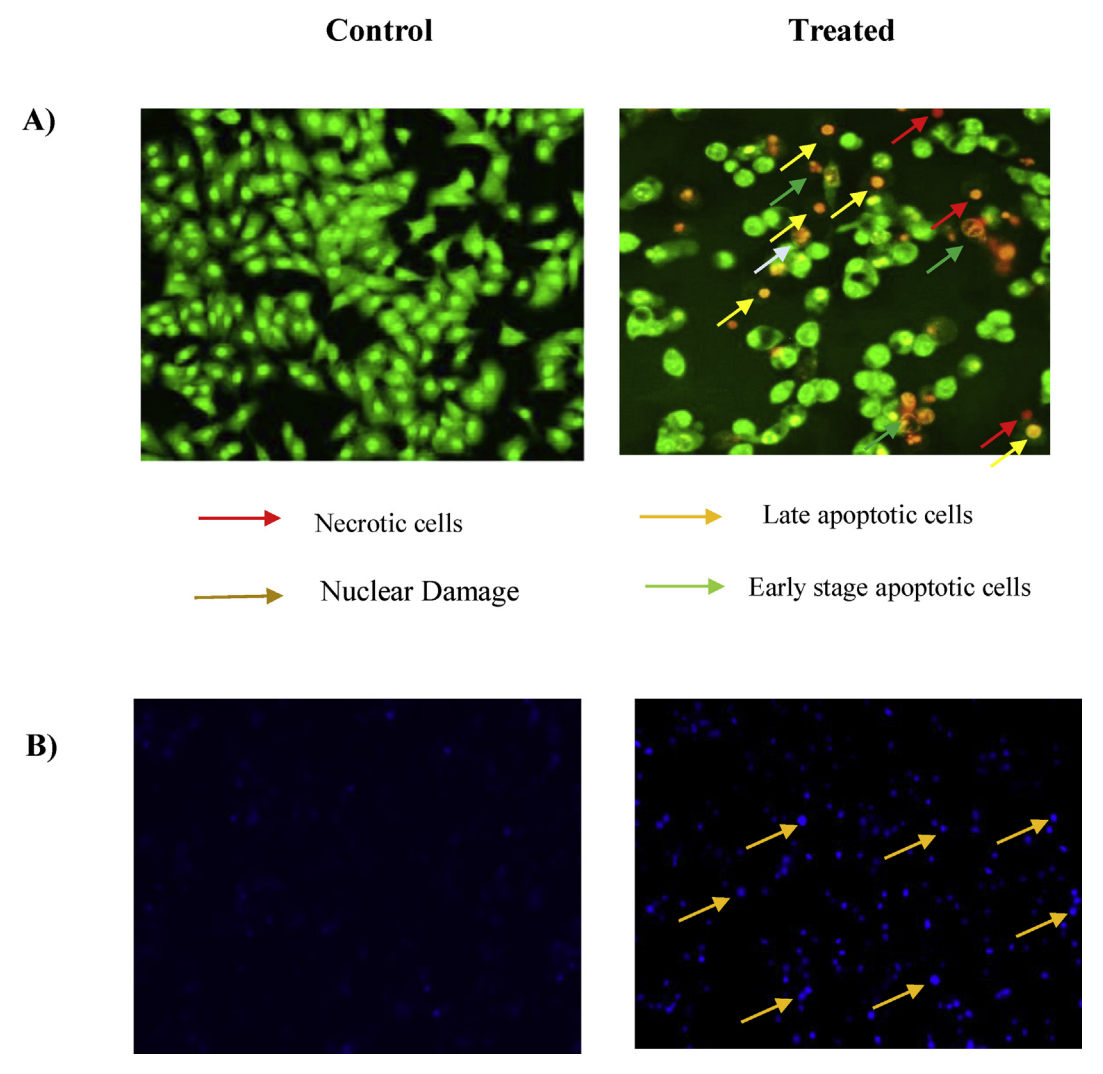


Fig. 7. Fluorescence microscopic analysis of A549 cells. A) Morphological changes of A549 cells to detect the various stages of apoptosis by AO/EB Staining. B) The number of apoptotic necrotic cells and nuclear damage were detected with their respective IC_{50} values of the C3 compound detected by Hoechst 33,258 Staining.

A549 cells were exposed to (60 µM) concentrations of C3 compound, it had been detected with intracellular ROS indicator DCFH-DA. In the presence of endogenously generated ROS, DCFH-DA is oxidised to release the fluorophore DCF. After 24 h treatment, ROS generation was gradually increased when compared to the untreated cells. As shown in (Fig. 8A). From this result revealed that lower DCF fluorescence intensity was detected with untreated cells when compared to the treated cells. Recent work proved that exposure of C3 compound induce a mitochondrial-dependent ROS response that significantly enhances the cytotoxic effect caused by nuclear DNA damage in cancer cells. The sensitization of the outer layer mitochondrial membrane is an important process to initiate apoptosis of A549 cells. Rhodamine 123 staining method was used to evaluate mitochondria membrane potential ($\Delta \psi m$) in treated and control. After 24 h treatment A549 cells were decreased as shown in (Fig. 8B) the uptake of Rhodamine 123. Results of the present study indicated that the C3 compound had induced apoptosis through an elevated level of ROS generation and alter the mitochondria membrane potential. We conclude from experimental data clearly emphasize enhanced generation of ROS and down regulation of $\Delta \psi m$ in cancer cells is a key pathway of apoptosis development that leads to cancer cell viability.

6. Conclusion

In summary, imidazole based heterocyclic compounds were designed to employ efficient inhibition of HDAC enzymes followed by synthetic methodologies in pure form was implemented and was tested for its inhibitory activity against HDAC enzymes. C3 compound had displayed the highest binding activities among their series of HDAC enzymes respectively. Molecular docking studies revealed that the binding interactions of the C3 compound had significant binding ability with the active site of the HDAC enzyme. Our results showed that the C3 compound had induced apoptosis by increasing the levels of ROS and loss of mitochondria membrane potential. This study clearly revealed that C3 compound is an effective epigenetic modulator of chromatin modifications of histone and non-histone proteins in treatment for lung cancer. We believe that these results encourage synthesis of new and similar compounds (more selective, more active and non-toxic derivatives) and tested against various cancers as an alternative treatment strategy in the near future.

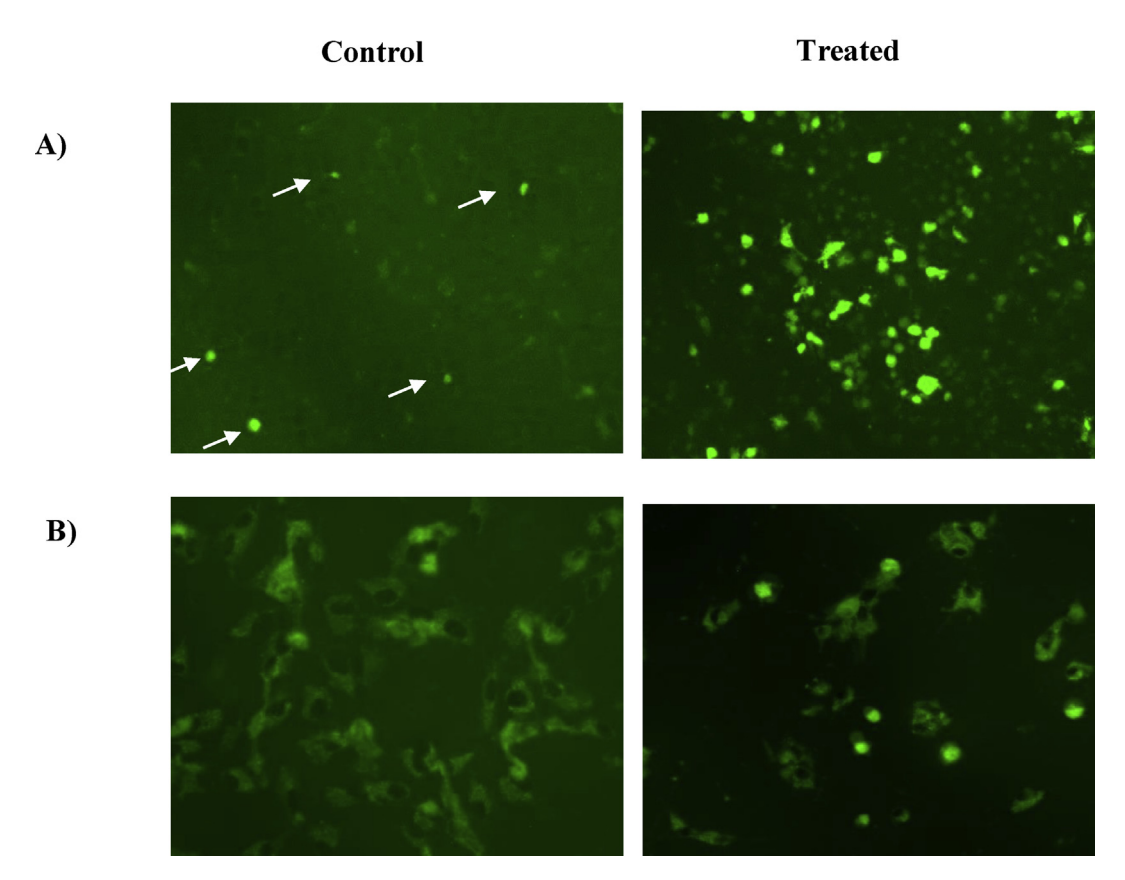


Fig. 8. A) ROS generation of C3 compound induced apoptosis through DCFH-DA staining. B) Rhodamine-123 staining was used to detect the loss of mitochondrial membrane potential when exposed to IC₅₀ doses of the C3 compound as compared to control. Images were taken at 100 μM with 20X magnification.

Credit of author statement

S.K performed the experiments. P.S performed microscopic studies. JM.J, K.M, G.P and V.R performed the bioinformatics experiments. K.S contributed in synthesising C3 compound. R.V conceptualized the entire work and wrote the manuscript. All authors reviewed the results and approved the version of the manuscript.

Declaration of competing interest

We declare no conflict of interest.

Acknowledgements

Kandasamy Saravanan is grateful to Science and Engineering Research Board (SERB), Department of Science and Technology, Government of India, for providing financial support through their junior research fellowship (JRF). Prabhu Subramani is grateful to DST PURSE for providing financial support through their junior research fellowship (JRF). We acknowledge Dr. C. Prahalathan and Dr. A. Antony Joseph Velanganni, Department of Biochemistry, Bharathidasan University, Tiruchirappalli, India, for their help with gel documentation and fluorescence microscopic studies. We are grateful to the Department of Science and Technology, Fund for Improvement of S&T Infrastructure in Universities and Higher Educational Institutions (DST-FIST and DST-PURSE) for their infrastructure support to our department.

Appendix A. Supplementary data

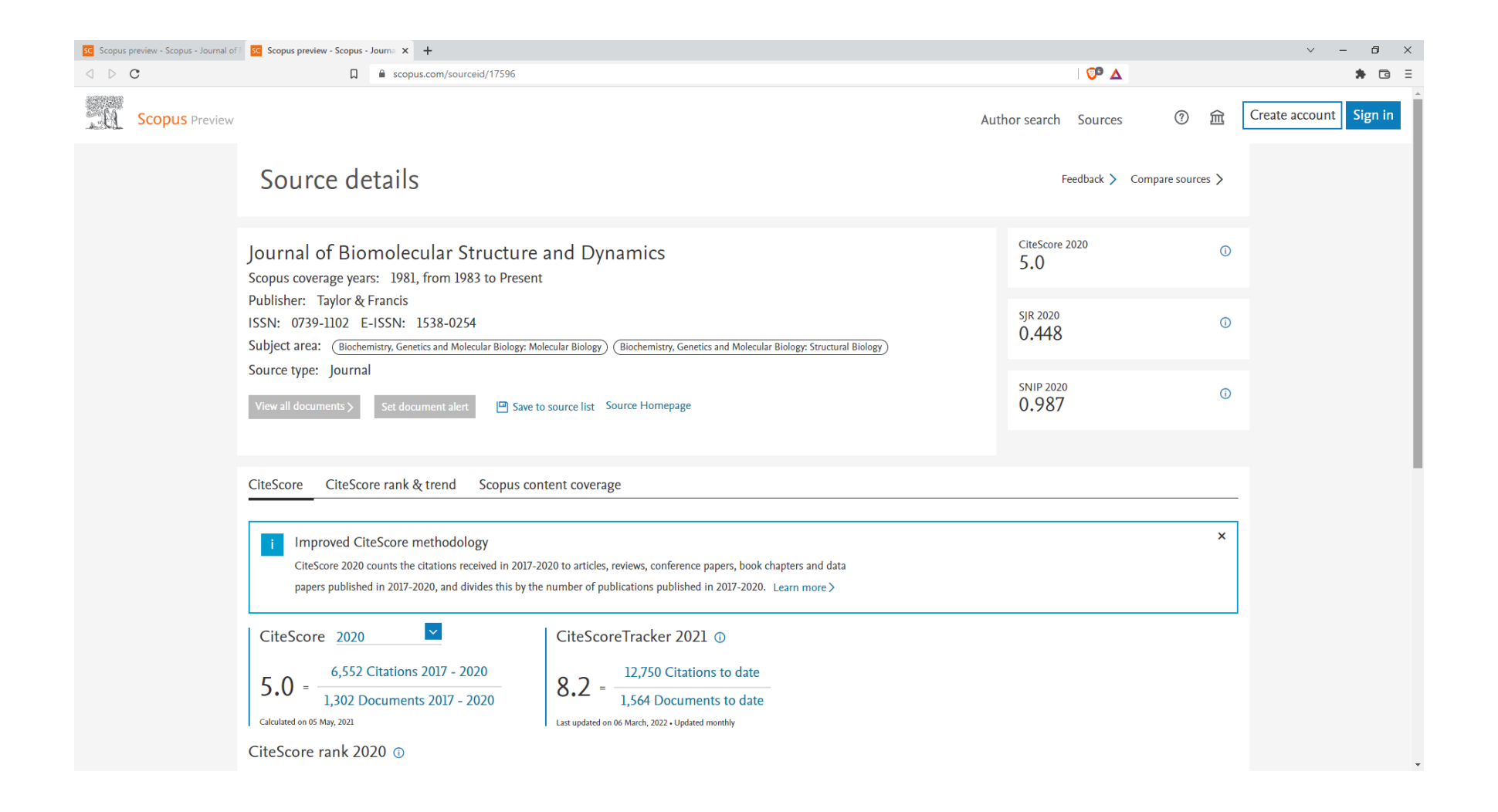
Supplementary data to this article can be found online at https://doi.org/10.1016/j.molstruc.2020.128177.

References

- [1] Mark A. Dawson, Tony Kouzarides, Cancer epigenetics: from mechanism to therapy, Cell 150 (1) (2012) 12–27.
- [2] B.S. Dwarakanath, et al., Targeting protein acetylation for improving cancer therapy, Indian J. Med. Res. 128 (1) (2008) 13–21.
- [3] Thomas A. Miller, David J. Witter, Sandro Belvedere, Histone deacetylase inhibitors, J. Med. Chem. 46 (24) (2003) 5097–5116.
- [4] Paul A. Marks, et al., Histone deacetylase inhibitors, Adv. Canc. Res. 91 (2004) 137–168.
- [5] Marielle Paris, et al., Histone deacetylase inhibitors: from bench to clinic, J. Med. Chem. 51 (6) (2008) 1505–1529.
- [6] Arunachalam Kalaiarasi, et al., Plant isoquinoline alkaloid berberine exhibits chromatin remodelling by modulation of histone deacetylase to induce growth arrest and apoptosis in the A549 cell line, J. Agric. Food Chem. 64 (50) (2016) 9542–9550.
- [7] C.A. Zahnow, et al., Inhibitors of DNA Methylation, Histone Deacetylation, and Histone Demethylation: a Perfect Combination for Cancer Therapy, vol. 130, Academic Press, 2016, pp. 55–111. Advances in cancer research.
- [8] Daiqing Liao, Profiling technologies for the identification and characterization of small-molecule histone deacetylase inhibitors, Drug Discov. Today Technol. 18 (2015) 24–28.
- [9] Rajeshwar P. Verma, Cytotoxicity of Heterocyclic Compounds against Various Cancer Cells: a Quantitative Structure—Activity Relationship Study, Bioactive Heterocycles III. Springer, Berlin, Heidelberg, 2007, pp. 53—86.
- [10] Pedro Martins, et al., Heterocyclic anticancer compounds: recent advances and the paradigm shift towards the use of Nano medicine's tool box, Molecules 20 (9) (2015) 16852–16891. Click2Drug—Encyclopedia—Chemical Compounds—Most Frequent Rings in FDA Approved Drugs. Available online: http://www.click2drug.org/encyclopedia/chemistry/fda-based-rings.html. (Accessed 5 June 2015).
- [11] Research, C. For D.E and new drugs at FDA: CDER's new molecular entities and new therapeutic biological products, Available online: http://www.fda.gov.

- Drugs/Development Approval process/Drug Innovation/default.htm. (Accessed 1 June 2015).
- [12] Gangavaram VM. Sharma, et al., Imidazole derivatives show anticancer potential by inducing apoptosis and cellular senescence, MedChemComm 5 (11) (2014) 1751–1760.
- [13] Scott A. Hollingsworth, Ron O. Dror, Molecular dynamics simulation for all, Neuron 99 (6) (2018) 1129–1143.
- [14] Thangavel Selvi, Kannupal Srinivasan, Boron trifluoride mediated ringopening reactions of trans-2-aryl-3-nitro-cyclopropane-1, 1-dicarboxylates. Synthesis of aroylmethylidene malonates as potential building blocks for heterocycles, J. Org. Chem. 79 (8) (2014) 3653–3658. Anne Marie J, Sid T (2008) Driving forces for ligand migration in the leucine transporter. Chem Biol Drug Des 72(4):265–272.doi.org/10.1111/j.1747-0285.2008.00707.x.
- [15] Hung-Ying Kao, et al., Isolation and characterization of mammalian HDAC10, a novel histone deacetylase, J. Biol. Chem. 277 (1) (2002) 187–193.
- [16] Xianbo Zhou, et al., Identification of a transcriptional repressor related to the noncatalytic domain of histone deacetylases 4 and 5, Proc. Natl. Acad. Sci. Unit. States Am. 97 (3) (2000) 1056–1061.
- [17] Edward Harder, et al., OPLS3: a force field providing broad coverage of druglike small molecules and proteins, J. Chem. Theor. Comput. 12 (1) (2016) 281–296.
- [18] J.B. Kevin, et al., Scalable algorithms for molecular dynamics simulations on commodity clusters, Proceedings of the ACM/IEEE Conference on Supercomputing (SC06) (2006).
- [19] Kevin J. Bowers, Ron O. Dror, David E. Shaw, The midpoint method for parallelization of particle simulations, J. Chem. Phys. 124 (18) (2006) 184109.
- [20] W.L. Jorgensen, D.S. Maxwell, J. Tirado-Rives, Development and testing of the OPLS all-atom force field on conformational energetics and properties of organic liquids, J. Am. Chem. Soc. 118 (1996) 11225—11236, https://doi.org/

- 10.1021/ja9621760.
- [21] G.A. Kaminski, R.A. Friesner, J. Tirado-Rives, W.L. Jorgensen, Evaluation and reparametrization of the OPLS-AA force field for proteins via comparison with accurate quantum chemical calculations on peptides, J. Phys. Chem. B 105 (2001) 6474–6487, https://doi.org/10.1021/jp003919d.
- [22] Ramesh Ummanni, et al., Altered expression of tumor protein D52 regulates apoptosis and migration of prostate cancer cells, FEBS J. 275 (22) (2008) 5703–5713.
- [23] Veronica Janson, et al., Phase-contrast microscopy studies of early cisplatininduced morphological changes of malignant mesothelioma cells and the correspondence to induced apoptosis, Exp. Lung Res. 34 (2) (2008) 49–67.
- [24] Shailaja Kasibhatla, et al., Acridine orange/ethidium bromide (AO/EB) staining to detect apoptosis, Cold Spring Harb. Protoc. 3 (2006) pdb—prot4493, 2006.
- [25] Valérie Combaret, et al., Effect of bortezomib on human neuroblastoma: analysis of molecular mechanisms involved in cytotoxicity, Mol. Canc. 7 (1) (2008) 50.
- [26] Jun Wang, et al., Anticancer effect of salidroside on A549 lung cancer cells through inhibition of oxidative stress and phospho-p38 expression, Oncology letters 7 (4) (2014) 1159–1164.
- [27] Alessandra Baracca, et al., Rhodamine 123 as a probe of mitochondrial membrane potential: evaluation of proton flux through F0 during ATP synthesis, BiochimicaetBiophysicaActa (BBA)-Bioenergetics 1606 1–3 (2003) 137–146
- [28] Understanding reactivity of two newly synthetized imidazole derivatives by spectroscopic characterization and computational study, M. Hossain, T. Renjith, Y. Mary, K. Resmi, S. Armaković, S. Armaković, N. Ashis, G. Vijayakumar, C. Alsenoy, J. Mol. Struct. (2018), https://doi.org/10.1016/ i.molstruc.2018.01.029s. In Press.







Structural exploration of common pharmacophore based berberine derivatives as novel histone deacetylase inhibitor targeting HDACs enzymes

Saravanan Kandasamy^a, Manikandan Selvaraj^b, Karthikeyan Muthusamy^b, Naveena Varadaraju^a, Srinivasan Kannupal^c, Ashok Kumar Sekar^d and Ravikumar Vilwanathan^a

^aDepartment of Biochemistry, School of Life Sciences, Bharathidasan University, Tiruchirappalli, Tamil Nadu, India; ^bDepartment of Bioinformatics, Alagappa University, Karaikudi, Tamil Nadu, India; ^cSchool of Chemistry, Bharathidasan University, Tiruchirappalli, Tamil Nadu, India; ^dCentre for Biotechnology, Anna University, Chennai, Tamil Nadu, India

ARSTRACT

Histone deacetylase (HDAC) inhibitors, are new class of cancer chemotherapeutics used in clinical development. It plays a pivotal role in restoring the acetylation balance and lysine residual deacetylation in histone and non-histone proteins. Notably, HDAC inhibitors have been approved by FDA to treat different malignancies. Recently, we demonstrated berberine as pan inhibitor for HDAC. However, isoform specific inhibition of HDAC enzyme is highly warranted. Therefore, a pharmacophore based structural exploration of berberine is in need to be developed, berberine is composed of four portions namely: a) zinc binding group (ZBG), b) Linker (scaffold), c) connect unit (CU), and d) surface recognition moiety (SRM). We derived four berberine derivatives based on common HDAC inhibition pharmacophore, compound 4 possesses highest bit score by molecular docking and compound stability by HOMOs-LUMOs analysis. It is concluded that, structurally modified berberine derivatives shown better inhibition of HDAC enzymes offering improved clinical efficacy.

ARTICLE HISTORY

Received 18 March 2021 Accepted 26 December 2021

KEYWORDS

Histone deacetylase (HDAC); HDAC inhibitor; pharmacophore; berberine derivatives; zinc binding group (ZBG)

1. Introduction

Epigenetic modifications mainly DNA methylation and acetylation, are recognized as additional mechanisms contributing to the malignant phenotype. Acetylation and deacetylation are catalyzed by specific enzymes namely, histone acetyltransferase (HAT) and histone deacetylases (HDACs). The Histones are a primary target for the physiological functions of HDACs. Histone modification is a predominant determinant in the epigenetic silencing of genes and regulation of cellular processes, such as gene transcription and proliferation (Bhadra & Kumar, 2011). Histone acetylation is a reversible process whereby histone acetyltransferase (HAT) transfers the acetyl moiety from acetyl coenzyme A to the lysine; histone deacetylase (HDAC) removes the acetyl groups, re-establishing the positive charge in the histones. Alterations in both HATs and HDACs have been identified in tumor cells and may contribute to altered gene expression in many cancers. Particularly, HDACs are been found to be overexpressed in cancer cells, thereby modifying the chromatin structure through deacetylating the lysine residues of histone and non-histone proteins, leading to aberrant expression of oncogenic transcription factors. In humans, there are 18 HDAC enzymes divided into four different classes namely, class I (1-3 and 8), class II (4-7 and 9-10), class III (1-7) and class IV (11). Class I, II and IV are a group of enzymes that use Zn⁺ as a co-factor to catalyze the removal of acetyl groups from lysine residues in histone and cellular proteins. Class III HDACs are Sirtuin (SIRT) family of proteins containing seven proteins including SIRT1 and SIRT2 (Bhadra & Kumar, 2011; Bhatti et al., 2019). These enzymes are NAD⁺ dependent and do not contain zinc as the other HDACs. HDAC inhibitors prevent the subtraction of acetyl groups from lysine tails of histones by blocking the active site of zinc dependent HDAC enzymes, also they have capacity to arrest the cell cycle and activate the tumor suppressor and apoptotic pathway in a variety of cancer cells (Bhowmik et al., 2012). HDAC inhibition triggers the apoptotic pathway in cancer cells, HDACi are classified into different classes depending on their structures such us hydroxamates, cyclic peptides, short chain fatty acids, aliphatic acids and benzamides (Cordell et al., 2001; Dokmanovic et al., 2007). Trichostatin A (TSA) belongs to hydroxamates group is the first discovered natural product (Dokmanovic et al., 2007). Another HDACi, depsipeptide (romidepsin), naturally extracted from Chromobacterium violaceum belonging to the cyclic peptide groups (Frank et al., 2016). Aliphatic acid and benzamides groups are also established and revolving under several clinical phases for multiple cancer treatments (Galloway et al., 2020). Till now, more than 20 HDACi have entered the clinical studies. FDA has approved four HDACi like Vorinostat (SAHA) (Figure 1(A)), Romidepsin, Panobinostat, and Belinostat for treating distinct

A) Berberine

Figure 1. Structures of Berberine (A) and designed berberine derivatives 1–4.

malignancies (Geng et al., 2006). Some other HDACi are currently in clinical trial to treat various cancers (Gornall et al., 2010). Classically HDACs are zinc dependent enzymes bearing a highly conserved catalytic domain with a zinc ion (Hu & Lutkenhaus, 2003). Therefore, a wide range of natural and synthetic derivatives have been identified as potent HDACi. HDACi derivatives are structurally diverse group compounds with attractive antitumor properties, majority of them consists of a zinc binding group (ZBG) interacting with zinc ion. Moreover, HDACi share other common features such us zinc binding group (ZBG), linker, connect unit (CU) and surface recognition moiety (SRM), which interacts with residues on of the the rim active site (Imanshahidi Hosseinzadeh, 2008).

Berberine is an isoquinoline quaternary alkaloid found in *Berberis aristata*, with variable pharmacological activities and a broad panel of target genes in various cancer cells (Ortiz et al., 2014). We recently reported the HDAC inhibition activity of berberine in NSCLC cells (Kalaiarasi et al., 2016). Number of reports exhibit the anticancer properties of berberine against a variety of different cell lines, operating through various mechanisms (Habtemariam, 2020). The anticancer activity of berberine appears to be derived from its ability to form strong complexes with nucleic acids to induce DNA damage,

topoisomerase poisoning, and inhibition of gene transcription (Zou et al., 2017). Berberine has suggested that 9 and 13 positions are critical for topoisomerase inhibition and quadruplex binding (Krishnan & Bastow, 2000). Moreover, derivatives of berberine substitutions at the 9 and 13 positions have shown better anticancer activity in human cancer cells (Lin et al., 2020) besides enhanced antifungal and antibacterial activities (Olleik et al., 2020). HDAC inhibition, and binding specificity of the berberine-HDAC enzyme were reported in our laboratory (Kalaiarasi et al., 2016). Many studies revealed that 9-substituted berberine enhances the DNA binding and also induce novel self-structure formations in single stranded poly (A) (Islam et al., 2011), than the parent berberine. Even though the precise molecular basis of the biological activities is still under debate, the structure of the berberine represents biologically important skeleton and also an attractive natural lead compound for the introduction of various chemical modifications in appropriate positions, in search for more selective, discriminated and narrowed medical indications Figure 1 (Brahmachari, 2015). Synthetic chemistry is also used to design new compounds or to improve the efficacy or safety of drugs that have been already used in cancer therapy. Based on these observations, we aimed to enhance the structural diversity and affinity with the zinc binding group of HDAC enzyme.



2. Materials and methods

All the computational and molecular dynamics studies were conceded by centos v7.0 Linux platform with Intel®core[™] i7-4470 CPU @ 3.40 GHZ processor along with the installed software package Schrodinger, LLC New York, 2018-4 (Nagamani et al., 2016).

2.1. Ligand preparation

The four compounds were retrieved from the Pubchem database (http://pubchem.ncbi.nlm.nih.gov/). Furthermore, the compounds were set by using ligprep module Schrodinger 2018-4. LigPrep module generated 1000 conformers in Preprocess (100-step) and Post-process (50) minimization steps. The force field geometry was optimized in the macro model and atomic charges were computed via the OPLS3 force field, which increased the accuracy of functional groups. These conformers were filtered by relative energy, the high energy conformers were ejected and the best conformers were generated (Shah et al., 2020).

2.2. Protein structure preparation and receptor grid generation

The X-ray crystal structures of 1T64, ICMR, 2VQM, 3C5K, 3C10, 3MAX, 4BKX, and 4A69 were primed by using protein preparation wizard of Maestro, Schrodinger 2018-4. The missing residues and atoms of the crystal structure were added and water molecules were removed by protein preparation wizard of Maestro Schrodinger 2018-4. Additionally, these structures were optimized and minimized through the OPLS3 force field. Furthermore, the co-crystal ligand was absent in the targeted proteins, so site map was created by using the sitemap program of Schrodinger 2018-4. The top scoring sited was taken for (active site) receptor grid generation. The receptor grid was generated by using glide grid program of Schrodinger 2019-4. The glide grid program identifying an amino acid position in the targeted protein. Correspondingly, the grid file was used for docking protocol (Jayaraj et al., 2019; Kirubakaran et al., 2012).

2.3. Molecular docking analysis

The four compounds were docked into the active site of targeted proteins by using Grid-Based Ligand Docking with Energetics (GLIDE) module of Schrodinger Maestro. Extra precision (XP) mode of the docking parameters were used to dock the four compounds in the active site of targeted proteins. The best compound was selected based on the Glide scoring function, Glide energy and the number of hydrogen bond interactions for the further study (Loganathan & Muthusamy, 2019).

2.4. Density functional theory (DFT)

Density functional theory was done through the Jaquar, version 7.8 (Schrödinger, LLC, New York, NY, 2015- 4. Hybrid DFT with Becke's three-parameter functional and the Lee- Yang-Parr

correlation functional (B3LYP) -/-6-31 G** basic set level was used to complete the geometry optimization of the preferred ligands. The B3LYP hybrid function is observed to evaluate the properties and reactions of organic molecules. Furthermore, the ligands molecular electrostatic potential map (MESP), frontier molecular orbitals (i.e. Highest Occupied Molecular Orbitals (HOMOs) and Lowest Unoccupied Molecular Orbitals (LUMOs), and HOMO-LUMO energy gap (HLG) were calculated using the jaguar model (Jayaraj et al., 2021).

2.5. Homology modeling and validation

The homology modeling of targeted proteins was performed by PRIME module (prime, version 4.1, Schrodinger, LLC, and New York-1). The geometry and energy profile were constructed using PRIME. Furthermore, the structure was validated by using Procheck, and phi and psi torsions angles were analyzed for the backbone of crystal structure of proteins, with the assistance of Ramachandran plot. The modeled structures energy criterion was compared with huge set of known protein structures (Bhatti et al., 2019).

2.6. Molecular dynamic simulation

The molecular dynamics simulation investigations were carried out using academic software (Schrodinger, Inc., LLC, and New York, USA) (Desmond, Schrodinger, 2015). Desmond is using the neutral territory approach, commonly known as the midway method. This was accomplished by effectively employing a high level of computing parallelism. The conformational stability and flexibility of the a) 4A69, b) 1T64, c) 4BKX, d) 3MAX, e) 2VQM, f) 3C10, g) 3C5K, and h) ICMR proteins with berberine derivative 4th compound were predicted using Desmond. To verify the stiffness of the protein and ligand complex, MD simulations of a) 4A69, b) 1T64, c) 4BKX, d) 3MAX, e) 2VQM, f) 3C10, g) 3C5K, h) ICMR were conducted using Desmond. The docked protein-ligand complexes were solved with the simple point energy (SPC), and a system builder was used to create a water mode in an orthorhombic box. On complete charge of the system, the crossing water molecules were eliminated, and the system was counteracted by a sufficient amount of Na+/cl- counter ions with a permanent salt concentration of 0.15 M. To improve stability, the primed system was used in conjunction with the Desmond's default relaxation procedure to run Molecular Dynamics simulations for 100 ns with a random condition in the number of atoms, pressure, and temperature (NPT) ensemble. Molecular dynamics (MD) simulation studies have also been conducted on the best hit substances. The stability of protein is examined by calculating the RMSD value (Bhatti et al., 2019).

3. Results and discussion

3.1. Homology modelling

Homology modeling was used to identify the unknown 3D structure depending on the experimentally proved 3D

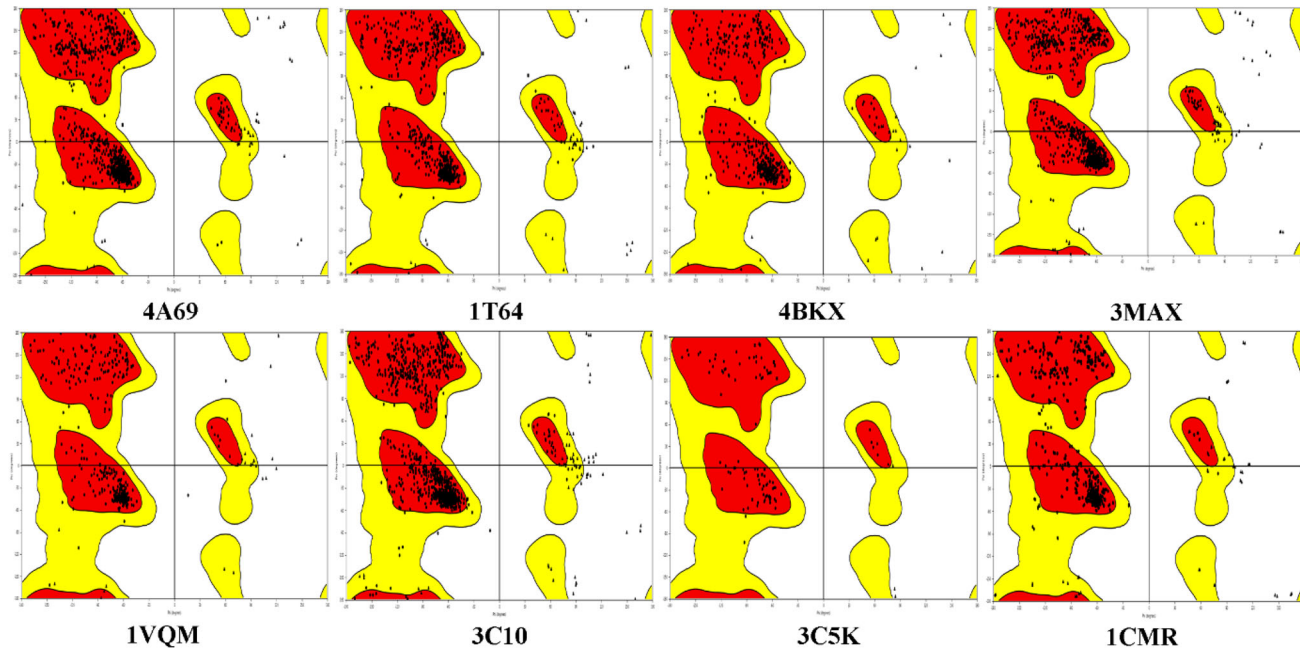


Figure 2. Ramachandran plot analysis of a) 4A69, b) 1T64, c) 4BKX, d) 3MAX, e) 2VQM, f) 3C10, g) 3C5K, h) ICMR proteins.

Table 1. Docking score for Berberine derivatives compounds with 4BKX protein.

			HDAC 1 (4BKX)		
S. no	Compound	Glide score (kcal/mol)	Glide energy (kcal/mol)	No. H bonds	Interacting amino acids
1.	Berberine (A)	-1.591	-26.630	1	HIS 57 (H-bond)
2.	Berberine derivatives 1	-5.633	-54.763	6	His57, Glu62, Glu63, Thr65, Lys66, Asp70
3.	Berberine derivatives 2	-5.063	-52.580	5	His57, Glu62, Glu63, Lys66, Asp70
4.	Berberine derivatives 3	-3.753	-46.726	2	Lys66, Glu62
5.	Berberine derivatives 4	-4.435	-45.310	3	Lys66, Glu63, Lys126

structure of homologous protein. The targeted protein sequences were retrieved from the uniprot database, the FASTA sequence was submitted to BLAST analysis. The targeted proteins were selected as suitable template. Maximum 70% sequences are identified with 85% guery sequence, which was taken and modeled by the prime Schrodinger 2018-4 suite. Furthermore, the modeled structure was validated by using Procheck, Phi/Psi distribution, stereo chemical and energetic properties.

Ramachandran plot showed the modeled 1T64 protein and showed 90.3% of residues were from favored region, 9.1% was from the allowed region, 0.5% was generic, 0.2% was from the disallowed region of the plot. ICMR protein showed 88.7% residues were from favored region, 10.7% was from the allowed region, 0.6% was generic, 0.0% was from the disallowed region of the plot, 2VQM protein showed 90.8% residues were from favored region, 8.3% was from the allowed region, 0.9% was generic, 0.0% was from the disallowed region of the plot, 3C5K protein shows 91.0% residues were favored region, 7.9% was from the allowed region, 1.1% was generic, 0.0% was from the disallowed region of the plot, 3C10 protein showed 89.3% residues were from favored region, 10.1% was from the allowed region, 0.5% was generic, 0.0% was from the disallowed region of the plot, 3MAX protein showed 91.5% residues were from favored region, 8.3% was from the allowed region, 0.9% was generic, 0.0% was from the disallowed region of the plot, 4BKX protein showed 90.4% residues were from favored region, 9.6% was from the allowed region, 0.0% was generic, 0.0% was from the disallowed region of the plot, 4A69 protein showed 89.7% residues were from favored region, 10.0% was from the allowed region, 0.3% was generic, and 0.0% was from the disallowed region of the plot, the plot image was shown in Figure 2. Accordingly, the results show that the 3D structures, stereochemical properties and other quality factors were in suitable range.

3.2. Molecular docking analysis

Molecular docking was used to estimate the stability of targeted proteins and ligand interactions. In this study, we docked four compounds in the active site of 1T64, 2VQM, 3C5K, 3C10, 3MAX, 4BKX, and 4A69 proteins. Glide XP docking affirms that the identified four compounds were bound to the active site of targeted protein and favors many interactions, furthermore having good docking score.

3.2.1. Molecular docking study of HDAC 1 (4BKX) protein

The Berberine, Berberine derivatives 1, 2, 3, 4 was docked against HDAC 1 (4BKX) protein, the compounds docking score ranging from -5.633 to -3.753, kcal/mol. Among all the compounds Berberine derivatives 1 had a good binding score and was interacting with the His57, Glu62, Glu63, Thr65, Lys66, Asp70 residues. The docking results were shown in Table 1.

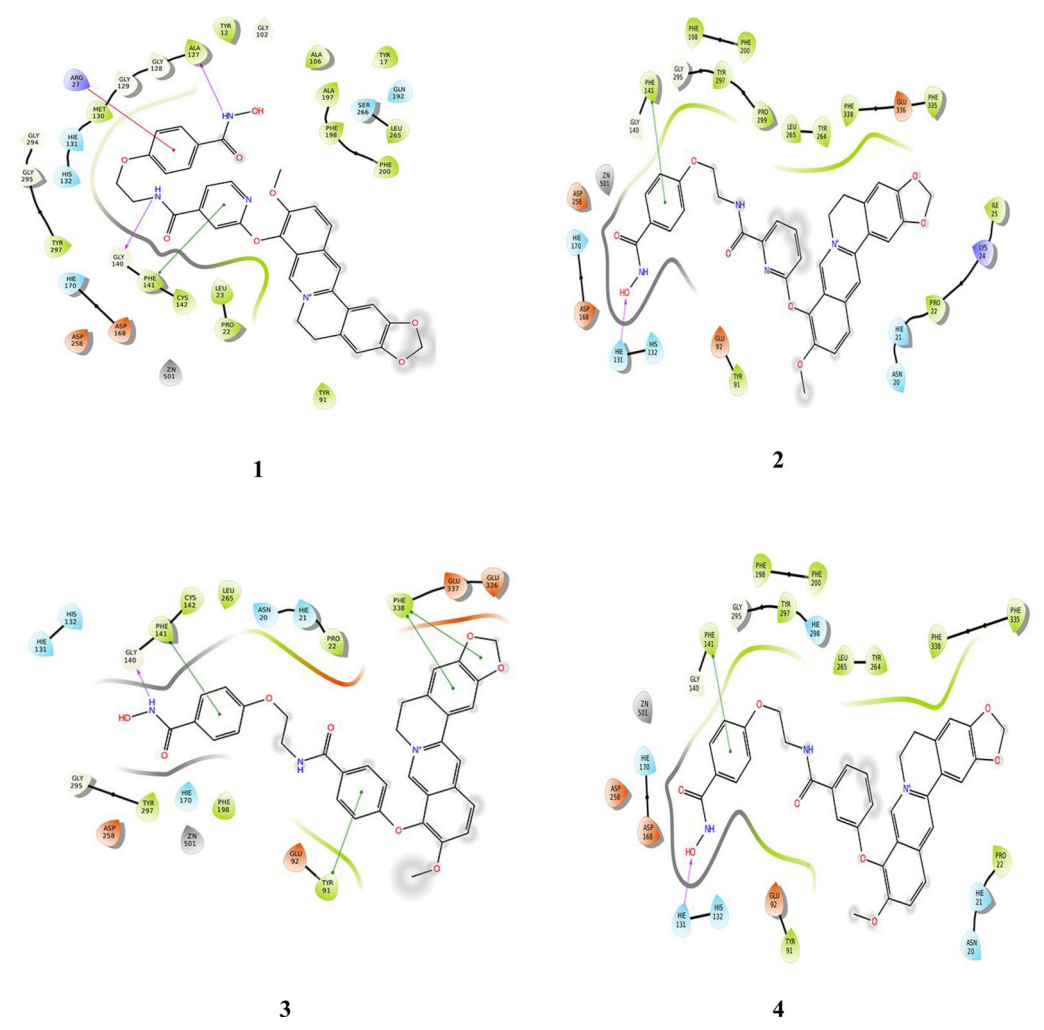


Figure 3. 2D interactions of berberine derivatives (1-4) with the amino acid residues of HDACs protein (PDB ID: 4BKX). Pink color represents the hydrogen bond interactions, green color represents the pi-pi interactions, red color represents the pi-cation interaction, and red with blue combination represents the salt bridges.

Table 2. Docking score of Berberine derivatives compounds with 4A69 protein.

	HDAC 3 (4A69)							
S. no	Compound	Glide score (kcal/mol)	Glide energy (kcal/mol)	No. H bonds	Interacting amino acids			
1.	Berberine (A)	-2.849	-27.343	3	LYS 475 _H-bond), ARG 265 (Pi-Pi), ARG 301 (Pi-Pi, Pi-Cation)			
2.	Berberine derivatives 1	-5.478	-60.290	2	Val96, Tyr18			
3.	Berberine derivatives 2	-4.270	-43.192	4	Asp93, Asp92, Gly91, Phe144			
4.	Berberine derivatives 3	-4.376	-47.013	5	Phe200, Asp93, Asp92, Ala20, Gly91			
5.	Berberine derivatives 4	-5.270	-57.304	3	Asp93, val96, Tyr18			

3.2.2. Binding mode analysis of HDAC 1 (4BKX) protein

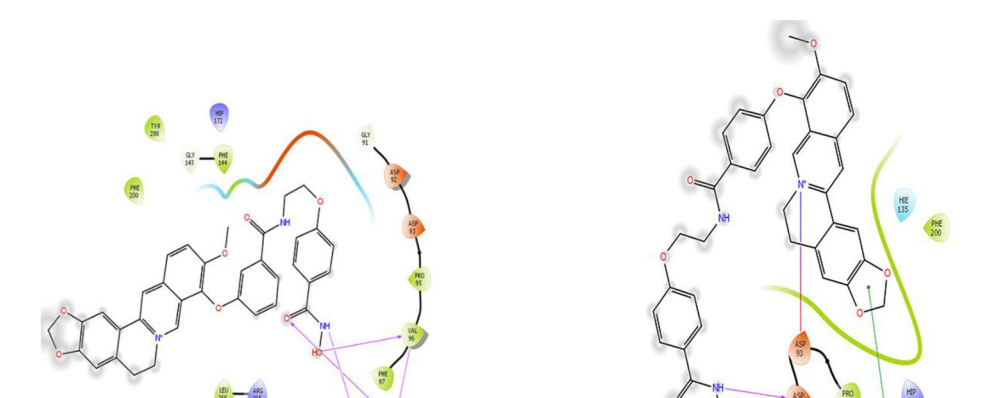
The binding mode of berberine derivative 1st had a high binding affinity (-5.633 kcal/mol), which forming hydrogen bond interactions with Glu62, Thr65, Lys66, Asp70 residues (Figure 3, (1)). The binding mode of 2nd compound had second highest binding affinity (-5.063 kcal/mol), making hydrogen bond interactions with Glu63, Lys66, Asp70 residues (Figure 3, (2)). The binding mode of 4th compound was making hydrogen bond interactions with Lys66, Lys126 and with binding affinity of -4.435 kcal/mol (Figure 3, (4)). The binding mode of 3rd compound was making hydrogen bond interactions with Lys66, Glu62 and binding affinity was -3.753 kcal/mol (Figure 3, (3)). The docking results showed the compounds having high binding affinity and was needed to inhibit 4BKX protein.

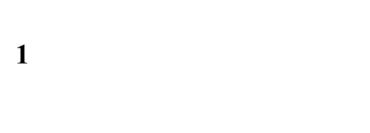
3.2.3. Molecular docking study of HDAC 3 (4A69) protein

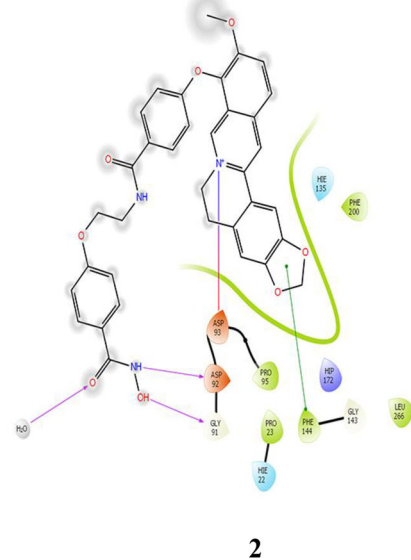
The Berberine, Berberine derivatives 1, 2, 3, 4 were docked with HDAC 3 (4A69) protein, the compounds docking score was ranging from -5.478 to -2.849 kcal/mol. Among all the compounds Berberine derivatives 1 showed a good binding score and was interacting with the Val96, Tyr18 residues. The docking results were shown in Table 2.

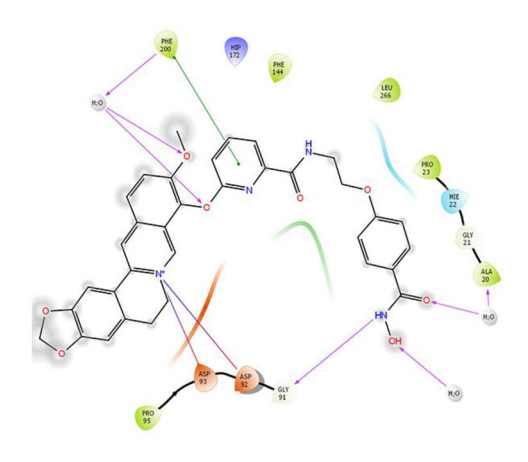
3.2.4. Binding mode analysis of HDAC 3 (4A69) protein

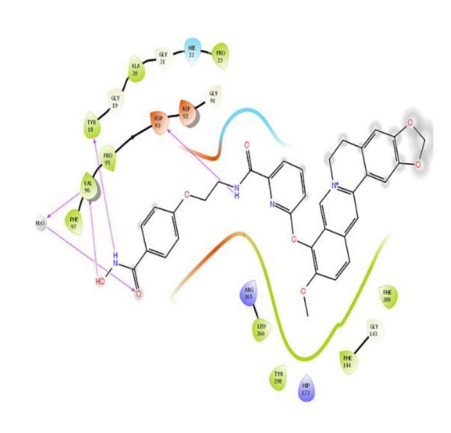
The binding mode of 2nd compound had second highest binding affinity (-4.270 kcal/mol), making hydrogen bond interactions with Asp92, Gly91 residues (Figure 4, (2)). The binding mode of 3rd compound was making hydrogen bond











3 Figure 4. 2D interactions of berberine derivatives (1-4) with the amino acid residues of HDACs protein (PDB ID: 4A69).

Table 3. Docking score for Berberine derivatives compounds with 2VQM protein.

HDAC 4 (2VQM)								
S. no	Compound	Glide score (kcal/mol)	Glide energy (kcal/mol)	No. H bonds	Interacting amino acids			
1.	Berberine (A)	-2.852	-31.691	2	PHE 168 (Pi-Pi), HIE 198(Pi-Cation)			
2.	Berberine derivatives 1	-6.163	-55.309	2	Arg154, Phe168			
3.	Berberine derivatives 2	-6.441	-60.560	6	Arg37, His159, Arg154, Tyr170, Phe168, Glu120			
4.	Berberine derivatives 3	-5.575	-49.501	2	Phe168, Gly167			
5.	Berberine derivatives 4	-5.877	-54.296	3	Phe168, Phe227, Glu120			

interactions with Phe200 Ala20, Gly91 and binding affinity -4.376 kcal/mol (Figure 4, (3)). The binding mode on 4th compound was making hydrogen bond interactions with Asp93, val96, Tyr18 and binding affinity are -5.270, kcal/mol (Figure 4, (4)). The binding mode of 1st compound making hydrogen bond interactions with Val96, Tyr18 and binding affinity was -5.478, kcal/mol (Figure 4, (1)). The docking results showed the compounds that have high binding affinity was needed to inhibit 4A69 protein. From all these results, it is concluded that these compounds might show promising inhibitory activity against all the targeted proteins. Finally, the identified compounds could have promising agonistic effect on targeted proteins.

3.2.5. Molecular docking study of HDAC 4 (2VQM) protein

The Berberine, Berberine derivatives 1, 2, 3, 4 was docked with HDAC 4 (2VQM) protein, the compounds docking score ranging

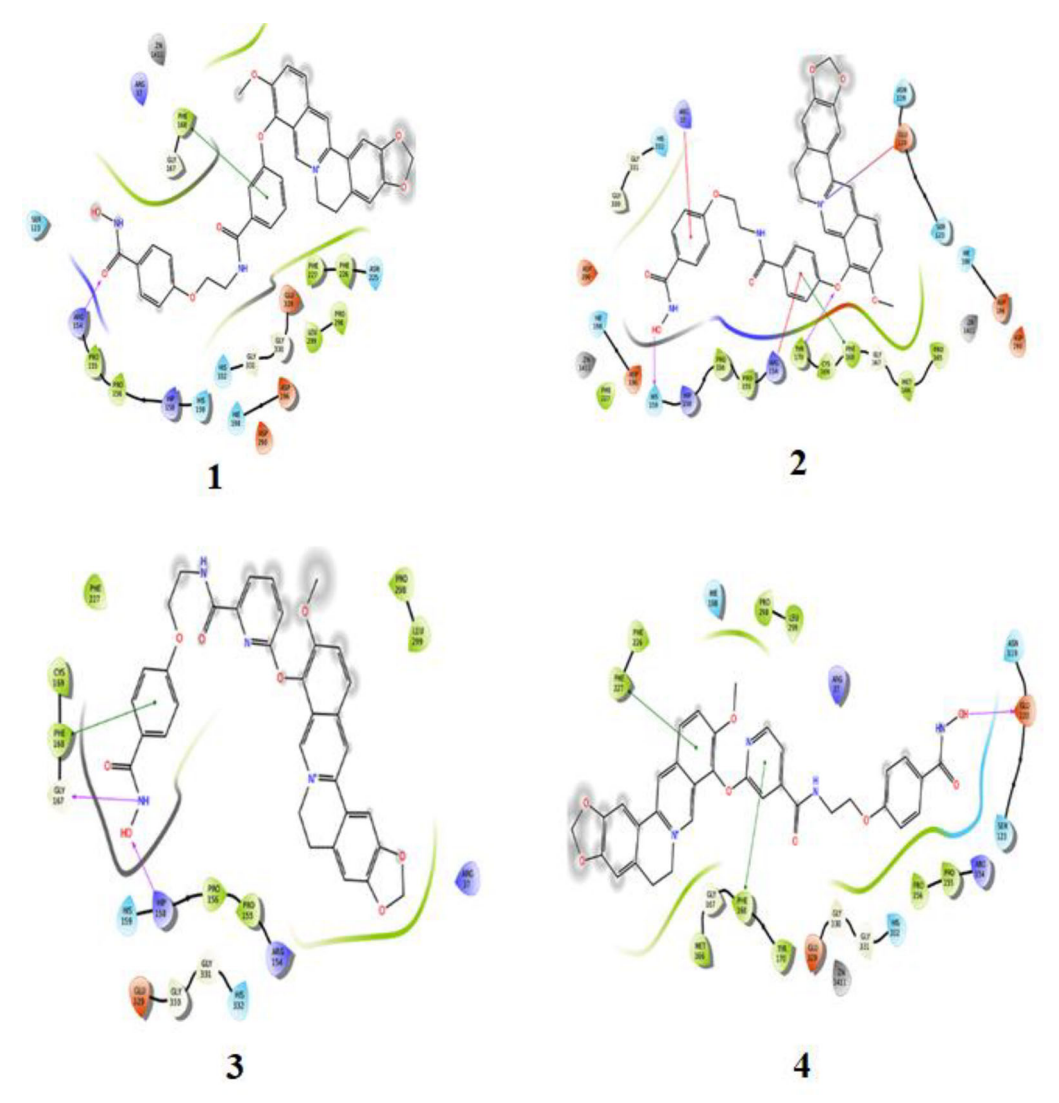


Figure 5. 2D interactions of berberine derivatives (1-4) with the amino acid residues of HDACs protein (PDB ID: 2VQM).

Table 4. Docking score for Berberine derivatives compounds with 3C5K protein.

HDAC 6 (3C5K)							
S. no	Compound	Glide score (kcal/mol)	Glide energy (kcal/mol)	No. H bonds	Interacting amino acids		
1.	Berberine (A)	-3.528	-23.908	3	ARG 47 (H-Bond, Pi-Pi, Pi-Cation), TRP 35 (Pi-Pi), TRP 74 (Pi-Cation)		
2.	Berberine derivatives 1	-4.636	-45.290	3	Asp70, Arg47, Trp74		
3.	Berberine derivatives 2	-3.558	-35.141	2	Tyr81, Asp70		
4.	Berberine derivatives 3	-4.308	-42.321	3	Trp35, Trp74, Arg47		
5.	Berberine derivatives 4	-3.158	-35.921	4	Trp35, Trp74, Arg47, Trp76		

from -6.441 to -2.852, kcal/mol. Among the all compounds, 2nd compound showed good binding score and which was interacting with the Arg37, His159, Arg154, Tyr170, Phe168, Glu120 residues. The docking results were shown in Table 3.

3.2.6. Binding mode analysis of HDAC 4 (2VQM) protein

The binding mode of compound 2nd compound had a high binding affinity (-6.441 kcal/mol), which forming hydrogen bond interactions His159, residues (Figure 5, (2)). The binding mode of 1st compound had second highest binding affinity (-6.163 kcal/mol), making hydrogen bond interactions with Arg154 (Figure 5, (1)). The binding mode of 4th compound was making hydrogen bond interactions with Glu120 with binding affinity -5.877 kcal/mol (Figure 5, (4)). The binding mode of 3rd compound making hydrogen bond interactions with Gly167 and binding affinity was -5.575 kcal/mol (Figure 5, (3)). The docking results showed the compounds that have high binding affinity and was needed to inhibit 2VQM protein.

3.2.7. Molecular docking study of HDAC 6 (3C5K) protein

The Berberine, Berberine derivatives 1, 2, 3, 4 was docked with HDAC 6 (3C5K) protein, the compounds docking score ranging from -4.636 to -3.158, kcal/mol. Among the all compounds Berberine derivative 1 showed good binding score and was

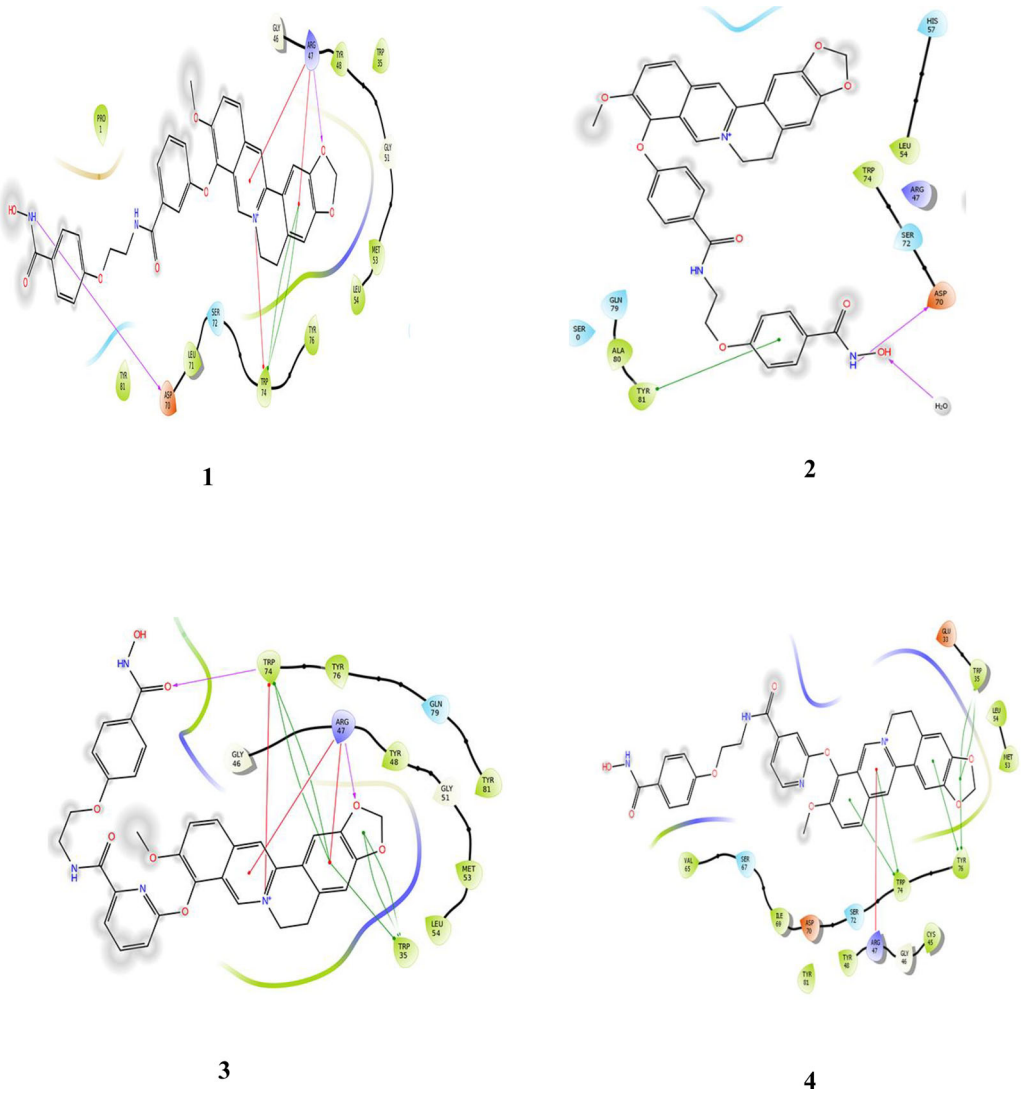


Figure 6. 2D interactions of berberine derivatives (1-4) with the amino acid residues of HDACs protein (PDB ID-3C5K).

 Table 5. Docking score for Berberine derivatives compounds with 3C10 protein.

	HDAC 7 (3C10)							
S. no	Compound	Glide score (kcal/mol)	Glide energy (kcal/mol)	No. H bonds	Interacting amino acids			
1.	Berberine (A)	-2.08	-27.574	1	HIE 709 (H-Bond)			
2.	Berberine derivatives 1	-7.572	-56.967	2	Gly678, His843			
3.	Berberine derivatives 2	-7.498	-55.493	1	Gly678			
4.	Berberine derivatives 3	-7.880	-56.311	4	Gly678, Phe679, Asp626, Phe738			
5.	Berberine derivatives 4	-8.376	-59.132	2	Gly678, His843			

interacting with the Asp70, Arg47, Trp74 residues. The docking results were shown in Table 4.

3.2.8. Binding mode analysis of HDAC 6 (3C5K) protein

The binding mode of 1st compound had a high binding affinity (-4.636 kcal/mol), forming hydrogen bond interactions Asp70 residues (Figure 6, (1)). The binding mode of 3rd compound has second highest binding affinity (-4.308 kcal/mol), making hydrogen bond interactions with Trp74, Arg47 (Figure 6, (3)). The binding mode on 4th compound was not making any hydrogen bond interactions and binding affinity

was –3.158, kcal/mol (Figure 6, (4)). The binding mode of 2nd compound making hydrogen bond interactions with Asp70 and binding affinity was –3.558, kcal/mol (Figure 6, (2)). The docking results showed the compounds that have high binding affinity and was needed to inhibit 3C5K protein.

3.2.9. Molecular docking study of HDAC 7 (3C10) protein

The Berberine, Berberine derivatives 1, 2, 3, 4 was docked by HDAC 7 (3C10) protein, the compounds docking score ranging from -8.376 to -2.08, kcal/mol. Among the all compounds 4 showed good binding score and was interacting

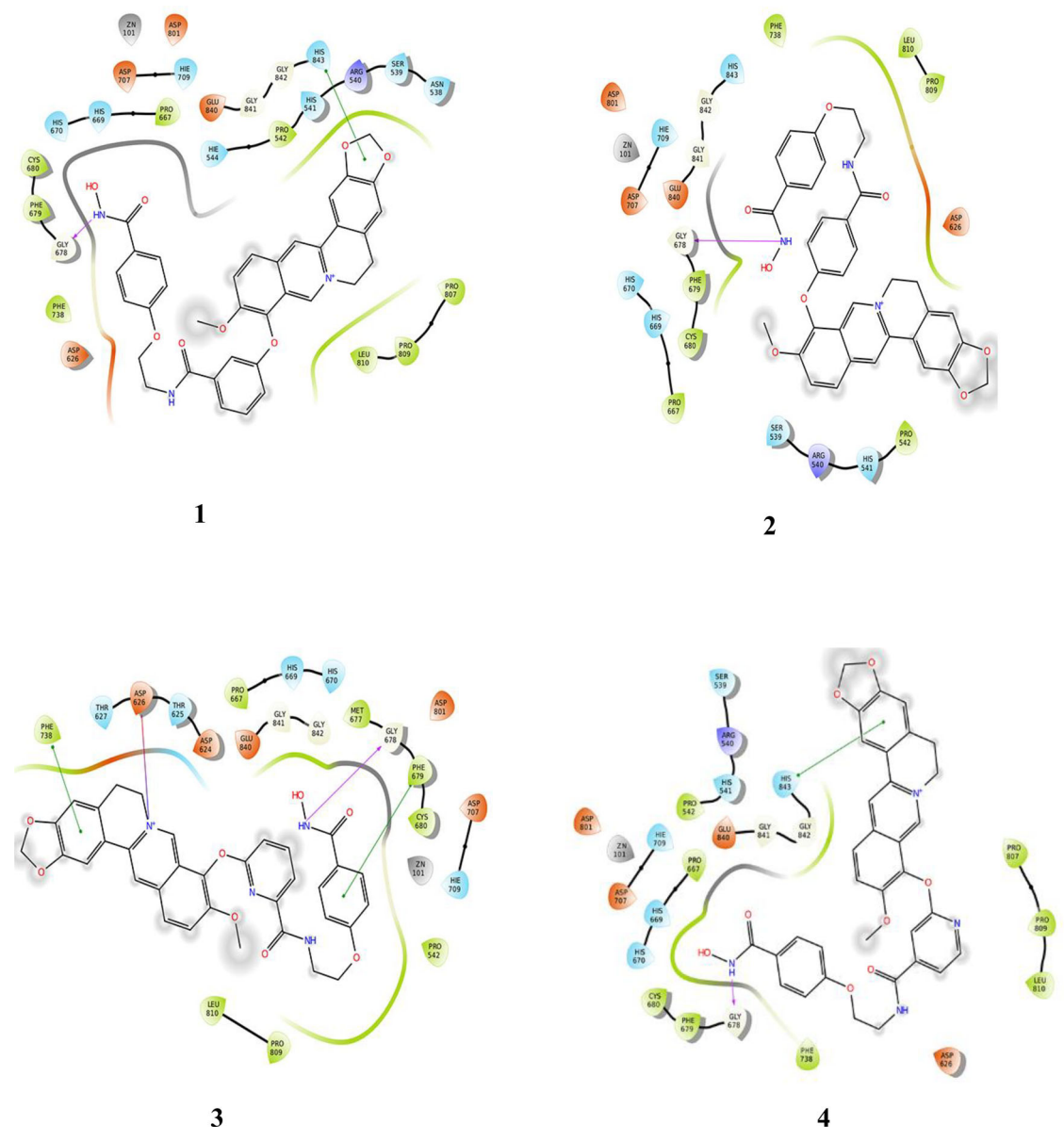


Figure 7. 2D interactions of berberine derivatives (1-4) with the amino acid residues of HDACs protein (PDB ID: 3C10).

Table 6. Docking score for Berberine derivatives compounds with 1T64 protein.

	HDAC 8 (1T64)							
S. no.	Compound	Glide score (kcal/mol)	Glide energy (kcal/mol)	No. H bonds	Interacting amino acids			
1.	Berberine (A)	-4.727	-28.627	3	TYR 306 (H-bond), PHE 152 (Pi-Pi), PHE 208 (Pi-Pi, Pi-Cation)			
2.	Berberine derivatives 1	-6.016	-46.297	4	Leu308, Tyr111, Tyr306, Phe152,			
3.	Berberine derivatives 2	-6.123	-50.582	3	Ala339, Lys36, Tyr100			
4.	Berberine derivatives 3	-6.612	-48.963	3	Phe152, Tyr306, Tyr111			
5.	Berberine derivatives 4	-5.590	-44.704	5	Phe152, Gly342, Árg313, Ala339, Asn307			

with the Gly678, His843 residues. The docking results were shown in Table 5.

3.2.10. Binding mode analysis of HDAC 7 (3C10) protein

The binding mode of 4th compound had a high binding affinity (-8.376 kcal/mol), forming hydrogen bond interactions Gly678 residues (Figure 7, (4)). The binding mode of 3rd compound was making hydrogen bond interactions with Gly678 with binding affinity -7.880 kcal/mol (Figure 7, (3)). The binding mode on 1st compound was making hydrogen bond interactions with Gly678 and binding affinity was -7.572, kcal/mol (Figure 7, (1)). The binding mode of 2nd compound making hydrogen bond interactions with Gly678 and binding affinity was -7.498, kcal/mol (Figure 7, (2)). The docking results showed the compounds that have high binding affinity and was needed to inhibit 3C10 protein.

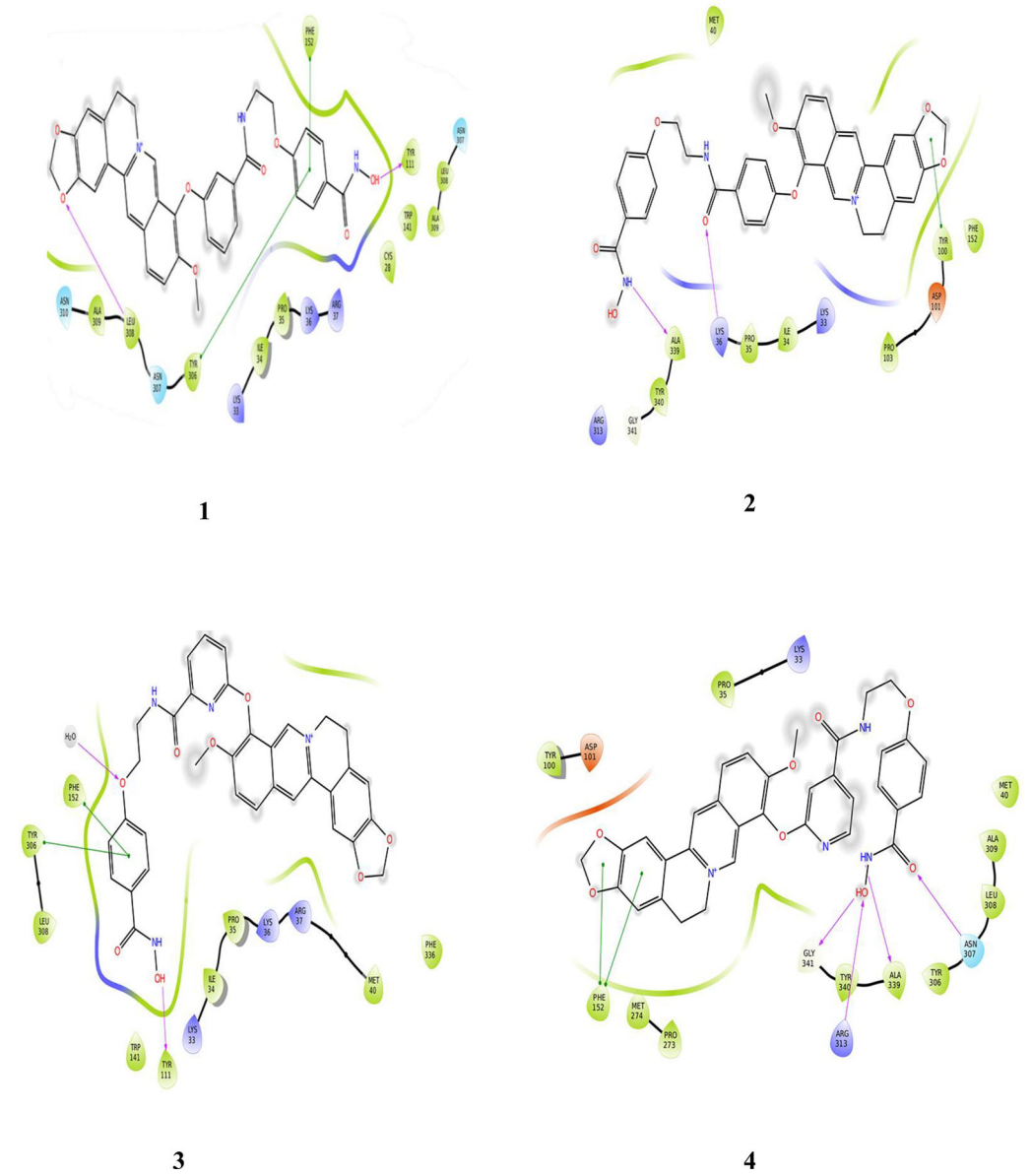


Figure 8. 2D interactions of berberine derivatives (1-4) with the amino acid residues of HDACs protein (PDB ID: 1T64).

3.2.11. Molecular docking study of HDAC 8 (1T64) protein

The Berberine, Berberine derivatives 1, 2, 3, 4 was docked with HDAC 8 (1T64) protein, the compounds docking score ranging from –6.612 to –4.727, kcal/mol. Among the all compounds 3 showed good binding score and was interacting with the Phe152, Tyr306, and Tyr111 residues. The docking results were shown in Table 6.

3.2.12. Binding mode analysis of HDAC 8 (1T64) protein

The binding mode of 3rd compound had a high binding affinity (-6.612 kcal/mol), forming hydrogen bond interactions Tyr111 (Figure 8, (3)). The binding mode of 2nd compound was making hydrogen bond interactions with Ala339, Lys36 residues with binding affinity -6.123 kcal/mol (Figure 8, (2)). The 1st compound making hydrogen bond interactions with Leu308, Tyr11, which binding affinity was -6.016, kcal/mol (Figure 8, (1)). The binding mode of 4th compound making hydrogen

bond interactions with Gly342, Arg313, Ala339, Asn307 and binding affinity was –5.590, kcal/mol (Figure 7, (4)). The docking results showed the compounds having high binding affinity and was needed to inhibit a 1T64 protein.

3.3. DFT analysis and salvation energy calculation

The four molecules were used for DFT analysis. The HOMOs and LUMOs for the four identified compounds are showed in Figure 9. The four Compounds and their HOMOs values are -0.21639, -0.21527, -0.21427, -0.21512 and -0.20361. Further the following compounds LUMOs values are -0.10658, -0.10536, -0.10172, -0.10331 and -0.02463 was shown in Table 7. The differentiation of HOMOs and LUMOs energy was explained as energy gap or band gap of the electronic excitation energy, which play a vital role in determining the stability and reactivity of the compounds. Overall the HOMOs and LUMOs eigen values for the four

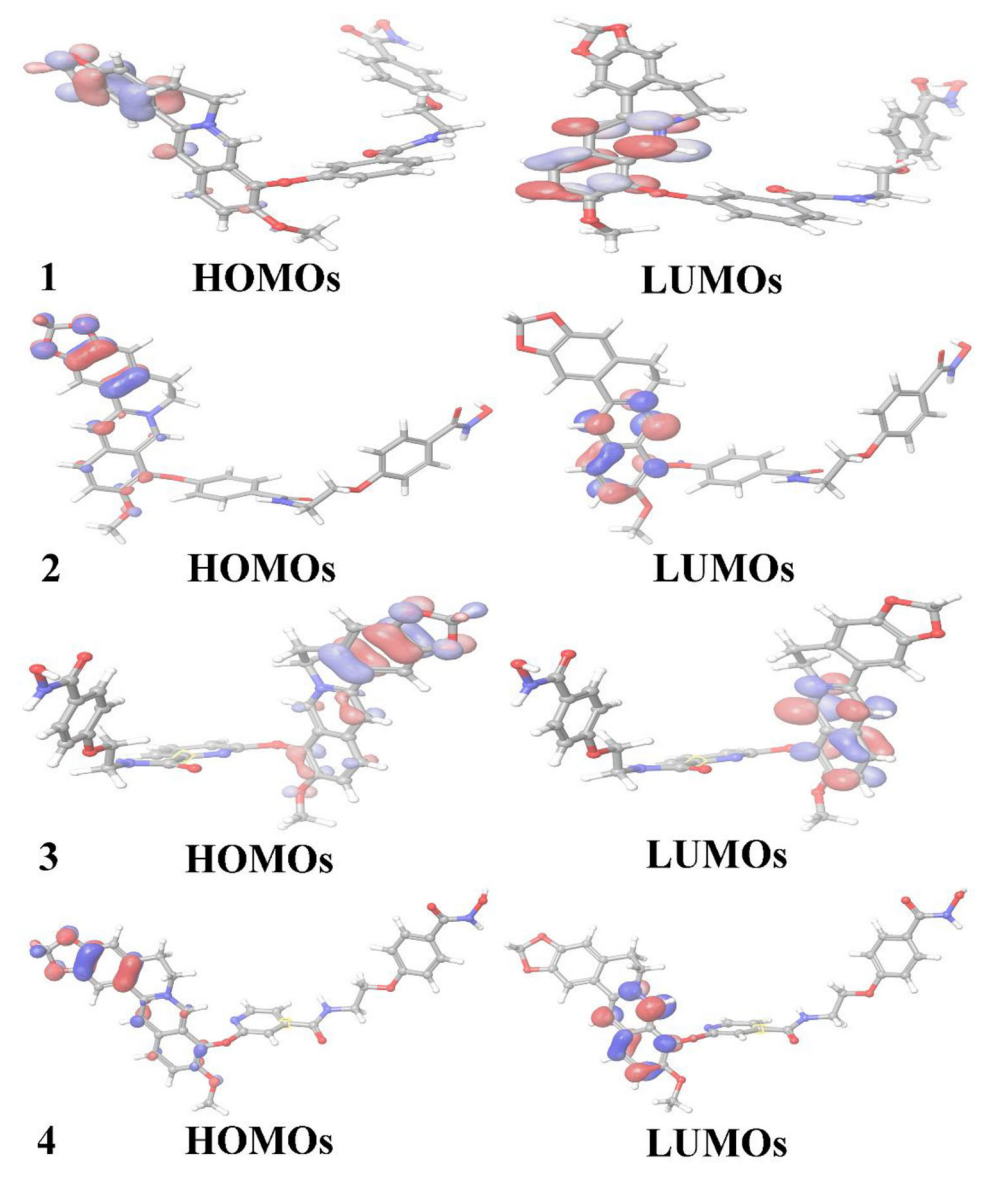


Figure 9. HOMOs and LUMOs of berberine derivatives compounds.

Table 7. HOMO, LUMO, HLG and MESP ranges from lead molecules in DFT calculation.

Compounds	HOMO (eV)	LUMO (eV)	Solvation energy kcal/mol	MESP (kcal/mol)
1	-0.21639	-0.10658	–0.10 kcal/mol	-48.1684 to -43.9049
2	-0.21527	-0.10536	-0.11 kcal/mol	-51.4436 to -48.0324
3	-0.21427	-0.10172	-0.10 kcal/mol	-48.9199 to -44.0796
4	-0.21512	-0.10331	–0.11 kcal/mol	-65.8124 to -61.4435

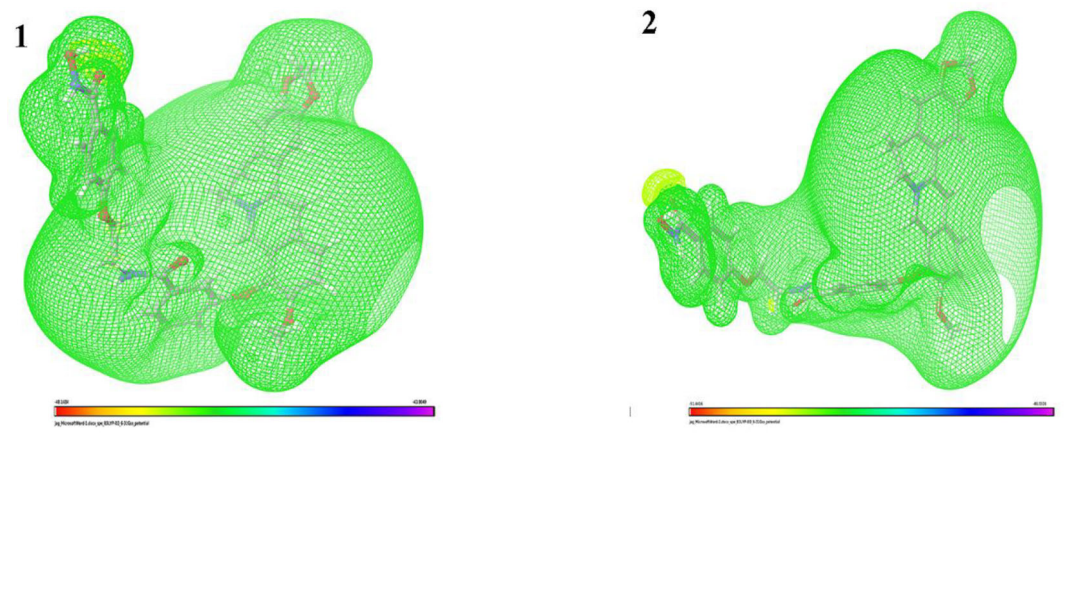
compounds are more negative and positive in nature, precise a compound having an electron donor and acceptor ability. Therefore, the stero electronic paring of ligand receptor is a crucial way to determine the protein ligand interactions, so the stereo electronic paring was measured by 3D-MESP and other electronic parameters. The MESP values of four compounds are as shown in Table 7. MESP isosurface are shown in Figure 10. The most negative electrostatic potential was yellow coloured and the most positive electrostatic potential was green coloured. Therefore, the salvation energy was used to determine the solubility of compounds. The berberine derivative compounds salvation energy values were more negative in nature (shown in Table 7), which represents that compounds have a more aqueous solubility.

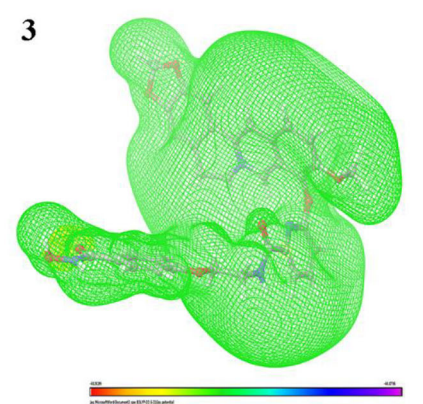
3.4. Molecular dynamics

For molecular dynamics simulations, protein-ligand complexes were considered. In complex dynamics, computational methods were more valuable for evaluating protein flexibility and releasing the dynamics model. Added, we discovered the methods were quite stable, and that the simulations were acceptable for further research.

3.5. Root mean square deviation (RMSD) analysis

The magnitude of confirmation drift of the protein was evaluated using the Root Mean Square Deviation (RMSD) of backbone atoms as a function of time in an array with





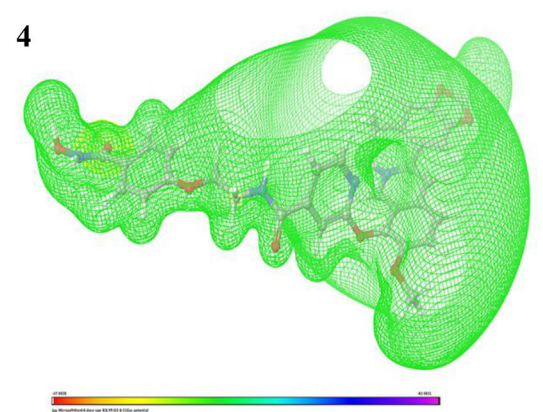


Figure 10. MESP mapping of berberine derivatives compounds.

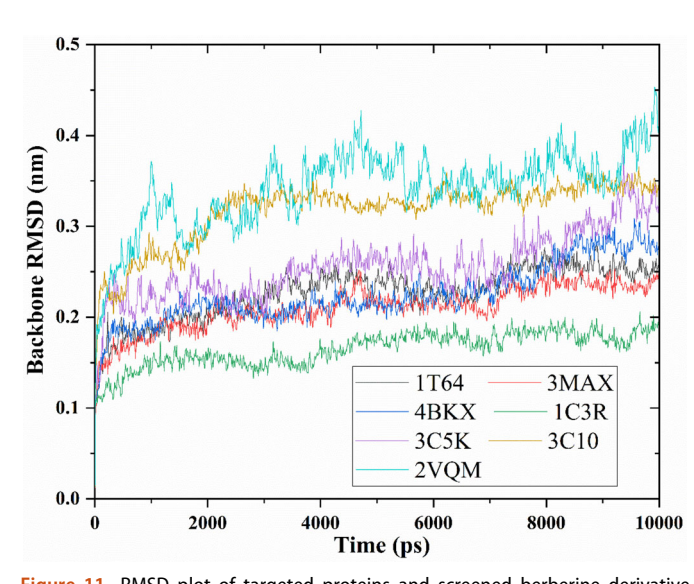


Figure 11. RMSD plot of targeted proteins and screened berberine derivative 4th compound complexes.

regard to the starting structure. The RMSD plots of the 4A69, 1T64, 4BKX, 3MAX, 2VQM, 3C10, 3C5K, ICMR with berberine derivative 4th compound are shown in Figure 11. Every simulation was distinguished by a preliminary rise in RMSD in the first 100 ns due to recreation of the models in water.

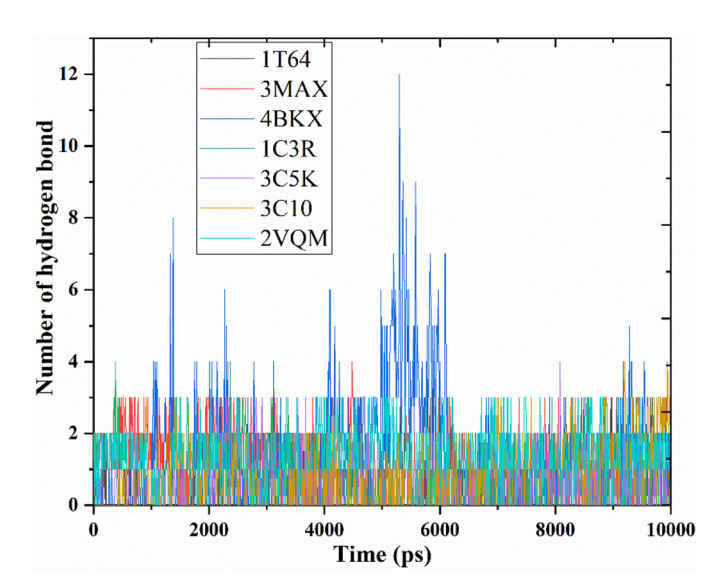


Figure 12. Hydrogen bond contact of berberine derivative 4th compound in the active site targeted proteins.

The RMSD plots of the 4A69, 4BKX, 3MAX, 2VQM, 3C10, 3C5K, ICMR with berberine derivative 4th compound stabilized between 80 ns and 100 ns with RMSD values of 0.3 Å, 0.25 Å, 0.2 Å, 0.4 Å, 0.3 Å, 0.3 Å, 0.15 Å, which let out stability



of the protein-ligand complex. Furthermore, overall the berberine derivative 4th compound is having below 0.4 Å, and lets out a compound that has more stability with the targeting HDACs enzymes proteins.

3.6. Hydrogen bond analysis

During the simulation period, the temporal dependency of hydrogen bonds between receptor and drug like molecules was studied in order to estimate drug molecule binding in the active site of 4A69, 4BKX, 3MAX, 2VQM, 3C10, 3C5K, ICMR proteins. The best hit compound's biological effects were linked to the observed intermolecular hydrogen bonding, according to the findings. The HDACs enzymes inhibitory molecule revealed stable hydrogen bonding interactions during the simulation time period, which gave a hint on its attractions towards the protein-ligand complexes Figure 12.

4. Conclusion

We performed this study to determine the impact of structural modification of berberine derivatives to adapt the common pharmacophore for HDAC inhibition activity and explore promising lead structure. Four compounds were tested for HDAC inhibition by molecular docking studies and stability of the compound were identified by DFT, molecular dynamics and salvation energy calculation. The docking studies provided us with invaluable data to estimate the free energy of binding, the binding mode, and the inhibition constant, all of which are promising tools for the discovery of new, active inhibitors useful as pharmacological agents. The conventional modifications at the 9th position of Mono Odemethylation of berberine using trimethylsilyl iodide would give a derivative with hydroxy group resulting in improved activities compared to berberine. Among the tested compounds, the compound 4 showed highest binding energy and potent HDAC inhibition. Finally, our results indicate that with high in silico inhibitory potency, compound 4 is suitable for further experimental analysis.

Acknowledgements

We acknowledge Dr. Karthikeyan Muthusamy Department of Bioinformatics, Alagappa University, Karaikudi, Tamil Nadu, for their help with Bio-informatics studies India, Dr. Kannupal Srinivasan, School of Chemistry, Bharathidasan University, Tiruchirappalli-620 024, Tamil Nadu, India, for their help with designing the compound. We are grateful to the Department of Science and Technology, Fund for Improvement of S&T Infrastructure in Universities and Higher Educational Institutions (DST-FIST and DST-PURSE) for their infrastructure support to our department.

Disclosure statement

Authors declare no conflict of interest.

Funding

The first author Kandasamy Saravanan is grateful to Indian Council of Medical Research (ICMR), Government of India, New Delhi, for providing

financial support through their senior research fellowship (SRF) Scheme (F.No. 45/19/2020-BIO/BMS).

ORCID

Karthikeyan Muthusamy (h) http://orcid.org/0000-0001-7755-3381

References

- Bhadra, K., & Kumar, G. S. (2011). Therapeutic potential of nucleic acidbinding isoguinoline alkaloids: Binding aspects and implications for drug design, Medicinal Research Reviews, 31(6), 821-862.
- Bhatti, V., Kwatra, K. S., Puri, S., & Calton, N. (2019). Histopathological spectrum and immunohistochemical profile of lung carcinomas: A 9year study from a tertiary hospital in North India. International Journal of Applied & Basic Medical Research, 9(3), 169-175.
- Bhowmik, D., Hossain, M., Buzzetti, F., D'Auria, R., Lombardi, P., & Kumar, G. S. (2012). Biophysical studies on the effect of the 13-position substitution of the anticancer alkaloid berberine on its DNA binding. The Journal of Physical Chemistry B, 116(7), 2314-2324.
- Brahmachari, G. (2015). Bioactive natural products: Chemistry and biology. John Wiley & Sons.
- Cordell, G. A., Quinn-Beattie, M. L., & Farnsworth, N. R. (2001). The potential of alkaloids in drug discovery. Phytotherapy Research. An International Journal Devoted to Pharmacological and Toxicological Evaluation of Natural Product Derivatives, 15(3), 183-205.
- Dokmanovic, M., Clarke, C., & Marks, P. A. (2007). Histone deacetylase inhibitors: Overview and perspectives. Molecular Cancer Research : MCR. 5(10), 981-989.
- Frank, C. L., Manandhar, D., Gordân, R., & Crawford, G. E. (2016), HDAC inhibitors cause site-specific chromatin remodeling at PU. 1-bound enhancers in K562 cells. Epigenetics & Chromatin, 9(1), 1-17. https:// doi.org/10.1186/s13072-016-0065-5
- Galloway, J. B., Norton, S., Barker, R. D., Brookes, A., Carey, I., Clarke, B. D., Jina, R., Reid, C., Russell, M. D., Sneep, R., Sugarman, L., Williams, S., Yates, M., Teo, J., Shah, A. M., & Cantle, F. (2020). A clinical risk score to identify patients with COVID-19 at high risk of critical care admission or death: an observational cohort study. Journal of Infection, 81(2), 282-288. https://doi.org/10.1016/j.jinf.2020.05.064
- Geng, L., Cuneo, K. C., Fu, A., Tu, T., Atadja, P. W., & Hallahan, D. E. (2006). Histone deacetylase (HDAC) inhibitor LBH589 increases duration of gamma-H2AX foci and confines HDAC4 to the cytoplasm in irradiated non-small cell lung cancer. Cancer Research, 66(23), 11298-11304. https://doi.org/10.1158/0008-5472.CAN-06-0049
- Gornall, K. C., Samosorn, S., Tanwirat, B., Suksamrarn, A., Bremner, J. B., Kelso, M. J., & Beck, J. L. (2010). A mass spectrometric investigation of novel quadruplex DNA-selective berberine derivatives. Chemical Communications (Cambridge, England), 46(35), 6602–6604.
- Habtemariam, S. (2020). Recent advances in berberine inspired anticancer approaches: from drug combination to novel formulation technology and derivatization. Molecules, 25(6), 1426. https://doi.org/10. 3390/molecules25061426
- Hu, Z., & Lutkenhaus, J. (2003). A conserved sequence at the C-terminus of MinD is required for binding to the membrane and targeting MinC to the septum. Molecular Microbiology, 47(2), 345-355. https://doi.org/ 10.1046/j.1365-2958.2003.03321.x
- Imanshahidi, M., & Hosseinzadeh, H. (2008). Pharmacological and therapeutic effects of Berberis vulgaris and its active constituent, berberine. Phytotherapy Research: PTR, 22(8), 999-1012. https://doi.org/10.1002/ ptr.2399
- Islam, M. M., Basu, A., & Kumar, G. S. (2011). Binding of 9-O-(ω-amino) alkyl ether analogues of the plant alkaloid berberine to poly (A): insights into self-structure induction. MedChemComm, 2(7), 631-637. https://doi.org/10.1039/c0md00209g
- Jayaraj, J. M., Krishnasamy, G., Lee, J.-K., & Muthusamy, K. (2019). In silico identification and screening of CYP24A1 inhibitors: 3D QSAR pharmacophore mapping and molecular dynamics analysis. Journal of



- Biomolecular Structure & Dynamics, 37(7), 1700–1714. https://doi.org/10.1080/07391102.2018.1464958
- Jayaraj, J. M., Reteti, E., Kesavan, C., & Muthusamy, K. (2021). Structural insights on Vitamin D receptor and screening of new potent agonist molecules: Structure and ligand-based approach. *Journal of Biomolecular Structure & Dynamics*, 39(11), 4112–4148. https://doi.org/10.1080/07391102.2020.1775122
- Kalaiarasi, A., Anusha, C., Sankar, R., Rajasekaran, S., John Marshal, J., Muthusamy, K., & Ravikumar, V. (2016). Plant isoquinoline alkaloid berberine exhibits chromatin remodeling by modulation of histone deacetylase to induce growth arrest and apoptosis in the A549 cell line. Journal of Agricultural and Food Chemistry, 64(50), 9542–9550.
- Kirubakaran, P., Muthusamy, K., Dhanachandra Singh, K., & Nagamani, S. (2012). Homology modeling, molecular dynamics, and molecular docking studies of Trichomonas vaginalis carbamate kinase. *Medicinal Chemistry Research*, 21(8), 2105–2116. https://doi.org/10.1007/s00044-011-9719-9
- Krishnan, P., & Bastow, K. F. (2000). The 9-position in berberine analogs is an important determinant of DNA topoisomerase II inhibition. *Anti-Cancer Drug Design*, 15(4), 255–264.
- Lin, H.-J., Ho, J.-H., Tsai, L.-C., Yang, F.-Y., Yang, L.-L., Kuo, C.-D., Chen, L.-G., Liu, Y.-W., & Wu, J.-Y. (2020). Synthesis and in vitro photocytotoxicity of 9-/13-lipophilic substituted berberine derivatives as potential anticancer agents. *Molecules*, 25(3), 677. https://doi.org/10.3390/molecules25030677

- Loganathan, L., & Muthusamy, K. (2019). Investigation of drug interaction potentials and binding modes on direct renin inhibitors: A computational modeling studies. *Letters in Drug Design & Discovery*, 16(8), 919–938. https://doi.org/10.2174/1570180815666180827113622
- Nagamani, S., Muthusamy, K., & Marshal, J. J. (2016). E-pharmacophore filtering and molecular dynamics simulation studies in the discovery of potent drug-like molecules for chronic kidney disease. *Journal of Biomolecular Structure & Dynamics*, 34(10), 2233–2250. https://doi.org/ 10.1080/07391102.2015.1111168
- Olleik, H., Yacoub, T., Hoffer, L., Gnansounou, S. M., Benhaiem-Henry, K., Nicoletti, C., Mekhalfi, M., Pique, V., Perrier, J., Hijazi, A., Baydoun, E., Raymond, J., Piccerelle, P., Maresca, M., & Robin, M. (2020). Synthesis and evaluation of the antibacterial activities of 13-substituted berberine derivatives. *Antibiotics*, 9(7), 381. https://doi.org/10.3390/antibiotics9070381
- Ortiz, L. M. G., Lombardi, P., Tillhon, M., & Scovassi, A. I. (2014). Berberine, an epiphany against cancer. *Molecules (Basel, Switzerland)*, 19(8), 12349–12367. https://doi.org/10.3390/molecules190812349
- Shah, B., Modi, P., & Sagar, S. R. (2020). In silico studies on therapeutic agents for COVID-19: Drug repurposing approach. *Life Sciences*, *252*, 117652. https://doi.org/10.1016/j.lfs.2020.117652
- Zou, K., Li, Z., Zhang, Y., Zhang, H.-Y., Li, B., Zhu, W.-L., Shi, J.-Y., Jia, Q., & Li, Y.-M. (2017). Advances in the study of berberine and its derivatives: a focus on anti-inflammatory and anti-tumor effects in the digestive system. *Acta Pharmacologica Sinica*, 38(2), 157–167. https://doi.org/10.1038/aps.2016.125